

Mining Science and Technology

Горные науки
и технологии

Vol.
Том 9 №3
2024



<https://mst.misis.ru/>

<https://t.me/MinSciTech>



Activities of the Mining Science and Technology (Russia) (Gornye nauki i tekhnologii) international journal are aimed at developing international scientific and professional cooperation in the field of mining.

The journal target audience comprises researchers, specialists in the field of mining, representatives of academic and professional communities.

The journal publishes original papers describing research findings, experience in the implementation of projects in mining industry, review publications.

The journal seeks to develop interdisciplinary areas that contribute to progress in mining, for example, technological and environmental safety, project organization and management in mining industry, development of territories, legal aspects of natural resource use, and other areas studied by researchers and practitioners. The journal always welcomes new developments. Papers are accepted in English or Russian.

EDITOR-IN-CHIEF

Vadim L. Petrov, Prof., Dr.Sci.(Eng.), University of Science and Technology MISIS, Moscow, Russian Federation

DEPUTIES EDITOR-IN-CHIEF

Oleg I. Kazanin, Prof., Dr.Sci.(Eng.), Saint Petersburg Mining University, St. Petersburg, Russian Federation

Svetlana A. Epshtein, Dr.Sci.(Eng.), University of Science and Technology MISIS, Moscow, Russian Federation

EDITORIAL BOARD

Zach Agioutantis, Prof., Ph.D., University of Kentucky, Lexington, Kentucky, USA

Maksim A. Bogdasarou, Prof., Dr.Sci.(Geol. and Min.), Brest State A. S. Pushkin University, Brest, Belarus

Grigory Yu. Boyarko, Prof. Dr. Sci. (Econ.), Cand. Sci. (Geol. and Miner.), National Research Tomsk Polytechnic University, Tomsk, Russian Federation

Xuan Nam Bui, Prof., Dr.Sci., Hanoi University of Mining and Geology, Duc Thang – Bac Tu Liem, Hanoi, Vietnam

Carsten Drebenstedt, Prof., Ph.D., Freiberg University of Mining and Technology, Freiberg, Germany

Faramarz Doulati Ardejani, Prof., Ph.D., Colledge of Engineering, University of Tehran, Tehran, Iran

Mikhail S. Ershov, Prof., Dr.Sci.(Eng.), National University of Oil and Gas "Gubkin University", Moscow, Russian Federation

Akper A. Feyzullaev, Prof., Dr.Sci.(Geol. and Min.), Institute of Geology and Geophysics of the National Academy of Sciences of Azerbaijan, Baku, Azerbaijan

Ochir Gerel, Prof., Dr.Sci.(Geol. and Min.), Geoscience Center, the Mongolian University of Science and Technology, Ulaanbaatar, Mongolia

Zoran Gligorić, Prof., Dr.Sci. (Mining-Underground Mining), University of Belgrade, Belgrade, Republic of Serbia

Monika Hardygora, Prof., Ph.D., Wroclaw University of Technology, Wroclaw, Poland

Nikolae Ilias, Prof., Dr.Sci.(Eng.), University of Petrosani, Petrosani, Romania

Vladislav Kecojevic, Prof., Ph.D., Benjamin M. Statler College of Engineering and Mineral Resources, West Virginia University, Morgantown, West Virginia, USA

Aleksey A. Khoreshok, Prof., Dr.Sci.(Eng.), Gorbachev Kuzbass State Technical University, Kemerovo, Russian Federation

Vladimir I. Klishin, Prof., Dr.Sci.(Eng.), Institute of Coal, Siberian Branch, Russian Academy of Sciences, Kemerovo, Russian Federation

Vladimir N. Koshelev, Prof., Dr.Sci.(Chem.), National University of Oil and Gas "Gubkin University" (Gubkin University), Moscow, Russian Federation

Jyant Kumar, Prof., Ph.D-Geotech.Eng., Indian Institute of Science, Bengaluru, India

Vladimir A. Makarov, Prof., Dr.Sci.(Geol. and Min.), Siberian Federal University, Krasnoyarsk, Russian Federation

Sergey I. Malafeev, Prof., Dr.Sci.(Eng.), Vladimir State University named after Alexander and Nikolay Stoletovs, Vladimir, Russia

Oleg S. Misnikov, Prof., Dr.Sci.(Eng.), Tver State Technical University, Tver, Russian Federation

Valery V. Morozov, Prof., Dr.Sci.(Eng.), University of Science and Technology MISIS, Moscow, Russian Federation

Igor M. Petrov, Dr.Sci.(Eng.), Infomine Research Group LLC, Moscow, Russian Federation

Bakhadirzhan R. Raimzhanov, Prof., Dr.Sci.(Eng.), University of Science and Technology MISIS (branch), Almalyk, Uzbekistan

Bayan R. Rakishev, Prof., Dr.Sci.(Eng.), Kazakh National Research Technical University named after K.I. Satpayev, Alma-Ata, Kazakhstan

Oscar Jaime Restrepo Baena, Prof., Ph.D., National University of Colombia, Medellín, Colombia

Alexander N. Shashenko, Prof., Dr.Sci.(Eng.), National Mining University, Dnipro, Ukraine

Vadim P. Tarasov, Prof., Dr.Sci.(Eng.), University of Science and Technology MISIS, Moscow, Russian Federation

Denis P. Tibilov, Prof., Dr.Sci.(Econ.), Moscow State Institute of International Affairs (University) under the Ministry of Foreign Affairs of Russia, Moscow, Russian Federation

Niyaz G. Valiev, Prof., Dr.Sci.(Eng.), The Ural State Mining University, Ekaterinburg, Russian Federation

Natalia Zhuravleva, Prof., Dr.Sci.(Eng.), West Siberian Testing Center JSC (WSTCenter JSC), Novokuznetsk, Russian Federation

Vera V. Yurak, Assoc. Prof., Dr. Sci. (Econ.), Ural State Mining University, Yekaterinburg; Institute of Economics, Ural Branch of the Russian Academy of Sciences, Yekaterinburg, Russian Federation

EDITORIAL COUNCIL

Yuri G. Agafonov, Assoc. Prof., Cand.Sci.(Eng.), University of Science and Technology MISIS, Moscow, Russian Federation

Michael R. Filonov, Prof., Dr.Sci.(Eng.), University of Science and Technology MISIS, Moscow, Russian Federation

Leonid A. Plashchansky, Prof., Cand.Sci.(Eng.), University of Science and Technology MISIS, Moscow, Russian Federation

Yuri I. Razorenov, Prof., Dr.Sci.(Eng.), Platov South-Russian State Polytechnic University, Novocherkassk, Russian Federation

EXECUTIVE SECRETARY

Daria P. Galushka, University of Science and Technology MISIS, Moscow, Russian Federation

QUARTERLY

FOUNDED in 2016

REGISTRATION

The journal science and applied research journal is registered by the Federal Service for Communication, IT and Mass Communication Control on August 10, 2015.
Registration Certificate E-No. ФС77-62652

INDEXATION

Scopus, CAS, EBSCO, DOAJ, РИНЦ, ВИНТИ РАН, Dimensions, BASE, J-Gate, Jisc Library Hub Discover.

FOUNDER AND PUBLISHER



MISIS
UNIVERSITY

University of Science and Technology
MISIS

CONTACT

4 Leninsky Prospect, Moscow 119049, Russian Federation

Phone: +7 (495) 955-00-77

e-mail: send@misis.ru



This work is licensed under a
[Creative Commons Attribution 4.0 License](https://creativecommons.org/licenses/by/4.0/).



Деятельность научно-практического журнала «Горные науки и технологии» (Mining Science and Technology (Russia)) направлена на развитие международного научного и профессионального сотрудничества в области горного дела.

Целевая аудитория журнала – исследователи, специалисты в области горного дела, представители академического и профессионального сообществ.

В журнале публикуются оригинальные статьи, описывающие результаты исследований, опыт реализации проектов в горнопромышленном комплексе, обзорные публикации.

Журнал стремится развивать такие междисциплинарные направления, как технологическая и экологическая безопасность, организация и управление проектами в горной промышленности, развитие территорий, правовые аспекты использования природных ресурсов и другие, которые способствуют прогрессу в горном деле и реализуются исследователями и практиками.

ГЛАВНЫЙ РЕДАКТОР

Петров Вадим Леонидович, проф., д.т.н., Университет науки и технологий МИСИС, г. Москва, Российская Федерация

ЗАМЕСТИТЕЛИ ГЛАВНОГО РЕДАКТОРА

Казанин Олег Иванович, проф., д.т.н., Санкт-Петербургский горный университет, г. Санкт-Петербург, Российская Федерация

Эпштейн Светлана Абрамовна, д.т.н., Университет науки и технологий МИСИС, г. Москва, Российская Федерация

РЕДАКЦИОННАЯ КОЛЛЕГИЯ

Агиутантис Зак, проф., д-р наук, Университет Кентукки, г. Лексингтон, Кентукки, США

Богдасаров Максим Альбертович, проф., д.г.-м.н., Брестский государственный университет им. А.С. Пушкина, г. Брест, Беларусь

Боярко Григорий Юрьевич – проф., д.э.н., к.г.-м.н., Национальный исследовательский Томский политехнический университет, г. Томск, Российская Федерация

Буи Суан Нам, проф., д-р наук, Ханойский университет горного дела и технологий, г. Ханой, Вьетнам

Валиев Нияз Гадым оглы, проф., д.т.н., Уральский государственный горный университет, г. Екатеринбург, Российская Федерация

Герел Очир, проф., д.г.-м.н., Центр геолого-геофизических исследований, Монгольский университет науки и технологий, г. Улан-Батор, Монголия

Глигорич Зоран, проф., д-р наук, Белградский университет, г. Белград, Республика Сербия

Дребенштедт Карстен, проф., д-р наук, Технический университет Фрайбургская горная академия, г. Фрайбург, Германия

Дулати Ардежани Фарамарз, проф., д-р наук, Инженерный колледж, Тегеранский университет, г. Тегеран, Иран

Ершов Михаил Сергеевич, проф., д.т.н., Российский государственный университет нефти и газа (национальный исследовательский университет) им. И.М. Губкина, г. Москва, Российская Федерация

Журавлева Наталья Викторовна, проф., д.т.н., АО «Западно-Сибирский испытательный центр» (АО «ЗСИЦентр»), г. Новокузнецк, Российская Федерация

Илиаш Николае, проф., д.т.н., Университет Петрошани, г. Петрошани, Румыния

Кецоджевич Владислав, проф., д-р наук, Институт инженерного дела и минеральных ресурсов им. Бенджамина М. Статлера Университета Западной Вирджинии, г. Моргантаун, Западная Вирджиния, США

Клишин Владимир Иванович, проф., д.т.н., Институт угля Сибирского отделения Российской академии наук, г. Кемерово, Российская Федерация

Кошелев Владимир Николаевич, проф., д.х.н., Российский государственный университет нефти и газа им. И.М. Губкина, г. Москва, Российская Федерация

Кумар Джьянт, проф., д-р наук (геотехнический инжиниринг), Индийский институт науки (Indian Institute of Science), г. Бангалор, Индия

Макаров Владимир Александрович, проф., д.г.-м.н., Сибирский федеральный университет, г. Красноярск, Российская Федерация

Малафеев Сергей Иванович, проф., д.т.н., Владимирский государственный университет имени А.Г. и Н.Г. Столетовых, г. Владимир, Российская Федерация

Мисников Олег Степанович, проф., д.т.н., Тверской государственный технический университет, г. Тверь, Российская Федерация

Морозов Валерий Валентинович, проф., д.т.н., Университет науки и технологий МИСИС, г. Москва, Российская Федерация

Петров Игорь Михайлович, д.т.н., ООО «Исследовательская группа «Инфолайн»», г. Москва, Российская Федерация

Раимжанов Бахадиржан Раимжанович, проф., д.т.н., филиал Университета науки и технологий МИСИС, г. Алматы, Узбекистан

Ракишев Баян Ракишевич, проф., д.т.н., Казахский национальный исследовательский технический университет им. К.И. Сатпаева, г. Алма-Ата, Казахстан

Рестрепо Базна Оскар Хайме, проф., д-р наук, Национальный университет Колумбии, г. Медельин, Колумбия

Тарасов Вадим Петрович, проф., д.т.н., НИТУ «МИСиС», г. Москва, Российская Федерация

Тибилов Денис Петрович, проф., д.э.н., Московский государственный институт международных отношений (Университет) Министерства иностранных дел России, г. Москва, Российская Федерация

Фейзуллаев Акпер Акпер оглы, проф., д.г.-м.н., Институт геологии и геофизики (ИГГ) Национальной Академии Наук Азербайджана, г. Баку, Азербайджан

Хорешок Алексей Алексеевич, проф., д.т.н., Кузбасский государственный технический университет им. М.С. Горбачева, г. Кемерово, Российская Федерация

Шашенко Александр Николаевич, проф., д.т.н., Национальный горный университет, г. Днепр, Украина

Хардигора Моника, проф., д-р наук, Вроцлавский технологический университет, г. Вроцлав, Польша

Юрак Вера Васильевна, доц., д.э.н., Уральский государственный горный университет, г. Екатеринбург; старший научный сотрудник, Институт экономики Уральского отделения Российской академии наук (ИЭ УрО РАН), г. Екатеринбург, Российская Федерация

РЕДАКЦИОННЫЙ СОВЕТ

Агафонов Юрий Григорьевич, доц., к.т.н., Университет науки и технологий МИСИС, г. Москва, Российская Федерация

Плащанский Леонид Александрович, проф., к.т.н., Университет науки и технологий МИСИС, г. Москва, Российская Федерация

Разоренов Юрий Иванович, проф., д.т.н., Южно-Российский государственный политехнический университет (НПИ) им. М.И. Платова, г. Новочеркасск, Российская Федерация

Филонов Михаил Рудольфович, проф., д.т.н., Университет науки и технологий МИСИС, г. Москва, Российская Федерация

ОТВЕТСТВЕННЫЙ СЕКРЕТАРЬ

Галушка Дарья Петровна, Университет науки и технологий МИСИС, г. Москва, Российская Федерация

ПЕРИОДИЧНОСТЬ 4 раза в год

ОСНОВАН в 2016 году

РЕГИСТРАЦИЯ

Зарегистрирован Федеральной службой по надзору в сфере связи, информационных технологий и массовых коммуникаций 10 августа 2015 года.

Свидетельство о регистрации Эл № ФС77-62652.

ИНДЕКСИРОВАНИЕ

Scopus, CAS, EBSCO, DOAJ, РИНЦ, ВИНТИ РАН, Dimensions, BASE, J-Gate, Jisc Library Hub Discover.



Журнал открытого доступа.

УЧРЕДИТЕЛЬ И ИЗДАТЕЛЬ



МИСИС Университет науки и технологий
УНИВЕРСИТЕТ
НАУКИ И ТЕХНОЛОГИЙ

АДРЕС УЧРЕДИТЕЛЯ И ИЗДАТЕЛЯ

119049, г. Москва, Ленинский проспект, д. 4

КОНТАКТЫ РЕДАКЦИИ

Адрес: 119049, г. Москва, Ленинский проспект, д. 4

Телефон: +7 (495) 955-00-77

e-mail: send@misis.ru



Контент доступен под лицензией
Creative Commons Attribution 4.0 License.



CONTENTS

MINING ROCK PROPERTIES. ROCK MECHANICS AND GEOPHYSICS

Model of time-distance curve of electromagnetic waves diffracted on a local feature
in the georadar study of permafrost zone rock layers..... 199
K. O. Sokolov

Assessment of rating parameters of the rock mass conditions
at Udachny underground mine deep levels..... 206
E. V. Serebryakov, I. A. Zaytsev, A. A. Potaka

Application of hydrodynamic simulation on the basis of a composite model to improve
the efficiency of gas-condensate reservoir development..... 221
K. O. Tomskiy, M. S. Ivanova, E. D. Nikitin, L. A. Rudykh

BENEFICIATION AND PROCESSING OF NATURAL AND TECHNOGENIC RAW MATERIALS

“Invisible” noble metals in carbonaceous rocks and beneficiation products:
feasibility of detection and coarsening..... 231
T. N. Aleksandrova, A. V. Afanasova, V. A. Aburova

SAFETY IN MINING AND PROCESSING INDUSTRY AND ENVIRONMENTAL PROTECTION

Assessment of readiness of auxiliary mine rescue teams in coal mines 243
V. A. Rudenko

Investigation of thermodynamic parameters of the air environment in subway lines
with single-track and double-track tunnels 250
S. G. Gendler, M. S. Kryukova, E. L. Alferova

Assessment of the efficiency of wastewater treatment from coal enterprises
for suspended solids using various filtering materials..... 263
L. A. Ivanova, A. Yu. Prosekov, P. P. Ivanov, E. S. Mikhaylova, I. V. Timoshchuk, A. K. Gorelkina

Environmentally sound geotechnologies for leaching metals
from polymetallic ore processing wastes and wastewater 271
V. I. Golik, Yu. I. Razorenov, N. G. Valiev, O. A. Gavrina

Substantiation of environmental safety
in metro facility operations considering hydrogeological risks..... 283
S. A. Zhukov

POWER ENGINEERING, AUTOMATION, AND ENERGY PERFORMANCE

Stability of a controlled sucker-rod pump unit drive under operating conditions
and during voltage dips in the electrical network..... 292
M. S. Ershov, E. S. Efimov



СОДЕРЖАНИЕ

СВОЙСТВА ГОРНЫХ ПОРОД. ГЕОМЕХАНИКА И ГЕОФИЗИКА

Модель годографа электромагнитных волн, дифрагированных на локальном объекте при георадиолокационном изучении слоев горных пород криолитозоны 199
К. О. Соколов

Оценка рейтинговых показателей состояния горного массива глубоких горизонтов подземного рудника Удачный 206
Е. В. Серебряков, И. А. Зайцев, А. А. Потака

Применение гидродинамического моделирования на основе композиционной модели для повышения эффективности разработки газоконденсатной залежи 221
К. О. Томский, М. С. Иванова, Е. Д. Никитин, Л. А. Рудых

ОБОГАЩЕНИЕ, ПЕРЕРАБОТКА МИНЕРАЛЬНОГО И ТЕХНОГЕННОГО СЫРЬЯ

«Невидимые» благородные металлы в углеродистых породах и продуктах обогащения: возможность выявления и укрупнения 231
Т. Н. Александрова, А. В. Афанасова, В. А. Абурова

ТЕХНОЛОГИЧЕСКАЯ БЕЗОПАСНОСТЬ В МИНЕРАЛЬНО-СЫРЬЕВОМ КОМПЛЕКСЕ И ОХРАНА ОКРУЖАЮЩЕЙ СРЕДЫ

Оценка готовности вспомогательных горноспасательных команд угольных шахт 243
В. А. Руденко

Исследование термодинамических параметров воздушной среды на линиях метрополитенов с однопутными и двухпутными тоннелями 250
С. Г. Гендлер, М. С. Крюкова, Е. Л. Алферова

Оценка эффективности очистки сточных вод угольных предприятий от взвешенных веществ различными фильтрующими материалами 263
Л. А. Иванова, А. Ю. Просеков, П. П. Иванов, Е. С. Михайлова, И. В. Тимощук, А. К. Горелкина

Экологически чистые геотехнологии выщелачивания металлов из твердых и жидких отходов обогащения полиметаллического сырья 271
В. И. Голик, Ю. И. Разоренов, Н. Г. Валиев, О. А. Гаврина

Обоснование экологической безопасности при эксплуатации объектов метрополитена с учетом гидрогеологического риска 283
С. А. Жуков

ЭНЕРГЕТИКА, АВТОМАТИЗАЦИЯ И ЭНЕРГОЭФФЕКТИВНОСТЬ

Устойчивость регулируемого привода штанговой насосной установки в рабочих режимах и при провалах напряжения в сети 292
М. С. Ершов, Е. С. Ефимов



MINING ROCK PROPERTIES. ROCK MECHANICS AND GEOPHYSICS

Research paper

<https://doi.org/10.17073/2500-0632-2023-05-118>

UDC 53.072:551.553:621.37:551.34

**Model of time-distance curve of electromagnetic waves diffracted on a local feature in the georadar study of permafrost zone rock layers**K. O. Sokolov   

N.V. Chersky Mining Institute of the North of the Siberian Branch of the RAS, Yakutsk, Russian Federation

 k.sokolov@ro.ru**Abstract**

In GPR (georadar) studies, one of the most popular procedures for determining electromagnetic waves propagation velocity in a rock mass is the selection of theoretical hyperbolic time-distance curves and subsequent comparison with the time-distance curve obtained from a GPR measurement. This procedure is based on the model of homogeneous medium, but nowadays the subject of GPR study is often inhomogeneous media, such as horizontally layered media characteristic of loose permafrost zone sediments. The paper presents the findings of studying the formation of hyperbolic time-distance curves of georadar impulses in a horizontally layered medium without taking into account the dispersion and absorption of electromagnetic waves. On the basis of geometrical optics laws, formulas were derived to calculate the shape of the hyperbolic lineup of georadar impulses reflected from a local feature in a multilayer frozen rock mass. On the example of a permafrost zone rock mass containing a layer of unfrozen rocks, the effect of the thicknesses of rock layers and their relative dielectric permittivity on the apparent dielectric permittivity resulting from the calculation of the theoretical hyperbolic time-distance curve was shown. The conditions under which it is impossible to determine the presence of a layer of unfrozen rocks from a hyperbolic time-distance curve are also presented. The established regularities were tested on synthetic georadar radargrams calculated in the gprMax software program. The findings of the theoretical studies were confirmed by the comparison with the results of the analysis of the georadar measurements computer simulation data in the gprMax system (the relative error was less than 0.5%).

Keywords

model, rock mass, rocks, dielectric permittivity, velocity, hyperbola, layer, georadar, permafrost zone, gprMax

Acknowledgments

The study was performed within the framework of the state assignment of the Ministry of Science and Higher Education of the Russian Federation (Project No. 0297-2021-0020, EGISU NIOKTR (Unified State Information System for R&D Accounting) No. 122011800086-1).

For citation

Sokolov K.O. Model of time-distance curve of electromagnetic waves diffracted on a local feature in the georadar study of permafrost zone rock layers. *Mining Science and Technology (Russia)*. 2024;9(3):199–205. <https://doi.org/10.17073/2500-0632-2023-05-118>

СВОЙСТВА ГОРНЫХ ПОРОД. ГЕОМЕХАНИКА И ГЕОФИЗИКА

Научная статья

Модель годографа электромагнитных волн, дифрагированных на локальном объекте при георадиолокационном изучении слоев горных пород криолитозоныК. О. Соколов   

Институт горного дела Севера им. Н.В. Черского СО РАН, г. Якутск, Российская Федерация

 k.sokolov@ro.ru**Аннотация**

В георадиолокации одной из наиболее популярных процедур определения скорости распространения электромагнитных волн в массиве горных пород является подбор теоретических гиперболических годографов с последующим сравнением с годографом, полученным при георадиолокационном измерении. Эта процедура основана на модели однородной среды, но в настоящее время объектом изучения георадиолокации часто становятся неоднородные среды, такие как горизонтально-слоистые среды, характерные для рыхлых отложений криолитозоны. В статье представлены результаты исследования формирования гиперболических годографов георадиолокационных сигналов в горизонтально-слоистой среде без учета дисперсии и поглощения электромагнитных волн. На основе законов геометрии



ческой оптики выведены формулы, позволяющие рассчитать форму гиперболической оси синфазности георадиолокационных сигналов, отраженных от локального объекта в многослойном массиве мерзлых горных пород. На примере массива горных пород криолитозоны, содержащего слой незамерзших горных пород, показано влияние мощностей слоев горных пород и их относительной диэлектрической проницаемости на кажущуюся диэлектрическую проницаемость, получаемую в результате расчета теоретического гиперболического годографа. Также представлены условия, при которых невозможно определить наличие слоя незамерзших горных пород по гиперболическому годографу. Установленные закономерности апробированы на синтетических георадиолокационных радарограммах, рассчитанных в программе gprMax. Результаты теоретических исследований подтверждены сравнением с результатами анализа данных компьютерного моделирования георадиолокационных измерений в системе gprMax (относительная погрешность составила менее 0,5 %).

Ключевые слова

модель, массив, горные породы, диэлектрическая проницаемость, скорость, гипербола, слой, георадиолокация, криолитозона, gprMax

Благодарности

Работа выполнена в рамках государственного задания Министерства науки и высшего образования Российской Федерации (тема № 0297-2021-0020, ЕГИСУ НИОКТР № 122011800086-1).

Для цитирования

Sokolov K. O. Model of time-distance curve of electromagnetic waves diffracted on a local feature in the georadar study of permafrost zone rock layers. *Mining Science and Technology (Russia)*. 2024;9(3):199–205. <https://doi.org/10.17073/2500-0632-2023-05-118>

Introduction

One of the geophysical problems to be solved by using GPR (georadar) method is the study of physical and mechanical properties of rocks. However, accumulation of experimental data and development of methodological support for GPR in this area is much slower [1, 2] than in other areas [3] that leads to underestimation of the capabilities of the georadar method. The reasons that led to this state of affairs in georadar application can be different. One of them is the incorrect use of the procedure for determining the velocity v of electromagnetic wave (EMW) propagation using hyperbolic time-distance curves (lineups of georadar impulses). This procedure is the most common way to estimate EMW velocity [1], based on which the material part of the relative complex dielectric permittivity ϵ' , depending on moisture, density, and cryogenic state of rocks, is calculated [4]. In training manuals (both domestic [1, 2] and foreign [5, 6]), as well as in data processing manuals of georadar manufacturers (GSSI, GEOTECH) and American Society for Testing and Materials (ASTM) standard¹, justification of application of EMW propagation velocity determination by hyperbolic time-distance curves is given for the case when the host medium is homogeneous.

Currently, in the practice of georadar measurements [3, 7, 8], as well as in scientific works devoted to the automation of the search for hyperbolic time-distance curves in GPR data [9–11], including on a real-time basis [12], the study subject is, as a rule,

an inhomogeneous medium. As a consequence, the EMW propagation velocity determined by a hyperbola located in some layer is an averaged (integral) characteristic of all overlying layers, as mentioned in the work of one of the GPR classics [13]. When conducting georadar studies in a permafrost zone, it is possible to incorrectly assess the cryogenic state of rocks and, correspondingly, their physical and mechanical properties in the presence of a layer of thawed rocks, whose effect on the shape of the hyperbolic time-distance curve may be significant but insufficient for the result of v determination by the method of approximation of the time-distance curve by a hyperbola [2] proved to be within the range of values characteristic of thawed rocks. Thus, in a layered medium it is possible to determine the true velocity v of EMW propagation directly from the hyperbolic time-distance curve only in the first layer of rocks, and for the correct use of v values in the practice of georadar works it is necessary to establish the regularities of formation of EMW time-distance curves diffracted at a local feature in a layered rock mass. In order to achieve the above goal, the following tasks need to be accomplished:

- develop a model of a hyperbolic time-distance curve of impulses obtained in the study of a layered rock mass;

- establish the dependence of v and ϵ' determined from the hyperbolic time-distance curve on the values of v and ϵ' of the overlying layers;

- determine the influence of a thawed layer in a frozen rock mass on the v value calculated from the hyperbolic time-distance curve;

- verify the validity of the obtained theoretical results using the data of computer simulation.

¹ ASTM D6432-11, Standard guide for using the surface ground penetrating radar method for subsurface investigation, ASTM International, West Conshohocken, PA; 2011. <https://doi.org/10.1520/D6432-11>

Model of a hyperbolic time-distance curve of georadar impulses obtained from probing of a layered rock mass

EMW emitted by a georadar located at point x propagates in a layered rock mass according to Fermat's principle (gray solid line in Fig. 1), but in this paper we consider a model of EMW propagation along a raypath (black dashed line in Fig. 1) in a rock mass consisting of n layers of h_i thickness with given values of ε'_i and v_i with i ranging 1 to n . A local feature, indicated by the black circle in Fig. 1, is located in the last layer at depth h_0 . The distance h_r , traveled by the ray from georadar to the local feature, will be equal to:

$$h_r = \sqrt{(x - x_0)^2 + h_0^2}.$$

When moving the georadar along the profile, the x coordinate will increase, while h_r will correspondingly decrease, forming the left branch of the hyperbola and reaching a minimum at the point $x = x_0$, where the vertex of the hyperbola will be located. At $x > x_0$, the values of h_r will increase and correspond to the right branch of the hyperbola. In the intermediate layer numbered i , the ray travels a distance h_{ri} , which is greater than the thickness of the layer h_i at all points except x_0 :

$$h_{ri} = \frac{h_i}{\cos \alpha}, \quad i \in 1 \dots (n-1),$$

where

$$\alpha = \arcsin\left(\frac{x - x_0}{h_r}\right).$$

Since in the last layer the ray travels a distance smaller than h_n , then h_m will be equal to:

$$h_m = \frac{h_0 - \sum_{i=1}^{n-1} h_i}{\cos \alpha}.$$

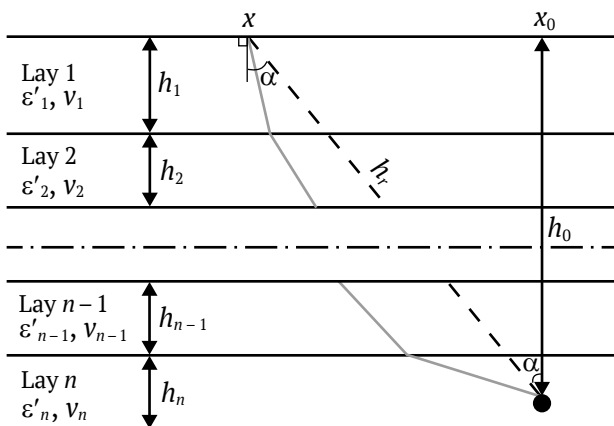


Fig. 1. Schematic diagram of the model of electromagnetic wave propagation in a layered rock mass

The ray propagation time in layer i :

$$t_{ri} = \frac{h_{ri}}{v_i}.$$

The total time t_r of the ray propagation from the georadar to a local feature will be:

$$t_r = \sum_{i=1}^n t_{ri}.$$

Then the averaged ray velocity will be equal to:

$$v_r = \frac{\sum_{i=1}^n h_{ri}}{t_r}.$$

Equation of a hyperbolic time-distance curve in a homogeneous medium [2]:

$$t = \frac{2h_r}{v}. \quad (1)$$

For a horizontally layered medium, equation (1) will take the following form:

$$t = \frac{2 \sum_{i=1}^n h_{ri}}{v_i} = \frac{2 \sum_{i=1}^n h_i}{v_i \cos \alpha} = \frac{2 \sum_{i=1}^n h_i}{\cos \left(\arcsin \frac{x - x_0}{h_r} \right)}.$$

Based on the basic trigonometrical identity and the positivity of the cosine function in the area of arcsine values, we transform the denominator of the fraction:

$$\begin{aligned} \cos \left(\arcsin \frac{x - x_0}{h_r} \right) &= \sqrt{1 - \left(\frac{x - x_0}{h_r} \right)^2} = \\ &= \frac{\sqrt{h_r^2 - (x - x_0)^2}}{h_r} = \frac{h_0}{h_r}. \end{aligned}$$

Then the equation of the hyperbolic time-distance curve of GPR impulses reflected from a local feature located in a layered rock mass can be represented as (2). When substituting parameters for a single-layer medium into equation (2), it coincides with expression (1):

$$t = \frac{2h_r}{h_0} \sum_{i=1}^n \frac{h_i}{v_i}. \quad (2)$$

When processing georadar data, the hyperbolic time-distance curve having the form corresponding to expression (2) is approximated by a hyperbola having the form according to equation (1). The values of EMW propagation velocity calculated as a result of such approximation are not true, but apparent (v_{app}), and represent some integral value of EMW velocities in all overlying layers. To determine the dependence of v_{app} on the values of v in the layers overlying the



local feature, we equate equations (1) and (2) to each other:

$$\frac{2h_r}{v_{app}} = \frac{2h_r}{h_0} \sum_{i=1}^n \frac{h_i}{v_i}.$$

And let's express v_{app} :

$$v_{app} = \frac{h_0}{\sum_{i=1}^n \frac{h_i}{v_i}}. \quad (3)$$

According to the known dependence $v = c/\sqrt{\varepsilon'}$ ($c = 300\,000\text{ km/s} = 0.3\text{ m/ns}$) [2], the apparent dielectric permittivity will be equal to:

$$\varepsilon'_{app} = \frac{c^2}{h_0^2} \left(\sum_{i=1}^n \frac{h_i}{v_i} \right)^2. \quad (4)$$

It is impossible to estimate the EMW propagation velocity in the rocks of a particular layer from the value of v_{app} , and it can be assumed that v of each layer is in the range of $v_{app} \pm \Delta v$. For example, if in GPR measurements of a permafrost rock mass with v in the narrow range of 100–150 m/ μsec (the average value $v_{avr} \approx 125\text{ m}/\mu\text{sec}$) [14] v_{app} will be higher than 100 m/ μsec , then the rock mass as a whole can be characterized as frozen. However, in such rock masses there may be a layer of rocks in thawed state, which can be detected by georadar data, but there is a problem with its identification [15]. In this connection there is a problem of determining the influence of a layer of rocks with a low value of v_{avr} on v_{app} .

To solve this problem, we used formula (3) and the fact that v of frozen rocks varies within narrow limits, and the velocity of EMW propagation in unfrozen (thawed) rocks v_{th} is much lower [2]. Let's represent a part of a frozen rock mass as layers of the same thickness h_{avr} , in each of which the EMW propagation velocity will be equal to the average value v_{avr} . The frozen part of the rock mass can be divided into layers arbitrarily, since at the same v their number and thickness do not affect the traveltime of GPR impulses that make up the hyperbolic lineup. The thickness h_{th} and velocity v_{th} in and thawed rock layer are represented as proportional to h_{avr} and v_{avr} :

$$h_{th} = k_h h_{avr}, \quad v_{th} = k_v v_{avr}.$$

After substitution into (3), we obtain an expression for the apparent velocity $v_{app,th}$ of EMW pro-

pagation in a frozen rock mass containing a layer of thawed rocks:

$$\begin{aligned} v_{app,th} &= \frac{h_0}{\sum_{i=1}^n \frac{h_i}{v_i}} = \frac{h_0}{\frac{h_{avr}}{v_{avr}} + \frac{h_{th}}{v_{th}}} = \frac{h_0}{\frac{h_{avr}}{v_{avr}} + \frac{k_h h_{avr}}{k_v v_{avr}}} \\ &= \frac{h_0}{\frac{h_{avr}}{v_{avr}} \left(1 + \frac{k_h}{k_v} \right)} = \frac{v_{avr} (n-1+k_h)}{\frac{h_{avr}}{v_{avr}} \left(n-1 + \frac{k_h}{k_v} \right)} = \frac{v_{avr} (n-1+k_h)}{\left(n-1 + \frac{k_h}{k_v} \right)}. \end{aligned} \quad (5)$$

At $k_h = 0$, according to formula (5), $v_{app,th} = v_{avr}$, i.e. it will correspond to frozen rock mass. In order to determine how v_{app} will change compared to v_{avr} in the presence of a low-velocity layer of thawed rocks, let us divide formula (3) with the frozen rock parameters h_{avr} and v_{avr} for all layers, denoted by $v_{app,fr}$ by expression (5):

$$\frac{v_{app,fr}}{v_{app,th}} = \frac{h_0}{n \frac{h_{avr}}{v_{avr}}} \frac{\left(n-1 + \frac{k_h}{k_v} \right)}{v_{avr} (n-1+k_h)} = \frac{n-1 + \frac{k_h}{k_v}}{n-1+k_h}. \quad (6)$$

Verification of the obtained theoretical expressions using computer simulation data

A simulation of GPR data was performed in the gprMax system [16], which has positively proved itself in studies devoted to the determination and analysis of hyperbolic lineups of GPR impulses [17–19]. The following parameters were used in the simulation: probing impulse – Ricker pulse with Fourier spectrum center frequency of 400 MHz, time-base sweep of 150, baseline of 0 mm. The data for the simulation are presented in the table below.

Input file text for gprMax for model #1:

```
#domain: 4 9.1 0.002
#dx_dy_dz: 0.002 0.002 0.002
#time_window: 150e-9
#material: 6 0 1 0 sloi1
#material: 4 0 1 0 sloi2
#waveform: ricker 10 0.4e9 my_ricker
#hertzian_dipole: z 0.1 9 0 my_ricker
#rx: 0.1 9 0
#src_steps: 0.01 0 0
#rx_steps: 0.01 0 0
#box: 0 0 0 4 9 0.002 sloi1
#box: 0 0 0 4 7 0.002 sloi2
#cylinder: 2 5 0 2 5 0.002 0.01 pec
```

Table

Parameters of rock mass models

Model No.	Quantity of layers	Layer thickness, m	ε'	v , m/ μs	h_0 , m
1	2	2; 7	6; 4	122.5; 150	4
2	3	2; 2; 4	8; 6; 4	100; 122.5; 150	6
3	5	1; 1; 1; 0.5; 2	6; 4; 6; 20; 4	122.5; 150; 122.5; 67; 150	4.5

The simulation result (out-file) was exported to the format of the GeoScan32 software program (of SPC GEOTECH manufacturer), in which the depth scale origin and the Baseline parameter equal to 1 were set. Fig. 2, a shows the results of the simulation (Model #1), the values of ε'_{app} , calculated using the “Hyperbola” procedure, and v_{app} . The traveltimes of impulses reflected from the lower boundary of layer 1 t_1 and from the local feature, the top of the hyperbola, t_h , according to formula (1) are equal to:

$$t_1 = 32.7 \text{ ns}; \quad t_h = t_1 + 26.7 = 59.4 \text{ ns}.$$

According to formulas (3) and (4), v_{app} and ε'_{app} are equal to:

$$v_{app} = 0.1349 \text{ m/ns} = 134.9 \text{ m/}\mu\text{s};$$

$$\varepsilon'_{app} = 4.9484.$$

Verification of the values obtained:

$$v = \frac{c}{\sqrt{\varepsilon'}} = 0.1349 \text{ m/ns}.$$

Thus, the relative error of the values of v_{app} and ε'_{app} calculated in the GeoScan32 program was 0.07 and 0.37%, respectively. For model No. 2, from the calculations by formulas (3) and (4), the values of $v_{app} = 123.7 \text{ m/}\mu\text{sec}$, $\varepsilon'_{app} = 5.8853$ were obtained.

To verify formula (6), we first calculate $v_{app,fr}$ for the model of frozen rock mass with thickness $h_0 = 5 \text{ m}$, consisting of $n = 5$ layers with $h = 1 \text{ m}$, $v = 122.5, 150, 122.5, 134.2, 150 \text{ m/}\mu\text{s}$ and $\varepsilon' = 6; 4; 6; 5; 4$. According to expression (3), $v_{app,fr} = 134.7 \text{ m/}\mu\text{s}$.

Further, instead of the fourth layer, we introduce a low-velocity layer (model No. 3 in the Table) with such parameters h_{th}, v_{th} so that the value of $v_{app,th}$ is in the range characteristic of thawed rocks. Let us set

the thickness of the thawed layer $h_{th} = 0.5 \text{ m}$ (thus h_0 decreases to 4.5 m) as half ($k_h = 0.5$) of the thickness of the averaged layer $h_{avr} = 1 \text{ m}$, and the EMW propagation velocity in it is two times less ($k_v = 0.5$) than the average value (at $\varepsilon'_{avr} = 5$) of $v_{avr} = 134.2 \text{ m/}\mu\text{s}$, i.e. $v_{th} = 67.1 \text{ m/}\mu\text{s}$, $\varepsilon'_{th} = (avr/v_{th})^2 = 20$. Other parameters of the simulated rock mass are presented in the Table. According to formula (3), $v_{app,th} = 121.2 \text{ m/}\mu\text{sec}$, which is confirmed by the result of the calculation of v_{app} based on the computer simulation data (Fig. 2, c), the relative error of which, compared to the exact value, was less than 0.5%.

Now we can calculate how the apparent EMW propagation velocity in the rock mass model has changed with the introduction of a low-velocity layer (into the model):

$$\frac{v_{app,fr}}{v_{app,th}} = 1.1114.$$

That is, in the presence of a low-velocity layer with the above parameters, v_{app} decreases by $\approx 10\%$. In order to obtain this result, we had to carry out the whole set of calculations to calculate v_{app} both for a fully frozen rock mass and for the case with a layer of unfrozen (thawed) rocks. Such calculations can be substantially simplified if we use formula (6), which allows to obtain the same result with accuracy to thousandths:

$$\frac{v_{app,fr}}{v_{app,th}} = \frac{n-1 + \frac{k_h}{k_v}}{n-1 + k_h} = 1.1111.$$

To confirm that formula (6) is correct when the frozen part of a rock mass is subdivided into an arbitrary number of layers, calculations were performed

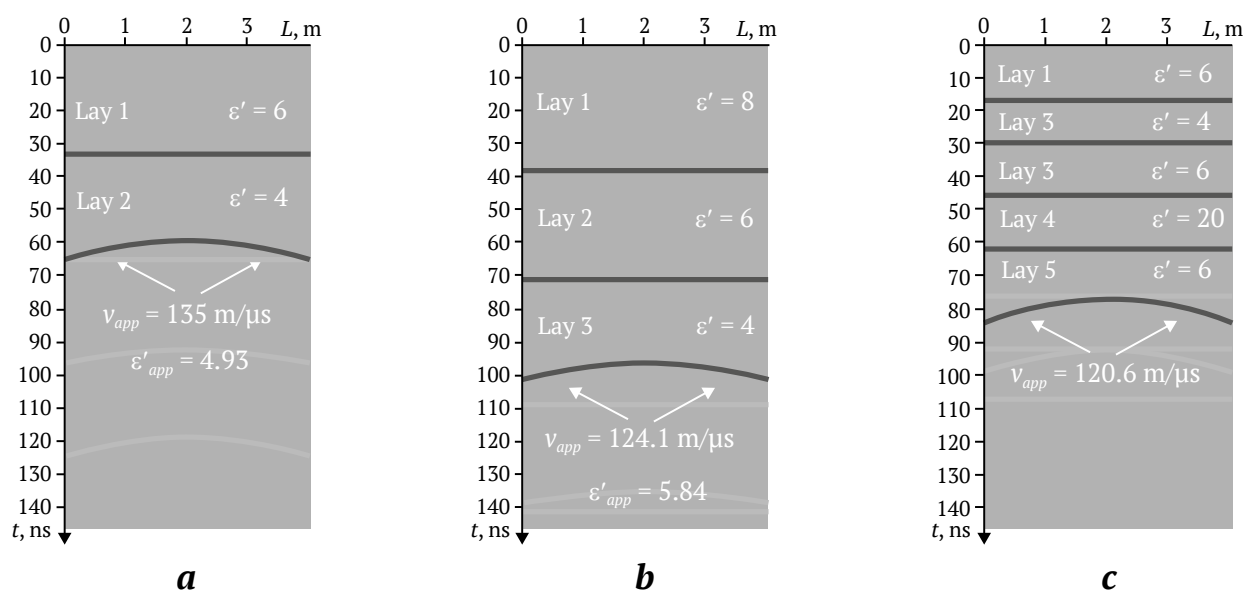


Fig. 2. Synthetic radargrams of models Nos. 1(a), 2(b) and 3(c)



for the model with 3 and 9 layers. Only one parameter, k_h , changes, for instance, at $n = 3$ ($h = 2, 0.5, 2$ m), $k_h = 0.25$, at $n = 9$ (thickness of each layer is 0.5 m), $k_h = 1$:

$$n = 3 \rightarrow \frac{v_{app.fr}}{v_{app.th}} = 1.1111;$$

$$n = 9 \rightarrow \frac{v_{app.fr}}{v_{app.th}} = 1.1111;$$

In general, to determine whether $v_{app.th}$ will be within the range of the values characteristic of frozen rocks, for example, in Central Yakutia, at arbitrary k_h , k_v , we substitute into formula (5) the averaged values characteristic of this region, $v_{avr} = 125$ m/ μ s and $v_{app.th} = 100$ m/ μ s [14], then with a very significant difference between $v_{app.fr}$ and $v_{app.th}$:

$$\frac{v_{app.fr}}{v_{app.th}} = 1.25$$

we obtain from (5):

$$100 = \frac{125(n-1+k_h)}{n-1+\frac{k_h}{k_v}},$$

from where

$$\frac{n-1+k_h}{n-1+\frac{k_h}{k_v}} = 0.8. \quad (7)$$

When $v_{app.th}$ increases or $v_{app.fr}$ decreases, expression (7) will be greater than 0.8, and the ratio $v_{app.fr}/v_{app.th}$ will decrease, which will lead to difficulties in interpreting GPR data to identify the presence of a layer of thawed rocks on the basis of analyzing the hyperbolic time-distance curve of GPR impulses. The estimation of the feasibility of detecting the

layer of thawed rocks based on the values of parameters k_h , k_v according to formula (7) was performed for the region of Central Yakutia. For other regions the calculation should be accomplished with the corresponding values of EMW propagation velocities in frozen and thawed rocks.

Conclusions

The performed study allowed to develop a model of hyperbolic time-distance curve of GPR impulses reflected from a local feature located in a rock mass with an arbitrary number of layers. On the basis of the developed model, the expressions for the apparent values of electromagnetic wave propagation velocity and the material part of the relative complex dielectric permittivity calculated from the hyperbolic time-distance curve of georadar impulses were obtained. The obtained expressions allowed us to determine how the velocity of electromagnetic wave propagation in a rock mass containing a layer of unfrozen (thawed) rocks decreases compared to a fully frozen rock mass. The findings of the theoretical studies were confirmed by comparison with the results of the analysis of the data of the georadar measurements computer simulation in the gprMax system (the relative error was less than 0.5%).

The results obtained in the course of the study are of great importance for the development of methodological support of GPR for determining electrophysical properties of rocks, which will increase the reliability of the assessment of their physical and mechanical properties, especially in the area of permafrost occurrence. Practical application of the obtained results in studies aimed at automated determination of electrophysical properties of rocks and soils by hyperbolic time-distance curves will allow to create a database with up-to-date information on dielectric permittivity of rocks.

References

1. Starovoitov A.V. Interpretation of georadar data. Moscow: MSU Publ. House; 2008. 192 p. (In Russ.)
2. Vladov M.L., Sudakova M.S. Georadar. From physical fundamentals to upcoming trends. Moscow: GEOS Publ. House; 2017. 240 p. (In Russ.)
3. Lombardi F., Podd F., Solla M. From its core to the niche: insights from GPR applications. *Remote Sens.* 2022;14(13):3033. <https://doi.org/10.3390/rs14133033>
4. Frolov A.D. Electrical and elastic properties of frozen rocks and ice. Pushchino: ONTI PNTs RAS Publ.; 1998. 515 p. (In Russ.)
5. Persico R. *Introduction to ground penetrating radar: inverse scattering and data processing*. New Jersey: Wiley-IEEE Press; 2014. 392 c. <https://doi.org/10.1002/9781118835647.ch2>
6. Jol H.M. *Ground penetrating radar: theory and application*. Elsevier; 2008. 544 p. <https://doi.org/10.1016/B978-0-444-53348-7.X0001-4>
7. Dyakov A. Yu., Kalashnik A.I. *Methodological fundamentals of GPR studies of mining features*. Apatity: FITs KSC RAS Publ.; 2021. 110 p. (In Russ.) <https://doi.org/10.37614/978.5.91137.443.3>



8. Solla M., Perez-Gracia V., Fontul S. A review of GPR application on transport infrastructures: troubleshooting and best practices. *Remote Sens.* 2021;13(4):672. <https://doi.org/10.3390/rs13040672>
9. Wunderlich T., Wilken D., Majchczack B.S. et al. Hyperbola detection with retinanet and comparison of hyperbola fitting methods in GPR data from an archaeological site. *Remote Sensing.* 2022;14:3665. <https://doi.org/10.3390/rs14153665>
10. Mertens L., Persico R., Matera L., Lambot S. Automated detection of reflection hyperbolas in complex gpr images with no a priori knowledge on the medium. In: *IEEE Transactions on Geoscience and Remote Sensing.* 2016;1:580–596. <https://doi.org/10.1109/TGRS.2015.2462727>
11. Lei W., Hou F., Xi J. et al. Automatic hyperbola detection and fitting in GPR B-scan image. *Automation in Construction.* 2019;106:102839. <https://doi.org/10.1016/j.autcon.2019.102839>
12. Dou Q., Wei L., Magee R., Cohn A.G. Real-time hyperbola recognition and fitting in GPR data. In: *IEEE Transactions on Geoscience and Remote Sensing.* 2017;55(1):51–62. <https://doi.org/10.1109/TGRS.2016.2592679>
13. Daniels J.J. Fundamentals of ground penetrating radar. In: *Symposium on the Application of Geophysics to Engineering and Environmental Problems.* 1989;1:62–142. <https://doi.org/10.4133/1.2921864>
14. Omelyanenko A.V., Fedorova L.L. Georadar studies of permafrost. Yakutsk: YaSC SB RAS Publ.; 2006. 136 p. (In Russ.)
15. Yakupov V.S. *Geophysics of permafrost zone.* Yakutsk: Yakutsk State University Publ.; 2008. 342 p. (In Russ.)
16. Warren C., Giannopoulos A., Giannakis I. gprMax: Open source software to simulate electromagnetic wave propagation for Ground Penetrating Radar. *Computer Physics Communications.* 2016;209:163–170. <https://doi.org/10.1016/j.cpc.2016.08.020>
17. Wunderlich T., Wilken D., Majchczack B.S., et al. Hyperbola detection with RetinaNet and comparison of hyperbola fitting methods in GPR data from an archaeological site. *Remote Sensing.* 2022;14:3665. <https://doi.org/10.3390/rs14153665>
18. Dewantara D., Parnadi W.W. Automatic hyperbola detection and apex extraction using convolutional neural network on GPR data. *Journal of Physics: Conference Series.* 2022;1:012027. <https://doi.org/10.1088/1742-6596/2243/1/012027>
19. Wang H., Ouyang S., Liao K.-F., Jin L.-N. GPR B-SCAN image hyperbola detection method based on deep learning. *Acta Electronica Sinica.* 2021;49(5):953–963. <https://doi.org/10.12263/DZXB.20200635>

Information about the author

Kirill O. Sokolov – Cand. Sci. (Eng.), Senior Researcher, N.V. Chersky Mining Institute of the North of the Siberian Branch of the RAS Yakutsk, Russian Federation; ORCID [0000-0002-4179-9619](https://orcid.org/0000-0002-4179-9619), Scopus ID [56457950500](https://scopus.org/56457950500), ResearcherID [P-8843-2016](https://orcid.org/P-8843-2016); e-mail k.sokolov@ro.ru

Received 11.05.2023

Revised 08.03.2024

Accepted 04.05.2024




MINING ROCK PROPERTIES. ROCK MECHANICS AND GEOPHYSICS

Research paper

<https://doi.org/10.17073/2500-0632-2023-12-192>

UDC 622.02

**Assessment of rating parameters of the rock mass conditions at Udachny underground mine deep levels**E. V. Serebryakov¹  , I. A. Zaytsev², A. A. Potaka²¹ Institute of Earth Crust SB RAS, Irkutsk, Russian Federation² Udachny Mining and Processing Complex, PJSC AK ALROSA, Mirny, Russian Federation serebryakov.e.v@mail.ru**Abstract**

Geotechnical rating classification systems of rock masses are an important tool in the design of underground mining systems. They are especially relevant at the early stages of project development, when primary mining and geological information is available to a limited extent. The presented work shows an approach to the collection of initial information and calculation of RMR (Rock Mass Rating) and Q Index for the rock mass of deep levels of the Udachny underground mine exploiting the kimberlite pipe of the same name. Since the classifications are multi-component systems, they impose heavy demands on the scope and quality of primary data, which can be met by applying an integrated data collection system. The bulk of these were obtained by acoustic televiewer tool (ATV) combined with geologic and structural logging of non-oriented core. Data on physical and mechanical properties of rocks, stress-strain state, and hydrogeological conditions were also used. The ratings were calculated interval by interval along holes, in which acoustic logging was performed. The acoustic wave amplitude parameter, which depends on the physical properties of a rock mass and the degree of its structural disturbance, was proposed as one of the criteria for distinguishing geotechnical intervals. The moderate level of correspondence between Q and RMR systems was established to be due to the different “sensitivity” and structure of the input parameters. Using the calculated ratings, the rock masses of ore bodies and host sediments were evaluated for stability (classes/categories have been assigned), and the optimal method and parameters of workings support were determined. The geotechnical database accumulated during the research process provides the feasibility of calculating alternative ratings such as MRMR, RMI, GSI, etc., without the use of transient equations.

Keywords


rating classification, RMR, Q, Udachnaya kimberlite pipe, televiewer, jointing, rock mass stability, supports

For citation

Serebryakov E. V., Zaytsev I. A., Potaka A. A. Assessment of rating parameters of the rock mass conditions at Udachny underground mine deep levels. *Mining Science and Technology (Russia)*. 2024;9(3):206–220. <https://doi.org/10.17073/2500-0632-2023-12-192>

СВОЙСТВА ГОРНЫХ ПОРОД. ГЕОМЕХАНИКА И ГЕОФИЗИКА

Научная статья

Оценка рейтинговых показателей состояния горного массива глубоких горизонтов подземного рудника УдачныйЕ. В. Серебряков¹  , И. А. Зайцев², А. А. Потака²¹ Институт земной коры СО РАН, г. Иркутск, Российская Федерация² Удачинский горно-обогатительный комбинат, ПАО «АК «АЛРОСА», г. Мирный, Российская Федерация serebryakov.e.v@mail.ru**Аннотация**

Геомеханические рейтинговые классификации массивов являются важным инструментом при проектировании подземных технологий отработки месторождений. Особенно актуальны они на ранних стадиях разработки проекта, когда первичная горно-геологическая информация доступна в ограниченном объеме. В представляемой работе показан подход к сбору исходной информации и расчету рейтинга RMR и индекса Q для массива горных пород глубоких горизонтов подземного рудника Удачный, обрабатывающего одноименную кимберлитовую трубку. Поскольку классификации являются многокомпонентными системами, они предъявляют высокие требования по объему и качеству первичной информации, выполнение которых возможно путем применения комплексной системы сбора данных.



Основной их объем получен посредством акустического телевьюверного каротажа, совмещенного с геолого-структурной документацией неориентированного керна. Также использованы данные о физико-механических свойствах пород, напряженно-деформированном состоянии и гидрогеологических условиях. Расчет рейтингов произведен поинтервально вдоль стволов скважин, в которых производился акустический каротаж. В качестве одного из критериев для выделения геомеханических интервалов предложен параметр амплитуды акустической волны, зависящий от физических свойств породного массива и степени его структурной нарушенности. Установлен средний уровень связи между Q и RMR, что обусловлено разной «чувствительностью» и структурой входных параметров. С помощью рассчитанных рейтингов массив рудных тел и вмещающих отложений оценен по степени устойчивости (присвоены классы/категории), а также определены оптимальные способ и параметры крепления выработок. Накопленная в процессе проведения исследований база геомеханических данных обеспечивает возможность расчета альтернативных рейтингов, таких как MRMR, RM_i , GSI и др., без использования переходных уравнений.

Ключевые слова

рейтинговая классификация, RMR, Q , кимберлитовая трубка Удачная, телевьювер, трещиноватость, устойчивость массива, крепление

Для цитирования

Serebryakov E.V., Zaytsev I.A., Potaka A.A. Assessment of rating parameters of the rock mass conditions at Udachny underground mine deep levels. *Mining Science and Technology (Russia)*. 2024;9(3)206–220. <https://doi.org/10.17073/2500-0632-2023-12-192>

Introduction

Rating classifications in their current form were formed as a result of accumulation of huge practical experience of specialists, accumulated in the course of comprehensive study of rock masses in a variety of mining and geological conditions. Despite the widespread introduction of numerical simulation methods developed back in the 1970s, rating classifications do not lose their relevance even nowadays, being used as a means of short-term prediction of rock mass behavior. In the world mining practice the following geotechnical classifications are most widely used: Rock Mass Rating RMR [1, 2], rock mass quality index for underground mining Q (the Norwegian Geotechnical Institute Tunneling Quality Index), Barton [3, 4], mining rock mass rating MRMR [5, 6], geological strength index GSI [7, 8]. In their structure, the classifications take into account to some extent all the characteristics of a rock mass that can potentially reduce its strength compared to the initial strength of intact rock. These characteristics include: physical and mechanical properties of rocks, the degree of disturbance of a rock mass by structural defects (faults, joints, layering elements), frictional properties of the structural defects, as well as water content and stress-strain state of a rock mass.

Since the classifications are multi-component systems, they impose heavy demands on the scope and quality of primary data, which can be met by applying an integrated data collection system. For early stages of design, a high level of quality and promptness in their collection is provided by an integrated study, including televiewer logging combined with the results of non-oriented core logging [9, 10]. A similar

integrated study was applied in the collection of initial data for the calculation of RMR and Q rating parameters for deep levels of the Udachny underground mine. The main findings of the conducted research are presented in this paper.

Subject of research

The Udachnaya kimberlite pipe is one of the largest diamond deposits, which is currently being exploited by underground mining. The deposit is represented by two pillar-shaped ore bodies – Udachnaya-Zapadny (Zapadny Ore Body, ZOB) and Udachnaya-Vostochny (Vostochny Ore Body, VOB), composed of a typical formations for pipes of the Yakutsk diamondiferous province: porphyritic kimberlite of early generations and autolithic kimberlite breccia of the final stages of magmatism [11]. The rocks of the sedimentary complex hosting the pipe, as well as halogenic sediments occur as xenoliths. The sedimentary xenoliths predominantly occur within the ZOB, where they form so-called floating reefs [12]. The thick salt deposits within the kimberlite pipe are a unique feature of the structure of the Zapadny ore body. A possible process responsible for the presence of the salts in the pipe is the alteration of the deposit kimberlites by external saline groundwater [13]. The pipe is hosted by carbonate and carbonate-clayey rocks (limestones, dolomites, marls) of Early-Late Cambrian.

The open-pit development of the deposit was carried out until 2014. The depth of the open pit was 640 m, the bottom elevation was –320 masl. Stripping and mining of the reserves of the first stage below the pit bottom up to –580 masl is currently performed by

underground method by the system of induced block caving/sublevel caving. Preparation of the second stage reserves occurring between –580 and –1080 masl levels is carried out by drilling deep holes from underground mine workings.

Methodology of data collection and analysis

The procedure for determining the rating parameters of a rock mass is quite simple and boils down to assigning a certain score (from existing tabular forms) for one or another type of source data and performing the required mathematical operations with these values to obtain the desired values of the final rating. The RMR classification system was developed in 1973 by Bieniawski [1] and has undergone several modifications over the years, the latest of which was implemented in 2014 [14]. The RMR rating is calculated using the following formula:

$$RMR = J_{A1} + J_{A2} + J_{A3} + J_{A4} + J_{A5} + J_B, \quad (1)$$

where J_{A1} is rating of rock mass strength; J_{A2} is rating of rock mass quality; J_{A3} is rating of joint spacing in a rock mass; J_{A4} is rating of joints characteristics; J_{A5} is rating of rock mass water content; J_B is rating of joints orientation in relation to an excavation axis.

The J_{A4} rating characterizing a rock mass jointing is determined by the following expression:

$$J_{A4} = J_{A4/1} + J_{A4/2} + J_{A4/3} + J_{A4/4} + J_{A4/5}, \quad (2)$$

where $J_{A4/1}$ is joint roughness rating; $J_{A4/2}$ is joint length rating; $J_{A4/3}$ is joint aperture rating; $J_{A4/4}$ is joint mineral infilling rating; $J_{A4/5}$ is joint wall weathering rating.

The index of rock mass quality in underground mining Q (the Norwegian Geotechnical Institute Tunneling Quality Index) was proposed by Barton N., Lien R., Lunde J. in 1974 [3]. Q value ranges from 0.001 to 1000 on a logarithmic scale and is determined by the following formula:

$$Q = \frac{RQD}{J_n} \times \frac{J_r}{J_a} \times \frac{J_w}{SRF}, \quad (3)$$

where RQD – rock mass quality; J_n – number of joint systems; J_r – joint roughness; J_a – degree of joint wall alteration and mineral infilling (joint cohesion); J_w – rock mass water content; SRF – stress reduction factor.

The simplicity of the calculations for determining the rating parameters implies high requirements to the quality and completeness of the initial data. In the present work, the initial geological and structural data was collected by drilling 73 vertical and slightly inclined holes within the ore bodies with access to the host sediments (Fig. 1). The holes were drilled from –465 masl level. This drilling campaign was performed with complete sampling of non-oriented core.

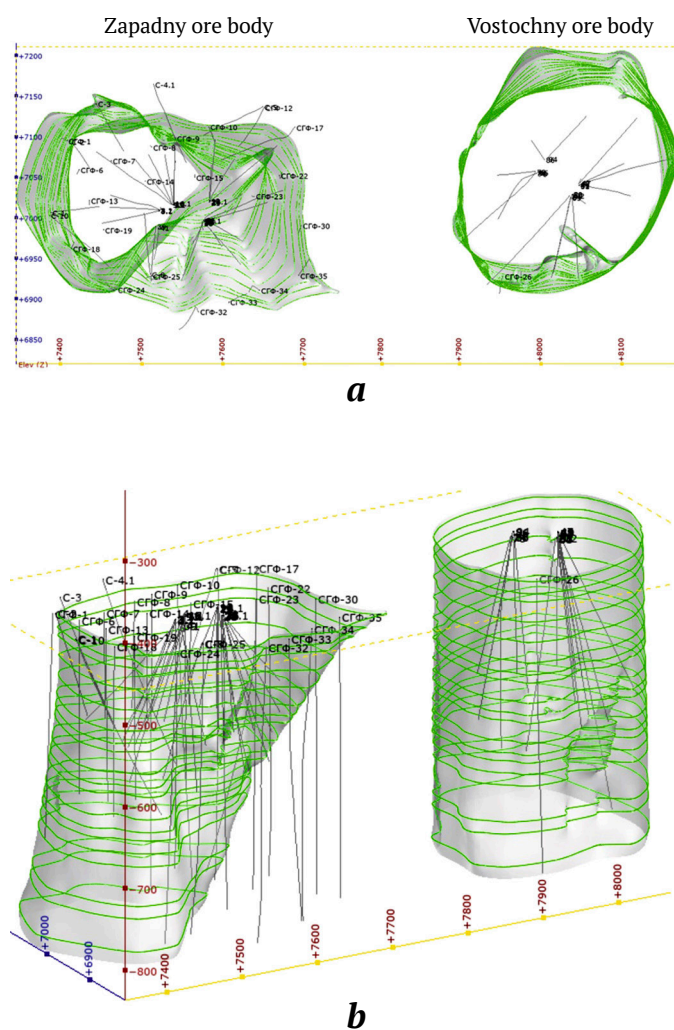


Fig. 1. Location of the holes used for televiewer logging: a – plan view; b – view from the south-west. Depth interval: –465 ... –850 masl

The strength properties of the kimberlite and host sediments rock mass were determined based on the results of laboratory tests of core samples. The samples were collected from the kimberlite, host sediments (dolomite, limestone), and the host sediment xenoliths. The tests were carried out in the Geotechnics laboratory of Yakutniiproalmaz Institute according to the methods set forth in GOST (GOST 21153.2–84 Rocks).

Structural disturbance of the rock mass was established by means of televiewing (acoustic) logging of geotechnical holes. Field geophysical works were carried out by specialists of Botuobinskaya exploration expedition using QL-40ABI probe jointly produced by Advanced Logic Technology and Mount Sopris Instruments.

The principle of an acoustic televiewer operation is continuous ultrasonic scanning of a hole walls

along its entire depth [15, 16]. The acoustic wave generated by the transmitter travels from the instrument to the contact with a rock, the reflected echo signal returns and, passing through the acoustic window, is picked up by the acoustic sensor (Fig. 2).

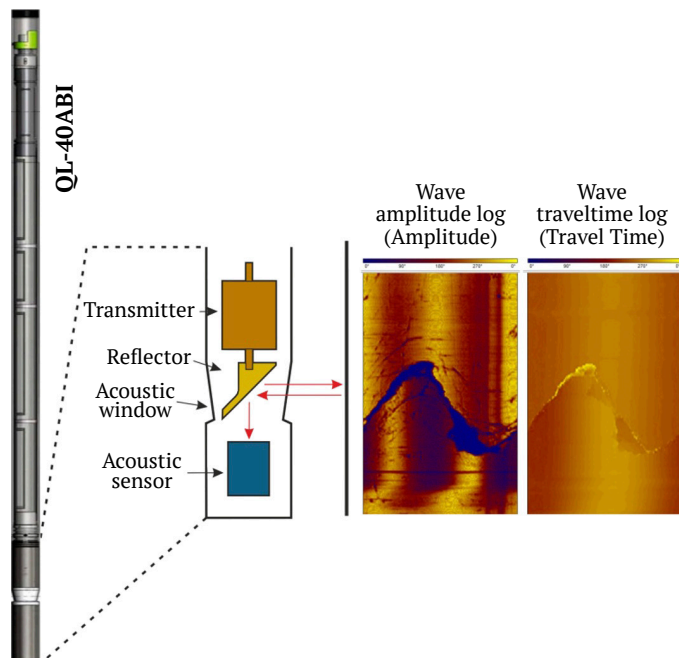


Fig. 2. Schematic diagram of an acoustic televiewer

The instrument records the amplitude of the acoustic wave and the time it takes for the emitted signal to travel from the acoustic window to a hole wall and back during the scanning process, and logs this data along the hole (see Fig. 2). Flat structures (joints, veins, layers, etc.) are converted into sinusoids (Figs. 2, 3) as a result of a hole cylinder scanning during log processing, and the amplitude of the sinusoids indicates the dip angle of a structure. The greater the amplitude, the steeper the dip angle. Due to the built-in high-precision positioning module, which includes a three-axis ferro-probe magnetometer and accelerometer, an oriented in space image is obtained, which makes it possible to automatically determine true dips and strikes of joints.

Interpretation of the results of the televiewer studies was carried out by the paper authors in the WellCAD program software¹. In addition to the logs themselves, the results of structural and photo logging of core were also included in the processing. Using the latter, the Core Image Cropper module generated a single log of photos positioned along a hole and georeferenced in depth. This allowed further comparison of logging results with drilling data and

¹ <https://www.alt.lu/products-wellcad/>

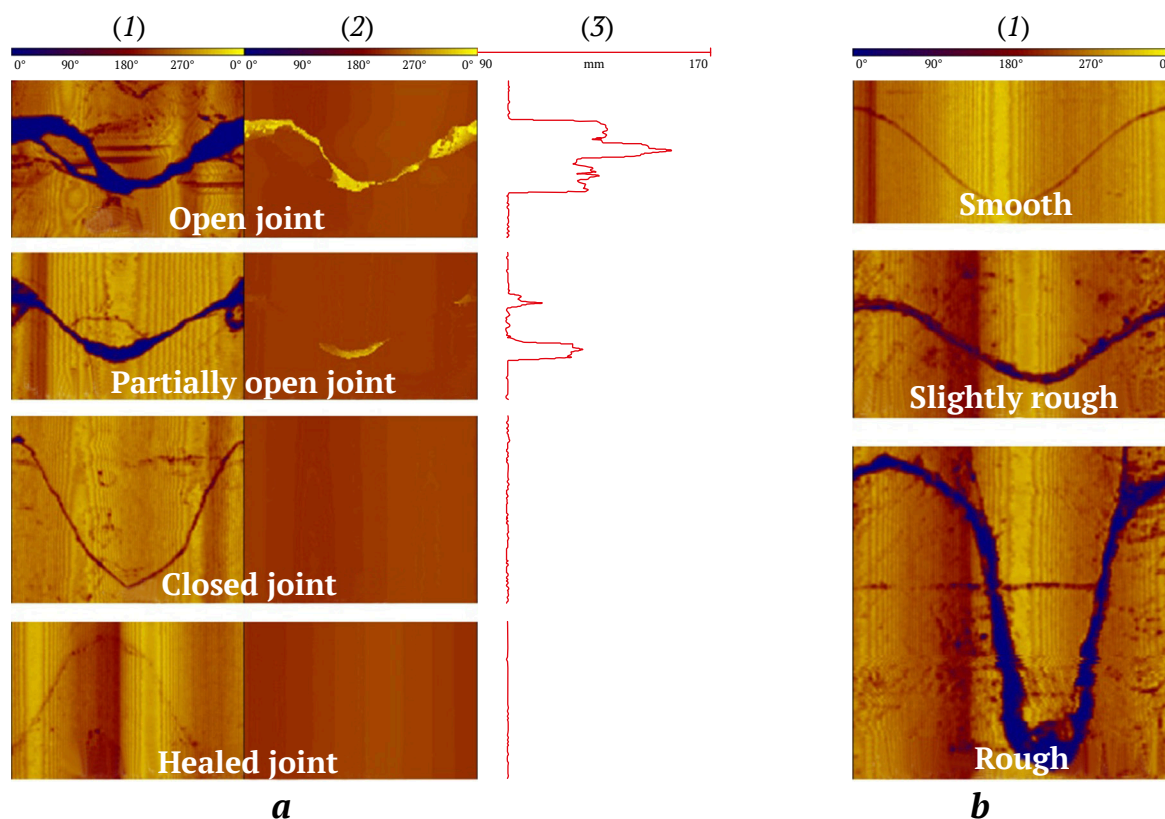


Fig. 3. Classification of joints by type (a) and wall roughness (b):

- 1 – display of the hole wall expressed in the amplitude of the acoustic wave (yellow color – high values, blue – low values);
- 2 – display of the hole wall expressed in the wave traveltime (yellow color – high values, blue – low values);
- 3 – log of the acoustic caliper

rejection of incorrectly recorded joints. The direct distinguishing and characterization of joints was performed in the ISI (Image & Structure Interpretation) module. Four main types of structures were defined and the first of these was an open joint. It is characterized by low wave amplitude and increased time for which the wave travels from the instrument to a hole wall and back, compared to an intact fragment [17]. In this case, on the acoustic caliper plot, a large anomaly will correspond to the area of an open joint (Fig. 3, a).

The second type of structures is a partially open joint. Visually in the amplitude field it is similar to a fully open one, but in the time field it does not have a single pronounced anomaly. The third type of structure, closed joints, is characterized by the absence of any anomalies in the wave traveltime log and caliper log. At that, such joints are displayed as thin lines of reduced amplitude values. Joint infilling also affects their visualization in logs. For instance, structures filled with solid minerals, due to the impedance difference, often have increased amplitude values, but at the same time are not distinguished on the time logs. Clay or gypsum infilling is expressed as low amplitude

anomalies. If it is partially washed out of the joints during drilling, the wave traveltime increases, which is reflected by the appearance of anomalies in the corresponding log.

The frictional properties of joints and primarily their wall roughness can be determined from amplitude images [18, 19]. At the same time, they can be determined most accurately and reliably for smooth, slightly rough, and roughly rough joints [17, 20] (Fig. 3, b). In order to validate the frictional properties of joints and their further subdivision, structural core logging was used [21]. In addition to roughness, it is used to determine the types and thickness of mineral infilling, which are difficult to establish reliably through hole logging.

Numerical assessment of the degree of a rock mass disturbance by joint was carried out by determining the RQD parameter and the number of joints per linear meter of an investigated hole. For this purpose, the WellCAD program software has appropriate modules that use the joint data (depth, dip and strike) extracted in the process of log interpretation for calculation (Fig. 4).

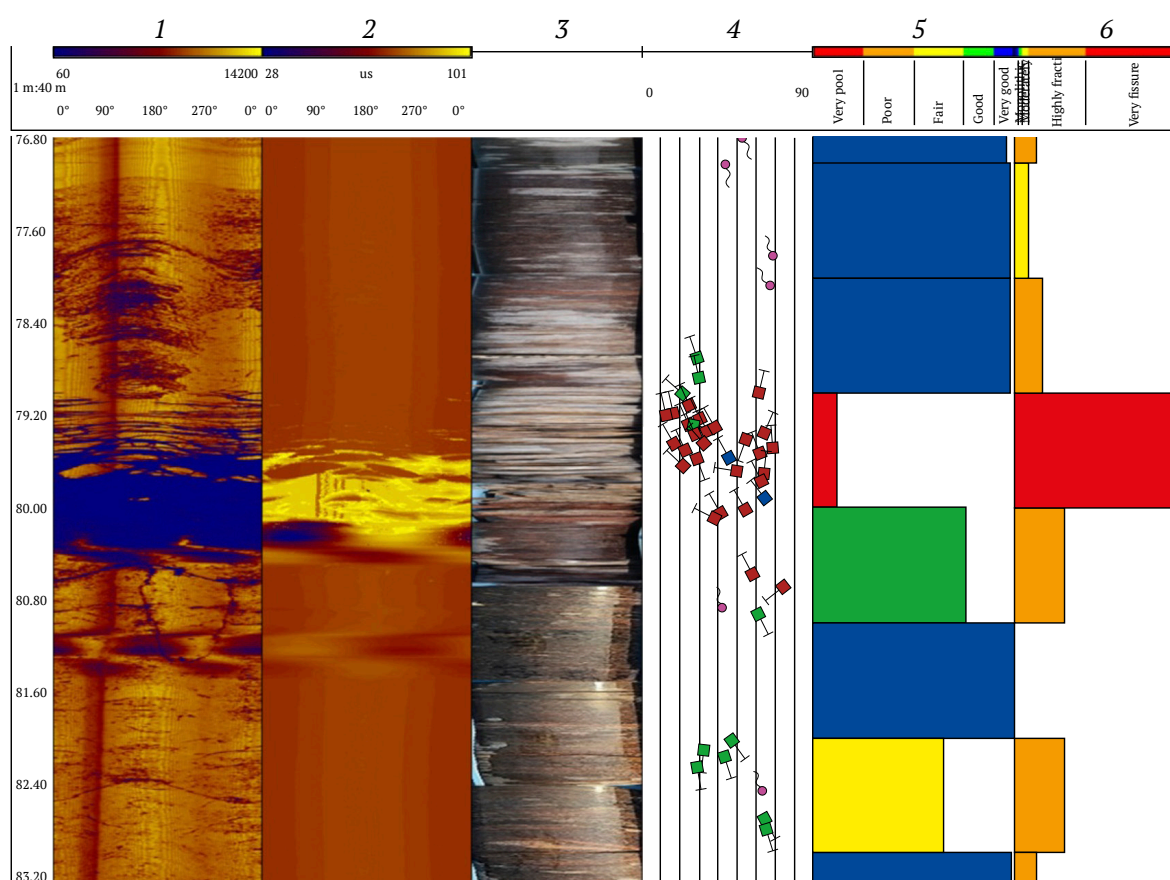


Fig. 4. Calculation of quantitative parameters of structural disturbance of the mass:

- 1 – hole wall mapping expressed in acoustic wave amplitude (yellow – high values, blue – low values);
- 2 – hole wall mapping expressed in wave traveltime (yellow – high values, blue – low values); 3 – core photo;
- 4 – “tadpole” joint plot; 5 – joint frequency per linear meter; 6 – RQD. Vertical scale 1 : 40

Findings

The rock mass of the studied deposit consists of three lithologic domains of the first order – the host terrigenous-carbonate sediments and the diatreme kimberlite bodies themselves. Within the distinguished large units, the evaluation of rating parameters from hole data was performed for individual geotechnical intervals representing sections of a rock mass with continuous lithology, physical and mechanical properties, and structural features. As a rule, lithology and structural features are confidently determined during geotechnical core logging, but the distinguishing intervals of similar physical and mechanical properties of rocks is often a problem, because even within the boundaries of one lithology there can be a wide variation of strength properties. To solve the problem, this research utilizes the property of rocks to reflect acoustic waves. The extent of this reflection is directly related to the physical properties and condition of a hole surface. A smooth wall formed in compact rocks reflects more energy and thus has a higher amplitude than a rough

wall. The reflectivity of walls formed in hard and/or monolithic rock is higher than those intersected in soft or intensely jointed rock. The rocks with a large proportion of clay component are characterized by the smallest amplitudes due to energy absorption. The same applies to joints, especially open joints or joints with soft infilling. In the amplitude logs they are shown in blue shades according to the adopted color scheme (see Fig. 3). An example of selecting intervals based on the amplitude of an acoustic wave is shown in Fig. 5.

Fig. 5, *a* presents a fairly clear dependence of the wave amplitude (columns 1 and 3) on the degree of joint disturbance of the rock mass, expressed through the number of joints per linear meter of a hole (column 4). The most structurally disturbed areas with high values of joint frequency index (intervals 4 and 6) are characterized by low amplitude values. Fig. 5, *b*, in contrast, shows a relatively monolithic, virtually joint-free fragment. In the 140–154 m interval, the acoustic wave amplitude (columns 1 and 3) clearly shows an area with significantly higher

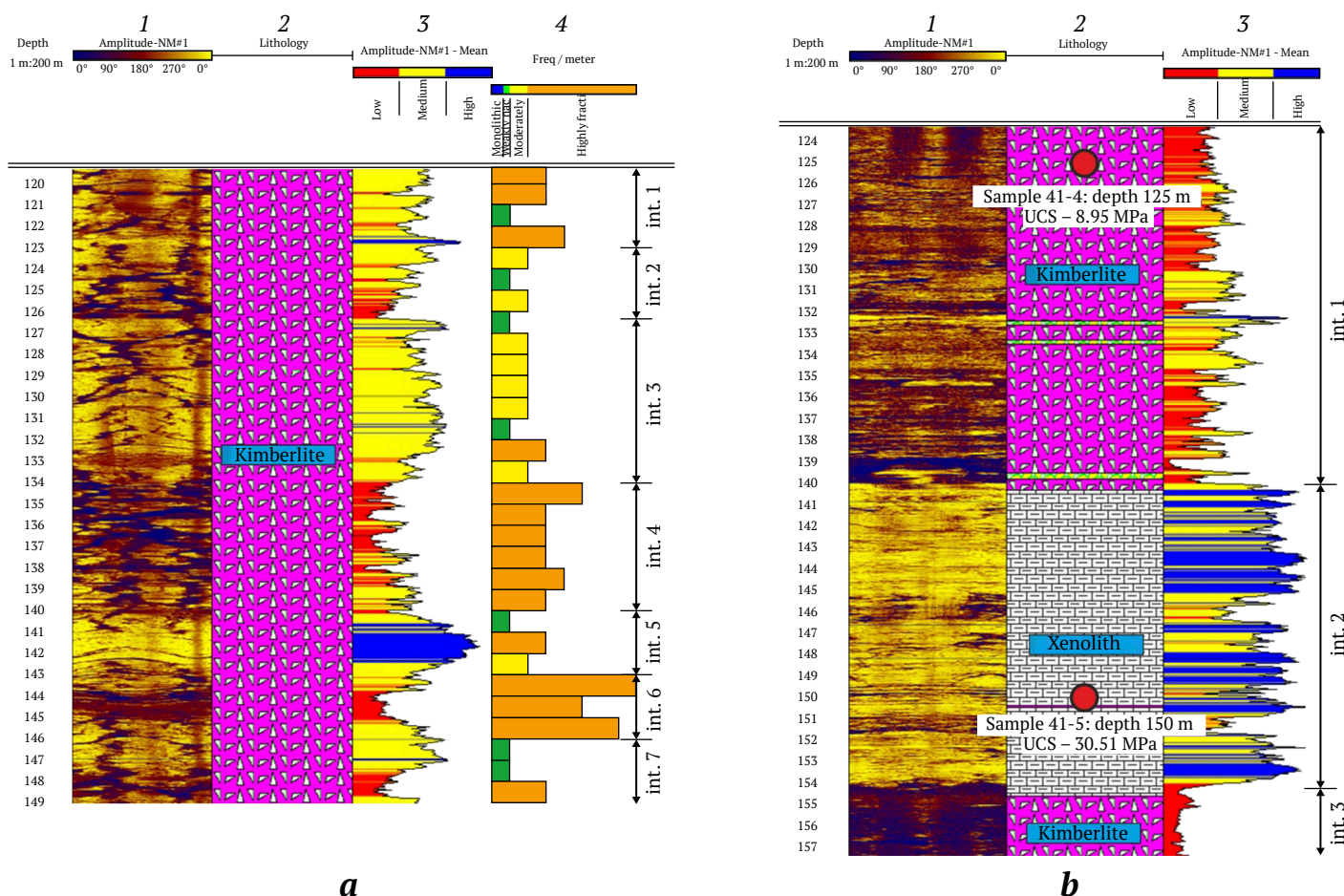


Fig. 5. Example of geotechnical intervals selection by acoustic wave amplitude:

1 – mapping of hole wall expressed in acoustic wave amplitude (yellow color – high values, blue – low values); 2 – lithology column;

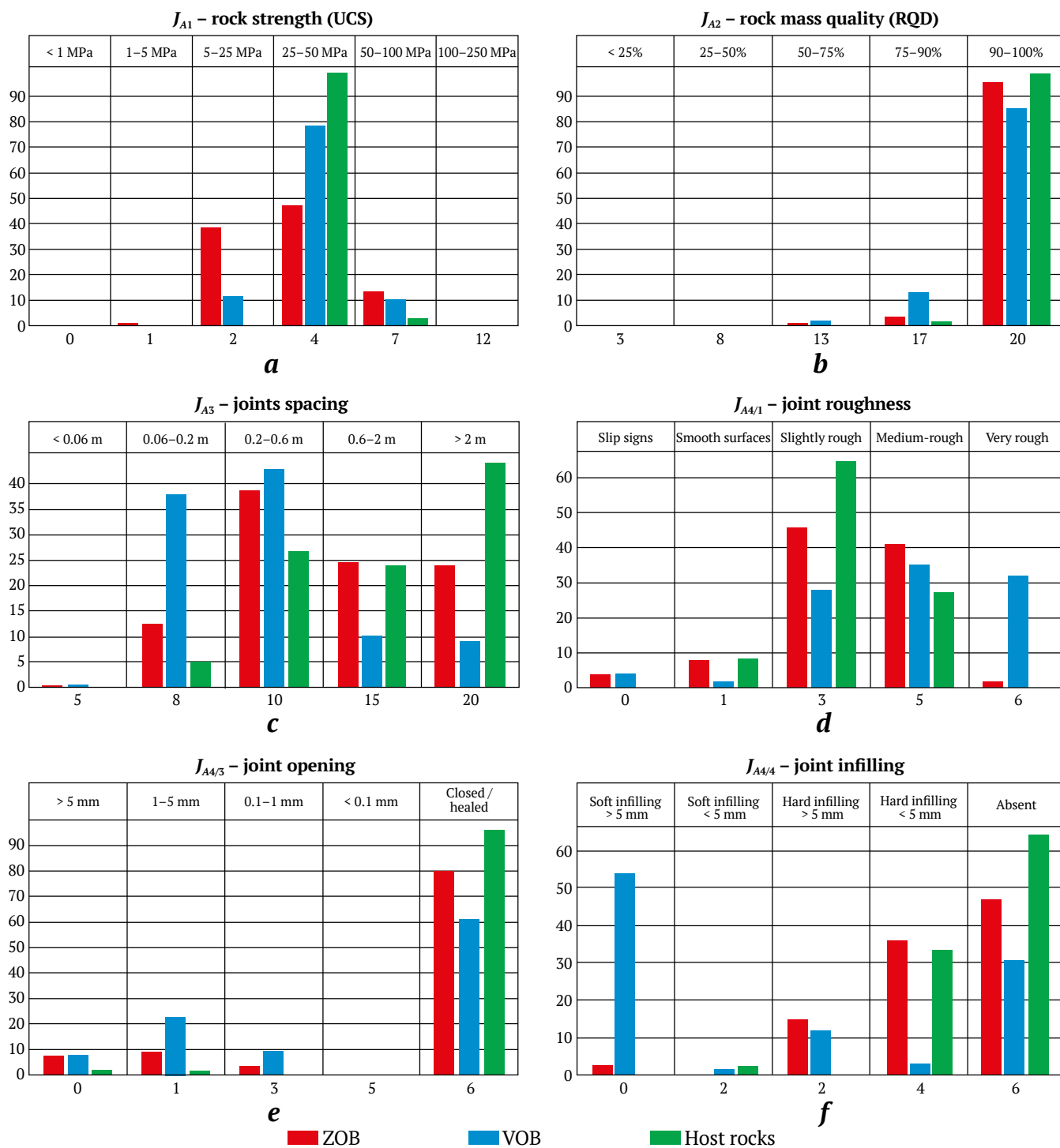
3 – averaged acoustic wave amplitude calculated for one turn of the transmitter; 4 – joint frequency per linear meter.

Vertical scale 1 : 200



values, which corresponds to the sedimentary rock xenolith in the matrix rock mass of the kimberlite breccia recorded by the results of geological logging of the hole core (column 2). At 125 and 150 m, samples were collected from kimberlite and xenolith

showing uniaxial compressive strength (UCS) values of 8.95 and 30.51 MPa, respectively, indicating that there is a relationship between rock strength properties and acoustic wave amplitude, which was revealed in a number of studies [22, 23].



Parameter	Value
$J_{A4/2}$ – joint length	2 (3–10 m)
$J_{A4/5}$ – weathered joint walls	6 (unweathered)
J_{A5} – water inflow	4 (drip)
J_B – orientation of joints to a hole axis	–5 (moderately favorable)

Fig. 6. Histograms of distribution of input parameters for RMR rating calculation

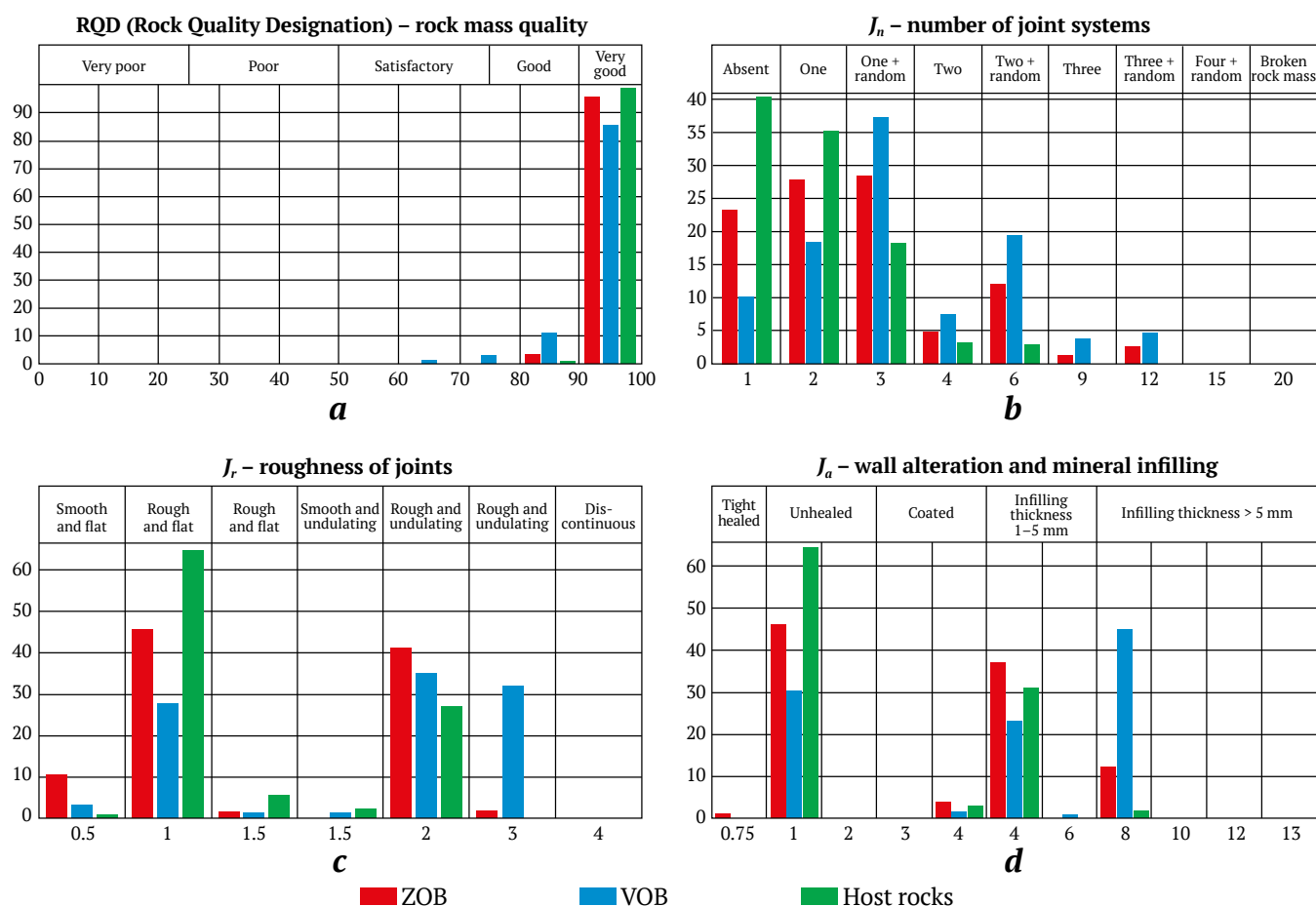


A total of 4,636 geotechnical intervals were identified for 73 holes. The length of an interval ranges from one meter for areas with complicated structures to six meters for those with relatively simple structures. The results of estimation of each input parameter separately for the selected lithologic domains are presented in the form of histograms in Figs. 6 и 7.

For the rocks hosting the pipe, uniaxial compressive strength ranges 28.14–71.73 MPa with a mean value of 41.05 MPa (Fig. 6, *a*). The highest degree of variability in strength properties is characteristic of kimberlite breccia of the ZOB and VOB (including porphyritic kimberlite and autolithic breccia). The measured strength values range 2.15 to 119.48 MPa with a mean value of 32.54 MPa. The large variation of the uniaxial compression strength values of kimberlites is explained by the fact that their physico-mechanical and strength properties depend on their mineralogical and chemical composition and particle size distribution. These characteristics vary considerably among the kimberlites, both in area and depth. In addition, the kimberlites are subject to hypergene alter-

ation, which leads to changes in their mineral composition and, consequently, to variations in strength characteristics [24]. In general, the obtained values of strength characteristics correspond to rock of low, moderate, medium, and high strength according to the existing classification [25]. At the same time, the overwhelming volume of the ore bodies is occupied by kimberlites of low and moderate strength.

RQD values vary widely, from 50 up to 100% (Fig. 6, *b*, Fig. 7, *a*), with average values with low coefficient of variation exceeding 90%, which corresponds to very good quality of rock masses for all lithologies [26]. It should be noted that the final RQD value is significantly affected by the quality of drilling, the orientation of a hole with respect to joints, and differences in joint spacing. For example, RQD = 0 when joint spacing is 100 mm or less, while RQD = 100 when the spacing is 110 mm or more. Another disadvantage is that RQD does not provide information on core fragments <10 cm, i.e., no weight is given to whether rejected fragments up to 10 cm in length are loose or compact (hard) rock.



Parameter	Value
J_w – water inflow	0.66 (medium)
SRF – stress reduction factor	2.5 (low stress, single tectonic zones)

Fig. 7. Histograms of distribution of input parameters for calculating Q rating

Joint spacing was defined as the inverse of the joint modulus (number of joints per unit length (linear meter)). For correct estimation of this parameter, the orientation of a hole with respect to the joints in the rock mass is important, as demonstrated in Fig. 8, which shows three logged intervals disturbed by joints with the same distance between them equal to 0.1 m.

In the first interval (50–51 m), within which joints are located perpendicular to the core axis, joint modulus is equal to 10 joints/lin. m. For the second interval (51–52 m) with joints located at an angle of 45° to the axis, a modulus equal to 7 joints/lin. m was obtained. Finally, for the third interval (52–53 m) with an angle between the core axis and the joints of 20° , the modulus is 4 joints/lin. m. The true joint modulus was obtained only for the first interval, while for the other two intervals the modulus proved to be underestimated. In this case, the example considers only one joint system, while in a real rock mass, as a rule, two or more systems and several random (unsystematic) joints are developed, which affect the final value of the modulus. That is why, Terzaghi weighting was used in the calculation of this parameter [27]. It proportionally increases the “weight” of joints in a sample set (weighted average of each joint in a set) that are located at an angle other than right angle to a hole axis. The more acute the angle between a joint and a hole axis, the greater the value of the Terzaghi coefficient.

The rock mass of sediments hosting the pipe can be classified as practically monolithic (jointing class I according to SNIP II-94–80) with the average joint spacing more than 1.5 m (Fig. 6, c). For the rock masses of kimberlite bodies, there is almost a threefold excess of the joint frequency index in the VOB rock mass, indicating that it is significantly more disturbed. This confirms earlier conclusions based on the results of structural logging of the mine workings walls [28]. The kimberlites are medium-jointed rocks (class III,

0.5–1 m joint spacing), while the VOB kimberlites are highly jointed (class IV, 0.1–0.5 m joint spacing).

Lower values of joint frequency are observed for halogenic deposits, which are explained by their rheological properties, namely increased plasticity, which compensates for the applied tectonic and lithostatic loads. The xenoliths within kimberlite bodies are characterized by higher jointing than the host rock strata. In all likelihood, this is due to the processes of additional disturbance during the intrusion of kimberlite melt.

Estimating the true extent of joints is a very non-trivial task, especially from hole data, due to their three-dimensional nature, limited manifestation, and high variability of parameters. This parameter can be most accurately obtained by visual tracing of disturbances along the walls of outcrops or mine workings. However, the size of mine workings is often smaller than the extent of joints/faults, making it impossible to accurately determine their length. Statistical analysis of joint measurements performed within the underground mine workings [28] showed that joints up to three meters long predominate in the rock mass. It should be noted that this figure is largely approximate, as the estimate of the extent of larger joints and local faults is limited by the cross-section of mine workings (about 5 m). Taking into account the data obtained during structural studies in the Udachny open pit, the average joint length is assumed to be 3–10 m as a design average.

Based on the results of core logging, it was found that in the rock masses of both host sediments and kimberlite bodies rough joints of flat, undulating, and stepped configurations significantly dominate (see Fig. 6, d, Fig. 7). Moreover, joints in the kimberlite are more often characterized by greater roughness than joints in the sedimentary rocks. Roughness of joints without infilling increases the friction angle across them and hence increases the shear resistance in the plane of the defect. Also within the rock mass and

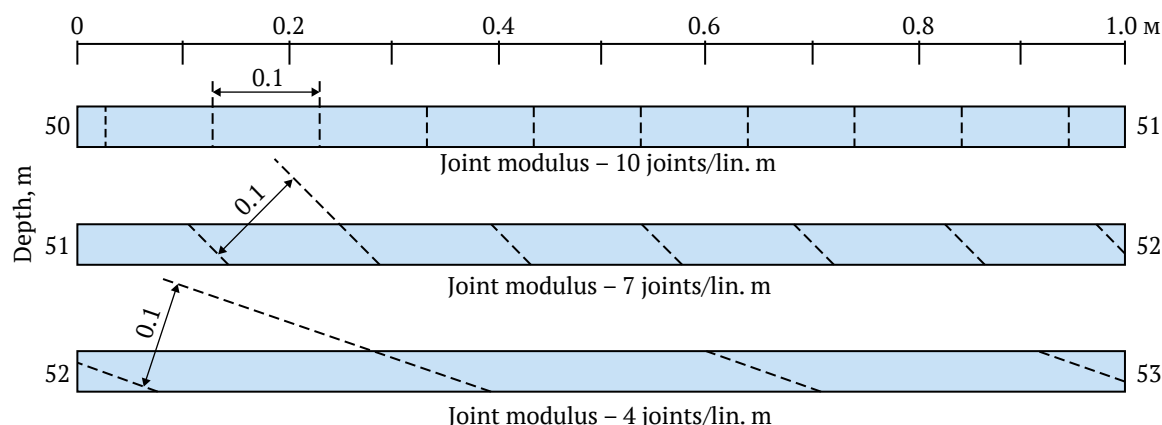


Fig. 8. Example of joint modulus calculation based on a hole core logging data (depth increases from left to right)



especially in the endo/exocontact zone, joints with slickensides were noted. The presence of displacement signs on the joint planes, such as slickensides and slip grooves, having dip along the dip of the joint planes significantly reduces the shear resistance.

At low degrees of roughness, the greatest influence on joint shear strength is exerted by the strength properties of the mineral infilling. Most of the joints in the kimberlite of the Zapadny ore body and the host sediments have no mineral infilling (see Fig. 6, e). The main joint infilling is carbonates with subordinate importance of sulfates and halogenic rocks. Joints with sulphide manifestations are significantly more common in ZOB, while in VOB a rather large number of joints demonstrates ferruginization of the walls. The main joint infilling in the kimberlite joints of the Vostochny ore body is rock salt. For the host rocks, salt-filled joints are not widespread, although a quarter of all joints recorded in the argillaceous limestone at the contact with the VOB are salt-filled. Clay and quartz are also noted in single joints. The latter is more often found in the form of druses and vugs and is associated with the hydrothermal stage of kimberlite alteration [29]. The vast majority of the filled joints are 1 to 5 mm thick, less frequently 5 to 10 mm thick. The greatest thickness is characteristic of joints filled with salt and calcite.

Based on the results of the analysis of interval jointing diagrams, it was found that the studied rock mass is characterized by the prevalence of one, less often two joint systems complicated by single unsystematic (random) joints (see Fig. 7, b). This is due to low tectonic activity in the deposit location area (central part of the Siberian Platform) and the absence of large high-rank faults. The largest number of joint systems is recorded in the exo-endocontact zone, which demonstrates increased disturbance due to thermodynamic effects from the intrusion of several portions of kimberlite melt.

The main source of water inflow to the deposit is the Middle Cambrian Aquifer Complex (MCAC) with two aquifers with enhanced filtration properties [12]. The MCAC groundwater is highly mineralized, gas-saturated, confined to limestone-dolomite sediments of the Middle-Lower Cambrian [30]. The va-

lues of formation pressures vary from 4.5 to 15.6 MPa, and the water inflows range from 0.6 to 228 l/min, which suggests medium level of water inflow into underground mine workings at deep levels of the mine. Consequently, the parameter J_{A5} from the RMR system is assumed to be 4, which corresponds to drip, and the parameter J_w of the Q system is assumed to be 0.66 – the water inflow level is medium.

The data on the stresses acting in the rock mass, which can be used to estimate the SRF factor in the calculation of the Q rating, are obtained from the results of investigations by the method of measuring hydraulic fracturing. In terms of effective stresses, the rock mass can be conditionally categorized as class B (strong rocks with stress (pressure) problems)². In this case, the SRF factor is estimated by the ratio σ_c/σ_1 , where σ_c is the uniaxial compressive strength; σ_1 is the maximum stress (Table 1).

The obtained high SRF values indicate potentially rockburst hazardous conditions of the deposit development in the studied depth interval. At the same time, according to the mine's geological service specialists, no dynamic manifestations of rock pressure (“crackle” in the rock mass, intensive roof breaks, “flaking” of rocks on the contour and in pillars, rock bursts) were observed during driving development workings at –480, –580 (–630) levels. Analysis of photologging of geotechnical hole cores showed the absence of large volumes of core diking, which is characteristic of brittle-elastic rocks under high-stress conditions, which also indicates a low potential for rockburst hazard of the rock mass at the investigated depths. The contradiction between the calculated data and the behavior of the rock mass in practice can be explained by the fact that as the necessary conditions for the rockburst manifestations, in addition to exceeding the compressive strength of rocks by the acting loads, it is required the rate of loading of rocks to exceed the rate of development of plastic or elastic-viscous deformations [31]. In absence of direct data confirming the presence of high stresses in the rock mass, a SRF value of 2.5 was adopted as a design value.

² Using the Q-system. Rock mass classification and support design. NGI. 2015. 56 p.

Table 1

Estimation of SRF (stress reduction factor)

Level	Rocks	σ_1 , MPa	σ_c , MPa	σ_c/σ_1	SRF
–465	Kimberlite (ZOB)	22.75	2.15–119.48	0.09–5.25	0.5–400
–465	Kimberlite (VOB)	20*	3.89–98.11	0.19–4.9	5–400
–480	Host rocks	26.8	27.9–71.3	1.04–2.66	50–400
–580	Host rocks	31.35	27.9–71.3	0.89–2.27	50–400

* no in-situ measurements of stress in VOB were performed

Findings Discussion

Application of the approach described above to the collection and analysis of mining and geological information on the studied deposit allowed to calculate RMR and Q ratings and on their basis to perform categorization of the rock mass condition (Fig. 9).

According to the classification of Bieniawski [2] the considered lithologic domains include areas of poor, satisfactory, and good condition, which corresponds to IV, III, and II categories of rock masses in terms of stability. According to the averaged values, the ZOB and VOB kimberlites belong to the third category, while the host sediments have a intermediate value between the second and third categories. The average stable condition time ranges from 6 months (for spans up to 8 m) to 10 hours (for spans up to 2.5 m).

The Q rating is characterized by a range of values from 0.18 to 105.6. This variation in minimum and maximum values is due to the fact that the Barton's classification uses a logarithmic scale with a spread of 10^6 . Based on median values, the VOB kimberlites refer to class D with poor rock mass condition. Most of the ZOB rock masses can be categorized as Class C with a medium condition. The rocks that host the pipe

predominantly fall into Class C with a medium rock mass condition.

The obtained estimated values of rating parameters are preliminary and rather conservative, requiring validation in the course of mining operations. This is due to the fact that the collection of geological and geotechnical information necessary for the calculation in the required volume and with the required level of data reliability is associated with numerous limitations. Thus, some of the input components for calculating the ratings were estimated from indirect data and assumed to be constants for the whole rock mass. This concerns the length of joints, water content of rock mass at the design depths, orientation of joints in relation to the design workings, and stresses acting in the rock mass. In the absence of the possibility of accurate estimation of missing parameters, the use of two or more classification systems in the design of deposit development methods provides a more complete and comprehensive picture of the geotechnical conditions of a rock mass and potential risks in its development, as the authors of the rating systems themselves say [2, 35].

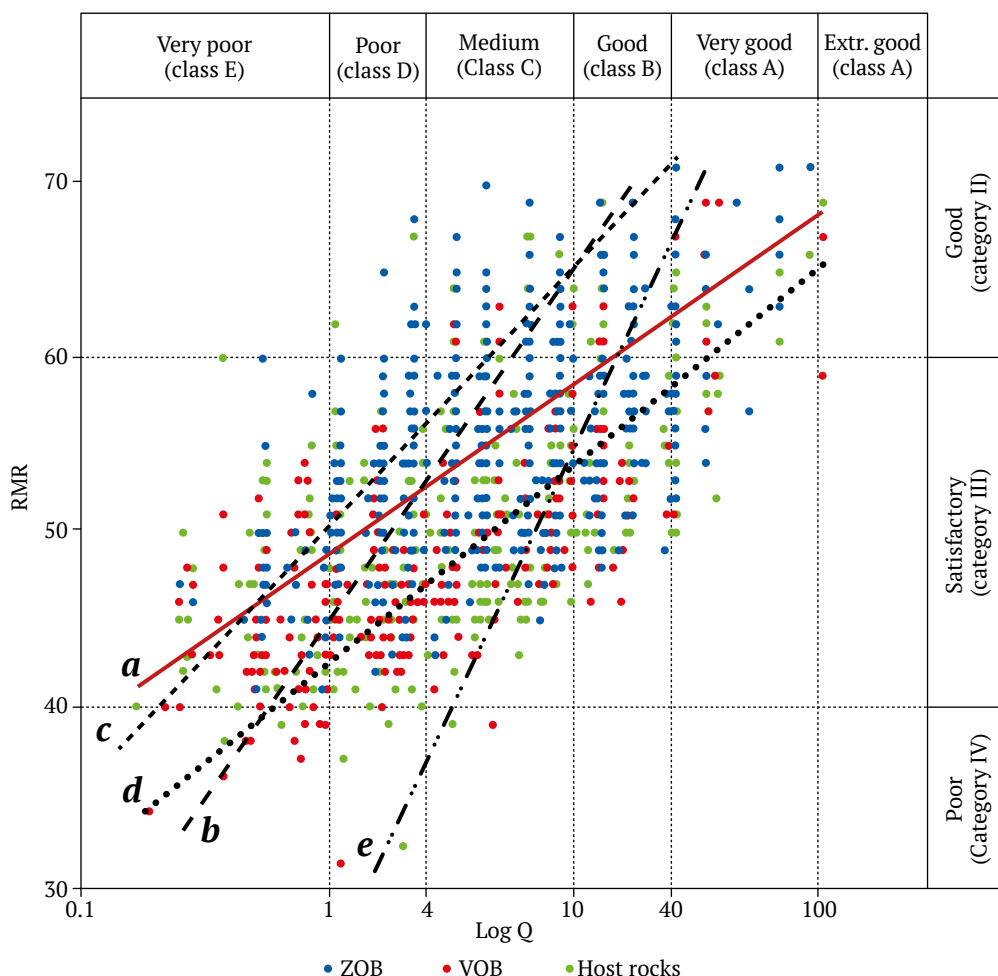


Fig. 9. Scatter diagram of RMR and Q rating scores: a – this study results, b – [2], c – [32], d – [33], e – [34]

Although there are many similarities between the RMR and Q classification systems, the different “sensitivity” of the parameters used and their structure result in the fact that the same rock mass areas characterized by different classifications can have significant differences in the final values, as shown in the scatter correlation diagram (see Fig. 9). As can be seen, for $Q = 1$ RMR varies over a wide range from 32 to 62, and for a RMR value of 50, the Q rating varies from 0.5 to 45. This moderate correlation is due to several reasons. The Q rating does not directly take into account the strength characteristic of rocks. Although an attempt was made in [36] to introduce uniaxial compression strength into the scheme for calculating the Q_c rating, this correction was not widely used. The RMR system does not take into account overstress conditions (rock-bursts) and is designed for applications with stresses up to 25 MPa, while for the Q system the active stresses in the rock mass are determined by the ratio of J_w and SRF values. Besides, the Q and RMR systems characterize fault zones differently. In the RMR system, no special parameter is used, while in the Q system the influence of faults is taken into account indirectly through the SRF parameter. In addition, the correlation depends on the type and structure of a rock mass, as demonstrated

in numerous works [2, 32–34]. Some of the correlation curves are shown in Fig. 9. Since the rock mass under consideration is a combined rock mass, i.e., consisting of a layered and a non-layered components, the influence of the rock mass structure will be high.

The RMR and Q systems work best in a blocky rock mass, so its degree of disturbance, expressed through the RQD, or joint spacing, is often the most important input parameter on which the resulting value of both ratings depends. Given the previously mentioned shortcomings of the RQD parameter as a measure of structural disturbance of a rock mass, the potential error that this parameter introduces into the resulting ratings should be taken into account and evaluated.

Despite the above-mentioned discrepancies, each of the systems allows to characterize the geotechnical condition of a rock mass, to determine the category of a rock mass in terms of stability, the time of stable conditions, the type of driving and the system of working support. The choice of the basic classification system should be made based on the tasks to be solved and the set of input data. In practice, the Q system using the nomogram developed by the Norwegian Geotechnical Institute (Fig. 10) is more popular in the selection of systems of underground mine support.

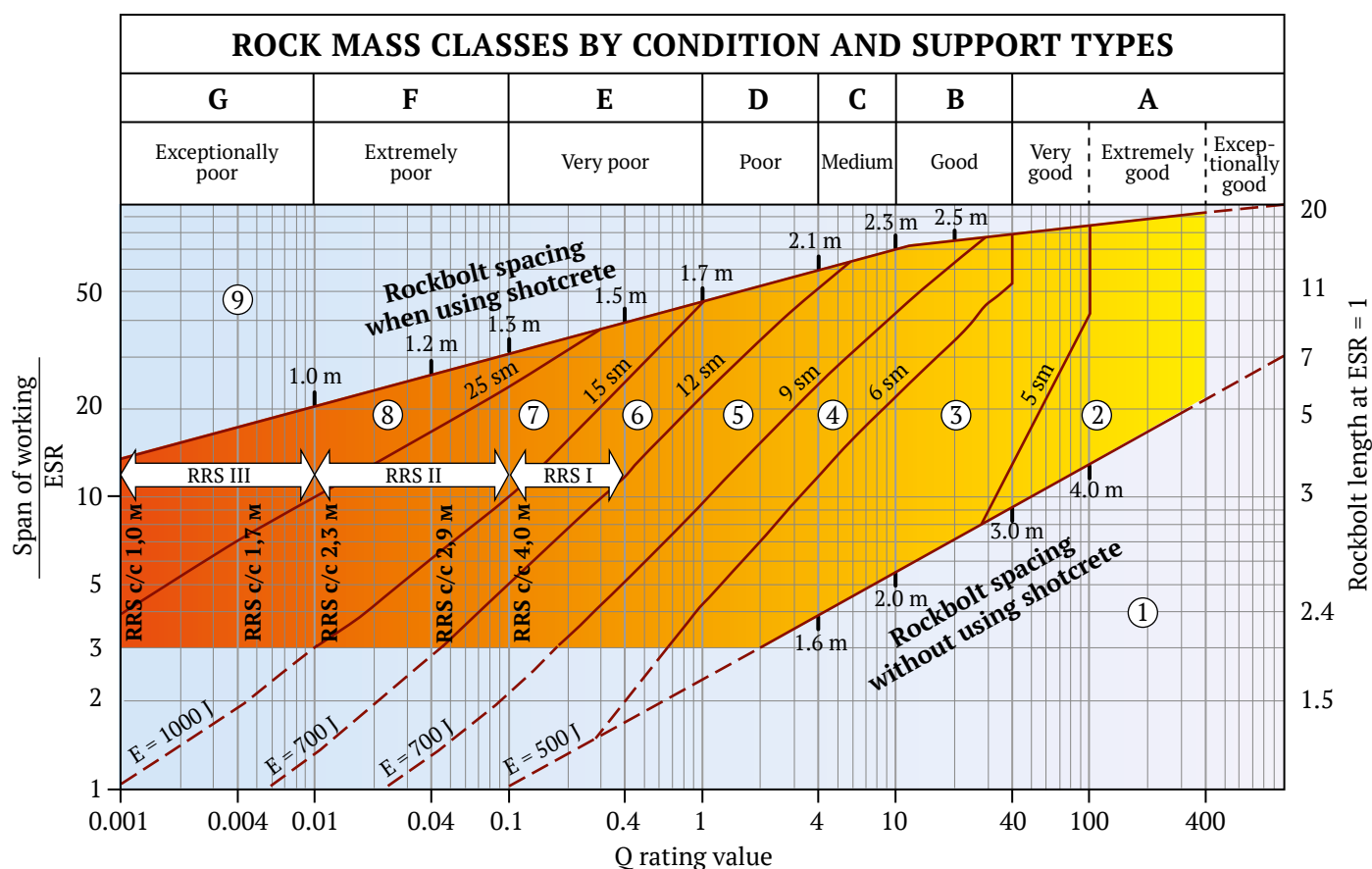


Fig. 10. Nomogram for selection of workings support parameters based on Q rating
Source: Using the Q-system. Rock mass classification and support design. NGI. 2015. 56 p.



Evaluation of the optimum characteristics of the support is carried out with the use of additional parameters: “equivalent dimension” (ED) and “Excavation Support Ratio” ESR [3]. For the Udachny mine, two options of mine workings (excavations) were considered: permanent workings with ESR equal to 1.6, as well as face-ends for which ESR is equal to 1. The span of excavations was taken as 5 m, hence the span/ESR ratio (vertical scale on the left in Fig. 10) for permanent excavations is 3.1, for face-ends, 5. Due to the obtained range of Q rating values in the nomogram (Fig. 10), the following support recommendations were proposed. Four types of support were recommended for permanent excavations. Local (scattered) support with reinforced concrete rockbolts of 2 m long with rockbolt spacing of 1–4 m for areas with very strong, strong, and medium rock mass according to the stability categories (classes A, B, and C). Systematic rock bolting with similar rockbolt parameters in combination with disperse-reinforced shotcrete 5–6 cm thick for D class rocks. For areas of very weak rocks (fault zones, areas of contact alteration) it is recommended to reduce the distance between rockbolts with a simultaneous increasing thickness of the layer of shotcrete to 9–12 cm. For mine workings face-ends, similar parameters of support are defined depending on the category of a rock mass, but it is recommended to increase the length of rockbolts up to 2.5 m, as well as a sequential decrease in the rockbolt spacing and increasing the thickness of shotcrete layer as the category of stability of a rock mass declines.

Conclusion

The application of a comprehensive data collection system including acoustic televiewer hole logging and geological and structural logging of non-oriented core, as well as the use of the results of laboratory studies of physical and mechanical properties of rocks, in-situ measurements of stress-strain state and water inflow allowed to calculate the rating parameters of rock mass condition according to RMR and Q classification systems for the deep levels of the Udachny underground mine. Based on them, the ore bodies and host sediments rock masses were assessed for stability (classes/categories were assigned), and the optimal method and parameters of mine workings support were determined. A database of geotechnical data has been accumulated, which can be used to calculate other ratings such as MRMR [5], RMI [37], GSI [7], etc., without transient equations, if necessary.

It should be noted that the calculation of the ratings is an iterative procedure that is repeated as new data becomes available and lasts for the entire period of a mine’s operation, and the studies obtained at the current stage require updating in the course of mining.

Rating classifications are an important tool for assessing a rock mass condition and are largely used as a means of short-term prediction of its behavior. The empirical basis of rating systems introduces a limitation to their use as key data sources in engineering decision making, especially in complicated mining and geologic environments. Integration of the ratings with analytical and numerical simulation methods looks like the most promising approach to account for the uncertainty and variability of rock mass properties in the design and operation of underground mines.

References

1. Bieniawski Z.T. Engineering classification of jointed rock masses. *Civil Engineer in South Africa*. 1973;15(12):335–344.
2. Bieniawski Z.T. *Engineering rock mass classifications*. New York: Wiley;1989. 251 p.
3. Barton N., Lien R., Lunde J. Engineering classification of rock masses for the design of rock support. *Rock Mechanics*. 1974;6:189–236. <https://doi.org/10.1007/BF01239496>
4. Barton N. Some new Q-value correlations to assist in site characterization and tunnel design. *International Journal of Rock Mechanics and Mining Sciences*. 2002;39:185–216.
5. Laubscher D.H. Geomechanics classification system for the rating of rock mass in mine design. *Journal of the Southern African Institute of Mining and Metallurgy*. 1990;90(10):257–273. [https://doi.org/10.1016/0148-9062\(91\)90830-F](https://doi.org/10.1016/0148-9062(91)90830-F)
6. Laubscher D.H., Jakubec J. The MRMR Rock mass classification for jointed rock masses. In: Hustrulid W.A., Bullock R.L. (Eds.) *Underground Mining Methods: Engineering Fundamentals and International Case Histories*. Littleton, Colorado: SME; 2001. Pp. 475–481.
7. Hoek E. Strength of rock and rock masses. *ISRM News Journal*. 1994;2(2):4–16.
8. Hoek E., Brown E.T. The Hoek–Brown failure criterion and GSI – 2018 edition. *Journal of Rock Mechanics and Geotechnical Engineering*. 2019;11(3):445–463. <https://doi.org/10.1016/j.jrmge.2018.08.001>
9. Gwynn X., Brown M.C., Mohr P.J. Combined use of traditional core logging and televiewer imaging for practical geotechnical data collection. In: Dight P.M. (ed.) *Slope Stability 2013: Proceedings of the 2013*



- International Symposium on Slope Stability in Open Pit Mining and Civil Engineering*. Perth: Australian Centre for Geomechanics; 2013. Pp. 261–272. https://doi.org/10.36487/ACG_rep/1308_13_Mohr
10. Serebriakov E.V., Gladkov A.S., Gapfarov T.D. Modern methods of data collection for structural damage assessment in rock mass: Review. *Mining Informational and Analytical Bulletin*. 2023;(9):160–177. (In Russ.) https://doi.org/10.25018/0236_1493_2023_9_0_160
 11. Kostrovitsky S.I., Spezičius Z.V., Yakovlev D.A. et al. *Atlas of primary diamond deposits of the Yakutsk kimberlite province*. Mirny: MGT LLC Publ.; 2015. 480 p. (In Russ.)
 12. Kolganov V.F., Akishev A.N., Drozdov A.V. *Mining and geologic features of primary diamond deposits of Yakutia*. Mirny: ALROSA, Yakutniproalmaz Institute Publ.; 2013. 568 p. (In Russ.)
 13. Kopylova M.G., Kostrovitsky S.I., Egorov K.N. Salts in southern Yakutian kimberlites and the problem of primary alkali kimberlite melts. *Earth-Science Reviews*. 2013;119:1–16. <https://doi.org/10.1016/j.earscirev.2013.01.007>
 14. Celada B., Tardáguila I., Varona P. et al. Innovating tunnel design by an improved experience-based RMR system. In: *Proceedings of the World Tunnel Congress 2014 – Tunnels for a Better Life*. Foz do Iguaçu, Brazil, 9–15 May 2014. PP. 1–9.
 15. Peyras L., Rivard P., Breul P. et al. Characterization of rock discontinuity openings using acoustic wave amplitude – Application to a metamorphic rock mass. *Engineering Geology*. 2015;193:402–411. <https://doi.org/10.1016/j.enggeo.2015.05.014>
 16. McKenna G.T.C., Roberts-Kelly S.L. Televiwer imaging of boreholes; benefits and considerations for interpretation in the absence of physical rock core. In: Lehane B., Acosta-Martinez H.E., Kelly R. (Eds.) *Geotechnical and Geophysical Site Characterisation, ISC'5*. Sydney, Australia: Australian Geomechanics Society; 2016. Pp. 291–296.
 17. Serebriakov E.V., Gladkov A.S. Application of acoustic televiwer in the assessment of structural disturbance and geomechanical state of the rock mass. In: *Engineering and Ore Geophysics 2023. Collection of papers of the 19th scientific and practical conference and exhibition*. Moscow: EAGE GEOMODEL LLC; 2023. Pp. 329–333. (In Russ.)
 18. Bae D.S., Kim K., Koh Y., Kim J. Characterization of joint roughness in granite by applying the scan circle technique to images from a borehole televiwer. *Rock Mechanics and Rock Engineering*. 2011;44:497–504. <https://doi.org/10.1007/s00603-011-0134-9>
 19. Thomas R.D.H., King A.M., Neilsen J.M. Assessing waviness from televiwer for incorporation within defect plane shear strength models. In: *Proceedings of the 48-th US Rock Mechanics/Geomechanics Symposium*. 1–4 June 2014, Minneapolis, Minnesota.
 20. Barton N., Choubey V. The shear strength of rock joints in theory and practice. *Rock Mechanics*. 1977;10:1–54. <https://doi.org/10.1007/BF01261801>
 21. Fredrick F.D., Nguyen T., Seymour C., Dempers G. Geotechnical data from optical and acoustic televiwer surveys. *The AusIMM Bulletin*. 2014:62–66.
 22. Katic N., Chalmers R., Christensen H.F. OATV for strength estimations in Copenhagen Limestone. In: *Proceedings of the 17th Nordic Geotechnical Meeting Challenges in Nordic Geotechnic*. 2016. Pp. 169–176.
 23. Kao H.-Ch., Chou P.-Y., Lo H.-Ch. An innovative application of borehole acoustic image and amplitude logs for geotechnical site investigation. *Acta Geophysica*. 2020;68(6):1821–1832. <https://doi.org/10.1007/s11600-020-00493-2>
 24. Podgaetskiy A.V. The influence of the mineralogical compound on the formation of physical and mechanical properties of kimberlites. *Mining Informational and analytical bulletin*. 2011;(8):105–110. (In Russ.)
 25. Palmstrom A. Measurement and characterization of rock mass jointing. In: Sharma V.M., Saxena K.R. *In-situ Characterization of Rocks*. A.A. Balkema Publishers; 2001.
 26. Deere D.U. *Rock quality designation (RQD) after twenty years*. U.S. Army Corps of Engineers Vicksburg, MS: Waterways Experimental Station; 1989. 93 p.
 27. Terzaghi R. Sources of error in joint surveys. *Géotechnique*. 1965;15(3):287–304. <https://doi.org/10.1680/geot.1965.15.3.287>
 28. Serebryakov E.V., Gladkov A.S. Geological and structural characteristics of deep-level rock mass of the Udachnaya pipe deposit. *Journal of Mining Institute*. 2021;250:512–525. <https://doi.org/10.31897/PMI.2021.4.4>
 29. Filippov A.G. Hydrothermal quartz from kimberlites of Yakutia. *Geologiya i Geofizika*. 1992;(11):108–115. (In Russ.)
 30. Alekseev S.V., Alekseeva L.P., Gladkov A.S. et al. Brines in deep horizons of the Udachnaya kimberlite pipe. *Geodynamics & Tectonophysics*. 2018;9(4):1235–1253. (In Russ.) <https://doi.org/10.5800/GT-2018-9-4-0393>



31. Petukhov I.M. *Rock bursts at coal mines*. 2nd revised and enlarged edition. St. Petersburg: FGUP “State Research Institute of Mining Geotechnics and Mine Surveying – MSC VNIMI” Publ.; 2004. 238 p. (In Russ.)
32. Barton N. The influence of joint properties in modelling jointed rock masses. In: *8th ISRM Congress*. September 25–29, 1995. International Society for Rock Mechanics and Rock Engineering. Pp. 1023–1032.
33. Sayeed I., Khanna R., Empirical correlation between RMR and Q systems of rock mass classification derived from Lesser Himalayan and Central crystalline rocks. In: *International Conference on «Engineering Geology in New Millennium»*. New Delhi, 27–29 October, 2015. Pp. 1–12.
34. Sadeghi S., Sharifi Teshnizi E., Ghoreishi B. Correlations between various rock mass classification/characterization systems for the Zagros tunnel-W Iran. *Journal of Mountain Science*. 2020;17(1):1790–1806. <https://doi.org/10.1007/s11629-019-5665-7>
35. Barton N., Bieniawski Z.T. RMR and Q-Setting records. *Tunnels and Tunnelling International*. 2008;26–29.
36. Barton N. Some new Q-value correlations to assist in site characterisation and tunnel design. *International Journal of Rock Mechanics and Mining Sciences*. 2002;39(2):185–216. [https://doi.org/10.1016/S1365-1609\(02\)00011-4](https://doi.org/10.1016/S1365-1609(02)00011-4)
37. Palmstrom A. Characterizing rock masses by the Rmi for use in practical rock engineering: Part 1: The development of the Rock Mass index (Rmi). *Tunnelling and Underground Space Technology*. 1996;11(2):175–188.

Information about the authors

Evgeny V. Serebryakov – Cand. Sci. (Geol. and Mineral.), Researcher at the Laboratory of Engineering Geology and Geoecology, Institute of Earth Crust SB RAS, Irkutsk, Russian Federation; ORCID [0000-0001-7280-7784](https://orcid.org/0000-0001-7280-7784); e-mail serebryakov.e.v@mail.ru

Ilya A. Zaytsev – Chief Geologist, Udachny Mining and Processing Complex, PJSC AK ALROSA, Mirny, Russian Federation; e-mail zaytsevia@alrosa.ru

Andrey A. Potaka – Head of the Geotechnical Monitoring Department, Udachny Mining and Processing Complex, PJSC AK ALROSA, Mirny, Russian Federation; e-mail potakaaa@alrosa.ru

Received 14.12.2023

Revised 21.02.2024

Accepted 02.04.2024



MINING ROCK PROPERTIES. ROCK MECHANICS AND GEOPHYSICS

Research paper

<https://doi.org/10.17073/2500-0632-2023-10-176>

UDC 550.8.053

**Application of hydrodynamic simulation on the basis of a composite model to improve the efficiency of gas-condensate reservoir development**K. O. Tomskiy¹ , M. S. Ivanova¹ , E. D. Nikitin² , L. A. Rudykh¹ ¹ North-Eastern Federal University named after M.K. Ammosov, Yakutsk, Russian Federation² University of Science and Technology MISIS, Moscow, Russian Federation kirilltom@mail.ru**Abstract**

At the moment, the use of digital models in the development of oil and gas fields is an effective tool for making informed tactical and strategic decisions to maximize the extraction of hydrocarbon reserves in a field. At the same time, the permanent increase in the share of hard-to-recover reserves leads to an accelerated increase in the role of simulation of reservoir hydrocarbon systems in the development of oil and gas fields. Many gas-condensate fields in Eastern Siberia can be characterized as reservoirs with low permeability and porosity and difficult thermobaric conditions, and, as a result, the issue of improving the efficiency of the development of such reservoirs to increase the cumulative production of gas and condensate is relevant. If the initial reservoir pressure of a gas-condensate field corresponds to the dewpoint pressure, dropout of a significant amount of retrograde condensate is observed when the pressure in the reservoir decreases. Condensate dropout in the pore space of a reservoir leads to a decrease in both the condensate recovery factor (CRF) and the gas recovery factor (GRF). The predictive calculations of the development of a gas-condensate reservoir by vertical and horizontal wells were carried out with the use of the hydrodynamic simulator T-Navigator of a domestic manufacturer Rock Flow Dynamics. The calculations were performed under various process conditions on the example of a gas-condensate field, which is characterized by complicated thermobaric conditions (the initial reservoir pressure corresponds to the dewpoint pressure), while the target process parameter was the amount of condensate dropout in the reservoir. Based on the results of the study, the main conclusion can be drawn. The development of the reservoir by horizontal wells can significantly reduce the reservoir drawdown pressure compared to vertical wells, while the condensate dropout in the reservoir occurs in a larger volume; the condensate becomes immobile and prevents further gas production, reducing the total production of condensate. An increase in reservoir condensate recovery in the course of the development of a gas-condensate reservoir by vertical wells compared to horizontal wells is observed under certain reservoir conditions corresponding to the simulation performed in this study, namely, at low reservoir permeability and porosity and the presence of a saturated gas-condensate system.

Keywords

condensate recovery factor, composite model, gas-condensate field, multicomponent model, retrograde condensate, mathematical model, condensate recovery, gas recovery factor

For citation

Tomskiy K. O., Ivanova M. S., Nikitin E. D., Rudykh L. A. Application of hydrodynamic simulation on the basis of a composite model to improve the efficiency of gas-condensate reservoir development. *Mining Science and Technology (Russia)*. 2024;9(3):221–230. <https://doi.org/10.17073/2500-0632-2023-10-176>

СВОЙСТВА ГОРНЫХ ПОРОД. ГЕОМЕХАНИКА И ГЕОФИЗИКА

Научная статья

Применение гидродинамического моделирования на основе композиционной модели для повышения эффективности разработки газоконденсатной залежиК. О. Томский¹ , М. С. Иванова¹ , Е. Д. Никитин² , Л. А. Рудых¹ ¹ Северо-Восточный федеральный университет имени М.К. Аммосова, г. Якутск, Российская Федерация² Университет науки и технологий МИСИС, г. Москва, Российская Федерация kirilltom@mail.ru**Аннотация**

На текущий момент использование цифровых моделей при разработке нефтяных и газовых месторождений является эффективным инструментом принятия обоснованных тактических и стратегических решений для максимального извлечения углеводородных запасов на месторождении. При этом



постоянное увеличение доли трудноизвлекаемых запасов приводит к ускоренному нарастанию роли моделирования пластовых углеводородных систем при разработке нефтяных и газовых месторождений. Многие газоконденсатные месторождения Восточной Сибири можно охарактеризовать как залежи с низкими фильтрационно-емкостными свойствами и сложными термобарическими условиями, и, как следствие, актуальным является вопрос повышения эффективности разработки подобных залежей для увеличения накопленной добычи газа и конденсата. В случае если начальное пластовое давление газоконденсатного месторождения соответствует давлению начала конденсации, наблюдается выпадение значительного количества ретроградного конденсата при понижении давления в пласте. Выпадение конденсата в поровом пространстве пласта приводит к понижению как коэффициента извлечения конденсата (КИК), так и коэффициента извлечения газа (КИГ). С помощью гидродинамического симулятора Т-Навигатор отечественного производителя Rock Flow Dynamics были произведены прогнозные расчеты разработки газоконденсатной залежи вертикальными и горизонтальными скважинами. Расчеты производились при различных технологических режимах на примере газоконденсатного месторождения, который характеризуется сложными термобарическими условиями (начальное пластовое давление соответствует давлению начала конденсации), при этом целевым технологическим параметром являлось количество выпавшего конденсата в пласте. По результатам исследования можно сделать основной вывод – разработка залежи горизонтальными скважинами позволяет значительно снижать депрессию на пласт по сравнению с вертикальными, при этом конденсат в пласте выпадает по большему объему, становится неподвижным и препятствует дальнейшей добыче газа, снижая общую добычу конденсата. Увеличение конденсатоотдачи пласта при разработке газоконденсатной залежи вертикальными скважинами по сравнению с горизонтальными скважинами наблюдается при определенных пластовых условиях, соответствующих проделанному в настоящей работе моделированию, а именно при низких фильтрационно-емкостных свойствах пласта и наличии насыщенной газоконденсатной системы.

Ключевые слова

коэффициент извлечения конденсата, композиционная модель, газоконденсатное месторождение, многокомпонентная модель, ретроградный конденсат, математическая модель, конденсатоотдача, коэффициент извлечения газа

Для цитирования

Tomskiy K. O., Ivanova M. S., Nikitin E. D., Rudykh L. A. Application of hydrodynamic simulation on the basis of a composite model to improve the efficiency of gas-condensate reservoir development. *Mining Science and Technology (Russia)*. 2024;9(3):221–230. <https://doi.org/10.17073/2500-0632-2023-10-176>

Introduction

At present, the use of geological and hydrodynamic simulation in the development of oil and gas fields is an effective way to make informed tactical and strategic decisions for the effective extraction of hydrocarbon reserves in a field. At the same time, the permanent increase in the share of hard-to-recover reserves leads to an accelerated increase in the role of simulation of reservoir hydrocarbon systems in the development of oil and gas fields [1–3].

The most common model in the development of oil and gas fields is a non-volatile oil model, in which an oil and gas system is simulated using two components: oil and gas, which, in turn, can be dissolved in oil [4–6].

The simulation of a gas-condensate reservoir requires a complex compositional model of three-phase filtration, due to the fact that, when developing a gas-condensate reservoir, it is necessary to take into account the actual composition of the reservoir fluid [7–9].

When the pressure isothermal drops below a critical point (dewpoint) during development, the phenomenon of retrograde condensation occurs in the

pore space of the reservoir. Fields with such characteristics are called gas-condensate fields [10–12].

The intensity of gas-condensate dropout, in addition to pressure, also depends on the component composition and physical and chemical properties of the phases. Changes in fluid composition occur under the influence of depth, surface tension, and viscosity. At the same time, a decrease in the cross-section of filtration channels leads to a decrease in permeability and, correspondingly, to a decrease in productivity [13–15].

The use of horizontal wells in comparison with vertical wells leads to a decrease in the reservoir drawdown pressure, which leads to less condensate dropout in the pore space and, correspondingly, to an increase in the final condensate recovery in the field. At the same time, it should be noted that there are few comparative studies of the use of horizontal and vertical wells in conditions of low reservoir permeability in order to increase the final condensate recovery [16–18].

The purpose of this work is to select the optimal option of a field development using hydrodynamic simulation to increase condensate recovery of

a gas-condensate field characterized by low permeability and porosity and initial reservoir pressure equal to the dewpoint pressure.

In order to achieve the goal, the following tasks were solved in the study:

- construction of two options for the development of a gas-condensate reservoir based on a hydrodynamic composite model: development by vertical wells (option 1) and horizontal wells (option 2);

- comparative analysis of the proposed options for the development of a gas-condensate reservoir characterized by low permeability and porosity.

Description of the composite model: the hydrodynamic model (Fig. 1) is represented by a selected fragment of the field.

Parameters adopted for simulation:

Height along Z (average) – 35.7 m;

Initial reservoir pressure – 29.1 MPa;

Reference depth – 2860 m;

Initial reservoir temperature – 80 °C;

Porosity – 0.09 – 0.169, decimal quantities;

Horizontal permeability – 0.0001556 – 0.0271019 μm^2 ;

Net/gross ratio (NTG) (average) – 0.6572, decimal quantities.

Reservoir gas component composition:

CO_2 – 0.273; N_2 – 1.045; CH_4 – 80.842; C_2H_6 – 6.044; C_3H_8 – 3.761; $i\text{C}_4\text{H}_{10}$ – 0.790;

$n\text{C}_4\text{H}_{10}$ – 0.921; C_5H_{12} and higher – 6.324 % mole.

Properties of the gas-condensate fluid:

Reservoir pressure – 29.10 MPa; Temperature – 80 °C; potential condensate content – 290 g/m³; mole fraction of dry gas – 0.937 decimal quantities; super-

compressibility coefficient under initial conditions – 0.902; fluid dewpoint pressure – 29.10 MPa [19].

Fluid properties were simulated based on the data from gas-condensate studies. Based on the data on the composition and properties of the reservoir fluid obtained in the process of laboratory experiments, a composite model of the fluid was created.

Research Methodology

One of the ways to rationally increase the profitability of the development of gas and gas-condensate fields with productive formations with low reservoir permeability and occurring at great depths is the shift to a development system using horizontal wells. The main advantages of horizontal wells are an increase in the area of reservoir fluid filtration through the well walls and a decrease in a productive reservoir drawdown, which makes it possible to ensure sufficiently high gas and gas-condensate flow rates in low-permeability and low-capacity reservoirs, as well as to reduce the number of required production wells in a field.

Two options for reservoir development were considered in the work: three vertical wells – option 1; one horizontal well with a horizontal section length of 1,400 m – option 2 [19–21].

The selection of three vertical wells versus one horizontal well, as well as the length of the horizontal wellbore, was justified by the economic costs of well construction. Well positioning was based on the map of initial gas reserves and permeability, as well as on maps of the initial net gas thickness of the reservoir (Fig. 2, 3). In other words, the two options considered

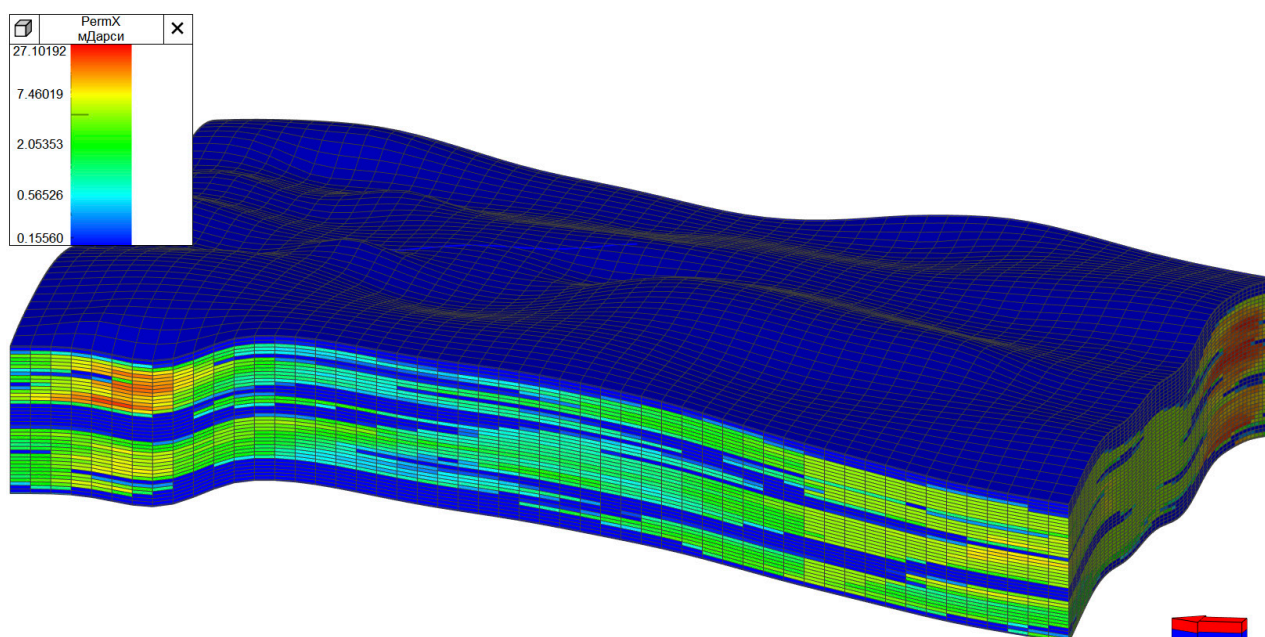


Fig. 1. Reservoir model used in calculations

are comparable in terms of well construction costs. In case of a change in the number of wells, namely additional drilling of a horizontal well or consideration of only two vertical wells as the first option – the conditions for the comparability of initial construction costs change.

Drawdown and gas withdrawal were taken as variable parameters for well operation. According to the accepted minimum possible bottomhole pressure in the field conditions, it was decided to switch to a bottomhole pressure of 3.5 MPa in case of failure to achieve the target indicators for flow rate and drawdown.

Further, the main indicators of the development of the reservoir fragment were calculated and compared with each other to find the most profitable option in terms of gas and gas-condensate production both in terms of well design (three vertical or one horizontal) and in terms of process conditions of operation.

The parameters of the process conditions of well operation adopted in the simulation for the options: gas flow rate of 600, 900, 1,500, and 2,100 thousand m³/day for one horizontal well; gas flow rate of 200, 300, 500, and 700 thousand m³/day for one vertical well; drawdown of 2, 3, 4, 5, and 6 MPa for each of the three vertical wells.

These parameters of the process conditions lie within the range of the changes in the actual parameters of the operation of vertical wells in the field.

Discussion

When developing a model of a gas-condensate reservoir with vertical wells, it is necessary to maintain significantly higher drawdowns compared to horizontal wells in order to achieve comparable flow rates. In this regard, in the case of vertical wells, there is a sharper drawdown in the bottomhole zone of a well, which causes more condensate dropout near the well, which ultimately leads to a decrease in the gas permeability of the bottomhole zone of a well. At the same time, at a certain distance from a well, smaller drawdowns are observed compared to the near-well zone, which ultimately leads to a greater amount of condensate dropout in the bottomhole zone compared to the rest of the reservoir. It is known that in the process of dropout, condensate forms three different areas of mobility near a vertical wellbore. In two of these zones, gas-condensate is present in mobile and immobile forms (Fig. 4) [9]. Correspondingly, most of the condensate in the bottomhole zone of a vertical well will occur in a mobile form.

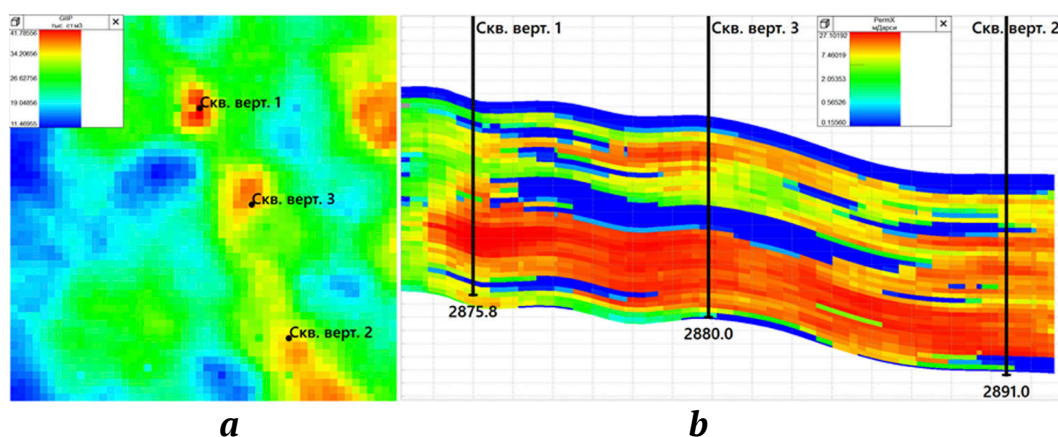


Fig. 2. Option 1 on the initial reserve map (a) and permeability map (b)

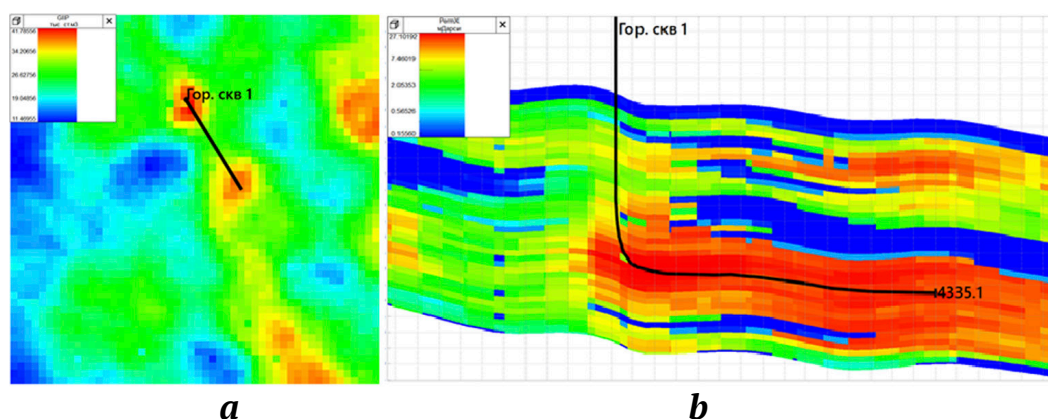


Fig. 3. Option 2 on the initial reserve map (a) and permeability map (b)

However, at the moment, there are very few studies regarding condensate dropout when using horizontal wells. In the case of developing a model of a gas-condensate reservoir with horizontal wells, we observe significantly lower drawdowns and high coverage of the reservoir by a horizontal wellbore, which, in turn, leads to condensate dropout at significant distances from the well, but in a smaller amount than in the bottomhole zone in the case of vertical wells. At the same time, the condensate formed (dropout) at considerable distances from a horizontal well will exist in an immobile form. As a result, this leads to an overall loss of cumulative condensate production.

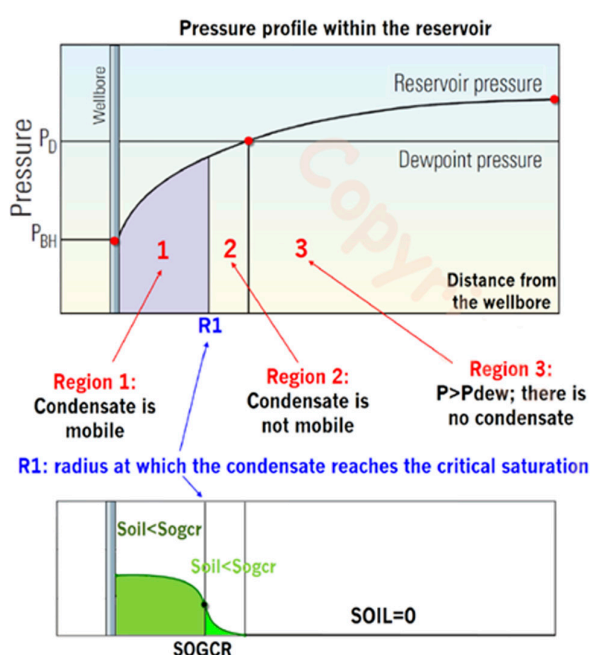


Fig. 4. Reservoir gas-condensate flow diagram [9]

Fig. 5 shows the change in condensate recovery (oil flow rate in the designation of the vertical axis) for a forecast period of 40 years with different flow rates of vertical wells. The figure shows that with high gas withdrawals (black line – 900 thousand m^3), at first, more condensate is produced, but then there is an intensive decrease in its production due to a large pressure gradient, leading to more condensate dropout in the reservoir. It can also be seen that with gas withdrawals of 200 thousand m^3/day (lilac line) the condensate flow rate is more uniform, and after 40 years of operation in this case, the maximum value of condensate recovery is observed, but the optimal amount of extraction should be selected based on the economic feasibility of developing the reservoir.

For optimal development mode and maximum condensate recovery over a given period of time, the flow rate level is selected that would justify from an economic point of view the extraction of gas reserves with a sufficient amount of condensate produced. Fig. 6 shows that the maximum condensate recovery (2,100 m^3) is achieved at a gas flow rate of 300 thousand m^3/day (blue line) for the period of well operation of 40 years.

Fig. 7 shows the condensate recovery time dependence at different flow rates of a horizontal well. Value of condensate recovery of a horizontal well at a flow rate of 2,700 thousand m^3/day corresponds to 620 m^3/day , while in the case of a vertical well with a flow rate of 900 thousand m^3/day (while the total flow rate of three vertical wells will also correspond to 2,700 thousand m^3/day), the condensate recovery corresponds to 760 m^3/day (see Fig. 5). Besides, on the graphs, we can observe certain “jumps”, which

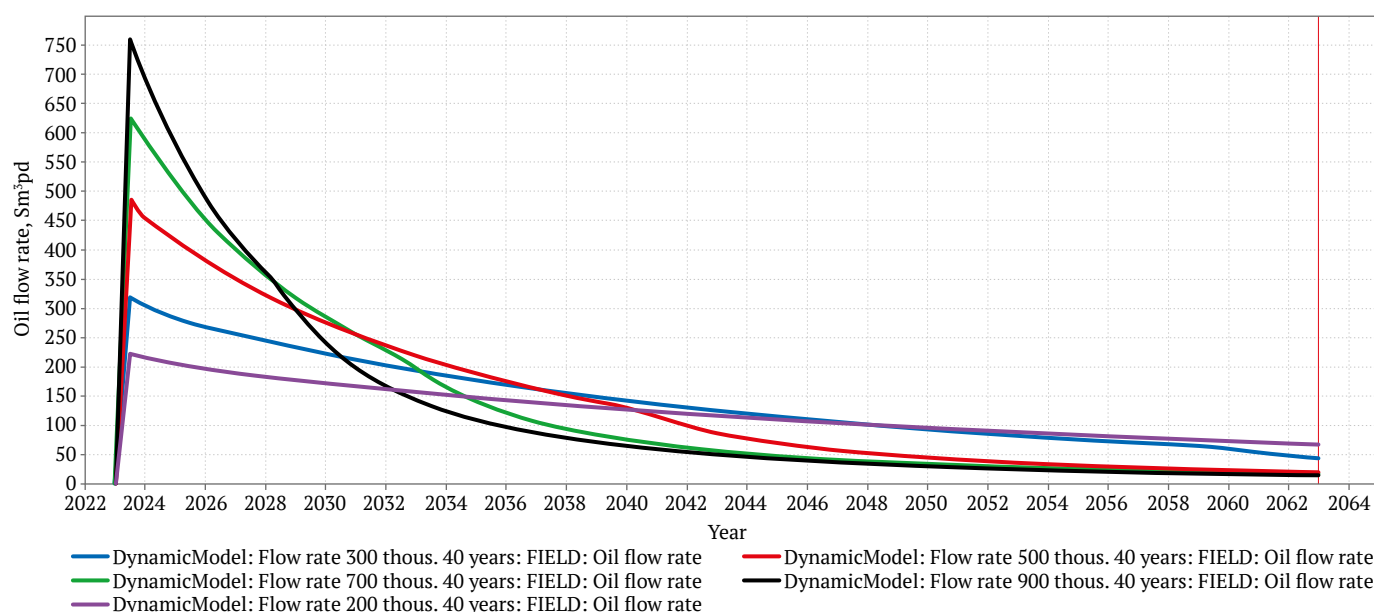


Fig. 5. Condensate recovery time dependence at different gas flow rates in the case of vertical wells (option 1)

is most likely due to the formation of a “condensate accumulation” in the pore space with the subsequent achievement of critical mobility of the formed condensate. Lower condensate recovery values of a horizontal well can be explained by lower values of drawdown in a horizontal wellbore, which leads to more uniform condensate formation (dropout) at a greater distance from the well and to more significant condensate losses in the reservoir under conditions of low permeability and porosity, since condensate under these conditions will exist in an immobile form.

Fig. 8 shows time dependencies of cumulative condensate production in the case of a horizontal well. The maximum cumulative condensate production is observed, same to the case of vertical wells, at a horizontal wellbore flow rate of 900 thousand m^3/day (corresponds to the case of a vertical well flow rate of 300 thousand m^3/day). However, the cumulative con-

densate production for a horizontal well over a 40-year operation period reaches 1,850 m^3/day , while in the case of vertical wells it is 2,100 m^3/day .

Fig. 9 presented gas flow rate graph for three vertical wells at different drawdowns corresponding to 2, 3, 4, 5, and 6 MPa (with a target flow rate of 700 thousand m^3/day) with the subsequent change to the bottomhole pressure control mode of 3.5 MPa if it is impossible to maintain the preset values of drawdowns. Analysis of the graphs shows that the lower the drawdown, the more steadily the required flow rates can be maintained during the life of a well.

Fig. 10 shows time dependencies of cumulative condensate production at different drawdowns of vertical wells corresponding to 2, 3, 4, 5, and 6 MPa (with a target flow rate of 700 thousand m^3/day). Analysis of the graphs shows that the optimal drawdown in the case of a prognosis for 40 years is 3 MPa.

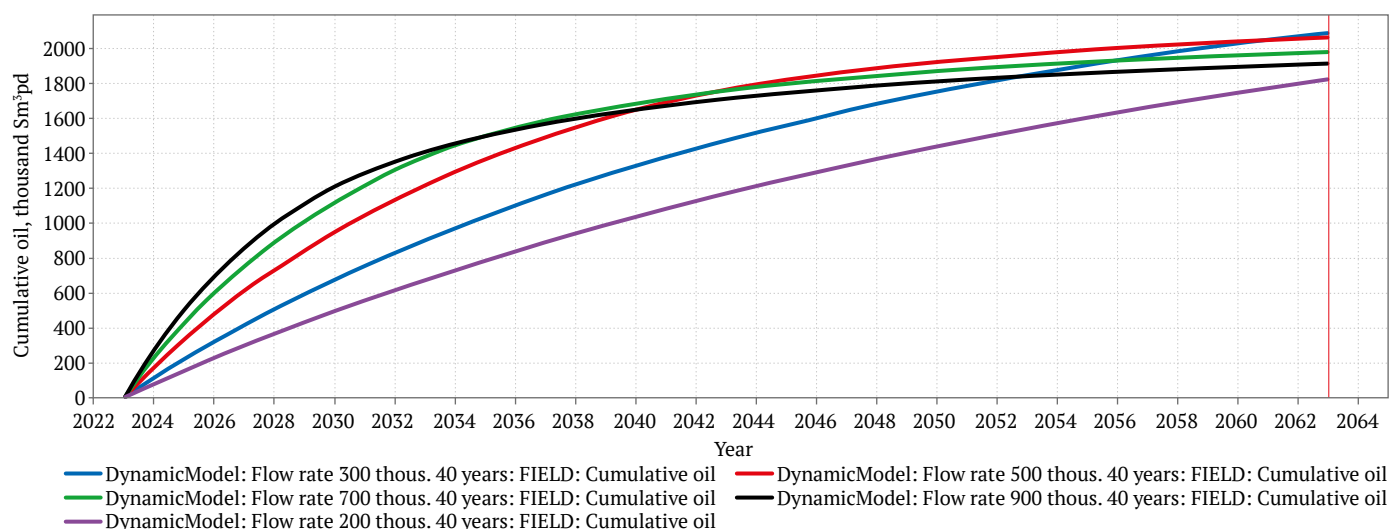


Fig. 6. Cumulative condensate production at different flow rates for vertical wells (Option 1)

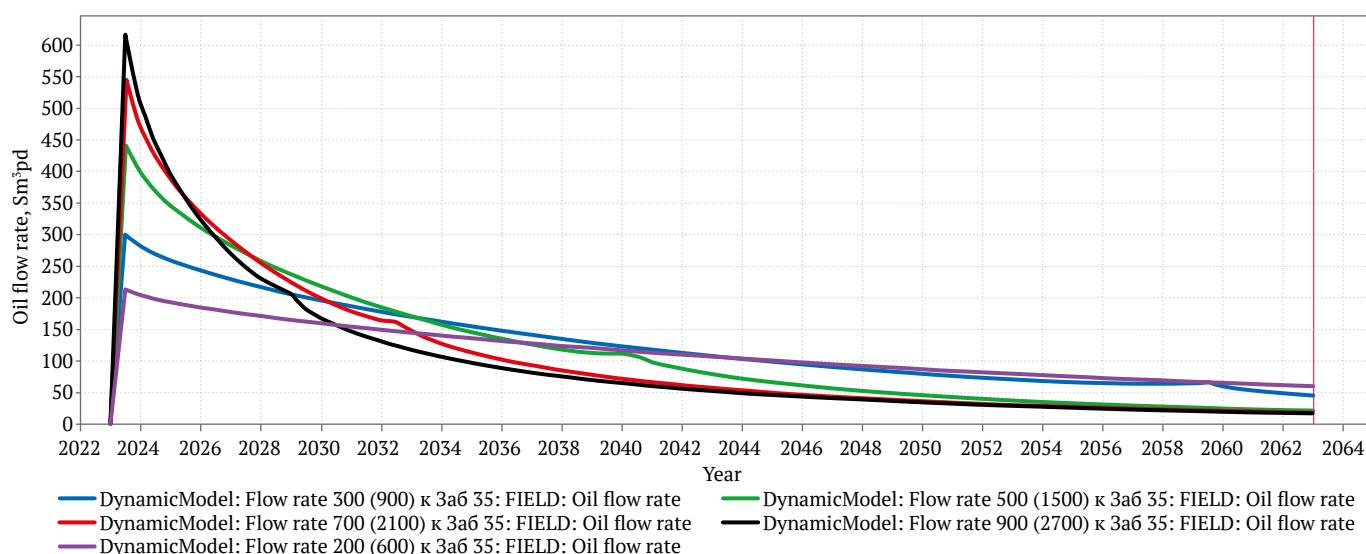


Fig. 7. Condensate recovery time dependence at different gas flow rates in the case of a horizontal well (Option 2)

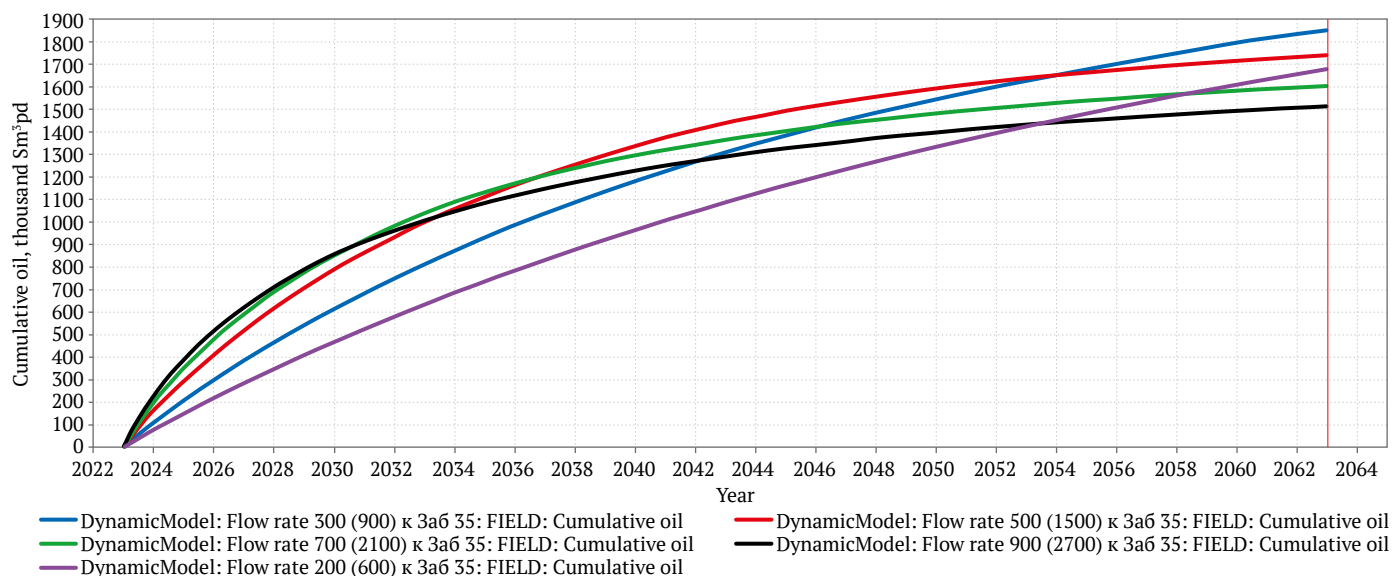


Fig. 8. Cumulative condensate production at different flow rates in the case of a horizontal well (Option 2)

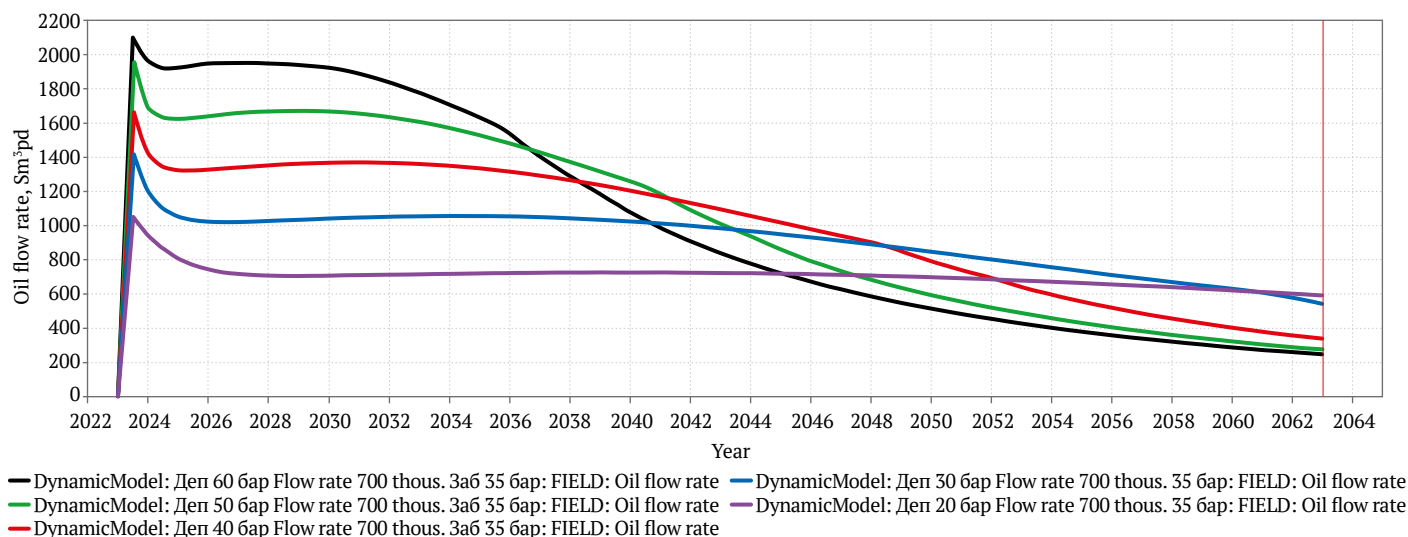


Fig. 9. Graph of changes in gas flow rates for three vertical wells at different drawdowns of 2, 3, 4, 5, and 6 MPa (Option 1)

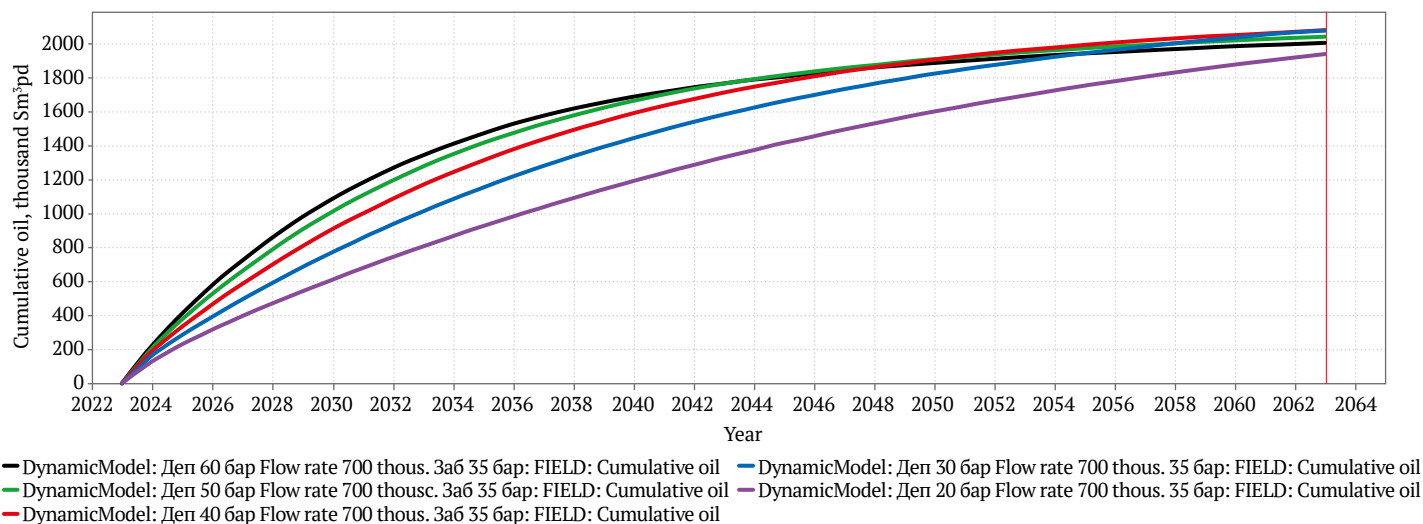


Fig. 10. Cumulative condensate production at different drawdowns for vertical wells (Option 1)

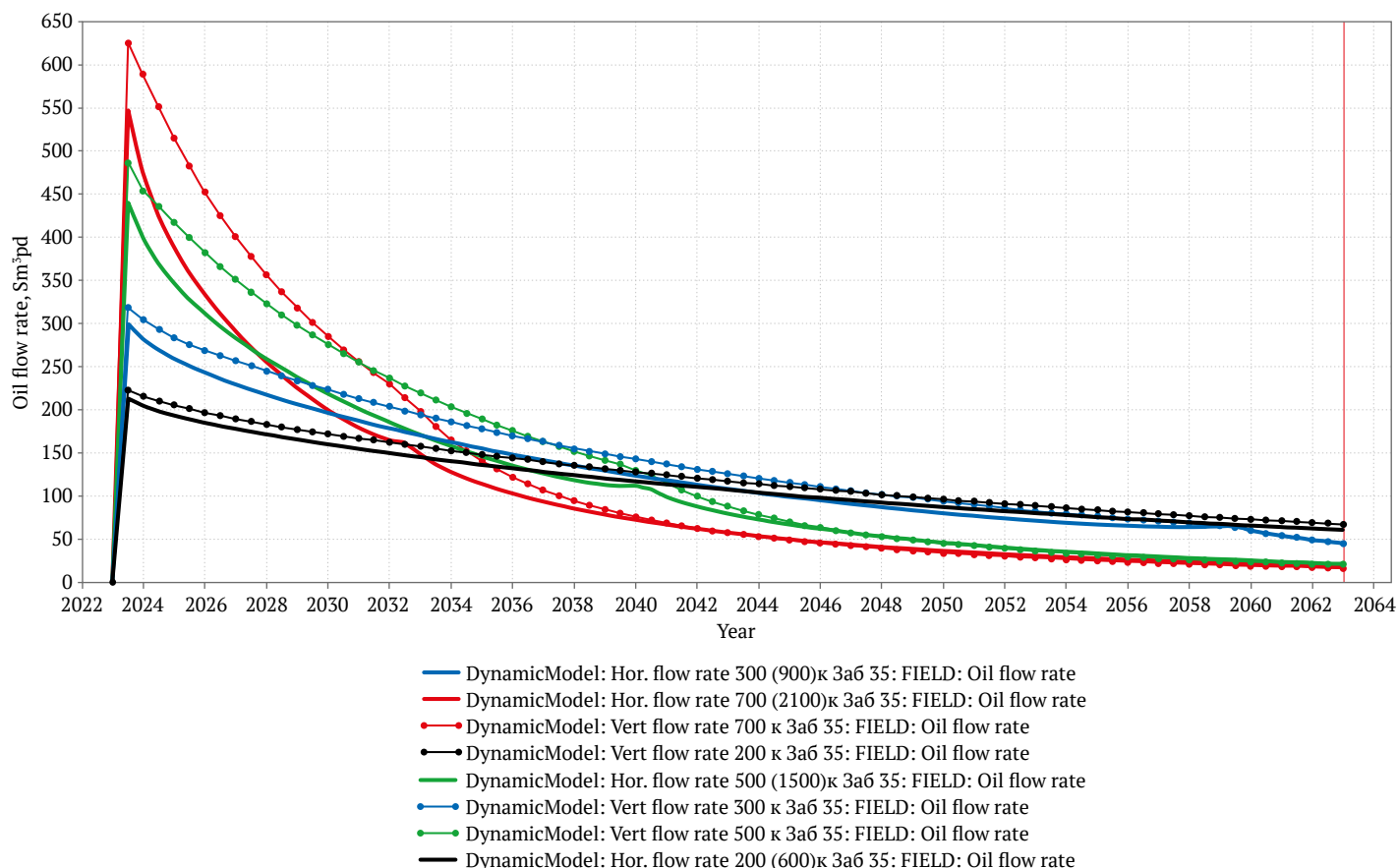


Fig. 11. Comparison of condensate recovery of vertical and horizontal wells at different flow rates (Options 1 and 2)

Fig. 11 shows comparative condensate recovery graphs in the cases of gas-condensate reservoir development by vertical and horizontal wells. The analysis shows that the condensate recovery of horizontal wells in all cases will be less than that of vertical wells. In the case of high initial flow rates, a comparability of the condensate recovery of the two options after 20 years of operation is observed, while in the case of low initial flow rates (200 thousand m^3/day for vertical wells and 600 thousand m^3/day for a horizontal well), the excess of condensate recovery of vertical wells compared to horizontal wells is observed during the entire development period.

Conclusions

1. Using hydrodynamic simulation based on a multicomponent (compositional) model, a comparative analysis of the development of a gas-condensate reservoir by vertical and horizontal wells was carried out, the results of which revealed the advantage of reservoir development by vertical wells compared to horizontal wells in terms of maximum condensate recovery. Field development by horizontal wells can significantly reduce reservoir drawdown

compared to vertical wells, with condensate dropout in the reservoir in large volume, becoming immobile and preventing further gas production, while reducing overall condensate production. An increase in reservoir condensate recovery in the course of the development of a gas-condensate reservoir by vertical wells compared to horizontal wells is observed under certain reservoir conditions corresponding to the simulation performed in this study, namely, at low reservoir permeability and porosity and the presence of a saturated gas-condensate system (the dewpoint pressure corresponds to the initial reservoir pressure).

2. A further more in-depth analysis of the development of a gas-condensate reservoir characterized by low permeability and porosity by horizontal wells is required from the point of view of other options for the optimal location of a horizontal wellbore in the reservoir in comparison with other options for the location of vertical wells in order to determine the area of occurring immobile condensate during the development, which ultimately has a significant impact on the cumulative condensate production.



References

1. Aziz Kh., Settari A. *Petroleum reservoir simulation*. London: Applied Science Publishers LTD; 1979. (Trans. ver.: Aziz Kh., Settari A. *Petroleum reservoir simulation*. 2nd ed. Moscow-Izhevsk: Institute of Computer Technology; 2004. 416 p. (In Russ.))
2. Pyatibratov P.V. *Hydrodynamic simulation of oil field development*. Moscow: Russian State University of Oil and Gas named after I.M. Gubkin Publ.; 2015. 167 p. (In Russ.)
3. Tomskiy K.O., Ivanova M.S., Oshchepkov N.S., Sokolov N.G. Determining the optimal location of a multilateral fishbone well, taking into account the peculiarities of the Srednebotuobinskoye oil and gas condensate field using hydrodynamic modeling. *Mathematical notes of NEFU*. 2022;29(4):95–112. (In Russ.) <https://doi.org/10.25587/SVFU.2023.68.12.008>
4. Kanevskaya R.D. *Mathematical simulation of hydrodynamic processes of hydrocarbon field development*. Moscow-Izhevsk: Institute for Computer Research Publ.; 2002. 140 p. (In Russ.)
5. Abasov M.T., Orudzhaliyev F.G. *Gas hydrodynamics and development of gas-condensate fields*. Moscow: Nedra Publ.; 1989. 262 p. (In Russ.)
6. Rodriguez F., Sancehs J., Galindo-Nava A. Mechanisms and main parameters affecting nitrogen distribution in the gas cap of the supergiant akal reservoir in the Cantarell Complex. In: *SPE Annual Technical Conference and Exhibition*. Houston, Texas, September 2004. <https://doi.org/10.2118/90288-MS>
7. Holditch S.A., Spivey J., Wang J.Y. Case history of a tight and abnormally pressured gas condensate reservoir. In: *SPE California Regional Meeting*. California, USA, 1985.
8. Afidick D., Kaczorowski N.J., Bette S. Production performance of retrograde gas reservoir: A case study of Arun field. In: *SPE Asia Pacific Oil and Gas Conference*. 1994.
9. Fan L., Harris B.W., Jamaluddin A., et al. Understanding gascondensate reservoirs. *Oilfield Review*. 2005;17(4):14–27.
10. Ursin J.R. Fluid flow in gas condensate reservoirs: The interplay of forces and their relative strengths. *Journal of Petroleum Science and Engineering*. 2004;(4):253–267. <https://doi.org/10.1016/j.petrol.2003.09.005>
11. Moses P.L., Wilson K. Phase equilibrium considerations in using nitrogen for improved recovery from retrograde condensate reservoirs. *Journal of Petroleum Technology*. 1981;33(02):256–262. <https://doi.org/10.2118/7493-PA>
12. Bergenov S.U., Chernova O.S., Zipir M.G. Methodology for assessing the expected starting flow rates of horizontal wells in gas and gas condensate fields. *Bulletin of the Tomsk Polytechnic University. Geo Assets Engineering*. 2020;331(3):207–212. (In Russ.) <https://doi.org/10.18799/24131830/2020/3/2563>
13. Aliev Z.S., Marakov D.A. Transition zone impact on reliability of gas reserves and well productivity. *Petroleum and Gas: Experiences and Innovation*. 2017;1(1):3–12. (In Russ.)
14. Fevang O., Whitson C.H. Modeling gas-condensate well deliverability. *SPE Reservoir Evaluation and Engineering*. 1996;11(4):221–222. <https://doi.org/10.2118/30714-PA>
15. Shandrygin A.N., Kazantsev M.A., Morev M.V., Badalov E.Z. Methodology for determining the productivity of horizontal wells based on the data of hydrodynamic modeling and exploration wells in gas condensate fields. *Science & Technology in the Gas Industry*. 2021;(2):52–59. (In Russ.)
16. Sayed M.A., Muntasheri G.A. Mitigation of the effects of condensate banking: a critical review. *SPE Production & Operations*. 2016;31(02):85–102. <https://doi.org/10.2118/168153-PA>
17. Nikolaev O.V., Shandrygin A.N., Baiburin R.A. et al. Optimization of the design and operation modes of horizontal holes in gas-condensate fields with complicated geological and climatic conditions. *Nauka i Tekhnika v Gazovoy Promyshlennosti*. 2021;(2):74–81. (In Russ.)
18. Hale P., Lokhandwala K. Advances in membrane materials provide new gas processing solutions. In: *Proceedings of the Laurance Reid Gas Conditioning Conference*. Norman, Oklahoma, USA, 2004. Pp. 165–182.
19. Tomskiy K.O., Nikitin E.D., Ivanova M.S. Analysis of the effectiveness of applying horizontal wells for the development of reserves of a gas condensate field with low filtration and capacitance properties. *Bulletin of the Tomsk Polytechnic University. Geo Assets Engineering*. 2023;(9):172–181. (In Russ.)
20. Brusilovsky A.I. *Phase transformations in the development of oil and gas fields*. Moscow: Graal Publ.; 2002. 575 p. (In Russ.)
21. Redlich O., Kwong J.N.S. On the thermodynamics of solutions: V: An equation of state. Fugacities of gaseous solutions. *Chemical Reviews*. 1949;44(1):233–244. <https://doi.org/10.1021/cr60137a013>



Information about the authors

Kirill O. Tomskiy – Cand. Sci. (Eng.), Head of the Department of Subsoil Use, Ammosov North-Eastern Federal University, Yakutsk, Russian Federation; ORCID [0000-0001-7612-5393](#), Scopus ID [58080759000](#); e-mail kirilltom@mail.ru

Mariya S. Ivanova – Cand. Sci. (Chem.), Associate Professor of the Department of Subsoil Use, Ammosov North-Eastern Federal University, Yakutsk, Russian Federation; ORCID [0000-0003-3272-9253](#), Scopus ID [7202135803](#); e-mail ims.06@mail.ru

Egor D. Nikitin – PhD-Student of the Department of Information and Communication Technologies, University of Science and Technology MISIS, Moscow, Russian Federation; ORCID [0009-0002-8211-5479](#); e-mail egornd1998@gmail.com

Lyubov A. Rudykh – Student of the Basic Department of Taas-Yuryakh Neftegazodobycha LLC, PJSC NK Rosneft, Polytechnic Institute (branch) Northeastern Federal University in Mirny, Mirny, Russian Federation; ORCID [0009-0006-5231-5276](#); e-mail lubovrudyh93@gmail.com

Received 26.10.2023

Revised 28.05.2024

Accepted 07.08.2024



BENEFICIATION AND PROCESSING OF NATURAL AND TECHNOGENIC RAW MATERIALS

Research paper

<https://doi.org/10.17073/2500-0632-2024-03-229>

UDC 622.7

**"Invisible" noble metals in carbonaceous rocks and beneficiation products: feasibility of detection and coarsening**

T.N. Aleksandrova , A.V. Afanasova , V.A. Aburova ✉

Empress Catherine II Saint Petersburg Mining University, Saint Petersburg, Russian Federation✉ aburovaleria@gmail.com**Abstract**

The decrease in the quality of raw materials coming for processing requires involvement of refractory ores in processing, the refractoriness of which is caused by the presence of organic carbonaceous matter sorption-active in relation to dissolved noble metals and impregnation of fine noble metals in mineral-carriers. In this connection, the actual research line is the development of new technological solutions with the use of energy methods of action in order to reduce the losses of valuable components in beneficiation tailings. Treatment with ultra-high frequency electromagnetic radiation has a number of advantages, including rapid and selective heating due to the differences in the ability of minerals to absorb this radiation. Carbon-containing materials represented by carbonaceous flotation concentrate and model samples of activated carbon with adsorbed silver were taken as the research subjects. Using the model samples as an example, the necessity of using magnetite to achieve coarsening fine silver particles during ultra-high frequency treatment was substantiated. The formation of active centers of local heating during the treatment in the points of magnetite addition was confirmed. The necessary content of magnetite of 10% for coarsening fine silver to spherical aggregates, the average size of which was 20–40 microns, was substantiated. Coarsening noble metal particles to sizes of 20–50 microns in treated carbonaceous concentrates containing silver and gold was achieved, when the substantiated amount of magnetite was added. Coarsened particles (aggregates) of noble metals can be recovered using traditional beneficiation methods.

Keywords

microwave treatment, carbonaceous concentrate, gold-bearing ores, model samples, flotation, silver, magnetite

Acknowledgments

The study was carried out within the framework of a grant from the Russian Science Foundation (Project No. 23-47-00109).

For citation

Aleksandrova T.N., Afanasova A.V., Aburova V.A. "Invisible" noble metals in carbonaceous rocks and beneficiation products: feasibility of detection and coarsening. *Mining Science and Technology (Russia)*. 2024;9(3):231–242. <https://doi.org/10.17073/2500-0632-2024-03-229>

ОБОГАЩЕНИЕ, ПЕРЕРАБОТКА МИНЕРАЛЬНОГО И ТЕХНОГЕННОГО СЫРЬЯ

Научная статья

**«Невидимые» благородные металлы
в углеродистых породах и продуктах обогащения:
возможность выявления и укрупнения**

Т.Н. Александрова , А.В. Афанасова , В.А. Абурова ✉

Санкт-Петербургский горный университет императрицы Екатерины II, г. Санкт-Петербург, Российская Федерация✉ aburovaleria@gmail.com**Аннотация**

По причине снижения качества поступающего на переработку сырья, вовлечения упорных руд, упорность которых обусловлена наличием сорбционно-активного по отношению к растворенным благородным металлам органического углеродистого вещества и вкрапленностью низкоразмерных благородных металлов в минералы-носители, актуальным направлением является разработка новых технологических решений с применением энергетических методов воздействия с целью снижения потерь ценных компонентов с хвостами обогащения. Обработка электромагнитным излучением сверх-



высокой частоты обладает рядом преимуществ, среди которых отмечаются быстрый и селективный нагрев за счет различий в способности поглощать минералами данное излучение. В качестве объекта исследования приняты углеродсодержащие материалы, представленные углеродистым флотационным концентратом и модельными навесками активированного угля с адсорбированным серебром. На примере модельных навесок обоснована необходимость использования магнетита для достижения укрупнения низкоразмерного серебра при сверхвысокочастотной обработке. Подтверждено образование активных центров локального нагрева в местах добавления магнетита в процессе обработки. Обосновано необходимое содержание магнетита для укрупнения низкоразмерного серебра до сферических агрегатов, средний размер которых составил 20–40 мкм, равное 10 %. Получено укрупнение частиц благородных металлов в обработанных углеродистых концентратах до размеров 20–50 мкм, содержащих серебро и золото, при добавлении обоснованного количества магнетита. Укрупненные частицы благородных металлов возможно извлекать с применением традиционных методов обогащения.

Ключевые слова

СВЧ обработка, углеродистый концентрат, золотосодержащие руды, модельные навески, флотация, серебро, магнетит

Благодарности

Работа выполнена в рамках гранта РНФ (проект № 23-47-00109).

Для цитирования

Aleksandrova T.N., Afanasova A.V., Aburova V.A. "Invisible" noble metals in carbonaceous rocks and beneficiation products: feasibility of detection and coarsening. *Mining Science and Technology (Russia)*. 2024;9(3):231–242. <https://doi.org/10.17073/2500-0632-2024-03-229>

Introduction

The development of technologies for processing of strategic raw materials is necessary to maintain the world economy at the current level in connection with the depletion of mineral resource base. Worsening the quality of gold- and silver-containing raw materials, involvement of lean and refractory ores in processing owes the actualization of scientific research aimed at increasing the recovery of valuable components into concentrates [1]. The analysis of existing studies has shown that some of the topical areas in the field of mineral beneficiation are increasing the efficiency of disintegration of mineral raw materials [2, 3], application of machine vision technology at various stages of beneficiation, synthesis of new flotation reagents [4–6], and the development of new reagent regimes [7–9].

The refractoriness of gold-bearing ores can be caused both by the presence of substances sorption-active in relation to dissolved gold and inclusions of fine noble metals in mineral-carriers, mainly in such minerals as pyrite, arsenopyrite, galena, etc. Ores in which both these features are present are referred to ores of double refractoriness. "Invisible" gold is referred to submicroscopic gold particles that are 1–100 nm in size and are not detected using optical or electron microscopy [10]. The presence of "invisible" gold and silver in ores complicates the selection of flow charts for their processing and owes the necessity for the development of new process solutions and improvement of existing ones.

The carbonaceous material contained in the double-refractory ores contaminates the concentrates produced and results in significant losses of valuable

components at the stage of metallurgical processing. The actual task of the existing research is to involve in processing carbonaceous products, going to tailings at most of the processing plants, in order to reduce losses of valuable components such as gold and silver [11–13].

In addition to native metal, silver in ores can be represented by dispersed inclusions in the host minerals, either as metallic or chemically bound silver. Chemically bound silver refers to various silver sulfides, for example, Ag_2S . The presence of fine silver associated with sulfide minerals, as well as in the case of gold, complicates its recovery at the cyanidation stage [14]. The recovery requires destruction of the matrix of the host minerals in order to provide the contact of reagents with the noble metal to dissolve it.

To date, there is a large amount of researches aimed at finding process solutions for the processing of refractory raw materials [15–17]. For double refractory ores, pretreatment to reduce the refractoriness of gold-bearing ores is required. The most common pretreatment methods are roasting, chlorination, pressure oxidation, bioleaching, and Albion technology. However, in addition to the traditional methods, research into the feasibility of using energy-based methods of action has become widespread [18, 19]. Ultra-high frequency (UHF) treatment is one of the promising methods whose advantages include fast and selective heating [20–22]. The selectivity of heating minerals is due to the differences in their heating rate, which in turn is connected with specific heat capacity, specific thermal conductivity, and relative dielectric constant. Recent researches



with the use of microwave treatment are aimed at increasing the efficiency of disintegration of mineral raw materials [23–25], studying the feasibility of using microwaves for sorting ores [26], reducing the content of harmful impurities in ores [27], studying the effect on surface properties and flotability of minerals [28], involvement of cyanide [29] and sulfide [30] tailings in the treatment. The melting temperature of “invisible” noble metals is much lower than the melting temperature of visible particles that predetermines the feasibility of their coarsening in the process of energy actions. For example, for Au, the melting point of a 1.6 nm diameter cluster is 257.85 °C [33], while that of a 1.9 nm diameter cluster is 318.85 °C [34]. For Ag, the melting point of a 4 nm diameter cluster is 449.85 °C [5], while that of a 5 nm diameter cluster is 509.85 °C [34]. Carbonaceous flotation products, as a rule, contain insignificant amounts of ore minerals, which requires sufficiently long time for microwave treatment in order to coarsen the particles. In this regard, the addition of magnetite in the process of treatment allows the creation of local heating centers. Table 1 systematizes the data of dependence of the achieved maximum heating temperature on the treatment time for sulfide mineral-concentrators of gold and products of their destruction after roasting.

Analysis of historical studies confirms the fact that magnetite is more active in relation to ultra-high frequency electromagnetic radiation and, in comparison with other minerals, reaches significantly higher heating temperatures. The low melting temperature of silver nanoclusters confirms the prospect of investigating the feasibility of their coarsening, since it is lower than the magnetite treatment heating temperature.

Thus, the purpose of this study was to reveal the mechanism of coarsening fine silver in the course of microwave treatment with the addition of magnetite using model samples and to justify the required content of magnetite to confirm the feasibility of silver coarsening in the course of microwave treatment of carbonaceous flotation concentrate samples to reduce losses of valuable components in tailings.

Research Materials and Techniques

1. Characterization of research subjects

The following carbon-containing materials were chosen as the research subjects:

1) carbonaceous flotation concentrate (produced by carbonaceous flotation from refractory sulphide gold-bearing ore);

2) model samples of activated carbon (after adsorption of silver).

The source of silver in the model sample was silver leaf, containing 99.9% Ag. Preparation of the model samples included: grinding of activated carbon, preparation of leaching solution, transition of silver leaf to liquid phase for two days (leaching), its subsequent contacting with activated carbon for three days. The leaching reagent is a mixture of iodine complex, amino acids, sodium chloride, urea, ammonium chloride, and sodium carbonate. After contacting the noble metal with activated carbon, filtration and drying of the obtained cake was carried out for subsequent microwave treatment.

The initial carbonaceous gold-bearing ore is characterized by the presence of fine inclusions of gold and insignificant amount of silver in the mineral-concentrators, such as pyrite and arsenopyrite, as well as organic carbonaceous matter sorption-active in relation to dissolved gold. The main valuable component is gold, the grade of which in the initial ore is 5.99 ± 0.29 g/t. Silver is a by-product, the grade of which is 0.29 ± 0.1 g/t.

2. Flotation beneficiation experiments

Separation of carbonaceous flotation concentrate from refractory gold-bearing ore was carried out using pneumomechanical flotation machine Flotation Bench Test Machine of Laarmann company with cell volume of 1.5 liters. The initial ore was subjected to grinding to particle size of 60% passing 71 µm, after which carbonaceous flotation was carried out with the addition of oxal frothing agent, the consumption of which was 85 g/t. The results of studying the obtained flotation products are presented in Table 2.

The obtained carbonaceous flotation concentrate after drying was subjected to microwave treatment, while the tailings of carbonaceous flotation went for additional grinding and subsequent sulfide flotation.

3. Microwave treatment

Microwave treatment of carbon-containing materials without and with the addition of different amount of magnetite (3, 5, 10, 15% by weight of a sample) was carried out using a Sineo UWave-2000 microwave oven, the range of possible setting of power in which was 100–1000 W. The coarseness of the added magnetite was –50 µm.

Table 1

Summary data on dependence of maximum microwave heating temperature on treatment time

No.	Mineral	Treatment time, min	Maximum temperature, °C	Reference
1	Magnetite	2.75	1,258	[31]
2	Pyrite	6.75	1,019	[31]
3	Pyrrhotite	1.75	886	[31]
4	Arsenopyrite	1.0	723	[31]
5	Hematite	7.0	182	[31]

Table 2

Results of research of refractory gold-bearing ore flotation products

Product Designation	Yield, %	Content [Grade], % [g/t]				Recovery, %			
		Au*	Ag*	C _{org}	S _{tot}	Au	Ag	C _{org}	S _{tot}
Carbonaceous flotation concentrate	2.42	2.91	0.12	27.14	0.95	1.19	0.94	40.54	1.36
Carbonaceous flotation tailings	97.58	5.99	0.31	0.99	1.71	98.81	99.06	59.46	98.64
Initial ore	100.00	5.92	0.31	1.62	1.69	100.00	100.00	100.00	100.00

4. Scanning electron microscopy

In order to confirm coarsening fine silver in model samples and carbonaceous flotation concentrate after microwave treatment with the addition of magnetite to create active centers of local heating, the study of the samples before and after the treatment was carried out using a Vega 3 LMH scanning electron microscope, combined with a system of X-ray energy dispersive microanalysis Oxford Instruments INCA Energy 250/X-max 20. The fine silver coarsening study was carried out with the determination of sizes of a minimum of 200 particles in each of the samples obtained. The carbonization of the samples was carried out using a Q150R E sputtering apparatus manufactured by Quorum Technologies Ltd.

5. Microwave heating temperature

Measuring the achieved temperature of microwave heating of samples was carried out using a FinePower DIN21H laser pyrometer. The measuring temperature range was –50 to 1,100 °C with an accuracy of ±2%.

Findings and Discussion

1. Processing of silver-containing model samples without magnetite addition

In order to confirm the feasibility of coarsening fine silver in the course of microwave treatment, an initial model sample with adsorbed silver before treatment was studied for comparison. Figure 1 shows the results of the sample study before treatment using scanning electron microscopy. Table 3 shows the findings of the elemental composition study for the spectrum shown in Fig. 1.

Based on the results obtained, the absence of visible silver was revealed, which was confirmed by the results of the elemental composition study, thus confirming its “invisibility”.

In order to confirm the necessity of adding magnetite to silver-containing model samples at microwave treatment for coarsening fine silver, the studies were carried out on model samples without magnetite addition. Figure 2 shows the results of scanning electron microscopy examination of the treated samples without magnetite addition. The results of the

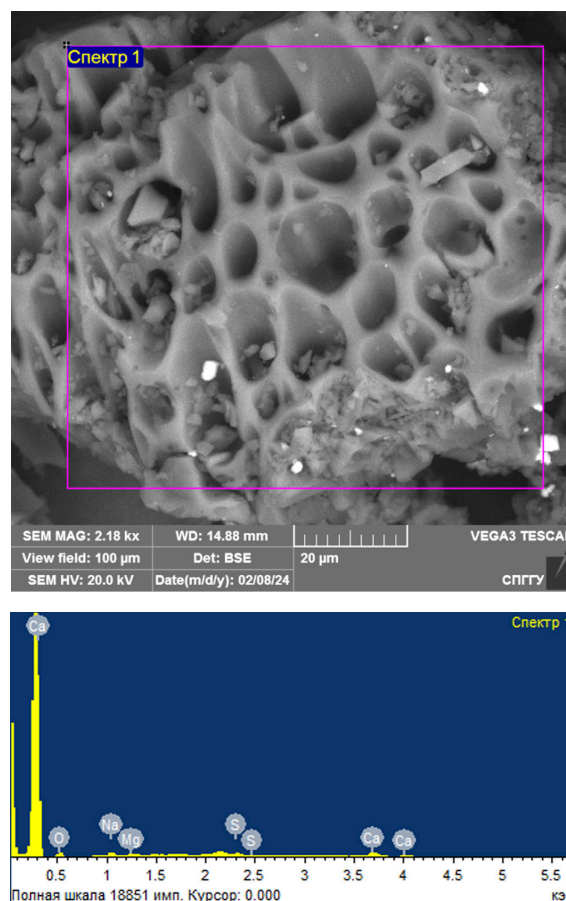


Fig. 1. Results of investigation of the initial model sample before microwave treatment using scanning electron microscopy

Table 3

The results of the study of elemental composition for the spectra presented in Fig. 1

Spectrum number	Content, weight %				
	O	Na	Mg	S	Ca
Spectrum 1	73.67	8.21	2.74	2.56	12.82

Table 4

The results of the study of elemental composition for the spectra presented in Fig. 2

Spectrum number	Content, weight %					
	O	Na	Mg	S	Ca	Ag
Spectrum 1	49.67	1.50	1.42	0.38	45.78	1.25
Spectrum 2	76.10	–	–	–	16.16	7.74

study of the elemental composition for the spectra in the studied samples are shown in Table 4.

The analysis of the obtained data allowed confirming the feasibility of coarsening fine silver particles using microwave treatment without addition of magnetite up to the average size equal to 5–10 microns. Despite the fact that coarsening is achieved at

the treatment without the addition of magnetite, the coarseness achieved in these studies does not allow extracting coarsened particles by traditional beneficiation methods. This fact predetermines the need to study the effect of the addition of different magnetite amounts to the studied model samples on coarsening fine silver particles.

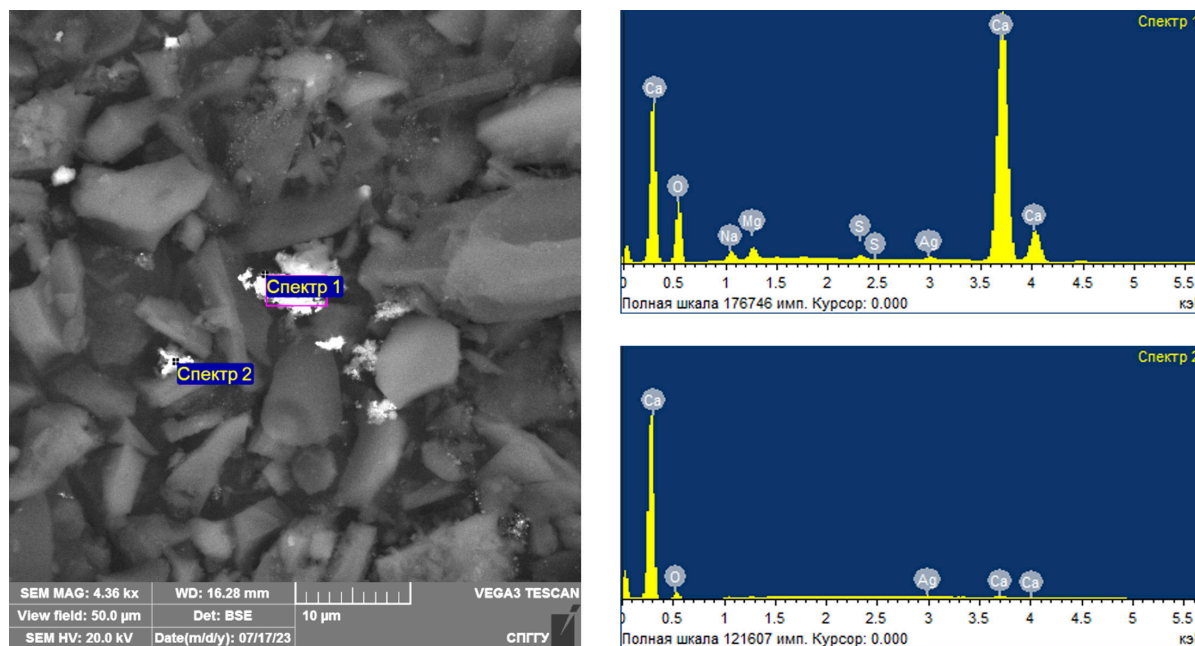


Fig. 2. Results of scanning electron microscopy study of model samples with coarsened silver after microwave treatment without magnetite addition

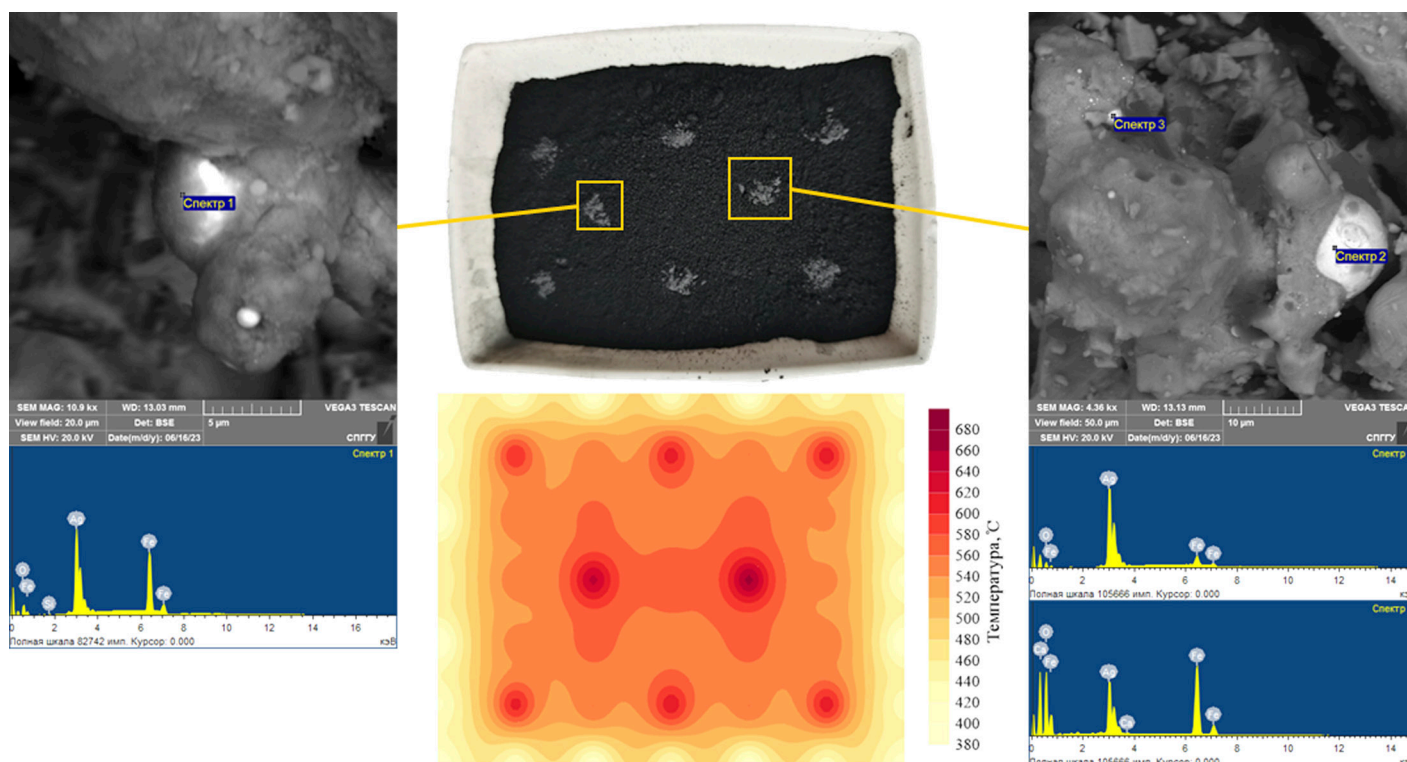


Fig. 3. Temperature mapping of silver-containing model sample at microwave treatment with addition of 10% magnetite with the results of sample examination at selected sampling points using scanning electron microscopy (gray – magnetite; black – model sample)

2. Processing of silver-containing model samples with magnetite addition

The studies aimed at establishing the necessary magnetite content to achieve maximum coarsening fine silver in the course of microwave treatment were carried out using silver-containing model samples. The magnetite contents were chosen at 3, 5, 10, and 15%. To confirm the generation of active centers of local heating in the course of microwave treatment of the model samples with the addition of magnetite, heating temperatures were measured over the whole area of the treated samples using a laser pyrometer. Fig. 3 shows the temperature mapping using an example of microwave treatment of a silver-containing model sample with 10% magnetite with sampling points for scanning electron microscopy study. The microwave heating temperature was measured immediately after the treatment. The results of the elemental composition study for the spectra shown in Fig. 3 are presented in Table 5.

The interpretation of the obtained data allows confirming arising active centers of local heating in the course of microwave treatment when magnetite was added to the model samples. In Fig. 3, the temperature peaks at the magnetite addition locations, which reach about 600 °C and higher, are clearly visible. At the same time, the heating temperature of the model sample itself is 540–560 °C. The presence of magnetite is confirmed by the results of the elemental composition study.

Table 5

The results of the elemental composition study for the spectra presented in Fig. 3

Spectrum number	Content, weight %				
	O	Si	Ca	Fe	Ag
Spectrum 1	10.17	0.12	–	42.22	47.48
Spectrum 2	11.69	0.11	–	11.51	76.69
Spectrum 3	35.06	–	0.24	41.40	23.30

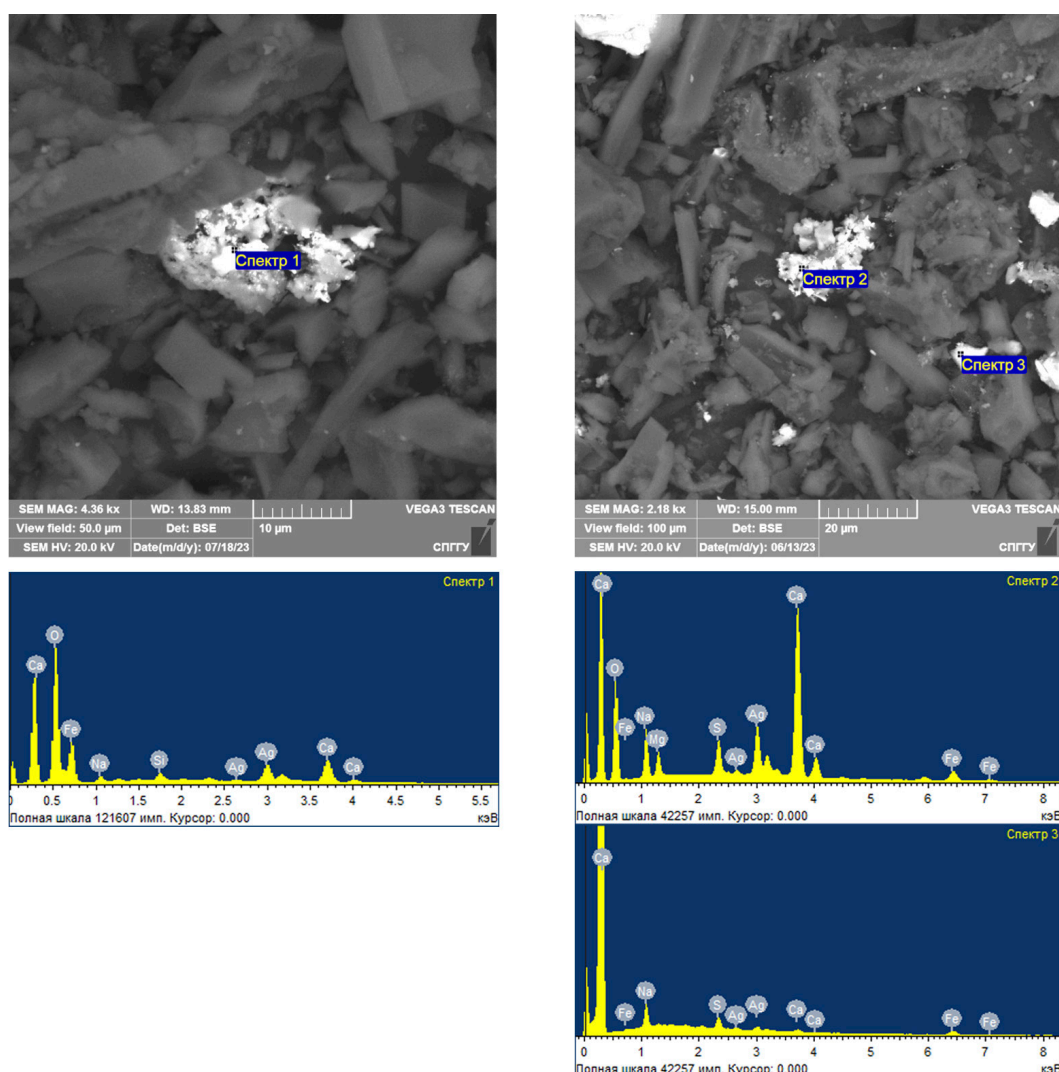


Fig. 4. Results of scanning electron microscopy study of model samples with coarsened silver after microwave treatment with addition of 3 (left) and 5 (right) % magnetite

The treated silver-containing model samples with magnetite addition were studied using a scanning electron microscope. Figs. 4 and 5 show the results of the study of these samples with magnetite content of 3, 5, 10, and 15%, respectively. The results of the study of elemental composition for the spectra shown in Figs. 4 and 5 are shown in Table 6.

The interpretation of the obtained data allows to confirm coarsening fine silver at addition of magnetite as a result of microwave treatment to the par-

ticle sizes exceeding the particle size formed in the samples without magnetite, as well as the increase of silver content in the coarsened particles. However, it is worth noting that at a magnetite content of 10%, if compared to the coarsened gold presented earlier in [36], spherical-shaped silver particles with an average size of 20–40 μm were found in the silver-containing model samples. This is because the melting point of silver is much lower than that of gold.

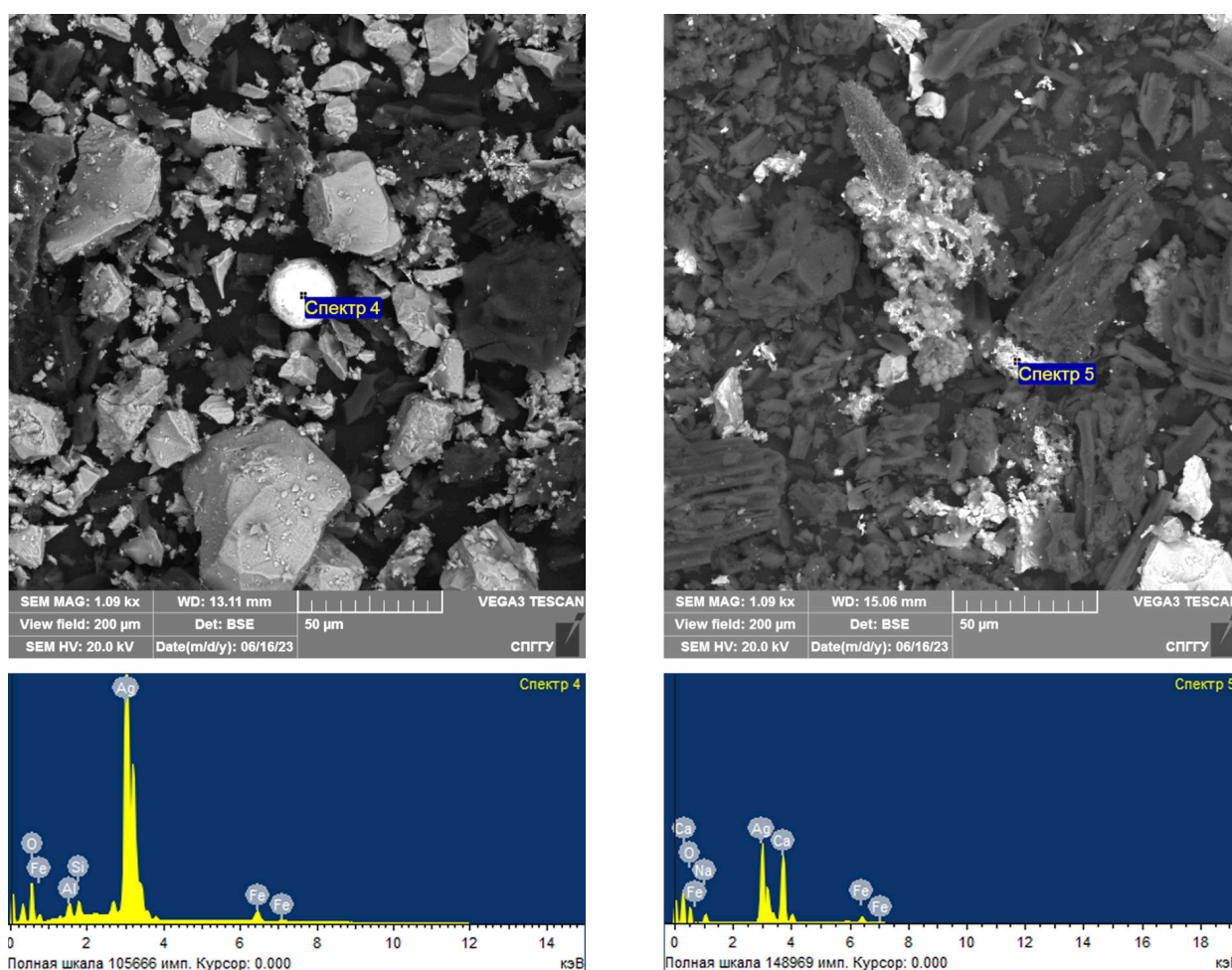


Fig. 5. Results of scanning electron microscopy study of model samples with coarsened silver after microwave treatment with addition of 10 (left) and 15 (right) % magnetite

Table 6

The results of the elemental composition study for the spectra presented in Figs. 4 и 5

Spectrum number	Content, weight %								
	O	Na	Mg	Al	Si	S	Ca	Fe	Ag
Spectrum 1	46.79	1.14	–	–	0.70	–	3.30	42.73	5.34
Spectrum 2	49.52	6.06	2.04	–	–	2.65	22.60	3.74	13.39
Spectrum 3	–	33.68	–	–	–	14.74	5.79	26.84	18.95
Spectrum 4	20.02	–	–	0.94	0.98	–	–	2.97	75.09
Spectrum 5	21.32	2.92	–	–	–	–	21.63	5.24	48.89

The obtained data on average and maximum sizes of coarsened noble metal particles (aggregates) depending on the magnetite content are presented in Table 7. Besides, Table 7 presents the degree of coarsening measured as the ratio of the average size of the coarsened silver particles to the estimated coarseness of the “invisible” silver.

Based on the obtained data analysis, it can be concluded that the addition of magnetite, which forms active centers of local heating, contributes to

coarsening fine silver particles in the course of microwave treatment, since the treatment of magnetite-free model samples allowed to coarsen the noble metal particles to smaller sizes if compared with the samples with magnetite. The obtained results allow justifying the necessary magnetite content of 10% to achieve maximum coarsening fine silver at microwave exposure to a coarseness of 20–40 μm . The formation of spherical silver particles can be explained by the lower melting point of silver compared to gold.

Table 7

Results of the study of the effect of magnetite content on coarsening fine silver in model samples with and without microwave treatment

Parameter	Value					
Magnetite content, %	0 (no treatment)	0	3	5	10	15
Average size of coarsened fine silver, μm	1–100 nm	5–10	10–15	10–20	20–40	10–15
Maximum size of coarsened fine silver, μm		39.0	43.0	92.3	123.1	102.0
Coarsening degree		75–7500	125–12500	150–15000	300–30000	125–12500
Average fineness of magnetite, μm	10–15					
Maximum fineness of magnetite, μm	49,0					

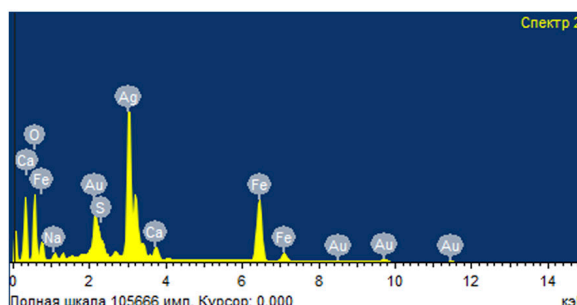
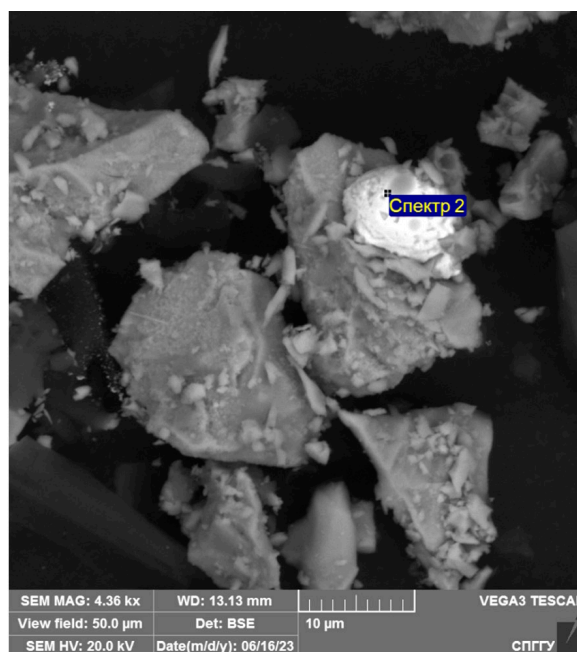
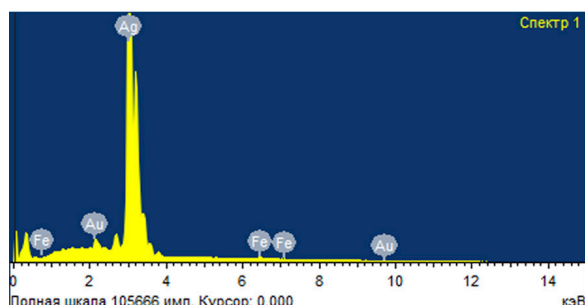
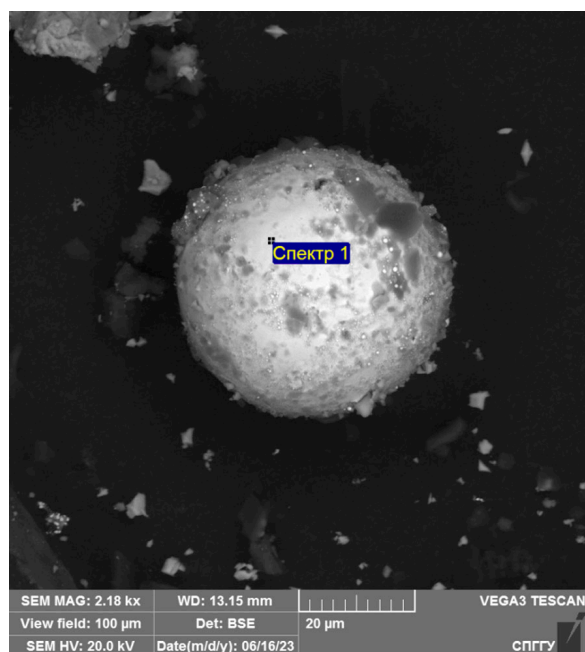


Fig. 6. Results of the study of treated carbonaceous concentrates with addition of 10% magnetite using scanning electron microscopy

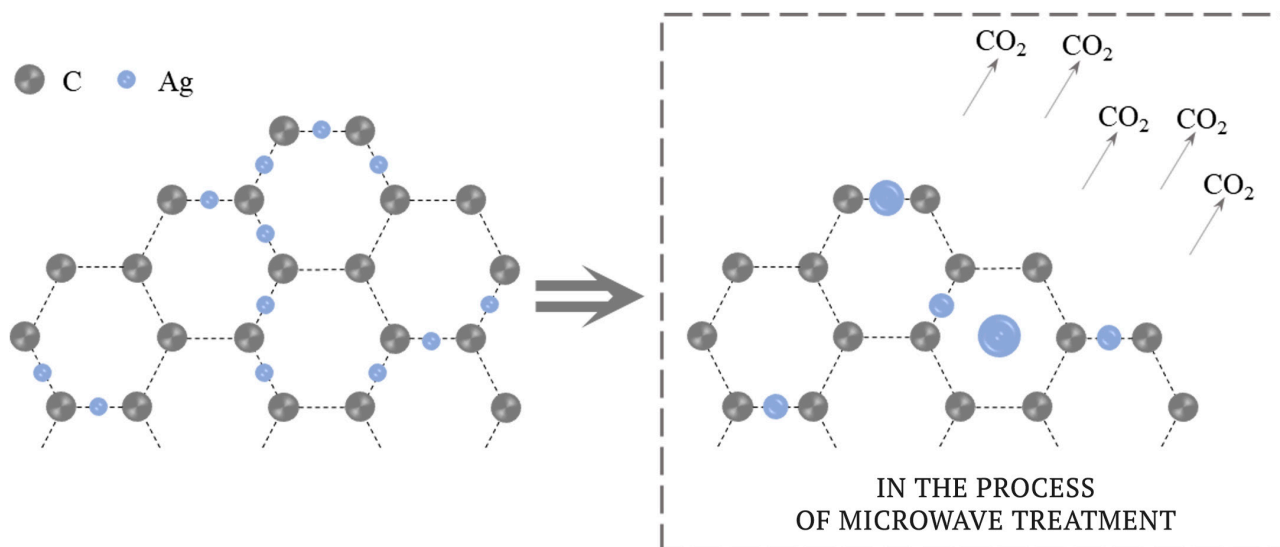


Fig. 7. Schematic representation of fine silver coarsening in the course of microwave treatment

3. Treatment of carbonaceous flotation concentrate with addition of substantiated amount of magnetite

The feasibility of silver coarsening with the addition of the previously substantiated magnetite amount in the course of microwave treatment was investigated on carbonaceous flotation concentrates. In [37], the feasibility of coarsening fine Au particles using 10% magnetite at microwave treatment of carbonaceous concentrate was confirmed. Fig. 6 presents the results of a scanning electron microscope study of the treated carbonaceous concentrate, confirming coarsening silver in the course of microwave treatment when added with magnetite in the amount of 10% of the sample weight. The elemental composition of the coarsened particles is presented in Table 8.

The interpretation of the obtained results allows to confirm coarsening silver particles in the course of microwave treatment of carbonaceous flotation concentrate added with 10% magnetite. The size of coarsened particles, which are characterized by spherical shape, after treatment is 20–50 microns. It is worth noting that, besides silver, characteristic peaks of gold were found in the coarsened aggregates according to the results of the study of the elemental composition. This indicates that silver was coarsened together with gold.

Microwave treatment contributes to increasing the temperature of the model sample, the main part of which is represented by activated carbon. When it is ignited in an oxidizing environment, the following phenomena occur:

- CO₂ formation;
- melting of adsorbed fine silver particles after combustion of a part of activated carbon and magnetite heating;

– coarsening due to silver movement into additional pores formed.

Fig. 7 shows a schematic representation of the mechanism of fine silver coarsening in the course of microwave treatment.

Fine silver coarsening is confirmed by the results of scanning electron microscopy examination of the treated silver-containing model samples. In the figures presented in this paper, the coarsened particles are observed both free (not tied with activated carbon and magnetite) and at the initial stage of coarsening directly on the activated carbon surface itself.

The results of the microwave treatment of carbonaceous flotation concentrate with the addition of 10% magnetite also confirmed the feasibility of fine silver coarsening. The achieved coarseness and the content (grade) of gold and silver in the coarsened spherical particles makes it possible to further extract them and, as a consequence, to reduce losses of valuable components with tailings. Centrifugal concentration can be considered as a potential method for the extraction of the coarsened particles [38].

Table 8
The results of the elemental composition study for the spectra presented in Fig. 6

Spectrum number	Content, weight %						
	O	Na	S	Ca	Fe	Au	Ag
Spectrum 1	–	–	–	–	0.96	3.84	95.20
Spectrum 2	26.59	1.12	0.50	1.48	20.46	12.83	37.02



Conclusion

The findings of the studies on microwave treatment of silver-containing model samples allowed substantiating the necessity of adding magnetite for fine silver coarsening. Based on the temperature mapping, the formation, in the course of the treatment, of active centers of local heating in the locations of magnetite addition was confirmed. The fine silver coarsening to spherical silver particles, whose average size was 20–40 μm , was achieved at a microwave

oven power of 1.0 kW and a treatment time of 3 min with 10% magnetite added. It was revealed that at similar microwave oven power and treatment time of 5 min, with 10% magnetite added, the greatest sizes of coarsened particles containing gold and silver equal to 20–50 μm were achieved. The microwave treatment findings showed that the silver coarsening occurs forming a gravity-extractable form of silver that allowed further investigation of its recovery using gravity concentration methods.

References

1. Fedotov P.K., Senchenko A.E., Fedotov K.V., Burdonov A.E. Studies of enrichment of sulfide and oxidized ores of gold deposits of the Aldan shield. *Journal of Mining Institute*. 2020;242:218–227. <https://doi.org/10.31897/PMI.2020.2.218>
2. Efimov D.A., Gospodarikov A.P. Technical and technological aspects of the use of Reuleaux triangular profile rolls in crushing units in the ore processing plant. *Mining Informational and Analytical Bulletin*. 2022;(10–2):117–126. (In Russ.) https://doi.org/10.25018/0236_1493_2022_102_0_117
3. Nikolaeva N.V., Kallaev I.T. Features of copper–molybdenum ore grinding. *Mining Informational and Analytical Bulletin*. 2024;(1):52–66. (In Russ.) https://doi.org/10.25018/0236_1493_2024_1_0_52
4. Lopéz R., Jordão H., Hartmann R. et al. Study of butyl-amine nanocrystal cellulose in the flotation of complex sulphide ores. *Colloids and Surfaces A: Physicochemical and Engineering Aspects*. 2019;579:123655. <https://doi.org/10.1016/j.colsurfa.2019.123655>
5. Chanturia V.A., Matveeva T.N., Ivanova T.A., Getman V.V. Mechanism of interaction of cloud point polymers with platinum and gold in flotation of finely disseminated precious metal ores. *Mineral Processing and Extractive Metallurgy Review*. 2016;37(3):187–195. <https://doi.org/10.1080/08827508.2016.1168416>
6. Matveeva T.N., Gromova N.K., Ivanova T.A., Chanturia V.A. Physicochemical effect of modified diethyldithiocarbamate on the surface of auriferous sulfide minerals in noble metal ore flotation. *Journal of Mining Science*. 2013;49(5):803–810. <https://doi.org/10.1134/S1062739149050158>
7. Owusu C., Agorhom E.A., Fosu S., Budu-Arthur E. Adsorption studies of sulphidic refractory gold ore. *Powder Technology*. 2020;375:310–316. <https://doi.org/10.1016/j.powtec.2020.07.063>
8. Yakovleva T.A., Romashev A.O., Mashevsky G.N. Digital technologies for optimizing the dosing of flotation reagents during flotation of non-ferrous metal ores. *Mining Informational and Analytical Bulletin*. 2022;(6–2):175–188. (In Russ.) https://doi.org/10.25018/0236_1493_2022_62_0_175
9. Aleksandrova T.N., Prokhorova E.O. Modification of properties of rock-forming minerals during flotation. *Mining Informational and Analytical Bulletin*. 2023;(12):123–138. (In Russ.) https://doi.org/10.25018/0236_1493_2023_12_0_123
10. Zakharov B.A., Meretukov M.A. *Gold: refractory ores*. Moscow: Ruda i Metally Publ. House; 2013. 452 p. (In Russ.)
11. Shumilova L.V., Kostikova O.S. Sulfidization of silver-polymetallic ores of “Goltsovoe” deposit for decreasing loss of silver in mill tailings. *Journal of Mining Institute*. 2018;230:160–166. <https://doi.org/10.25515/PMI.2018.2.160>
12. Rasskazova A.V., Sekisov A.G., Burdonov A.E. Activation leaching of difficult primary ore at Malmyzh deposit. *Mining Informational and Analytical Bulletin*. 2023;(1):130–141. (In Russ.) https://doi.org/10.25018/0236_1493_2023_1_0_130
13. Lavrik A.V., Konareva T.G., Rasskazova A.V. Recovery of submicron encapsulated gold from rebellious ore of Delken deposit. *Mining Informational and Analytical Bulletin*. 2021;(12–1):121–128. (In Russ.) https://doi.org/10.25018/0236_1493_2021_121_0_121
14. Lodeyshchikov V.V. *Technology of gold and silver extraction from refractory ores: in 2 vol. v. 1*, Irkutsk: JSC Irigredmet Publ.; 1999. 452 p. (In Russ.)
15. Grigoreva V.A., Boduen A.Ya. Prospects for refractory gold-sulfide ore processing. *Izvestiya. Non-Ferrous Metallurgy*. 2023;(6):22–34. <https://doi.org/10.17073/0021-3438-2023-6-22-34>
16. Petrov G.V., Gordeev D.V., Bekirova V.R. Comparison of methods for enhancing gold recovery from double refractory concentrates using the technology of autoclave oxidation. *iPolytech Journal*. 2023;27(4):809–820. (In Russ.) <https://doi.org/10.21285/1814-3520-2023-4-809-820>



17. Ivanik S.A., Ilyukhin D.A. Flotation extraction of elemental sulfur from gold-bearing cakes. *Journal of Mining Institute*. 2020;242:202–208. <https://doi.org/10.31897/PMI.2020.2.202>
18. Amankwah R.K., Pickles C.A. Microwave roasting of a carbonaceous sulphidic gold concentrate. *Minerals Engineering*. 2009;22(13):1095–1101. <https://doi.org/10.1016/j.mineng.2009.02.012>
19. Chanturiya V.A., Bunin I.Z. Advances in Pulsed Power Mineral Processing Technologies. *Minerals*. 2022;12(9):1177. <https://doi.org/10.3390/min12091177>
20. Wei W., Shao Z., Zhang Y. et al. Fundamentals and applications of microwave energy in rock and concrete processing – a review. *Applied Thermal Engineering*. 2019;157:113751. <https://doi.org/10.1016/j.applthermaleng.2019.113751>
21. Haque K.E. Microwave energy for mineral treatment processes – a brief review. *International Journal of Mineral Processing*. 1999;57(1):1–24. [https://doi.org/10.1016/S0301-7516\(99\)00009-5](https://doi.org/10.1016/S0301-7516(99)00009-5)
22. Amini A., Latifi M., Chaouki J. Electrification of Materials Processing via Microwave Irradiation: A Review of Mechanism and Applications. *Applied Thermal Engineering*. 2021;193:117003. <https://doi.org/10.1016/j.applthermaleng.2021.117003>
23. Pressacco M., Kangas J.J.J., Saksala T. Numerical modelling of microwave irradiated rock fracture. *Minerals Engineering*. 2023;203:108318. <https://doi.org/10.1016/j.mineng.2023.108318>
24. Shadi A., Ahmadihosseini A., Rabiei M. et al. Numerical and experimental analysis of fully coupled electromagnetic and thermal phenomena in microwave heating of rocks. *Minerals Engineering*. 2022;178:107406. <https://doi.org/10.1016/j.mineng.2022.107406>
25. Qin L., Chen G., Xu G. et al. Microscopic liberation mechanisms of oolitic iron ore under microwave irradiation and optimization of irradiation parameters. *Minerals Engineering*. 2022;178:107402. <https://doi.org/10.1016/j.mineng.2022.107402>
26. Duan B., Bobicki E.R., Hum S.V. Application of microwave imaging in sensor-based ore sorting. *Minerals Engineering*. 2023;202:108303. <https://doi.org/10.1016/j.mineng.2023.108303>
27. Siva L.M. da, Nascimento M., Oliveira E.M. de et al. Evaluation of the diffusional coefficient in the acid baking process using microwave energy to reduce phosphorus content in iron ore particles. *Minerals Engineering*. 2020;157:106541. <https://doi.org/10.1016/j.mineng.2020.106541>
28. Silva G.R. da, Espiritu E.R.L., Mohammadi-Jam S., Waters K.E. Surface characterization of microwave-treated chalcopyrite. *Colloids and Surfaces A: Physicochemical and Engineering Aspects*. 2018;555:407–417. <https://doi.org/10.1016/j.colsurfa.2018.06.078>
29. Li H., Long H., Zhang L. et al. Effectiveness of microwave-assisted thermal treatment in the extraction of gold in cyanide tailings. *Journal of Hazardous Materials*. 2020;384:121456. <https://doi.org/10.1016/j.jhazmat.2019.121456>
30. Kamariah N., Kalebic D., Xanthopoulos P. et al. Conventional versus microwave-assisted roasting of sulfidic tailings: mineralogical transformation and metal leaching behavior. *Minerals Engineering*. 2022;183:107587. <https://doi.org/10.1016/j.mineng.2022.107587>
31. Walkiewicz J.W., Kazonich G., McGill S.L. Microwave heating characteristics of selected minerals and compounds. *Minerals & metallurgical processing*. 1988;5:39–42. <https://doi.org/10.1007/BF03449501>
32. Farahat M., Elmahdy A.M., Hirajima T. Influence of microwave radiation on the magnetic properties of molybdenite and arsenopyrite. *Powder Technology*. 2017;315:276–281. <https://doi.org/10.1016/j.powtec.2017.04.023>
33. Golovenko Zh.V., Gafner S.L., Gafner Yu.Ya. Computer analysis of the structural properties of gold nanoclusters. *Fundamental Problems of Radio-Electronic Instrument Making*. 2010;7(2):11–16. (In Russ.)
34. Golovenko Zh.V., Gafner S.L., Gafner Yu.Ya. Investigation of structural states of gold nanoclusters by molecular dynamics method. *Fundamental Problems of Radio-Electronic Instrument Making*. 2008;8(2):83–86. (In Russ.)
35. Samsonov V.M., Sdobnyakov N.Y., Myasnichenko V.S. et al. A comparative analysis of the size dependence of the melting and crystallization temperatures in silver nanoparticles via the molecular dynamics and Monte-Carlo methods. *Journal of Surface Investigation: X-Ray, Synchrotron and Neutron Techniques*. 2018;12(6):1206–1209. <https://doi.org/10.1134/S1027451018050671> (Orig. ver.: Samsonov V.M., Sdobnyakov N.Y., Myasnichenko V.S. et al. A comparative analysis of the size dependence of the melting and crystallization temperatures in silver nanoparticles via the molecular dynamics and Monte-Carlo methods. *Poverkhnost'. Rentgenovskie, Sinkhrotronnnye i Neitronnye Issledovaniya*. 2018;(12):65–69. <https://doi.org/10.1134/S0207352818120168>)
36. Aleksandrova T.N., Nikolaeva N.V., Afanasova A.V. et al. Extraction of low-dimensional structures of noble and rare metals from carbonaceous ores using low-temperature and energy impacts at succeeding stages of raw material transformation. *Minerals*. 2023;13(1):84. <https://doi.org/10.3390/min13010084>



37. Afanasova A.V., Aburova V.A. Growth of low-dimensional structure noble metals in carbonaceous materials under microwave treatment. *Mining Informational and Analytical Bulletin*. 2024;(1):20–35. (In Russ.) https://doi.org/10.25018/0236_1493_2024_1_0_20
38. Amdur A.M., Fedorov S.A., Matushkina A.N. Extraction of gold from definitely processing ores and technogenic waste by their high-temperature treatment and subsequent centrifugal separation. *Mining Informational and Analytical Bulletin*. 2022;(11-1):95–106. (In Russ.) https://doi.org/10.25018/0236_1493_2022_111_0_95

Information about the authors

Tayana N. Aleksandrova – Dr. Sci. (Eng.), Professor, Corresponding Member of the Russian Academy of Sciences, Empress Catherine II Saint Petersburg Mining University, St. Petersburg, Russian Federation; ORCID [0000-0002-3069-0001](https://orcid.org/0000-0002-3069-0001), Scopus ID [57216873316](https://scopus.org/57216873316), ResearcherID [A-5418-2014](https://orcid.org/A-5418-2014); e-mail: Aleksandrova_TN@pers.spmi.ru

Anastasia V. Afanasova – Cand. Sci. (Eng.), Associate Professor, Empress Catherine II Saint Petersburg Mining University, St. Petersburg, Russian Federation; ORCID [0000-0002-8451-2489](https://orcid.org/0000-0002-8451-2489), Scopus ID [57188630049](https://scopus.org/57188630049), ResearcherID [AAH-4333-2019](https://orcid.org/AAH-4333-2019); e-mail: Afanasova_av@pers.spmi.ru

Valeria A. Aburova – PhD-Student, Empress Catherine II Saint Petersburg Mining University, St. Petersburg, Russian Federation; ORCID [0000-0002-1364-5006](https://orcid.org/0000-0002-1364-5006), Scopus ID [57503048800](https://scopus.org/57503048800); e-mail: aburovaleria@gmail.com

Received 13.03.2024

Revised 23.04.2024

Accepted 10.06.2024



SAFETY IN MINING AND PROCESSING INDUSTRY AND ENVIRONMENTAL PROTECTION

Research paper

<https://doi.org/10.17073/2500-0632-2024-03-234>

UDC 658.386:622.867

**Assessment of readiness of auxiliary mine rescue teams in coal mines**V. A. Rudenko  

Federal State Unitary Enterprise “Militarized Mine Rescue Unit” (FSUE “VGSC”), Moscow, Russian Federation

 rescue@vgsch.ru**Abstract**

The efficiency of mine rescue operations largely depends on how quickly efforts to localize and mitigate an accident are initiated. Given the remoteness of some mining enterprises, a decision was made to form auxiliary mine rescue teams composed of miners. However, there is ongoing debate regarding the effectiveness of the rescue operations carried out by these auxiliary teams. This paper presents data on the assessment of the readiness of auxiliary mine rescue teams in Russian coal mines. A survey of professional mine rescuers was conducted across all units and platoons, focusing on key aspects of auxiliary team operations. The results, based on expert evaluations, revealed the main challenges in training auxiliary team members and highlighted areas for improving the regulatory and methodological framework for mine rescue tactics. The second part of the paper presents the results of control-tactical exercises held at seven mines. These unannounced exercises took place at the end of a work shift and evaluated a wide range of knowledge, skills, abilities, and physical fitness among the auxiliary teams. Key evaluations included the accuracy of task allocation, tactical training, preparation for mine descent, the use of rescue equipment, first aid skills, theoretical knowledge, and physical fitness.

Keywords

militarized mine rescue units, auxiliary mine rescue team, coal mine, safety, accident, expert assessment, tactical exercises

For citation


Rudenko V.A. Assessment of readiness of auxiliary mine rescue teams in coal mines. *Mining Science and Technology (Russia)*. 2024;9(3):243–249. <https://doi.org/10.17073/2500-0632-2024-03-234>

**ТЕХНОЛОГИЧЕСКАЯ БЕЗОПАСНОСТЬ В МИНЕРАЛЬНО-СЫРЬЕВОМ КОМПЛЕКСЕ
И ОХРАНА ОКРУЖАЮЩЕЙ СРЕДЫ**

Научная статья

**Оценка готовности вспомогательных горноспасательных команд
угольных шахт**В. А. Руденко  

ФГУП «Военизированная горноспасательная часть» (ФГУП «ВГСЧ»), г. Москва, Российская Федерация

 rescue@vgsch.ru**Аннотация**

Эффективность ведения горноспасательных работ зависит от времени, когда приступили к локализации и ликвидации аварии. В связи с удалённостью некоторых горных предприятий было принято решение о создании вспомогательных горноспасательных команд из числа горнорабочих. При этом эффективность аварийно-спасательных работ, проводимых членами вспомогательных горноспасательных команд в настоящее время вызывает много споров. В данной работе приведены сведения по оценке готовности вспомогательных горноспасательных команд угольных шахт России. По всем отрядам и взводам было проведено анкетирование профессиональных горноспасателей по основным вопросам деятельности вспомогательных горноспасательных команд. Полученные методом экспертных оценок результаты позволили определить основные проблемы в подготовке членов вспомогательных горноспасательных команд, выявить направления совершенствования нормативно-правовой и методической базы по тактике ведения аварийно-спасательных работ. Во второй части работы представлены результаты проведенных контрольно-тактических учений, проведенных на семи шахтах. Учения проводились внепланово в конце рабочей смены. Проверялся целый спектр знаний, навыков, умений



и физическая подготовка членов вспомогательных горноспасательных команд. А именно проверялось правильность выдачи заданий, тактическая подготовка отделений, правильность подготовки к спуску в шахту и применения горноспасательного оборудования, навыки оказания первой помощи, теоретические знания и физическая подготовка.

Ключевые слова

военизированные горноспасательные части, вспомогательная горноспасательная команда, угольная шахта, безопасность, авария, экспертная оценка, тактические учения

Для цитирования

Rudenko V.A. Assessment of readiness of auxiliary mine rescue teams in coal mines. *Mining Science and Technology (Russia)*. 2024;9(3):243–249. <https://doi.org/10.17073/2500-0632-2024-03-234>

Introduction

The safety of mining operations is directly influenced by the qualifications of miners and technical staff. Currently, 38 higher education institutions and 114 colleges in Russia provide training for the mining industry [1, 2]. However, training in mining safety and mine rescue (a mandatory discipline) varies significantly in quality across educational institutions, with instructors of differing qualifications and often insufficient training facilities [3, 4]. Accidents in mining enterprises usually occur due to the low qualification of employees [5]. Moreover, only a few universities offer in-depth training in mine rescue [4, 6]. Abroad, where mine rescue is more advanced, there are no auxiliary mine rescue teams¹ [7]. In Russia, the preparation of personnel for accident localization and elimination in the initial stages is carried out only by the divisions of the Federal State Unitary Enterprise “Militarized Mine Rescue Unit” (FSUE “VGSC”).

The mine rescue service in Russia traces its origins back to the 32nd Congress of Mine Industrialists in 1907, where the decision was made to establish rescue stations at the most dangerous mines and pits. By 1920, over 40 stations had been set up, staffed by engineers, technical workers, and miners working part-time for additional pay.

The professional state mine rescue service of Russia, with a centralized management structure, was officially established on July 6, 1922, following the adoption of the government resolution “On Mine Rescue Operations in the RSFSR”². All mine rescue stations were brought under state control and tasked with rescuing people and mitigating accidents at all mining enterprises without exception.

In 1932, recognizing the extreme nature of mine rescue work in high-temperature, oxygen-deprived environments, and the need for strict command and execution of orders, the Council of Labour and Defence militarized the mine rescue units, placing them under the authority of the Department of Military Specialized Units and Air Defence of the People's Commissariat of Heavy Industry. This decision accelerated the development of mine rescue units in the country. Operational work became regulated by official charters, provisions, and instructions, with established ranks for personnel ranging from privates to senior officers. Uniforms and insignia were also introduced.

Until 2010, mine rescue services for mining operations were provided by various militarized mine rescue services, including FGKU “VGSC in Construction”, JSC “VGSC”, and FSUE “Metallurgbezopasnost”, which all shared the same mission – saving lives and eliminating accidents during mining operations in coal, mining, and underground construction industries.

In 2010, by Presidential Decree No. 554³ of May 6, 2010, the oversight of militarized mine rescue units was transferred to the Ministry of Emergency Situations (EMERCOM) of Russia.

In 2011, FSUE “SPO Metallurgbezopasnost” was renamed FSUE “Militarized Mine Rescue Unit”, and all operational units of JSC “VGSC” were incorporated into its structure.

At present, the Ministry of Emergency Situations of Russia includes five militarized mine rescue organizations: FSUE “VGSC”, FAU “VGSC in Construction”, FGKU “National Mine Rescue Centre”, FGKU “VGSC LNR”, and FGKU “VGSC DNR”. The total number of personnel in these organizations is 8,584.

Operational units of VGSC EMERCOM are territorially distributed across 40 regions of the Rus-

¹ Handbook of training in mine rescue and recovery operations. Workplace Safety North (WSN). North Bay Ontario; 2021. 378 p.; Western Canada Mine Rescue Manual Ministry of Energy and Mines. Office of the Chief Inspector of Mines; 2016. 195 p.

² Decree of the All-Russian Central Executive Committee and the Council of People's Commissars “On Mine Rescue in the RSFSR”. URL: <https://scgss.narod.ru/Postanovlenie.gif>

³ Presidential Decree of the Russian Federation No. 554, dated May 6, 2010, “On the Improvement of the Unified State System for the Prevention and Mitigation of Emergency Situations”. URL: <http://www.kremlin.ru/acts/bank/31043>

sian Federation (Fig. 1) and include 26 militarized mine rescue detachments, consisting of 71 platoons, 103 mine rescue posts, and 25 mine rescue stations equipped with specialized equipment, tools, and materials.

VGSCHEM units provide coverage for 2,350 hazardous industrial facilities in the mining industry, including 168 coal mines, 143 underground mineral extraction sites, 28 underground construction facilities, 1,259 open-pit mining sites, 224 mineral processing and enrichment plants, and 528 other hazardous production sites.

The VGSCHEM forces of Russia's EMERCOM comprise 5,487 personnel and 978 units of equipment (specifically: FSUE "VGSCHEM" – 3,922 personnel and 756 units of equipment; FAU "VGSCHEM in Construction" – 216 personnel and 53 units of equipment; FGKU "National Mine Rescue Centre" – 66 personnel and 13 units of equipment; FGKU "VGSCHEM LNR" – 448 personnel and 71 units of equipment; FGKU "VGSCHEM DNR" – 835 personnel and 85 units of equipment). Of these, 1,364 rescuers and 276 units of equipment are on round-the-clock duty.

The management of VGSCHEM within the central apparatus of EMERCOM is assigned to the Rescue Units Department, which is responsible for overseeing the activities of VGSCHEM, coordinating with regional branches of EMERCOM, and developing a unified

national policy for the development, training, and deployment of VGSCHEM.

A special role in the emergency protection system is given to Auxiliary Mine Rescue Teams (AMRT). To date, nearly 100,000 members of AMRT have been trained.

Each year, thousands of miners participate in both initial and refresher training (Fig. 2). The training follows a standardized and approved curriculum, conducted every three years. Additionally, every six months, members of the AMRT undergo team-based training in the use of isolating breathing apparatus.

To assess the necessity and effectiveness of the auxiliary mine rescue teams, research was conducted that included expert evaluations and tactical exercises at seven mines in Russia.

Research on the effectiveness of AMRT actions

A survey was conducted among the command staff of VGSCHEM, with 334 respondents participating. Of these, 89% of professional rescuers believe that auxiliary mine rescue teams should be established at mining enterprises.

However, 82% of respondents feel that AMRT members are exposed to less life-threatening risk than professional mine rescuers. Additionally, only 5% reported that AMRT members had been injured during accident localization and mitigation efforts.



Fig. 1. Deployment of units and composition of VGSCHEM forces within EMERCOM of Russia

An interesting result emerged when respondents were asked if AMRT members had ever refused to participate in emergency rescue operations (ERO). Responses were almost evenly split: 53% said yes, while 47% said no. This brings the issue of motivation into focus. It is one thing to be a member of the AMRT, but another to enter a mine during an accident and risk one's life and health.

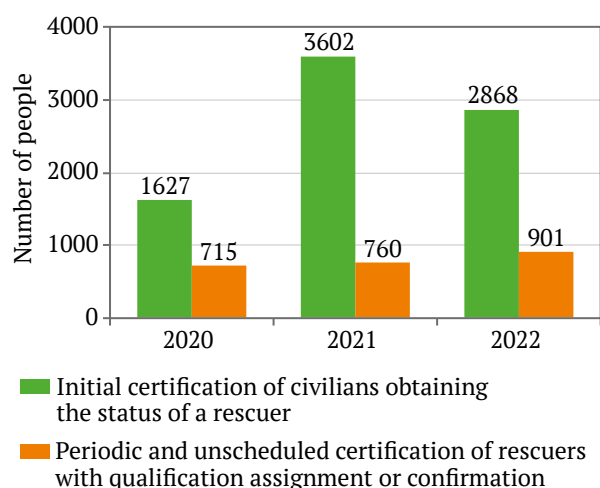
The main challenges in preparing AMRT members, according to the mine rescue community, are insufficient physical training, low proficiency in operating mine rescue equipment, and difficulties with self-organization. Nearly unanimously (75%), respondents agreed that the number of training hours for AMRT members needs to be increased. Currently, AMRT training lasts 72 hours as part of their certification.

Questions about the necessary number of AMRT members required for tasks such as first aid or firefighting remain unanswered (Fig. 3). Consequently,

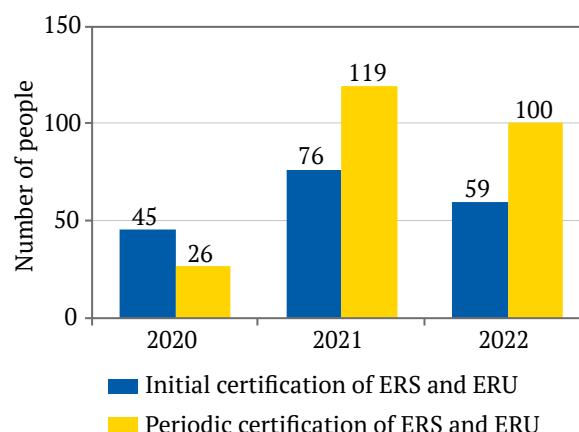
many questions arise regarding the tactics used by AMRT members during rescue operations. At present, there is no officially approved tactical document specifically for AMRT. In the absence of such a document, AMRT members rely on the regulations followed by professional mine rescuers during emergency response operations.

When asked, "What do AMRT members lack?" almost all respondents pointed to skills in working as part of a team.

It is crucial to understand how effective AMRT rescue operations truly are, especially considering the significantly different starting conditions they face compared to professional mine rescuers. For instance, an accident could occur at the end of a work shift, after AMRT members have already worked 6–8 hours at their regular jobs. Unlike professional mine rescuers, AMRT members do not have the same level of ingrained proficiency in using breathing apparatus, honed through repeated practice.

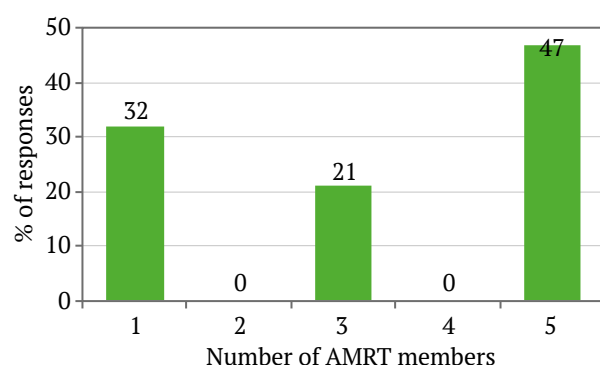


a

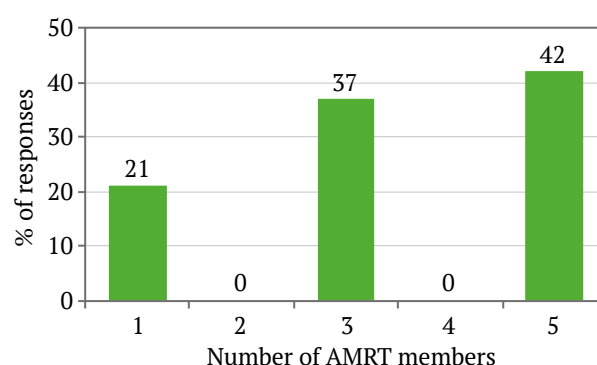


b

Fig. 2. Certification statistics of AMRT members (a) and emergency rescue services (units) (ERS/ERU) (b)



a



b

Fig. 3. The required minimum number of AMRT members: a) for providing first aid to the injured, b) for firefighting



safety protocols and miscalculated the time required to advance into the high-temperature zone (HTZ). At Mine “3”, the commander neglected to instruct the unit to secure themselves with ropes, failed to inform the team about the gas levels, and did not mention the need to disconnect from respirators when necessary. During movement through the mine and while inside the HTZ, both the commander and the team did not adhere to the correct practice of staying in the lower sections of the mine workings. At Mine “4”, the commander did not communicate the potential spread of the accident within the mine workings. Unit 1 proceeded to enter gas-filled areas directly at the entrance to the affected zone, where the air was being contaminated by the fire. At Mine “5”, the commander incorrectly calculated the oxygen supply needed to

advance in an atmosphere unsuitable for breathing. At Mine “6”, the commander did not notify the unit about the impacted areas or the potential spread of the accident.

In real situations, these and other errors could result in the deaths of AMRT members and worsen the accident.

Conclusion

Critical deficiencies were noted at all mines. The overall performance results are summarized in the diagram (Fig. 5). The biggest issues were in task allocation and the use of rescue equipment, while tactical preparation and first aid procedures were relatively stronger. These areas will be the focus of future improvements.

Table

Assessment of theoretical competence and physical fitness

No.	Year of birth	Current position	Position in AMRT at the mine	Education	Experience (years)	Test scores	Overall assessment of theoretical competence of AMRT members	Pull-up requirement (Yes/No)	Push-up requirement (Yes/No)
1.	1978	Deputy chief engineer	AMRT Leader	Higher	18	4	3.3	Yes	Yes
2.	1978	Mine foreman	Squad Leader AMRT No.1	Technical	15	3		No	Yes
3.	1987	Miner	AMRT Member	Higher	5	4		Yes	Yes
4.	1993	Stope miner	AMRT Member	Secondary	7	3		Yes	Yes
5.	1992	Underground equipment operator	AMRT Member	Secondary	4	3		No	Yes
6.	1983	Stope miner	AMRT Member	Secondary	15	3		Yes	No
7.	1995	Deputy section head	Squad Leader AMRT No.2	Secondary	10	3		Yes	Yes
8.	1995	Driller	AMRT Member	Secondary	3	3		Yes	Yes
9.	1989	Driller	AMRT Member	Technical	9	3		Yes	No
10.	1995	Miner	AMRT Member	Secondary	4	3		Yes	Yes
11.	1983	Stope miner	AMRT Member	Secondary	12	4		Yes	No

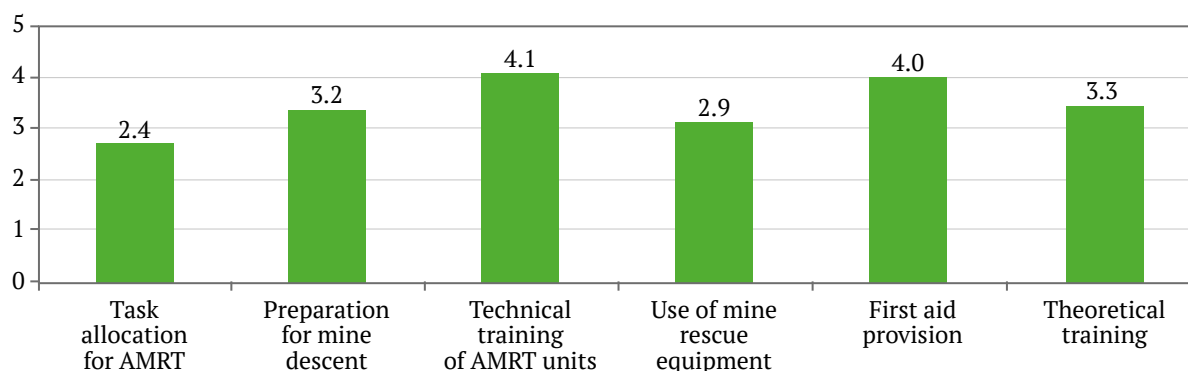


Fig. 5. Average chart of deficiencies in AMRT member training from control-tactical exercises



It should be noted that some types of accidents [8] are more complex, making it difficult to quickly locate the accident site. In such cases, the risk of AMRT members making incorrect decisions is higher.

Possible ways to improve safety and efficiency of AMRT operations:

1. Boost motivation by significantly increasing the additional compensation – currently, the supplementary pay ranges from 3–10% of base salary; by offering government guarantees of support for AMRT members in the event of injury during rescue operations; and by ensuring support for their families in the case of death or injury.

2. Increase the number of training hours for AMRT members, conduct unannounced inspections, and organize competitions across mining industry organizations.

3. Develop rescue operation tactics that account for the number of AMRT members available at the accident site, potential issues with team cohesion, and the physical condition of miners at different points in their work shift.

Only by implementing this comprehensive set of measures can the safety and effectiveness of AMRT rescue operations be improved.

References

1. Petrov V.L., Puchkov L.A. The system of higher mining education in Russia. *Eurasian Mining*. 2017;(2):57–60. <https://doi.org/10.17580/em.2017.02.14>
2. Petrov V.L. Analytical review of the training system for mining engineers in Russia. *Mining Science and Technology (Russia)*. 2022;7(3):240–259. <https://doi.org/10.17073/2500-0632-2022-3-240-259>
3. Kaledina N.O. Engineer training of mine rescue men. *Gornyi Zhurnal*. 2018;(5):86–89. (In Russ.) <https://doi.org/10.17580/gzh.2018.05.14>
4. Kobylkin S.S., Rudenko V.A. Training of miners in mine rescue. *Ugol'*. 2023;(11):30–42. (In Russ.) <https://doi.org/10.18796/0041-5790-2023-11-30-42>
5. Kolikov K.S., Grishin V. Yu., Ishkhineli O. G. Accidents and injuries at coal industry enterprises. *Okhrana Truda i Sotsial'noye Strakhovaniye*. 2020;(6):34–44. (In Russ.)
6. Kolikov K.S., Kaledina N.O., Kobylkin S.S. Mining Safety and Ecology Department: past, present and future. *Gornyi Zhurnal*. 2018;(3):21–28. (In Russ.) <https://doi.org/10.17580/gzh.2018.03.04>
7. Enright C., Ferriter R.L. *Mine rescue manual. a comprehensive guide for mine rescue team members*. Society for Mining, Metallurgy, and Exploration, Inc.; 2015. 196 p.
8. Kobylkin S.S., Kharisov A.R. Design features of coal mines ventilation using a room-and-pillar development system. *Journal of Mining Institute*. 2020;245:531–538. <https://doi.org/10.31897/PMI.2020.5.4>

Information about the author

Vitaly A. Rudenko – First Deputy General Director, Federal State Unitary Enterprise “Military Mine Rescue Unit” (FSUE “VGSC”), Moscow, Russian Federation; ORCID [0009-0002-7365-0015](https://orcid.org/0009-0002-7365-0015); e-mail rescue@vgsch.ru

Received 26.03.2024

Revised 14.04.2024

Accepted 22.05.2024



SAFETY IN MINING AND PROCESSING INDUSTRY AND ENVIRONMENTAL PROTECTION

Research paper

<https://doi.org/10.17073/2500-0632-2024-02-223>

UDC 624

**Investigation of thermodynamic parameters of the air environment in subway lines with single-track and double-track tunnels****S. G. Gendler¹  , M. S. Kryukova¹   , E. L. Alferova²  **¹ *Empress Catherine II St. Petersburg Mining University, St. Petersburg, Russian Federation*² *N.A. Chinakal Institute of Mining, Siberian Branch of the Russian Academy of Sciences, Novosibirsk, Russian Federation* s215068@stud.spmi.ru**Abstract**

The study of thermodynamic parameters in the air environment of subway lines is of particular relevance due to the substantial differences in air temperatures between Russian cities and those abroad. These temperature variations influence the formation of aerothermodynamic characteristics, which must be considered when selecting methods to ensure compliance with standard climatic parameters in subway systems. The objective of the study presented in this article was to identify, based on experimental data, the patterns governing aerothermodynamic processes, with the aim of providing recommendations for the standardization of air environment parameters in subway tunnels (both single- and double-track) located at different depths. The primary tasks of the research involved identifying the factors influencing the distribution and variation of temperature and humidity, conducting instrumental measurements of temperature and humidity distribution along the length of the transit tunnel sections under investigation, both in the absence of trains and during varying intensities of train movement. Proposals were then developed to apply the identified patterns in maintaining standard air parameters. The article posits that the selection of technical solutions for improving subway ventilation systems should be based on the unique features of aerothermodynamic processes, which depend on the structural characteristics of the transit tunnels and their depth. Experimental studies revealed the patterns governing the formation of ventilation and thermal regimes in single-track and double-track tunnels, as well as at junction sections, and provided recommendations for optimizing ventilation and thermal regimes to ensure compliance with climatic standards. Specifically, the study found that in deep single-track tunnels, the thermal regime is influenced by the presence of circulation loops between adjacent stations, created by the piston effect and the heat emissions from moving trains. Circulation loops in shallow single-track tunnels, by contrast, are characterized by strong aerodynamic connections with the surface, as surface air enters the stations and tunnels via pedestrian walkways and inclined passages. In double-track underground structures, in the absence of train movement, the variation in air temperature along the length of the transit tunnel is determined by the amount of heat accumulated in the surrounding ground during periods of train operation. When trains are in motion, the heat emitted by trains moving in opposite directions is evenly distributed along the tunnel, due to the near absence of a piston effect, resulting in a stable air temperature throughout the tunnel. However, the sections adjacent to stations experience localized increases in air temperature due to the maximum heat generated during braking and train stops, with tunnel air temperatures in these sections rising by 2–3 °C compared to those in the transit sections. In sections where both single-track and double-track tunnels are present, a potential rise in air temperature at the station adjacent to single-track tunnels is associated with the formation of circulation loops between the junction of different tunnel types and the station itself. Recommendations for normalizing the aerothermodynamic regime in the various tunnel types studied include provisions for mitigating potential summer air temperature increases above the standard levels by either increasing air flow or cooling the air in cross passages adjacent to stations. Methods for increasing air temperature may include organizational, aerodynamic, and heat engineering techniques.

Keywords

subway, tunnels, single-track tunnels, double-track tunnels, tunnel operation, tunnel ventilation, ventilation schemes, ventilation regime, thermal regime

For citation

Gendler S.G., Kryukova M.S., Alferova E.L. Investigation of thermodynamic parameters of the air environment in subway lines with single-track and double-track tunnels. *Mining Science and Technology (Russia)*. 2024;9(3):250–262. <https://doi.org/10.17073/2500-0632-2024-02-223>



ТЕХНОЛОГИЧЕСКАЯ БЕЗОПАСНОСТЬ В МИНЕРАЛЬНО-СЫРЬЕВОМ КОМПЛЕКСЕ И ОХРАНА ОКРУЖАЮЩЕЙ СРЕДЫ


Научная статья

Исследование термодинамических параметров воздушной среды на линиях метрополитенов с однопутными и двухпутными тоннелями

С. Г. Гендлер¹  , М. С. Крюкова¹   , Е. Л. Алферова²  

¹ Санкт-Петербургский горный университет императрицы Екатерины II, г. Санкт-Петербург, Российская Федерация

² Институт горного дела СО РАН им. Н. А. Чинакала, г. Новосибирск, Российская Федерация

 s215068@stud.spmi.ru

Аннотация

Актуальность проблемы термодинамических параметров воздушной среды на линиях метрополитена заключается в существенной разнице температур воздуха городов России и городами зарубежных стран. Данная температурная разница определяет и закономерности формирования аэротермодинамических параметров воздушной среды, которые необходимо учитывать при выборе способов обеспечения нормативных климатических параметров воздуха. Исследование, представленное в статье, проводилось с целью установления на основе экспериментальных данных закономерностей протекания аэротермодинамических процессов для последующей разработки рекомендаций по нормированию параметров воздушной среды в тоннелях метрополитена (однопутных и двухпутных), расположенных на разной глубине заложения. Основные задачи сводятся к определению факторов, оказывающих влияние на установление распределения температур (влажностей) и закономерностей их изменения, проведение инструментальных измерений распределения температур (влажностей) воздуха по длине исследуемых участков перегонных тоннелей как при отсутствии поездов, так и при их движении с различной интенсивностью; разработке предложений по использованию выявленных закономерностей для обеспечения нормативных параметров воздушной среды. Идея статьи состоит в том, что в качестве основы для выбора технических решений по совершенствованию систем вентиляции метрополитенов следует принимать выявленные особенности формирования аэротермодинамических процессов, зависящих от конструктивных параметров перегонных тоннелей и глубины их заложения. На основе выполненных экспериментальных исследований были выявлены закономерности формирования вентиляционных и тепловых режимов однопутных, двухпутных тоннелей и участка сопряжения и предложены мероприятия по совершенствованию вентиляционного и теплового режимов, обеспечивающих нормативные климатические условия. В частности, было установлено, что в однопутных тоннелях глубокого заложения тепловой режим определяется наличием циркуляционных контуров между соседними станциями, которые возникают в результате поршневого эффекта, и тепловыделениями от движущихся поездов; отличием циркуляционных контуров, сформировавшихся в подземных сооружениях мелкого заложения однопутного типа, является наличие плотной аэродинамической связи с поверхностью. Тем самым подземные сооружения мелкого заложения насыщаются поверхностным воздухом, который поступает на станции и в тоннели по пешеходным путям и наклонным ходам; в подземных сооружениях двухпутного типа при отсутствии движения подвижных составов характер изменения температуры воздуха по длине перегона определялся количеством теплоты, которая была аккумулирована грунтом в период движения поездов. Во время движения теплота, выделяемая поездами, движущимися навстречу друг другу при практическом отсутствии поршневого эффекта, равномерно распределяется по длине перегона. Это обуславливает постоянную температуру воздуха в тоннелях за исключениями участков, непосредственно прилегающих к станциям, где в период торможения и остановки поездов количество продуцируемой ими теплоты максимально, соответственно, температура тоннельного воздуха в пристанционных выработках увеличивается на 2–3 °С в сравнении с температурой на перегонах. На участках, включающих два типа подземных сооружений, возможный рост температуры воздуха на станции, прилегающей к однопутным тоннелям, связан с образованием циркуляционных контуров между участком сопряжения разных типов конструкции тоннелей и станции, прилегающей к ним. Также разработаны рекомендации по нормализации аэротермодинамического режима для рассмотренных типов тоннелей: при установленной возможности превышения в летнее время температурой воздуха нормативных параметров (значений) необходимо предусмотреть или резерв по его расходу, или его охлаждение в сбойках, прилегающих к станциям. Для повышения температуры воздуха могут быть использованы организационные, аэродинамические и теплотехнические методы.

Ключевые слова

метрополитен, тоннели, однопутные тоннели, двухпутные тоннели, эксплуатация тоннелей, вентиляция тоннелей, схемы проветривания тоннелей, вентиляционный режим, тепловой режим

Для цитирования

Gendler S. G., Kryukova M. S., Alferova E. L. Investigation of thermodynamic parameters of the air environment in subway lines with single-track and double-track tunnels. *Mining Science and Technology (Russia)*. 2024;9(3):250–262. <https://doi.org/10.17073/2500-0632-2024-02-223>



Introduction

Currently, subways operate in seven major cities across Russia. Each of these subway systems has its own specific characteristics in terms of structural design, technological approaches to construction and operation, and engineering support for their functioning, including ventilation systems (Table 1).

As shown in Table 1, the vast majority of subway lines consist of both deep and shallow single-track tunnels. However, in recent years, the construction of double-track tunnels has begun in the Moscow and St. Petersburg subway systems, facilitated by the development of modern construction geotechnologies utilizing mechanized tunnel shields (MTSs) [1]. The use of MTSs has made it possible to construct double-track tunnels even under the challenging engineering and geological conditions of St. Petersburg [2].

The prospects for using double-track tunnels have been demonstrated by many years of successful operation in numerous global megacities. According to publications [3], even in hot climates, the ventilation design solutions for double-track tunnels provide more comfortable air thermodynamic parameters during operation compared to their single-track counterparts.

In Russia, double-track tunnels have been successfully operated in Moscow and St. Petersburg. There are future plans to implement double-track sections in Novosibirsk and Yekaterinburg.

Research data [4, 5] indicate that the primary factors influencing the aerothermodynamic characteristics of the air environment in tunnels include: external meteorological conditions (Table 2); the geometric parameters of the tunnel alignment, which

Table 1

Characteristics of Subways in Russia [compiled by the authors]

No	City	Number of stations	Subway line composition				Systems for ensuring normative air parameters	
			Single-track tunnel lines		Double-track tunnel lines		Ventilation	Heating (cooling)
			Length, km	Depth, m	Length, km	Depth, m		
1	Moscow	306	~1010	~60	~11.57	~17–46	Yes	No (Yes)
2	St. Petersburg	72	~114	~70	~10.94	~10–68	Yes	No (Yes)
3	Nizhny Novgorod	16	~22	~10	–	–	Yes	Yes (Yes)
4	Kazan	11	~16.9	~10	–	–	Yes	No (no)
5	Samara	10	~11.6	~20	–	–	Yes	Yes (Yes)
6	Yekaterinburg	9	~13.8	20	–	–	Yes	Yes (Yes)
7	Novosibirsk	13	~15.9	10	–	–	Yes	Yes (Yes)

Table 2

Climatic conditions in Russian cities with operating subway systems [compiled by the authors]

No	City	Air temperatures	
		Average annual temperature, °C	Average winter / summer / January / July temperature, °C
1	Moscow	7.00	–7.5 / 20.3 / –5.5 / 20.5
2	St. Petersburg	6.75	–6.75 / 19.17 / –4.5 / 19.5
3	Nizhny Novgorod	5.88	–11.75 / 19.67 / –8.5 / 20
4	Kazan	5.25	–15.5 / 20 / –10 / 20.5
5	Samara	7.08	–13.25 / 7.08 / –9 / 22
6	Yekaterinburg	4.08	–18.75 / 18.5 / –10.5 / 20
7	Novosibirsk	2.67	–29.5 / 17.67 / –13.5 / 19
8	Madrid	17.42	18.25 / 28 / 7 / 30.5
9	Rome	18.29	10.17 / 27.83 / 7.5 / 29
10	London	13.29	13.25 / 20.16 / 6.5 / 21.5
11	Turin	13.71	10.25 / 22.67 / 5 / 24
12	Beijing	13.46	–4.25 / 26.33 / –2 / 27.5



affect the energy consumption for train movement; train operation parameters, such as speed and headway (i.e., the number of train pairs per hour); the tunnel depth relative to the surface; the type of transit tunnel (single- or double-track); ventilation schemes; and the presence of additional infrastructure between stations, such as cross-passages between single-track tunnels, ventilation structures for air supply, and other auxiliary facilities.

Table 2 positions 8–12 illustrate the differences between air temperatures in Russian cities where subway systems are located and cities abroad, where this mode of transport has seen significant development.

The harsh climate of Russia significantly affects the aerothermodynamic characteristics of the atmospheric air, which must be considered when developing measures to maintain optimal climate conditions [6].

The objective of this study is to identify, based on experimental data, the patterns of aerothermodynamic processes in subway tunnels (both single-track and double-track) located at various depths, with the goal of providing recommendations for standardizing air environment parameters.

The research methodology employed was based on experimental studies described in [7]. The mathematical models used to predict thermodynamic air parameters in underground transport systems allow for reliable verification of experimental results [8].

Experimental studies were conducted in various tunnel structures, including single-track and double-track tunnels at different depths in the St. Petersburg subway, as well as in shallow single-track tunnels in the Novosibirsk subway.

The main tasks addressed during the research include the following:

1. Instrumental measurements of temperature (and humidity) distribution along the studied sections of transit tunnels, both in the absence of trains and during their movement at various intensities (measured by the number of train pairs per hour, pairs/h);

2. Identification of the main factors influencing the observed temperature (and humidity) distributions;

3. Establishment of patterns in temperature and humidity changes;

4. Development of proposals for applying the identified patterns to ensure compliance with standard air environment parameters.

The central idea of the article is that the selection of technical solutions for improving subway ventilation systems should be based on the identified features of aerothermodynamic processes, which depend on the structural parameters of the transit tunnels and their depth.

Ventilation and thermal regimes of deep single-track tunnels

As shown in Table 1, the main subway lines in St. Petersburg consist of single-track tunnels with a depth of more than 50 meters.

In the summer of 2023, staff from St. Petersburg Mining University, in collaboration with GUP “Petersburg Metro”, carried out on-site measurements of air temperature and relative humidity in the tunnel section of the third Nevsky-Vasileostrovsky line, covering the interstation sections between the “Primorskaya”, “Vasileostrovskaya”, and “Gostiny Dvor” stations.

Temperature measurements, both during train operation and in periods without train movement, were taken using iButton Temperature Loggers with an accuracy of $\pm 0.5^\circ\text{C}$. These loggers were placed along the length of the mentioned sections (Fig. 1).

In ventilation ducts, the temperature loggers were mounted on vertical supports, while in transport zones, they were attached to the tunnel lining. Measurements were recorded at intervals of 120 seconds over seven days, and the data were stored in the logger’s memory. Once a week, the sensors were collected, and the data were transferred to electronic media (personal computer) using a special receiver device.

Surface temperature values of the tunnel lining and relative humidity were measured during periods without train movement using an infrared pyrometer and a hygrometer (TESTO 625), respectively.

The ventilation in the “Primorskaya”–“Vasileostrovskaya” and “Vasileostrovskaya”–“Gostiny Dvor” sections during both train operation and idle periods followed specific ventilation schemes. These schemes involved supplying outside air to the stations and nearby cross-passages, with the air then being extracted through ventilation shafts along the tunnel sections. In another scenario, outside air was introduced via the station and tunnel shafts, with the outgoing airflow exhausted through the “Gostiny Dvor” station.

In the selected segment, particularly the “Primorskaya”–“Vasileostrovskaya” section, ventilation units were operated in inflow/exhaust mode at full capacity: VOM-24R, FTDA-REV-200, with air flow rates of approximately 46–56.4 m³/s and air speeds of 4.6–5.64 m/s at a fan depression of ~922–1100 Pa.

In the “Vasileostrovskaya”–“Gostiny Dvor” track section, the following units were in use: VOM-18R, VOM-18-01, FTDA-REV-180, FTDA-REV-200. Air flow rates were ~48.6–74.8 m³/s (with speeds of 4.86–7.48 m/s) at fan depressions of ~990–1520 Pa.

The measurement results are presented in Figs. 2 and 3.

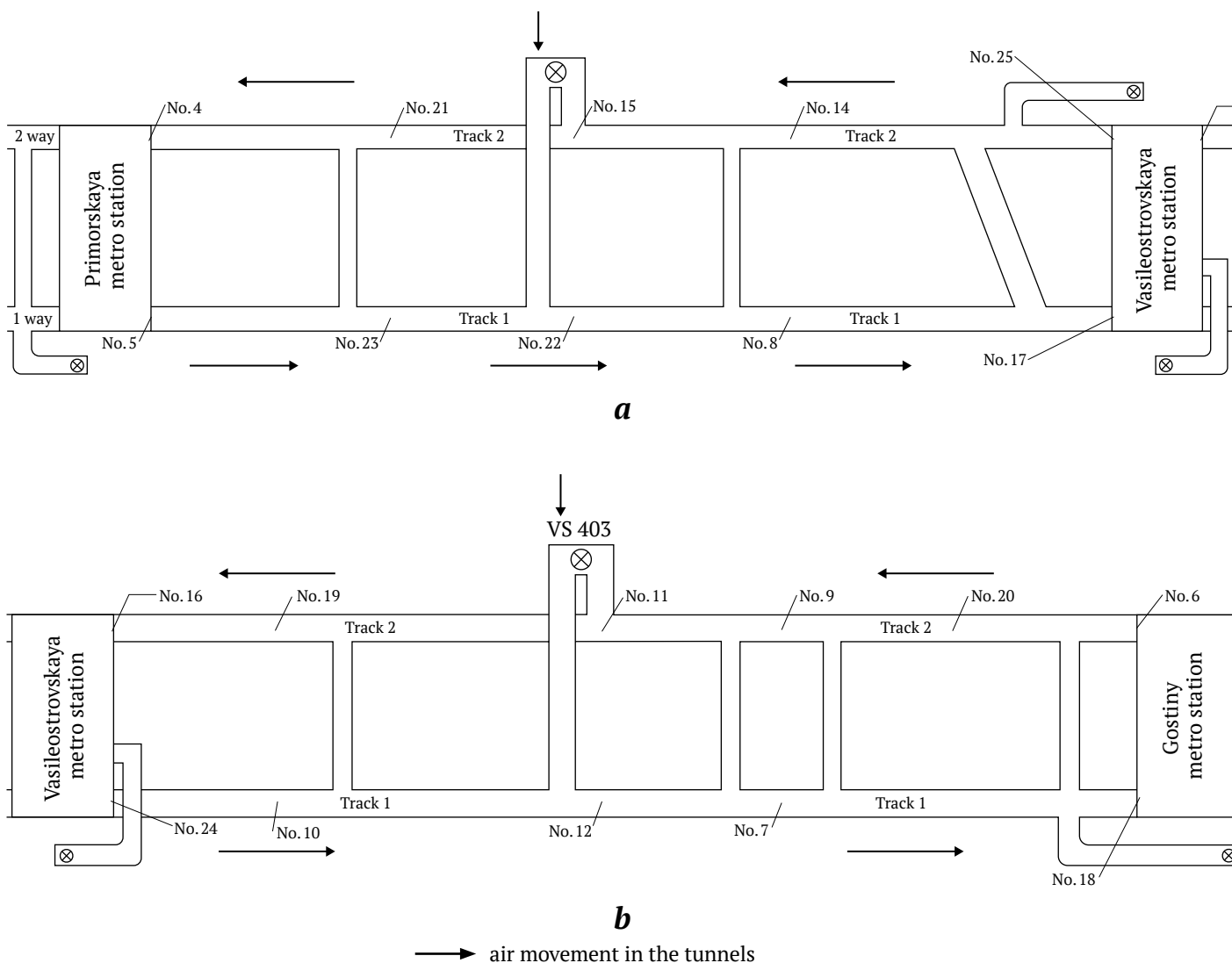


Fig. 1. Diagram of sensor placement for air temperature measurement in the single-track tunnel section of three subway lines:

a – section “Primorskaya”–“Vasileostrovskaya”; *b* – section “Vasileostrovskaya”–“Gostiny Dvor” [compiled by the authors]

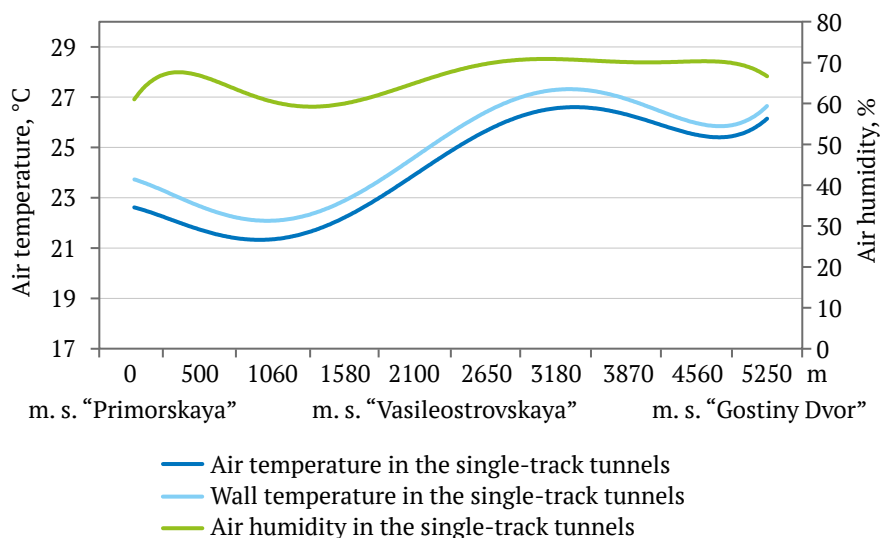


Fig. 2. Air and wall temperature distribution, and air humidity in the “Primorskaya”–“Vasileostrovskaya”–“Gostiny Dvor” section during periods without train movement [compiled by the authors]

Fig. 2 shows the temperature distribution graph of air, tunnel lining surface, and humidity in the tunnels of the “Primorskaya”–“Vasileostrovskaya”–“Gostiny Dvor” sections during periods without train movement.

The variation in air temperature distribution along the length of the tunnel segments is non-monotonic. The maximum temperature is observed near the station, while the minimum occurs in the middle of the section. This is due to the use of different ventilation schemes at various times of the day.

It is important to note that the air temperature is lower than the tunnel lining surface temperature, primarily because the surrounding ground heats up during the day, with train movement providing an additional heat source. The relative humidity of the air varies between 60% and 70%.

The distribution of air temperatures along the tunnel length during train movement is shown in Fig. 3.

An analysis of the measurement results shows that the pattern of air temperature variation along the tunnel length during train movement generally follows the same distribution as when trains are not running, with some differences in temperature values between the first and second tracks.

The conducted experimental studies demonstrated that the average air temperature in the tunnels and stations can exceed the surface air temperature by $\sim 14^\circ\text{C}$.

The reasons for this phenomenon include: significant heat emissions along the segments between stations (tunnel segments) and the use of daytime ventilation schemes that supply fresh air through ventilation shafts, leading to the formation of circulation loops.

In the tunnel section from the mixing point with outside air to the station, several factors influence the air temperature, such as increased air flow and heat

emissions from moving trains, heat exchange processes between the air, tunnel structures, and the surrounding rock, as well as mass exchange processes [9].

At the same time, the increase in train movement intensity has a dual effect: on the one hand, the total amount of emitted heat increases, and on the other, the air flow in the circulation streams also increases.

Based on the developed methodology for determining air distribution parameters in subway station ventilation cross-passages, taking into account the piston effect of trains, the authors conducted a series of calculations of heat emissions and air flow in the circulation streams during train movement to quantitatively assess the interaction of these factors.

The input data for the calculations include: an average train speed of 50 km/h; the number of cars – 8; tunnel cross-section – 21 m^2 ; and segment length – 500–3500 m. The main results of the calculations are presented in Fig. 4.

An analysis of the obtained data shows that, with a simultaneous increase in the number of train pairs per hour from 15 to 45 and the segment length from 500 to 3500 meters, the amount of circulation air (Q_c) increases by 2.5 times. Moreover, the ratio of the heat emitted by the trains to the circulation air flow (N_0) does not depend on the train intensity and varies between 4 and 8.75 for different segment lengths. At the same time, the ratio N_0 remains constant for each segment length.

Thus, it can be concluded that the air temperature in the transport zones of the tunnels is practically unaffected by the frequency of train traffic.

However, an increase in the circulation air flow may lead to another negative effect – an increase in the concentration of suspended dust, especially in the spring, when atmospheric dust levels are higher. This assumption is supported by a number of studies [12].

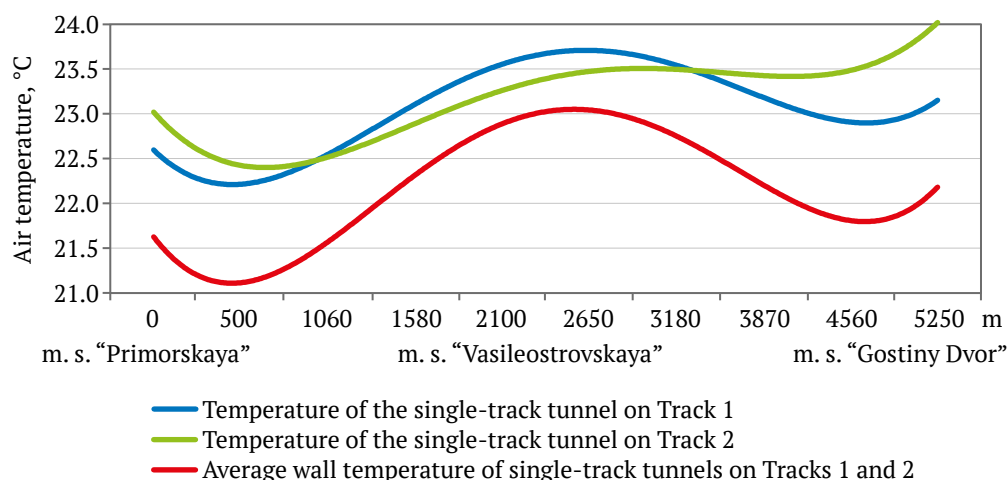


Fig. 3. Air and wall temperature distribution, and humidity in the “Primorskaya”–“Vasileostrovskaya”–“Gostiny Dvor” section during peak hours with 24 train pairs in operation [compiled by the authors]

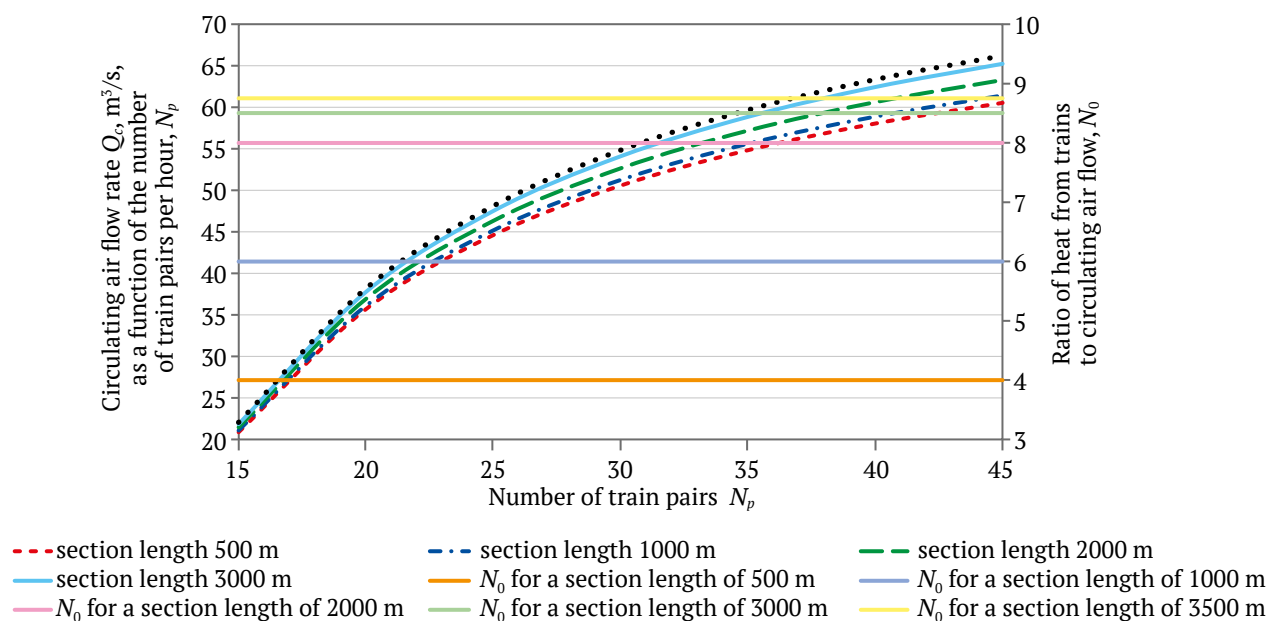


Fig. 4. Circulating air flow rate Q_c and the ratio of heat from trains to circulating air flow (solid line) as a function of train traffic intensity N_p (pairs/hour) [compiled by the authors]

During the operation of deep single-track tunnels, part of the heat from the rolling stock and other sources accumulates in the circulating loops. In the summer, this leads to an increase in the temperature of the tunnel air entering the stations (Fig. 2, 3). To reduce air temperature, it is possible to install refrigeration equipment in ventilation cross-passages near the stations, as described in [10].

In the winter, the circulating air, when mixed with cold outside air in the tunnel section, helps maintain a positive temperature at the stations.

Thus, the circulation loops play a dual role: in the summer, the heat accumulated in them causes additional warming of the air and progressive heating of the surrounding rock; in the winter, on the contrary, the circulating air allows for the maintenance of positive temperatures at the stations and in the tunnels [13].

Ventilation and thermal regimes of shallow single-track tunnels

A distinctive feature of the aerodynamic processes in shallow single-track tunnels, compared to those in deep tunnels, is that the circulating loops formed between stations (or cross-passages) have a close aerodynamic connection with the surface [14].

In deep subway lines, the temperature distribution along the length of the circulation loops forms in the horizontal plane and is determined only by the air flow initiated by the trains moving through parallel tunnels and the amount of heat emitted by them. In shallow tunnels, the external air entering the wor-

kings through cross-passages and pedestrian paths significantly influences the temperature distribution, as these circulating loops are fed by outside air even when the fans are not operating.

This means that the circulation loop forms in both the horizontal and vertical planes. This conclusion is confirmed by the measured air speeds at the stations “Ploshchad Gagarina-Mikheylovskogo”, “Rechnoy Vokzal”, “Sibirskaya”, and others in Novosibirsk.

Mixing the circulating air with external air leads to changes in the temperature distribution along the length of the circulation loop. While these changes do not lead to deviations from the standard parameters during the summer and spring periods, in the winter, the air temperature at the stations may significantly differ from the standard values, requiring the heating of outside air drawn in by the piston effect.

Based on the experimental research and numerical calculations performed, several proposals for managing the ventilation of shallow subway lines in Novosibirsk can be formulated (Fig. 5) [15].

Ventilation and thermal regimes of double-track tunnels

Field studies of the thermodynamic parameters of the air in double-track tunnels on the sections: “Dead End”–“Begovaya”–“Zenit” – the junction with the single-track tunnels leading to “Primorskaya” station (Fig. 6) were also conducted in the summer of 2023. The arrangement of sensors for measuring the thermodynamic parameters of the air is shown in Fig. 7.

The measurement methodology and equipment used were identical to those employed in the single-track tunnels.

In the selected sections (“Dead End”–“Begovaya”–“Zenit”–“Primorskaya”), fresh air was supplied through station ventilation shafts using Zitron ZVR1-18-75/6, ZVN 1-20-75/6, and FTDA-REV-200 units. Operating at 80% capacity, these units provided an airflow of $\sim 51 \text{ m}^3/\text{s}$ and an airspeed of $\sim 5.6 \text{ m/s}$ at a fan depression of 925 Pa.

Air extraction from the tunnels was carried out using FTDA-REV-180 units, located in the ventilation shafts at the “Begovaya”, “Zenit” stations, and in the dead-end section. These units, also operating at 80% capacity, provided an air extraction rate of $\sim 42 \text{ m}^3/\text{s}$ (with an airspeed of $\sim 5.6 \text{ m/s}$) at a fan depression of 925 Pa.

Figs. 8 and 9 show graphs illustrating the distribution of air temperature, tunnel lining surface

temperature, and humidity levels in the “Begovaya”–“Zenit” section during periods of no train movement. During the measurements, the outside air temperature was 7°C , and the relative humidity was 55%.

In the absence of train movement, the variation in the thermal regime along the section is due to the amount of heat stored in the ground during train passage. This is confirmed by the higher tunnel lining surface temperature compared to the air temperature and the distribution pattern of the air supplied by the fans along the tunnel section. Despite the heat emitted by the ground, the air temperature decreases along the section as it moves further from the “Zenit” station due to the influx of outside air, which has a significantly lower temperature than the tunnel lining surface temperature. The relative humidity along the section fluctuates within the range of 50–60%.

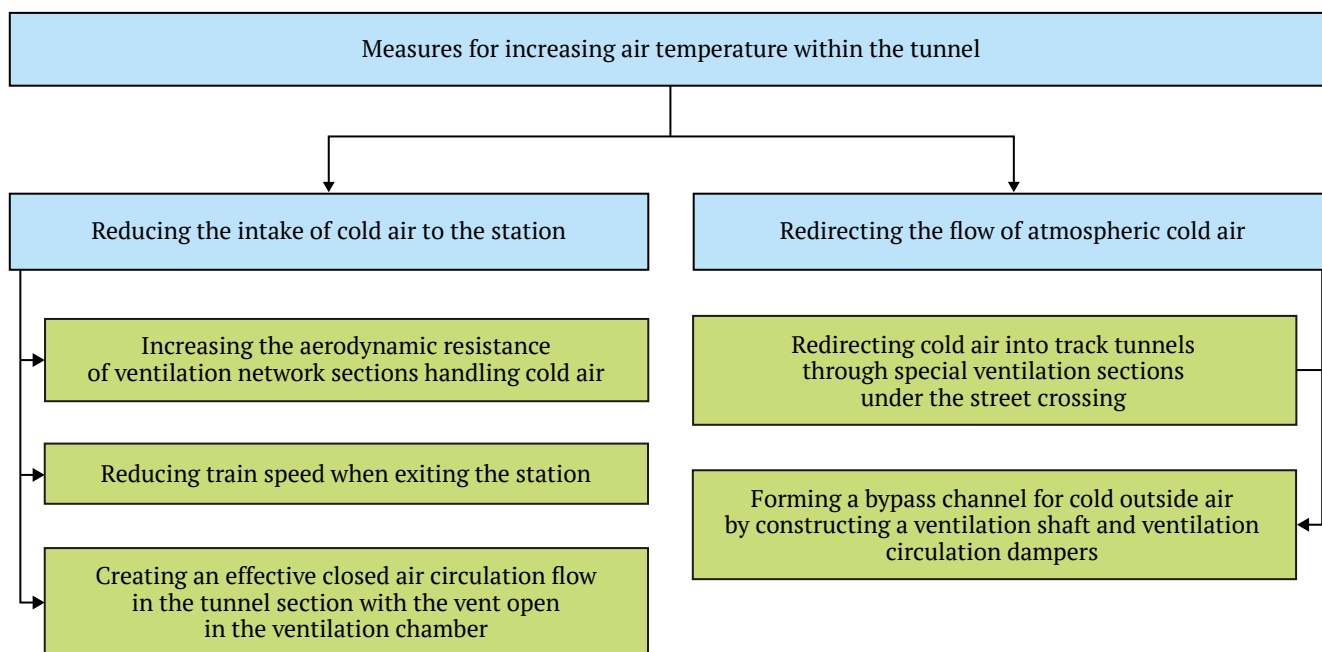


Fig. 5. Approaches to managing ventilation in shallow subway lines under the conditions of Novosibirsk [compiled by the authors]

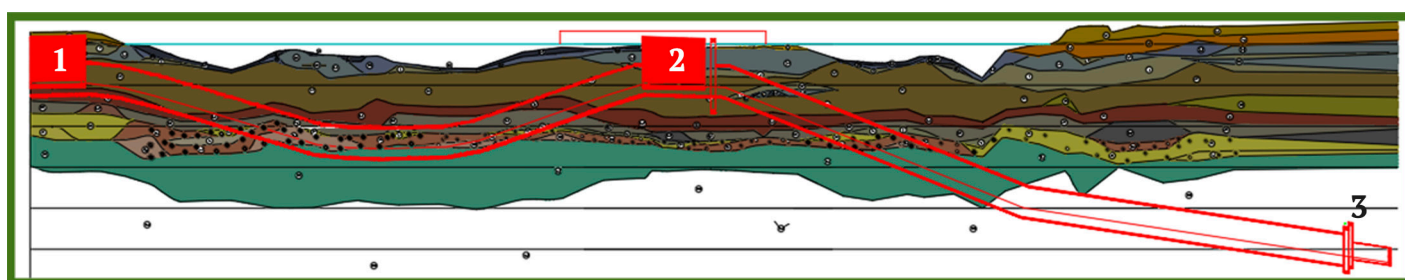


Fig. 6. Profile of the double-track section:

1 – “Begovaya”; 2 – “Zenit”; 3 – junction point of single-track and double-track tunnels [compiled by the authors]

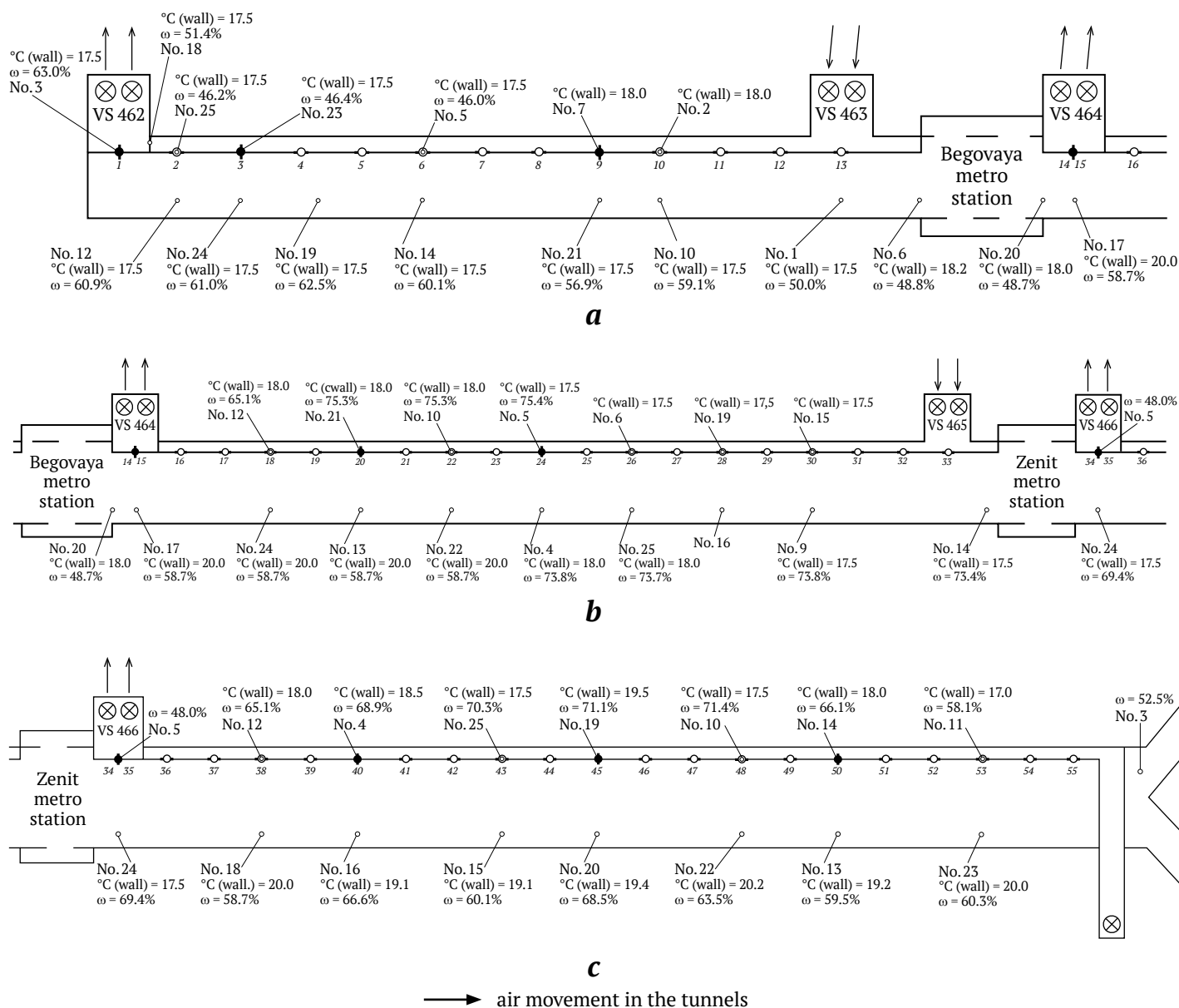


Fig. 7. Diagram of air temperature sensor placement in the double-track section of the third subway line: *a* – section “Dead End”–“Begovaya”; *b* – section “Begovaya”–“Zenit”; *c* – part of the “Zenit”–“Primorskaya” section up to the junction of single-track and double-track tunnels [compiled by the authors]

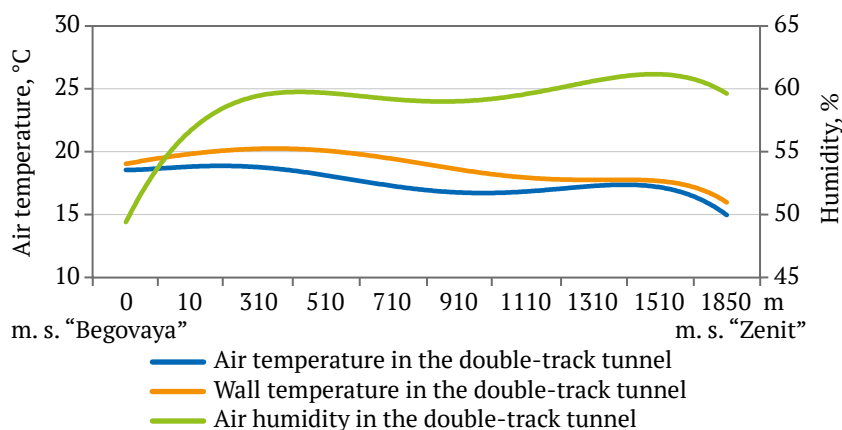


Fig. 8. Air temperature, tunnel lining surface temperature, and humidity distribution in the “Begovaya”–“Zenit” section during periods without train movement [compiled by the authors]

Compared to single-track tunnels, double-track tunnels exhibit a more comfortable thermal regime. This is due to the absence of circulating airflows caused by the movement of trains. In single-track tunnels, the heat emitted by moving trains accumulates over a prolonged period since a significant portion of it is not removed along with the outgoing air from the subway [16]. In subways with double-track transit tunnels, due to the lack of circulating airflows (piston effect), most of the heat is evenly distributed along the tunnel section [17]. The consistency of air temperature is maintained through heat removal, except in zones near the stations. In these zones, the intensity of heat generation is highest during train braking and stops. As a result, the air temperature exceeds the tunnel lining surface temperature, indicating the transfer of heat to the ground.

For sections with double-track tunnels, an increase in temperature is observed with higher train traffic intensity, which is directly related to the increase in heat emissions from the trains.

Ventilation and thermal regimes in sections with single-track and double-track tunnels

A key distinction in the ventilation and thermal regimes of the sections under consideration is the difference in airflow dynamics between the double-track and single-track tunnels. Single-track tunnel sections are ventilated through a combination of forced ventilation and the piston effect. Additionally, a circulation loop forms between the junction of the double-track and single-track tunnels and the stations closest to the junction [18].

In contrast, the ventilation of double-track tunnels is managed solely by shaft fans.

When trains are not operating, the temperature and humidity distribution along the section from “Zenit” station to “Primorskaya” station remains consistent for both double-track and single-track tunnels (Fig. 10). During the measurements, the outside air temperature was 13°C, and the humidity level was 69%.

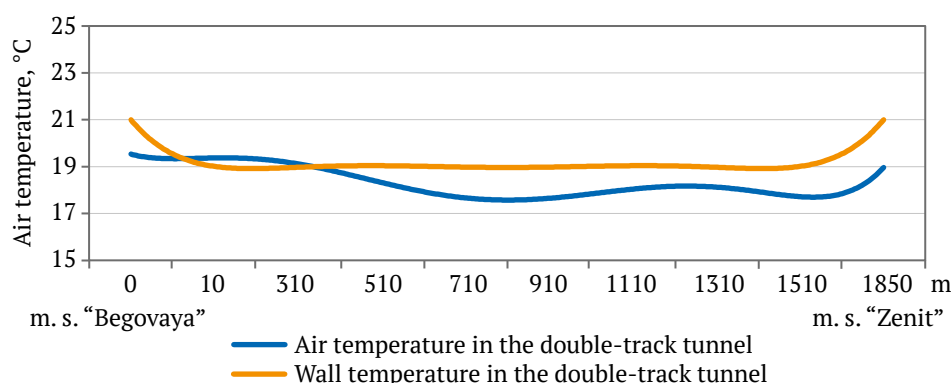


Fig. 9. Air temperature distribution in the “Begovaya”–“Zenit” section during peak hours with 24 train pairs in operation [compiled by the authors]

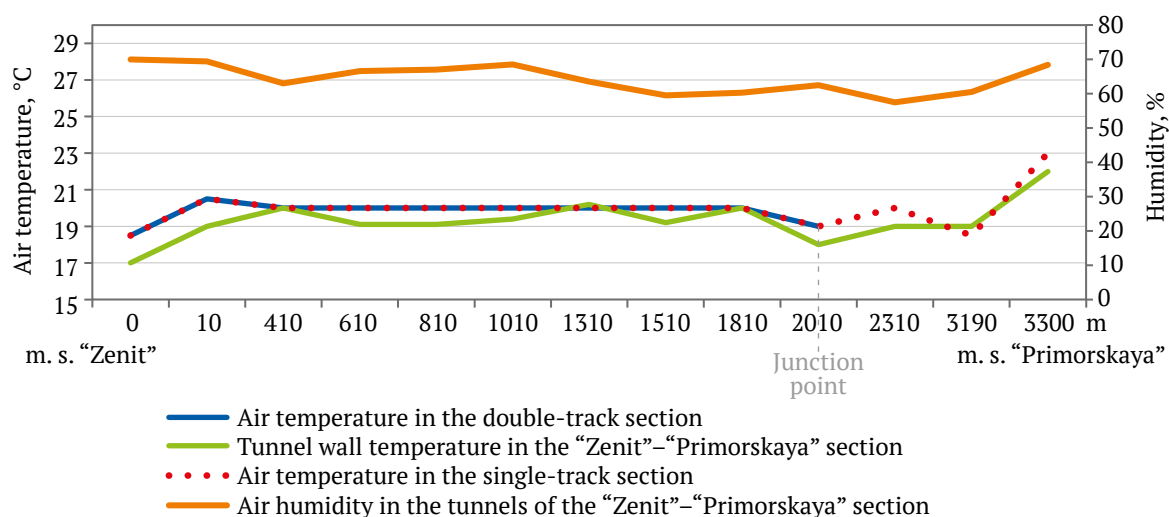


Fig. 10. Air temperature distribution in the “Zenit”–“Primorskaya” section during periods without train movement, with the junction point where the double-track tunnel transitions into two single-track tunnels [compiled by the authors]

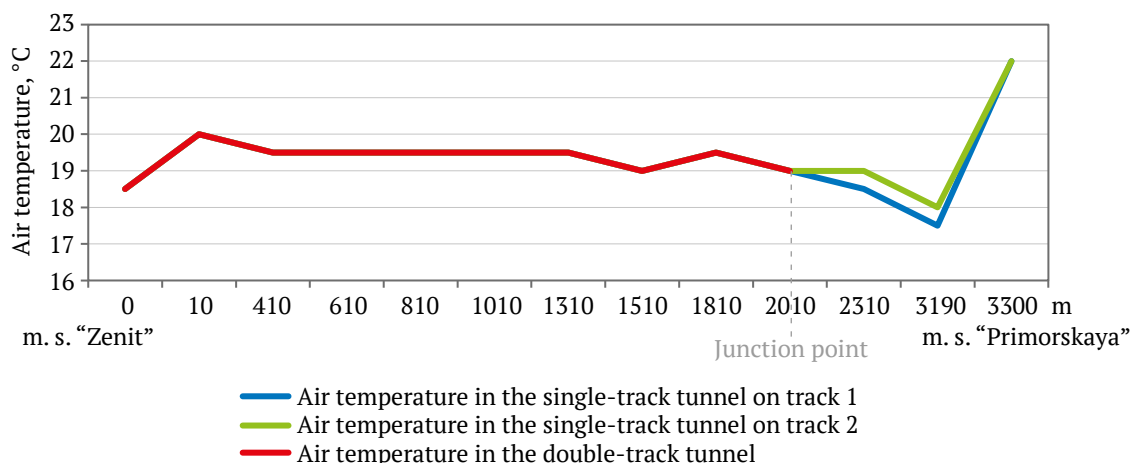


Fig. 11. Air temperature distribution in the “Zenit”–“Primorskaya” section during peak-hour train operation (24 pairs/hour) [compiled by the authors]

During train movement, when the air temperature beyond the junction with the double-track tunnels aligns with the typical temperature distribution found in single-track tunnels, it is possible for the temperature to exceed the absolute values observed in the single-track tunnels (Fig. 11). During the measurements, the outside air temperature was recorded at 17°C.

The above is confirmed by measurement results, which show that the air temperature in the double-track tunnel before the junction, at a point 2010 meters from “Zenit” station, was 19.5°C, while at “Primorskaya” station, it increased to 22–23°C. This increase is due to the circulation loop in the single-track section being fed with air from the double-track tunnel, which has a higher temperature than the outside air supplied from the surface, as is typical in standard ventilation schemes.

To lower the temperature regime in single-track tunnels, a ventilation method using outside air can be applied. This method involves supplying fresh air into the double-track tunnel through a specially designed shaft located at the end of the double-track section.

Conclusions

Based on the experimental research conducted, the patterns of ventilation and thermal regimes in single-track, double-track tunnels, and junction sections were identified, and measures were proposed to improve these regimes to ensure compliance with climate standards. Specifically, the following findings were made:

1. In deep single-track tunnels, the thermal regime is influenced by two main factors: air circulation between stations, caused by the piston effect, and heat emissions from moving trains. The temperature

distribution along the tunnels is uneven, with minimum values in the middle and maximum values at the stations. This phenomenon is a result of the ventilation system, which introduces fresh air into the tunnels and expels it at the stations. As train traffic intensity increases, there is no significant change in air temperature, which can be attributed to the rise in circulating air flow.

2. In shallow single-track tunnels, the circulation loop formed between stations is fed by outside air entering through pedestrian paths at the stations and tunnels. During the summer, this phenomenon does not significantly affect the temperature distribution. However, in winter, it can lead to a critical drop in temperature at the stations. Maintaining standard air parameters at the stations during the winter can be achieved through a combination of organizational, aerodynamic, and thermal engineering methods. The first method involves reducing the piston effect by slowing down the arrival and departure of trains. The second approach increases the aerodynamic resistance in sections of the ventilation system, facilitating the movement of cold atmospheric air or internal circulation loops. The third method involves using systems to heat the incoming outside air, such as air-thermal curtains.

3. In double-track tunnels, when trains are not in operation, the temperature variation along the tunnel is determined by the amount of heat retained in the ground during train movement. When trains are running, the heat emitted by trains moving in opposite directions, with minimal piston effect, is evenly distributed along the tunnel. This results in a consistent air temperature throughout the tunnels, except near stations, where braking and stopping generate maximum heat. Consequently, the air tem-



perature in these areas increases by 2–3°C compared to the rest of the tunnel.

In sections with both double-track and single-track tunnels, the rise in air temperature at stations near single-track tunnels is due to the formation of circulation flows between the junction of the double-track and single-track tunnels and the adjacent station.

4. Recommendations for normalizing the aerothermodynamic regime for the tunnel types studied include the following:

- In cases where air temperature may exceed standard values in the summer, provisions should be made for either an air flow reserve or air cooling in cross-passages near the stations.

- To increase air temperature, organizational, aerodynamic, and heat engineering methods can be applied: the first involves reducing the piston effect by lowering train speeds; the second involves increasing the aerodynamic resistance in ventilation network sections connected to the intake of outside air; and the third entails using systems to heat cold external air, such as air-thermal curtains.

- In sections that combine double-track and single-track tunnels, the potential rise in air temperature at stations near single-track tunnels can be mitigated by supplying outside air into the double-track tunnel through a shaft located at the end of the double-track section.

References

1. Yungmeister D.A., Yacheykin A.I. Rational design justification of the tunnel boring shield executive body for the conditions of the mines of Saint Petersburg Metrostroy. *Journal of Mining Institute*. 2021;249:441–448. <https://doi.org/10.31897/PMI.2021.3.13>
2. Dashko R.E., Lokhmatikov G.A. The Upper Kotlin clays of the Saint Petersburg region as a foundation and medium for unique facilities: an engineering-geological and geotechnical analysis. *Journal of Mining Institute*. 2022;254:180–190. <https://doi.org/10.31897/PMI.2022.13>
3. Maevski I. Features of tunnel ventilation systems design in hot climate. In: *Proceedings from 12th International Symposium on Aerodynamics and Ventilation of Vehicle Tunnels*. Portoroz, Slovenia, 11–13 July 2006. BHR Group; 2006. Pp. 331–347.
4. Kiyanitsa L.A. Determining analytical dependences for heat flow in soil from enclosed-type shallow underground subway stations with double-track tunnels. *Mining Informational and Analytical Bulletin*. 2018;(2):89–102. (In Russ.)
5. Zedgenizov D.V. To calculation of the coefficients of automatic regulator of tunnel fan capacity. *InterekspoGeo-Sibir*. 2021;2(3):213–218. (In Russ.) <https://doi.org/10.33764/2618-981X-2021-2-3-213-218>
6. Tsodikov V.Ya. Chapter III. Ventilation systems of subway tunnels and the main provisions of their calculations. In: *Ventilation and Heat Supply of Subways*. 2nd ed. Moscow: Nedra Publ.; 1975. (In Russ.)
7. Vardy A., Hagenah B. Full-scale flow measurements in a tunnel air shaft. In: *Proceedings from 12th International Symposium on Aerodynamics and Ventilation of Vehicle Tunnels*. Portoroz, Slovenia, 11–13 July 2006. BHR Group; 2006. Pp. 343–357.
8. Sahlin P., Eriksson L., Grozman P. et al. 1D models for thermal and air quality prediction in underground traffic systems. In: *Proceedings from 12th International Symposium on Aerodynamics and Ventilation of Vehicle Tunnels*. Portoroz, Slovenia, 11–13 July 2006. Pp. 261–267.
9. Kiyanitsa L.A., Unaspekov B.A. Estimate of air distribution in ventilation tunnel between subway station as function of piston effect. *Mining Informational and Analytical Bulletin*. 2021;(12):99–109. (In Russ.) https://doi.org/10.25018/0236_1493_2021_12_0_99
10. Gendler S.G., Kryukova M.S. Thermal management of metro lines with single-track tunnels. *IzvestiyaTul'skogo Gosudarstvennogo Universiteta. Nauki o Zemle*. 2022;(4):116–127. (In Russ.)
11. Gendler S.G., Kryukova M.S. Problems of operation of metro lines with double-track tunnels in a cold climate. *Izvestiya Tul'skogo Gosudarstvennogo Universiteta. Nauki o Zemle*. 2022;(2):77–87. (In Russ.)
12. Smirnyakov V.V., Rodionov V.A., Smirnyakova V.V., Orlov F.A. The influence of the shape and size of dust fractions on their distribution and accumulation in mine workings when changing the structure of air flow. *Journal of Mining Institute*. 2022;253:71–81. <https://doi.org/10.31897/PMI.2022.12>
13. Lugin I.V., Pavlov S.A., Irgibaev T.I. Justification of the parameters of ring models in the decomposition of the ventilation network of an extended metro line for the calculation of air distribution. *Interekspo Geo-Sibir*. 2022;2(3):214–220. <https://doi.org/10.33764/2618-981X-2022-2-3-214-220>
14. Kiyanitsa L.A., Lugin I.V., Krasyuk A.M. On air flow structure in station ventilation connections of subways. *Interekspo Geo-Sibir*. 2021;2(3):219–229. (In Russ.) <https://doi.org/10.33764/2618-981X-2021-2-3-219-229>



15. Krasnyuk A.M., Lugin I.V. Keeping of microclimate parameters at terminal station of subway line. *InterekspoGeo-Sibir*. 2019;2(4):122–130. (In Russ.) <https://doi.org/10.33764/2618-981X-2019-2-4-122-130>
16. Zhikharev S. Enhanced methodology for thermal management area assessment of metro lines. In: *E3S Web of Conferences. IV International Conference on Geotechnology, Mining and Rational Use of Natural Resources (GEOTECH-2024)*. 2024;525:05018. <https://doi.org/10.1051/e3sconf/202452505018>
17. Zhikharev S. Methodological approach to determining the area of air recycling on metro lines with double track tunnels. In: *E3S Web of Conferences. XIV International Conference on Transport Infrastructure: Territory Development and Sustainability (TITDS-XIV-2023)*. 2024;471:02022. <https://doi.org/10.1051/e3sconf/202447102022>
18. Karimov D. Numerical simulation of aerodynamic processes of air mass movement in underground tunnels taking into account piston impact of rolling stock. *Proceedings of Petersburg Transport University*. 2022;19(1):17–27. (In Russ.) <https://doi.org/10.20295/1815-588X-2022-19-1-17-27>

Information about the authors

Simeon G. Gendler – Dr. Sci. (Eng.), Professor, Head of the Department of Industrial Safety, Empress Catherine II Saint Petersburg Mining University, St. Petersburg, Russian Federation; ORCID [0000-0002-7721-7246](https://orcid.org/0000-0002-7721-7246), Scopus ID [56168675100](https://scopus.org/56168675100), ResearcherID [I-9283-2017](https://orcid.org/I-9283-2017); e-mail sgendler@mail.ru

Milana S. Kryukova – PhD-Student of the Department of Industrial Safety, Empress Catherine II Saint Petersburg Mining University, St. Petersburg, Russian Federation; ORCID [0000-0001-9632-3979](https://orcid.org/0000-0001-9632-3979), Scopus ID [58723622900](https://scopus.org/58723622900); e-mail s215068@stud.spmi.ru

Elena L. Alferova – Engineer, Researcher at the Chinakal Institute of Mining of the Siberian Branch of the Russian Academy of Sciences, Novosibirsk, Russian Federation; ORCID [0000-0001-9453-2355](https://orcid.org/0000-0001-9453-2355), Scopus ID [57193708767](https://scopus.org/57193708767); e-mail alfenok.ru@gmail.com

Received 22.02.2024

Revised 12.04.2024

Accepted 07.05.2024



SAFETY IN MINING AND PROCESSING INDUSTRY AND ENVIRONMENTAL PROTECTION

Research paper


<https://doi.org/10.17073/2500-0632-2024-03-227>

UDC 504.4.054

**Assessment of the efficiency of wastewater treatment from coal enterprises for suspended solids using various filtering materials**

L. A. Ivanova  , A. Yu. Prosekov  , P. P. Ivanov  , E. S. Mikhaylova  ,
I. V. Timoshchuk  , A. K. Gorelkina 

Kemerovo State University, Kemerovo, Russian Federation

 lyuda_ivan@mail.ru

Abstract

Suspended solids are the predominant pollutants in the wastewater of coal enterprises. The basic wastewater treatment system regulated in BAT No. 15 ITC-37–2017 does not ensure water quality meets the discharge standards for fishery water bodies. The gravitational sedimentation method used in this technology is effective for coarse particles. However, colloidal systems formed from fine insoluble fractions are challenging to separate in a gravitational field. As an effective method for removing suspended solids from wastewater, we recommend filtering through a stationary layer of granular filtering materials. The study investigates the kinetics and dynamics of filtering suspended particles from the wastewater of coal enterprises using various filtering materials. Sedimentation curves of suspended solids from quarry wastewater have been constructed. The dependence of wastewater treatment efficiency on the size of filtering material fractions has been identified. The study provides an evaluation of the effectiveness of using natural filtering materials for treating wastewater from coal enterprises. The experiments demonstrated that the most efficient and cost-effective granular filtering material is quartzite from the Bobrovskoye deposit, which we recommend using in a combination of fractions 20–50 and 0.7–12 mm (in a ratio of 1 : 2). The optimal flow rate of wash water during the regeneration of the granular filter is also determined.

Keywords

coal enterprises, quartzite, suspended solids, wastewater, filtration, mechanical treatment

Acknowledgments

This research was conducted within the framework of the comprehensive scientific and technical program for the full innovation cycle “Development and Implementation of a Complex of Technologies in the Fields of Exploration and Mining of Mineral Resources, Ensuring Industrial Safety, Bioremediation, and Creating New Deep Processing Products from Coal Raw Materials while Sequentially Reducing Environmental Impact and Risks to Population Life” approved by the Government of the Russian Federation Decree No. 1144-r dated 11.05.2022, with financial support from the Ministry of Science and Higher Education of the Russian Federation under Agreement No. 075-15–2022-1201 dated 30.09.2022.

For citation

Ivanova L. A., Prosekov A. Yu., Ivanov P. P., Mikhaylova E. S., Timoshchuk I. V., Gorelkina A. K. Assessment of the efficiency of wastewater treatment from coal enterprises for suspended solids using various filtering materials. *Mining Science and Technology (Russia)*. 2024;9(3):263–270. <https://doi.org/10.17073/2500-0632-2024-03-227>


ТЕХНОЛОГИЧЕСКАЯ БЕЗОПАСНОСТЬ В МИНЕРАЛЬНО-СЫРЬЕВОМ КОМПЛЕКСЕ И ОХРАНА ОКРУЖАЮЩЕЙ СРЕДЫ

Научная статья

Оценка эффективности очистки сточных вод угольных предприятий от взвешенных веществ различными фильтрующими материалами

Л. А. Иванова  , А. Ю. Просеков  , П. П. Иванов  , Е. С. Михайлова  ,
И. В. Тимошук  , А. К. Горелкина 

Кемеровский государственный университет, г. Кемерово, Российская Федерация

 lyuda_ivan@mail.ru

Аннотация

Взвешенные вещества являются преобладающими загрязнителями сточных вод угольных предприятий. Базовая система очистки сточных вод, регламентируемая в НДТ № 15 ИТС-37–2017, не обеспечивает качества очистки до нормативных значений сброса в водоемы рыбохозяйственного назначения.



Используемый в данной технологии метод гравитационного осаждения в прудах-отстойниках эффективен для грубодисперсных частиц. Однако формирующиеся коллоидные системы из мелкодисперсных нерастворимых фракций являются сложными для разделения в условиях гравитационного поля. В качестве эффективного метода удаления взвешенных веществ из сточных вод рекомендуем использовать фильтрование через стационарный слой фильтрующих зернистых материалов. В работе проведено исследование кинетики и динамики фильтрования взвешенных частиц из сточных вод угольных предприятий на фильтрующих материалах различной природы. Построены кривые гравитационного осаждения взвешенных веществ из карьерных сточных вод. Выявлена зависимость степени очистки сточных вод от размера фракций фильтрующих материалов. В работе приведены результаты оценки эффективности применения фильтрующих материалов природного происхождения для очистки сточных вод угольных предприятий от взвешенных веществ. Результаты экспериментов показали, что наиболее эффективным и доступным зернистым фильтрующим материалом является кварцит Бобровского месторождения, который мы рекомендуем использовать, комбинируя его фракции 2,0–5,0 и 0,7–1,2 (в соотношении 1 : 2). Определена оптимальная скорость подачи промывочных вод на этапе регенерации фильтра с зернистой загрузкой.

Ключевые слова

угольные предприятия, кварцит, взвешенные вещества, сточные воды, фильтрование, механическая очистка

Благодарности

Исследование выполнено в рамках комплексной научно-технической программы полного инновационного цикла «Разработка и внедрение комплекса технологий в областях разведки и добычи полезных ископаемых, обеспечения промышленной безопасности, биоремедиации, создания новых продуктов глубокой переработки из угольного сырья при последовательном снижении экологической нагрузки на окружающую среду и рисков для жизни населения», утвержденной Распоряжением Правительства Российской Федерации от 11.05.2022 г. №1144-р, при финансовой поддержке Министерства науки и высшего образования Российской Федерации, № соглашения 075-15-2022-1201 от 30.09.2022 г.

Для цитирования

Ivanova L. A., Prosekov A. Yu., Ivanov P. P., Mikhaylova E. S., Timoshchuk I. V., Gorelkina A. K. Assessment of the efficiency of wastewater treatment from coal enterprises for suspended solids using various filtering materials. *Mining Science and Technology (Russia)*. 2024;9(3):263–270. <https://doi.org/10.17073/2500-0632-2024-03-227>

Introduction

Suspended insoluble substances, formed as a result of drilling, blasting, excavation, and transportation of coal and rock at coal mines, are among the predominant pollutants in coal enterprise wastewater [1].

When organizing recirculating water supply systems, such as using wastewater to supply beneficiation plants, the high content of suspended solids in the water can lead to a reduction in the quality of the obtained concentrates, as well as increased wear on pipes and pumps.

Mineral dust particles form various systems in water depending on the degree of dispersion, such as suspensions, emulsions, colloidal solutions, etc.

Most coal mines located in the Kemerovo region (Kuzbass) have a wastewater treatment system corresponding to the basic treatment regulated by BAT No. 15 ITC-37–2017 “Coal Mining and Beneficiation”, which includes the process of sedimentation of suspended solids under the action of gravity in sedimentation ponds and filtration through the dam filter material [2].

Settling of quarry wastewater in sedimentation ponds is the most common method and is used in the first stage of treatment. This method is effective

for removing large particles with a size greater than 2 mm. For such particles, the efficiency of sedimentation reaches 90–100%. Moreover, this method allows the removal of 40–60% of coarse and medium sand particles with a size greater than 0.25 mm [3]. The presence of difficult-to-settle silty and clay particles smaller than 10 μm in high concentrations makes sedimentation ponds insufficiently effective. Typically, they do not allow achieving regulatory concentrations for suspended solids in discharged wastewater, even when using a cascade of filtering dams. Furthermore, sedimentation ponds with regulated water discharge are not adapted to function under conditions of sharp and significant changes in wastewater flow rates, which may be caused by the peculiarities of mining and meteorological conditions [4].

The main body of the filtering array is often made of [5]:

- native overburden rocks;
- coarse gravel with fractions of 100–200 mm;
- medium gravel with fractions of 60–100 mm;
- burnt rock;
- quartz sand or zeolite.

The use of native overburden rocks as a filtering material for the cascade of dams for treating quarry



wastewater has a significant drawback, which is the accumulation of predominant pollutants during operation, followed by their leaching, leading to an increase in their concentration in the treated water.

Monitoring the quality of discharged wastewater from coal mines showed that the quantitative content of suspended solids exceeds the regulatory values and varies throughout the year, with the maximum peak observed from May to July [6].

The aim of this study is to assess the efficiency of treating coal mine wastewater from suspended insoluble anthropogenic contaminants by filtration through a granular media layer.

The research tasks included:

- conducting field measurements of suspended solids content in coal mine wastewater;
- investigating the kinetics of gravitational sedimentation of suspended solids from wastewater;
- analyzing the filtering capacity of natural materials;
- determining the effectiveness of wastewater treatment from suspended solids by forming a working layer through a combination of different materials and fractions;
- determining the optimal flow rate of wash water during the regeneration of the granular filter.

Research Methods

We recommend using a non-reagent method of treating quarry wastewater from suspended solids – filtration [7–9]. This method can be used either independently or as one of the stages of a comprehensive zero-discharge technology, depending on the concentration of contaminants in the source water [10].

For analyzing suspended solids, we used the method described in PND F 14.1:2:4.254–2009 “Quantitative Chemical Analysis of Water. Method for Measuring Mass Concentrations of Suspended Solids and Ignited Suspended Solids in Samples of Drinking, Natural, and Wastewater by Gravimetric Method”.

The dispersed composition of suspended particles in wastewater was determined using a particle size analyzer according to GOST 8.774–2011.

Laboratory studies were conducted to select a filtering material for loading into a filter column installed at the inlet of the comprehensive zero-discharge wastewater treatment technology system.

Characteristics of research objects

To analyze the efficiency of wastewater treatment from suspended solids by filtration, natural materials of different chemical compositions were chosen as research objects (Table 1).

Results of research on wastewater treatment from suspended solids using filtering materials

The study of sedimentation of suspended solids under kinetic conditions was carried out using quarry water sampled from a sump in autumn and spring (with concentrations of 103 and 126 mg/dm³, respectively), where clay particles with a fraction size of 0.005 µm predominated.

The kinetics of gravitational sedimentation of suspended solids from wastewater is shown in Fig. 1. The analysis of the sedimentation curves reveals two stages, each with different process speeds. In the first 100 minutes, a significant reduction in the concentration of suspended solids is observed due to the sedimentation of particles predominantly larger than 0.005 µm. Subsequently, a significant decrease in the sedimentation rate of fine particles smaller than 0.002 µm occurs, which are difficult to separate under gravitational field conditions. The concentration of suspended solids in the samples reached its minimum value (20 mg/dm³) only on the fifth day and then remained unchanged.

The results of gravitational sedimentation showed that gravitational forces are insufficient to cause the settling of colloidal impurities. Another characteristic feature is the sediment's instability in both sedimentation and aggregation [11].

Table 1 1

Chemical composition of filtering materials, %

Filtering material	SiO ₂	Al ₂ O ₃	Fe ₂ O ₃ общ	MnO	CaO	MgO	Na ₂ O	K ₂ O
Zeolite from Holinsky deposit (Chita Region, Russia)	56.27	5.37	2.30	< 0.01	14.90	1.26	0.14	1.24
Sorbent AS (catalytic aluminosilicate) (Russia)	46.8	1.0	6.12	< 0.01	0.6	0.1	0.72	–
Filter-Ag (USA)	70–73	14	1.5–3.5	0.2–2.5	–	–	2.5	1.5
Filtering Material MFU (Russia)	80	7	5	4	–	–	3	–
Sorbent MS (catalytic aluminosilicate) (Russia)	16.9	0	9.53	1.7	0.34	6.2	0	–
Quartzite from Bobrovskoye deposit (Russia)	98.7	1.3	0.6	–	–	–	–	–

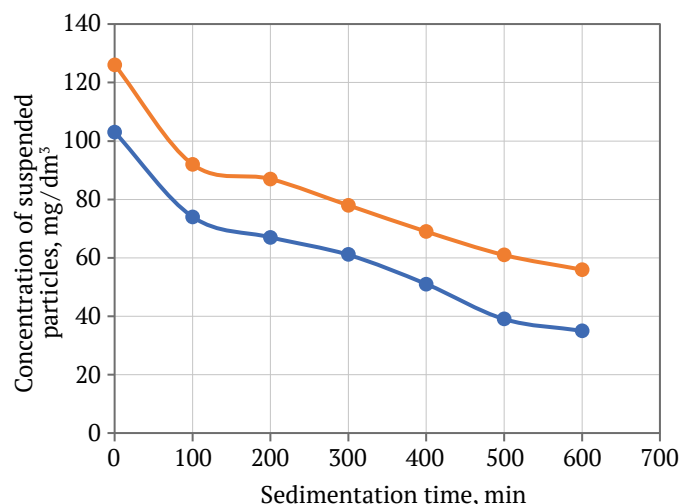


Fig. 1. Kinetics of gravitational sedimentation of suspended solids

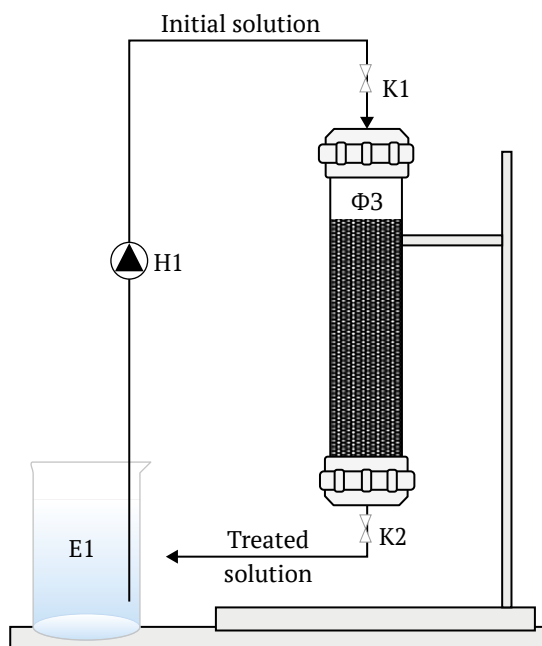


Fig. 2. Schematic diagram of the laboratory mechanical filtration setup

The obtained results confirm the need for further treatment of wastewater from suspended solids in the colloidal group after the sedimentation ponds, where laminar flow is organized for sufficient removal of coarse particles. An effective method for further treating wastewater from colloidal particles is dynamic filtration using column-type apparatuses with granular media [12].

Wastewater exiting sedimentation ponds, with a suspended solids concentration of 62 mg/dm³ and a predominant particle size of 0.005–0.02 μm, was passed through a laboratory setup, the schematic of which is shown in Fig. 2, where the filtering granular media was varied.

The laboratory setup consists of a filtering column with a granular media layer height of 0.50 m and a diameter of 0.1 m. The treated water is fed from the top at an initial rate of 8 m/h. The degree of wastewater treatment using various filtering media was determined after passing 200 liters.

Before the start of mechanical filtration, pre-treated and settled water was poured into tank E1, from which it was pumped by pump N1 into the filtering column FZ with granular media. The filtration rate was adjusted by valves K1 and K2. The resulting filtrate was collected in an intermediate tank.

The degree of wastewater treatment from suspended solids was calculated using the formula [13]:

$$\varepsilon = \frac{C_0 - C_k}{C_0} 100,$$

where ε is the degree of wastewater treatment, %; C_0 is the initial concentration of suspended solids, mg/L; C_k is the concentration of suspended solids at the column outlet after passing 200 liters of wastewater, mg/L.

The experiment results are presented in Table 2.

The laboratory experiment data showed that Filter Ag and quartzite from the Bobrovskoye deposit provide the highest degree of treatment of model solutions from suspended solids.

Table 2

Concentration of suspended particles and degree of wastewater treatment

Filtering material	Initial concentration of suspended solids, mg/L	Concentration of suspended solids at column outlet after passing 200 L of wastewater, mg/L	Degree of treatment, %
Filter Ag	62.32	1.47	97.64
Filtering material MFU	60.54	42.94	29.02
Sorbent AS	59.42	54.74	7.84
Zeolite from Holinsky deposit	68.20	22.73	66.67
Sorbent MS	62.34	29.75	52.24
Quartzite from Bobrovskoye deposit (fraction 2–5)	64.50	9.28	85.61

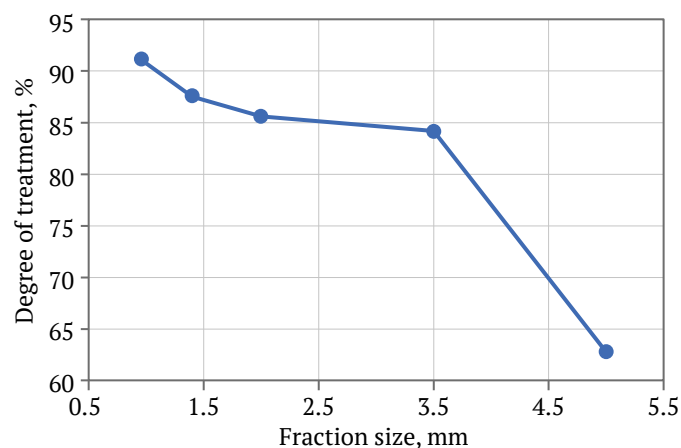


Fig. 3. Dependence of treatment degree on the fraction size of quartzite material from the Bobrovskoye deposit

The results of studying the influence of the fractional composition of the filtering material on the degree of treatment of model solutions from suspended solids were conducted on quartzite material from the Bobrovskoye deposit. The results are presented in Fig. 3.

As the experimental data indicated, the treatment degree decreases with increasing fraction size. This is explained by the increase in the size of the channels between the particles of the granular material, which reduces the hydraulic resistance of the stationary material layer and, accordingly, insufficiently decreases the kinetic energy of suspended particles for their retention in the filtering media layer.

A literature review showed that one of the ways to improve the efficiency of wastewater treatment from suspensions is to form a combined granular media loading [14]. Typically, the material with the largest particle size is used first in the direction of the treated wastewater flow, gradually decreasing it towards the column exit. Additionally, using the principle of combining filtering materials allows for a reduction in wastewater treatment costs [15, 16].

To compare the efficiency of combining granular media loading, a model setup with two layers of different fractions or filtering materials was assembled. The experiment results are presented in Table 3.

The analysis of experimental data showed that the highest degree of suspended solids removal is achieved when using a combination of filtering materials – quartz sand and Filter Ag (in a ratio of 1 : 2). The lowest degree of suspended solids removal was observed when using a combination of filtering materials—quartz sand with particles of 1.0–2.0 mm and zeolite (in a ratio of 1 : 2). At the same time, the highest unit cost of wastewater treatment is associated with loadings that include zeolites (which have a low degree of suspended solids removal) and Filter Ag (which is high cost and lacks local production in Russia).

Thus, the most effective and accessible granular filtering material is quartzite from the Bobrovskoye deposit, which we recommend using in a combination of fractions 2.0–5.0 and 0.7–1.2 (in a ratio of 1 : 2).

Table 3

Degree of wastewater treatment from suspended particles using a combined granular media layer

Filtering material	Amount of treated water before reaching MAC, L	Cost of loading for laboratory setup, Rubles	Unit cost of wastewater treatment per liter, Rubles/L
Quartzite from Bobrovskoye deposit, fraction 2.0–5.0/0.7–1.2 (in ratio 1 : 2)	480	150	0.31
Quartzite from Bobrovskoye deposit, fraction 2.0–5.0/0.8–2.0 (in ratio 1 : 2)	250	145	0.58
Quartzite from Bobrovskoye deposit, fraction 1.0–3.0/zeolite (in ratio 1 : 1)	180	162	0.90
Quartzite from Bobrovskoye deposit, fraction 1.0–3.0/zeolite (in ratio 1 : 2)	100	123	1.23
Quartzite from Bobrovskoye deposit, medium fraction 1.0–3.0/zeolite (in ratio 2 : 1)	250	140	0.56
Quartzite from Bobrovskoye deposit, fraction 2.0–5.0/Filter Ag (in ratio 1 : 2)	720	433	0.60
Quartzite from Bobrovskoye deposit, fraction 2.0–5.0/quartzite from Bobrovskoye deposit, fraction 0.7–1.2/Filter Ag (in ratio 1 : 1 : 1)	580	291	0.50

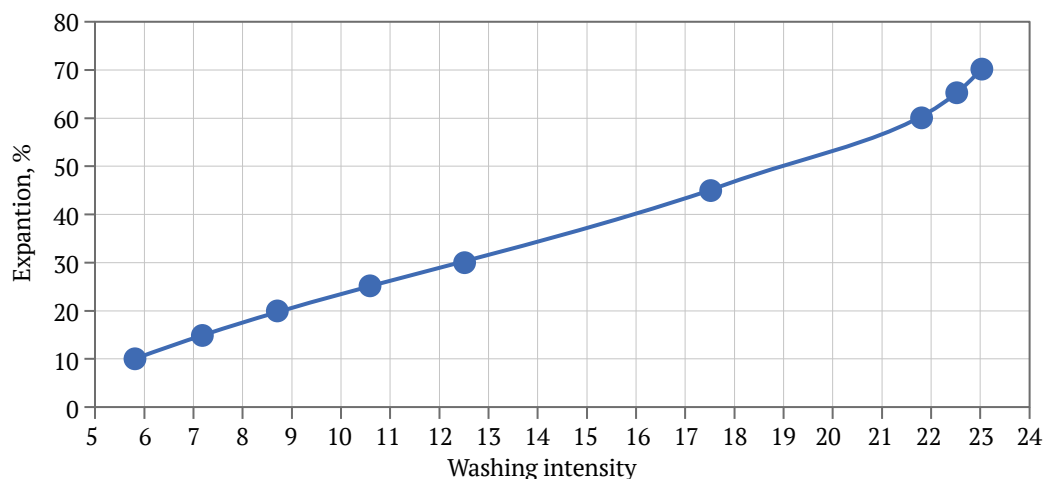


Fig. 4. Dependence of the expansion of quartzite media from the Bobrovskoye deposit, fraction 2.0–5.0/0.7–1.2 (in ratio 1 : 2), on washing intensity

To restore the filtering capacity of the granular media, its regeneration is carried out through backwashing.

The optimal percentage of granular media expansion during regeneration is 30% [17]. To achieve the desired expansion, each type of granular media requires its specific wash water flow rate.

To determine the optimal intensity of backwashing for the studied filtering materials, a series of experiments was conducted. The dependence of the filter layer expansion on the wash water flow rate was recorded on the filtering column described above. Wash water was supplied to the filtering column from below and drained from the top, with the washing intensity regulated by valve K2.

For each type of filter media, the dependence of its expansion on the wash water flow rate was determined. The graph of the expansion dependence for the quartzite media from the Bobrovskoye deposit, fraction 2.0–5.0/0.7–1.2 (in a ratio of 1 : 2), is presented in Figure 4.

Based on the analysis of the data, it can be concluded that the optimal wash water flow rate for effectively regenerating the combined filtering media – quartzite from the Bobrovskoye deposit, fractions 2.0–5.0/0.7–1.2 (in a 1 : 2 ratio) – is 12–13 L/m²·s.

Conclusion

Insoluble suspended substances are the primary pollutants in quarry wastewater. The simplest and most cost-effective method for treating this type of wastewater is filtration through a stationary granular layer of filtering material. Coal mining enterprises commonly use the wastewater treatment system recommended by BAT No. 15 ITC-37–2017 “Coal Mining and Beneficiation”. This system includes sedimentation ponds, which are open earthen basins constructed either by excavation (e.g., pit-type sedimentation ponds) or by damming natural ravines with combined mineral material dams (e.g., ravine-type sedimentation ponds). For additional treatment of quarry wastewater, we recommend filtration using granular media filters.

Among the materials studied, quartzite from the Bobrovskoye deposit, used in combination with various fractions for two-stage filtration, demonstrated the highest efficiency. To restore the filtering capacity of the granular media, backwashing is used for regeneration. For effective regeneration of the combined filtering media – quartzite from the Bobrovskoye deposit, fractions 2.0–5.0/0.7–1.2 (in a 1 : 2 ratio) – the optimal wash water flow rate is 12–13 L/m²·s.

References

1. Ivanova L.A., Salishcheva O.V., Timoshchuk I.V. et al. Major wastewater pollutants in coal mining. *Coke and Chemistry*. 2023;66(4):227–231. <https://doi.org/10.3103/S1068364X23700722>
2. Ivanova L., Golubeva N., Timoshchuk I. et al. Evaluation of the efficiency of wastewater treatment of a coal mining enterprise and its impact on the pollution of small rivers. *Ecology and Industry of Russia*. 2023;27(1):60–65. (In Russ.) <https://doi.org/10.18412/1816-0395-2023-1-60-65>



3. Krasavtseva E.A., Maksimova V.V., Makarov D.V., Masloboev V.A. Removal of suspended solids from industrial wastewater. *Journal of Mining Science*. 202;58(3):466–475. <https://doi.org/10.1134/S1062739122030140> (Orig. ver.: Krasavtseva E.A., Maksimova V.V., Makarov D.V., Masloboev V.A. Removal of suspended solids from industrial wastewater. *Fiziko-Tekhnicheskiye Problemy Razrabotki Poleznykh Iskopayemykh*. 2022;(3):136–146. (In Russ.) <https://doi.org/10.15372/FTPRPI20220314>)
4. Blinov S.M., Karavaeva T.I., Bokov D.A. Method of water clearing from suspended substances with use of drag's dumps. *Bulletin of Perm University. Geology*. 2012;(2):86–91. (In Russ.)
5. Tchaikovsky D.Ya., Tchaikovsky A.A., Arkanova I.A. Expediency of using quartz sand as a filtering granular material for water purification from suspended solids. *Vestnik Nauchnykh Konferentsiy*. 2016;(3–7):218–219. (In Russ.)
6. Gron V.A., Budnik E.V., Shakhrai S.G., Kondratyev V.V. New opportunities for coal deposit wastewater treatment. *Proceedings of Irkutsk State Technical University*. 2012;(9):183–189. (In Russ.)
7. Das A., Saha A.K., Sarkar Sh. et al. A multidimensional study of wastewater treatment. *International Journal of Experimental Research and Review*. 2022;28:30–37. <https://doi.org/10.52756/ijerr.2022.v28.005>
8. He L., Gao Z., Fan L., Tan T. The shock effect of inorganic suspended solids in surface runoff on wastewater treatment plant performance. *International Journal of Environmental Research and Public Health*. 2019;16(3):453. <https://doi.org/10.3390/ijerph16030453>
9. Shi J., Huang W., Han H., Xu C. Pollution control of wastewater from the coal chemical industry in China: Environmental management policy and technical standards. *Renewable and Sustainable Energy Reviews*. 2021;143:110883. <https://doi.org/10.1016/j.rser.2021.110883>
10. Zhang Sh., Wu Q., Ji H. Research on zero discharge treatment technology of mine wastewater. *Energy Reports*. 2022;8(2):275–280. <https://doi.org/10.1016/j.egyr.2022.01.014>
11. Yuan N., Zhao A., Hu Z. et al. Preparation and application of porous materials from coal gasification slag for wastewater treatment: A review. *Chemosphere*. 2022;287(2):132227. <https://doi.org/10.1016/j.chemosphere.2021.132227>
12. Mao G., Han Y., Liu X. et al. Technology status and trends of industrial wastewater treatment: A patent analysis. *Chemosphere*. 2022;288(2):132483. <https://doi.org/10.1016/j.chemosphere.2021.132483>
13. Gorelkina A.K., Timoshchuk I.V., Golubeva N.S. et al. Reduction of impact of mining on water ecosystems. *Mining Informational and Analytical Bulletin*. 2023;(7):64–75. (In Russ.). https://doi.org/10.25018/0236_1493_2023_7_0_64
14. Ivanova L., Timoshchuk I., Gorelkina A. et al. Removing excess iron from sewage and natural waters: selecting optimal sorbent. *Food Processing: Techniques and Technology*. 2024;54(2):398–411. (In Russ.) <https://doi.org/10.21603/2074-9414-2024-2-2516>
15. Mikhaylova E.S., Ivanova L.A. Technologies of full-cycle treatment of pit and surface wastewater for open-pit coal mining operations: trends and prospects. *Ugol'*. 2023;(9):63–69. (In Russ.). <https://doi.org/10.18796/0041-5790-2023-9-63-69>
16. Mkilima T., Meiramkulova K., Zandybay A. et al. Investigating the influence of column depth on the treatment of textile wastewater using natural zeolite. *Molecules*. 2021;26(22):7030. <https://doi.org/10.3390/molecules26227030>
17. Nikitin A.P., Dudnikova Y.N., Mikhaylova E.S., Ismagilov Z.R. Raman characteristics of Kuznetsk basin coal and coal-based sorbents. *Coke and Chemistry*. 2019;62(9):379–384. <https://doi.org/10.3103/S1068364X19090059>
18. Zvekov A.A., Zikov I.Y., Dudnikova Y.N. et al. Sorption of organic compounds by carbon sorbents from Kuzbass coals. *Coke and Chemistry*. 2019;62(6):240–244. <https://doi.org/10.3103/S1068364X19060103>

Information about the authors

Ludmila A. Ivanova – Cand. Sci. (Eng.), Associate Professor, Department of Technosphere Safety, Kemerovo State University, Kemerovo, Russian Federation; ORCID [0000-0002-4103-8780](https://orcid.org/0000-0002-4103-8780); e-mail lyuda_ivan@mail.ru

Alexander Yu. Prosekov – Dr. Sci. (Eng.), Professor, Corresponding Member of the Russian Academy of Sciences, Rector, Kemerovo State University, Kemerovo, Russian Federation; ORCID [0000-0002-5630-3196](https://orcid.org/0000-0002-5630-3196), Scopus ID [57194498125](https://orcid.org/57194498125), ResearcherID [C-7606-2014](https://orcid.org/C-7606-2014); e-mail rector@kemsu.ru

Pavel P. Ivanov – Cand. Sci. (Eng.), Associate Professor, Department of Mechatronics and Automation of Technological Systems, Kemerovo State University, Kemerovo, Russian Federation; ORCID [0000-0002-8086-3273](https://orcid.org/0000-0002-8086-3273), Scopus ID [57214880844](https://orcid.org/57214880844); e-mail ipp7@yandex.ru



Ekaterina S. Mikhaylova – PhD (Chemistry), Director of the Institute of Nano-, Bio-, Information, Cognitive and Socio-Humanitarian Technologies, Department of Technosphere Safety, Kemerovo State University, Kemerovo, Russian Federation, ORCID [0000-0002-0673-0747](https://orcid.org/0000-0002-0673-0747), Scopus ID [57189052967](https://scopus.org/57189052967); e-mail: e_s_mihaylova@mail.ru

Irina V. Timoshchuk – Dr. Sci. (Eng.), Professor, Department of Technosphere Safety, Kemerovo State University, Kemerovo, Russian Federation; ORCID [0000-0002-1349-2812](https://orcid.org/0000-0002-1349-2812), Scopus ID [56646335100](https://scopus.org/56646335100), ResearcherID [L-4795-2016](https://orcid.org/L-4795-2016); e-mail irina_190978@mail.ru

Alena K. Gorelkina – Dr. Sci. (Eng.), Professor, Department of Technosphere Safety, Kemerovo State University, Kemerovo, Russian Federation; ORCID [0000-0002-3782-2521](https://orcid.org/0000-0002-3782-2521); e-mail alengora@yandex.ru

Received 11.03.2024

Revised 23.04.2024

Accepted 10.06.2024



SAFETY IN MINING AND PROCESSING INDUSTRY AND ENVIRONMENTAL PROTECTION

Research paper

<https://doi.org/10.17073/2500-0632-2023-11-184>

УДК 504.55.054:622(470.6)

**Environmentally sound geotechnologies for leaching metals from polymetallic ore processing wastes and wastewater****V.I. Golik^{1,2}  , Yu.I. Razorenov³  ,
N.G. Valiev⁴  , O.A. Gavrina⁵  **¹ *Moscow Polytechnic University (MPU), Moscow, Russian Federation*² *North Caucasian Mining and Metallurgical Institute (NCSTU), Vladikavkaz, Russian Federation*³ *M.I. Platov South Russian State Polytechnic University (NPI), Novocherkassk, Russian Federation*⁴ *Ural State Mining University, Ekaterinburg, Russian Federation*⁵ *Research Institute of Comprehensive Exploitation of Mineral Resources of the Russian Academy of Sciences, Moscow, Russian Federation* v.i.golik@mail.ru**Abstract**

Global challenges (increased consumption of georesources, climatic changes, limited reserves) increase the relevance of the problems of growing waste accumulation and environmentally-sound modernization of mineral extraction. In this regard, the existing approaches to the design of geotechnologies for metal mining need to be improved based on a concept of so-called circulation waste management and ecologization of technological processes. The paper is devoted to the issue of formation of conceptual bases and directions of ecologization of geotechnologies at leaching metals from polymetallic ore processing wastes and wastewater. The study presents recommendations for improving in-situ leaching of ores in blocks, allowing to determine the optimal conditions for increasing the completeness of subsoil use and reducing environmental damage. It was revealed that at metal extraction with solution circulation through brine chambers the content of Na, Cl, SO₄ and Ca ions in dialysate was low, while without circulation through brine, it significantly exceeded corresponding MPCs. This proves the fundamental feasibility of controlling natural leaching processes by enhancing the oxidizing potential of natural solvents through the addition of industrial oxidizing agents. It was found that increasing the duration of agitation leaching (both with and without mechanoactivation) leads to a uniform expansion of the local maximums of Pb yield from the pulp when the minimum NaCl concentration decreases from 11–12 to 7% at H₂SO₄ concentration of 0.6%. One of key results of the study is justifying the expansion of the use of disintegrators to realize targeted activation of tailings. The practical significance of the obtained results lies in the proved feasibility of optimizing the flow sheet of electrochemical extraction of metals from wastewater on the basis of the obtained regularities of the use of brine circulation through brine chambers. In addition, the totality of the obtained results of using a disintegrator for re-extraction of lead from geomaterials will allow developing a methodology for calculating the parameters of mechanoactivation action to increase the degree of metal recovery from the tailings of North Ossetia-Alania's (Zgidskoe, Sadonskoe, Arkhonskoe deposits) polymetallic ores beneficiation. The most promising way for further research is to substantiate methods of using underground space for complete removal of wastes (wastewater and tailings) after their multistage treatment.

Keywords

tailings, wastewater, acid leaching, mechanochemical activation, Pb recovery, geotechnologies, waste management

For citationGolik V.I., Razorenov Yu.I., Valiev N.G., Gavrina O.A. Environmentally sound geotechnologies for leaching metals from polymetallic ore processing wastes and wastewater. *Mining Science and Technology (Russia)*. 2024;9(3):271–282. <https://doi.org/10.17073/2500-0632-2023-11-184>



ТЕХНОЛОГИЧЕСКАЯ БЕЗОПАСНОСТЬ В МИНЕРАЛЬНО-СЫРЬЕВОМ КОМПЛЕКСЕ И ОХРАНА ОКРУЖАЮЩЕЙ СРЕДЫ

Научная статья

Экологически чистые геотехнологии выщелачивания металлов из твердых и жидких отходов обогащения полиметаллического сырья

В.И. Голик^{1,2}   , Ю.И. Разоренов³  
Н.Г. Валиев⁴  , О.А. Гаврина⁵  

¹Московский политехнический университет (МПУ), г. Москва, Российская Федерация

²Северо-Кавказский горно-металлургический институт, (СКТИ), г. Владикавказ, Российская Федерация

³Южно-Российский государственный политехнический университет (НПИ) им. М.И. Платова,
г. Новочеркасск, Российская Федерация

⁴Уральский государственный горный университет (УГГУ), г. Екатеринбург, Российская Федерация

⁵Институт проблем комплексного освоения недр им. академика Н.В. Мельникова Российской академии наук,
г. Москва, Российская Федерация

 v.i.golik@mail.ru

Аннотация

Глобальные вызовы (рост потребления георесурсов, климатические изменения, ограниченность запасов) повышают актуальность проблем роста накопления отходов и экологической модернизации добычи минерального сырья. В связи с этим существующие подходы к проектированию геотехнологий добычи металлов нуждаются в совершенствовании на основе концепции циркуляционного управления отходами и экологизации технологических процессов. Статья посвящена вопросу формирования концептуальных основ и направлений экологизации геотехнологий при выщелачивании металлов из твердых и жидких отходов обогащения полиметаллического сырья. В исследовании предложены рекомендации по совершенствованию подземного выщелачивания руд в блоках, позволяющие определить оптимальные условия для повышения полноты использования недр и уменьшения ущерба окружающей среде. Выявлено, что при извлечении металлов с циркуляцией раствора через рассольные камеры содержание ионов (Na, Cl, SO₄ и Ca) в диализате было низким, а без циркуляции в рассоле существенно превышало ПДК (по Na, Cl, SO₄ и Ca). Это доказывает принципиальную возможность управления процессами подземного выщелачивания путем усиления окислительного потенциала растворителей за счет добавления промышленных окислителей. Установлено, что рост продолжительности агитационного выщелачивания (как с использованием, так и без механоактивации) приводит к равномерному расширению локальных максимумов выхода Pb из пульпы при снижении минимальной концентрации NaCl с 11–12 до 7 % при H₂SO₄ = 0,6 %. Одним из ключевых результатов исследования является обоснование расширения области использования дезинтеграторов для осуществления направленного активационного воздействия на хвосты обогащения. Практическое значение полученных результатов заключается в возможности оптимизации технологической схемы электрохимического извлечения металлов из техногенных стоков на основании полученных результатов применения циркуляции рассолов через рассольные камеры. Кроме того, совокупность полученных результатов использования дезинтегратора для повторного извлечения свинца из геоматериалов позволит разработать методику расчета параметров механоактивационного воздействия для повышения степени извлечения металлов из хвостов обогащения полиметаллического сырья РСО–Алания (Згидское, Садонское, Архонское месторождения). Наиболее перспективным направлением дальнейших исследований является обоснование путей использования подземного пространства для полного захоронения отходов (техногенных стоков и хвостов обогащения) после их многостадийной обработки.

Ключевые слова

хвосты обогащения, растворы/стоки, кислотное выщелачивание, механохимическая активация, извлечение Pb, геотехнологии, управление отходами

Для цитирования

Golik V.I., Razorenov Yu.I., Valiev N.G., Gavrina O.A. Environmentally sound geotechnologies for leaching metals from polymetallic ore processing wastes and wastewater. *Mining Science and Technology (Russia)*. 2024;9(3):271–282. <https://doi.org/10.17073/2500-0632-2023-11-184>



Introduction

Mining enterprises around the world step up the rate of accumulation of various types of waste, causing environmental degradation due to the growth of production, gradual transition to the mining of lean and disseminated ores, as well as due to the complication of mineral deposits mining conditions [1–3]. Big data from the enterprise can be used to reduce resource consumption and optimize reserves at mines using digital twin approach [4]. Digital models of geologic mineral reserves in combination with GIS technologies allow forming digital twins of deposits, determining the design of more rational mining methods [3]. At the same time, solutions to some environmental problems can be achieved by optimizing existing technological processes, as well as improving the quality of management of natural-technogenic systems [5, 6].

Heap leaching methods, which are widely used around the world, allow metals to be extracted more profitably from various types of low-grade ores. At the same time, even the existing level of understanding of its fundamentals does not allow to fully ensure environmentally sound implementation in the pursuit of sustainable development of mineral resource base [7]. This gives rise to the problem of formation of wastewater, dry waste dumps and dust contamination. Each dusting facility is characterized by individual peculiarities, which allows the use of process models to minimize emissions into the atmosphere, but does not allow to completely solve this problem [8]. Minimizing the consequences, i.e., hydrosphere pollution, requires the development of measures that take into account a whole set of mutually determined factors [9, 10]. Tailings storage facilities (TSFs) are anthropogenic deposits composed of ore processing tailings, which participate in environmental pollution with chemical ingredients due to natural and anthropogenic leaching processes [11–14]. Thus, in our country, more than 45 billion tons of solid waste (including dusting ones) have already been stockpiled in the form of waste dumps, of which beneficiation wastes annually add about 140 million m³/year to this figure [15].

The solution to waste problems in the recovery of polymetallic raw materials can be achieved with greening and widespread use of in-situ leaching geotechnologies. Progressive technologies of in-situ leaching in blocks are implemented in mining industry to maintain and strengthen the mineral resource bases of technologically developed countries [16, 17]. The history of implementing and development of the in-situ block leaching at nuclear industry enterprises of the USSR in Kazakhstan is described in [18]; at the

same time some processes remain insufficiently studied. Thus, for Jimidon ore field, increasing the availability for processing of low-grade reserves of polymetallic raw materials can be achieved by improving the quality of breaking (blasting) and selective energy consumption in the blasting preparation of ores [19]. At mining enterprises in Russia, primarily in the nuclear industry, in-situ block leaching methods are used in mining of a large share of commercial products, for example, at Priargunsky MCC. In this case, suboptimal topology of the surface well network is used, which does not allow the use of directional drilling to minimize the number of injection wells (when they are drilled in parallel to the ore body) that leads to an increase in waste generation with low efficiency of in-situ leaching [20].

The rate of leaching processes is determined by the metal content, the thickness of the diffusion layer and the diffusion coefficient. The rate of chemical reaction is crucial for the extraction of rare earth elements in the process of in-situ leaching (which is accompanied by ion migration, which gives it an electrochemical character) with two parameters being the most important: solution resistance and charge transfer resistance [21]. In addition, the maximum recovery corresponds to a high velocity of solution movement relative to the reaction surface. In the Caucasus, most of the exploited deposits are of the quartz-polymetallic type in the quartz-keratophyre formation, e.g., Sadonskoe. It is characterized by polymetallic and pyrrhotite types of mineralization. Water is the cause of the hydrolysis process. When a certain acidity is reached, iron sulfate reacts to form iron hydroxide. Of the methods of solution purification the most commonly used is chemical, the disadvantage of which is the possibility of environmental pollution by reagents in case of emergency violation of the process conditions.

The existing mathematical methods for controlling leaching processes require a large amount of a priori information about the structure and properties of the deposit, with one of the main methods being the method of expert reviews, which does not provide sufficient reliability of the results obtained [22, 23]. The noted features of mining practice are most acutely manifested in the implementation of processes where the error can reduce the performance of a process to an unacceptable level [24, 25]. For example, if the parameters of ore breaking for leaching are wrong, the highly efficient process with chemical dissolution of metals becomes impossible to use.

The existing approaches to the design of geotechnologies for metal extraction need to be improved based on the concept of circulation waste manage-



ment and greening of technological processes [26, 27]. Study [28] convincingly proved the necessity of solving the primary problems for “the transition to the circulation economy in the conditions of handling technogenic mineral formations”. The drawback of realizing the author’s idea of creating pathways to achieve the goal is the perception of the circulation approach as a “closed supply chain concept”. While, for example, for coal mine’s methane it is formulated as “conversion of waste (methane) into energy” [29, 30]. In this regard, the author’s hypothesis of “circulation management of tailings” consists in: “the optimization of technological processes of leaching, mechanochemical activation of geomaterials or other methods allowing to transform beneficiation tailings into the source of additionally recoverable metals with the subsequent use of tailings in production of building materials or at facilities for burial (inert filler of underground space)”.

In this regard, the **purpose** of the study is the formation of conceptual bases and directions of ecologization of geotechnologies at leaching metals from polymetallic ore processing wastes and wastewater. In this regard, the following **problems** should be solved: 1 – to analyze and classify measures to improve geotechnologies of underground metal leaching; 2 – to simulate the process of electrochemical metal extraction from wastewater; 3 – to substantiate the efficiency of metal extraction with the use of preliminary mechanochemical activation of dry tailings.

Methods

The study targets are technogenic deposits of North Ossetia-Alania (Russia). Intensive exploitation of ore deposits is accompanied by the formation of dumps of substandard ores and tailings of processing plants located in river valleys.

Quantitative values and parameters of wastewater in the conditions of the Sadonskoe ore cluster deposit are given in Table 1.

The volumes of storage of tailings from the processing plants of the North Caucasus are given in Table 2.

To assess the prospects in the field of improvement of underground geotechnologies, a retrospective review of the theory and practice of application of technological innovations at the enterprises of the Ministry of Atomic Energy and Industry of the USSR was carried out.

To solve the second problem, wastewater with electrochemically treated leaching reagents were tested. Sulfate-chloride wastewater of the Arkhonskoe deposit (North Ossetia-Alania) with predominance of sodium cations was tested at a unit in the

All-Union Research Institute of Chemical Technology (Moscow). The base for determining the performance of metal leaching from natural resources is the results of leaching of ores and their processing products in percolator columns using natural reagents.

The third problem was solved on the basis of testing of Mizursky processing plant tailings. The pulp was activated by high-energy grinding in DESI-11 unit with rotor speeds of 50 and 200 Hz for 0.25 and 1 h, respectively. To form a pulp, the ground tailings samples were screened using a 2.0 mm mesh sieve and mixed with the filtrate. The modeling technique was developed by analogy with the technique considered in [31–33], and consisted in data processing based on the Savitzky-Golei filter combined with three-dimensional interpolation using the method of R.J. Renka (Robert Renka) [34–36]. The algorithms were implemented as “scripts” (using Vi IMproved software (version 9.0)) in Python (version 2.7.10). The final three-dimensional plots were built using Gnuplot software (version 5.4).

Table 1

Characterization of industrial wastewater

Deposit	Wastewater volume, m ³ /h	Metal content, g/m ³
Sadonskoe	300	Lead – 5, zinc – 7
Zgidskoe	24	Lead – 5, zinc – 12
Kholstinskoe	70	Lead – 8, zinc – 25
Archonskoe	30	Lead – 65, zinc – 7
Khanikom-Kakadurskoe	150	Lead – 5, zinc – 100
Urupskoe	350	Copper – 12, zinc – 41, iron – 0.2
Tyrnyauz	400	Molybdenum – 37, tungsten – 45

Table 2

Ore processing tailings storage quantities

Tailings Storage Facility (TSF)	Quantity of beneficiation tailings, tons	Grades of Metals, %
Mizursky processing plant	3,000,000	Zinc – 0.15–0.25, lead – 0.13–0.19
Fiagdon processing plant	3,000,000	Zinc – 0.18–0.24, lead – 0.18–0.24
Electrozinc plant	3,000,000	–
Urupskoe processing plant	4,000,000	Zinc – 0.25–0.40, copper – 0.36–0.46, iron – 30–35
Tyrnyauz processing plant	120,000,000	Tungsten – 0.25–0.40, copper – 0.36–0.46, iron – 30–35%



Findings

Improvement of geotechnology of in-situ leaching of metals

Leaching of polymetallic raw materials is the process of filtration of aqueous solution through rock strata under the action of gravity, capillary forces at inter-phase boundaries or due to pressure gradients between injection and production (pumping-out) wells. The internal structure of a porous medium is random and its geometry can be described only approximately. In this connection, the determination of aqueous solutions flow parameters on the basis of hydraulic equations shall be approximated, with some degree of probability.

The main parameters of the filtration process are viscosity, permeability, velocity, and pressure of a liquid [37, 38]. A liquid moving in a porous medium is a non-Newtonian one, for which the relation describing the rate of strain change as a function of stress is described by the rheological law:

$$\tau_{xy} = \tau_0 + \mu \frac{\partial u_x}{\partial y}, \quad (1)$$

where μ is dynamic viscosity; τ_0 is initial shear stress; u_x is flow velocity in the direction being square with OX axis.

In a porous medium, a non-Newtonian liquid satisfies the equation of motion and the continuity equation in the absence of inflows and discharges:

$$\begin{aligned} \rho \frac{\partial \bar{V}}{\partial t} &= -\nabla \bar{p} + \nabla(\bar{\tau} - \rho \bar{V}' \bar{V}'), \\ \frac{\partial(\rho m)}{\partial t} + \nabla(\rho \bar{V}) &= 0, \end{aligned} \quad (2)$$

where ρ is density of medium; m is porosity; \bar{V} is the velocity vector; \bar{p} is pressure distribution; $\bar{\tau}$ is stress tensor.

The permeability of an ore-bearing formation differs depending on its density, but under the conditions of chaotic variation of filtration characteristics at each point of a formation it is possible to assume its state to be homogeneously permeable. If the filtration characteristics of a formation, porosity and permeability, vary from point to point, the formation is heterogeneous.

In a mathematical model of potential flow, the total formation flow rate is the sum of the flow rates of all layers (composing the formation). For simplification, a heterogeneous formation is modeled as a quasi-uniform formation with averaged formation permeability

$$k_{av} = \sum_i \frac{k_i h_i}{h}, \quad (3)$$

where k_i is permeability of the i -th layer; h_i is thickness of the i -th layer; h is thickness of the whole formation.

In generalized form, the model of diffusion of solution for leaching of metals from ores can be represented by the Fokker-Planck equation:

$$\frac{\partial W}{\partial t} = \left[- \sum_{i=1}^3 \frac{\partial}{\partial x_i} D_i^1(x_1, x_2, x_3) + \sum_{i=1}^3 \sum_{j=1}^3 \frac{\partial^2}{\partial x_i \partial x_j} D_{ij}^2(x_1, x_2, x_3) \right] W, \quad (4)$$

where $W(\bar{V}, t)$ is velocity probability density function; D^1 is flow drift vector; D^2 is diffusion tensor.

The presence of particles coarser than 5 mm in a layer adjacent to a solid phase increases the intensity of metal particles transport in the extracted liquid.

The optimal leaching method is the one that ensures the transit of metals into a mobile state with minimal ore preparation costs and provides permeability of the crushed ore for leaching solutions. Mineral extraction technologies, including leaching methods, and their individual components are evaluated by the criterion of the completeness of metal extraction from ores [39, 40]. It follows from the review of studies [41] that measures to improve in-situ leaching of ores in blocks (with controlled permeability of the blocks for leaching solutions) can be systematized (Table 3).

Simulation of efficiency of metal recovery from wastewater

The method of electrochemical softening of concentrated solutions through electrodialysis desalination consists in using the phenomenon of selectivity of ion-exchange membranes: cation-exchange membranes pass positive ions, while anion-exchange membranes pass negative ions.

Membrane electrolysis provides reagent-free softening of natural solutions and concentrating of minor elements. Electrodialysis and activation in diaphragm electrolyzers with decomposition of salt systems into acid and alkali and neutralization of solutions are rather promising. The disadvantage of the method is the deposition of hardly soluble compounds in brine chambers.

The parameters of metal recovery from a solution are determined for options with the solution circulation through brine chambers and without the circulation. Natural solutions are fed into the desalting chamber, and pure water is fed into the acid/alkali generation chamber. After that, the reagents required for the generation of alkali and acid (selected for the implementation of the technological cycle) are fed into the chambers. As the proportions of magnesium, calcium ions, and acids increases, the efficiency of the investigated process deteriorates due to a decrease in the quality of membrane contact with brine



due to the adhesion of carbonate precipitates and magnesium oxide. Energy consumption for removal of 1 kg of salt is 0.6 kW (at residual concentrations of $Zn = 0.3\text{--}0.4 \text{ mg/dm}^3$ and $Pb = 0.06\text{--}0.08 \text{ mg/dm}^3$, respectively).

To implement the author's approach, a series of tests was carried out for different schemes of brine (solution) circulation. The obtained performance data for these schemes are presented in Table 4 and Figs. 1, 2.

It follows from the surface analysis presented in Fig. 1, that the option of the electrochemical method

with brine circulation through brine chambers is the most efficient way to leach metals from industrial wastewater. Extraction of metals from brines is carried out in sorption and washing columns up to 4 m high and 1–1.5 m in diameter. Consumption of reagents per 1000 m³ of solution: cationite (anionite), 0.8 kg; regenerating reagent, 100–150 kg.

It follows from the analysis of the concentrations presented in Fig. 3, that the values for Na, Ca, Cl, and SO₄ significantly exceed the MPCs (Na – 6,089, Ca – 650, Cl – 4,600, and SO₄ – 153 mg/dm³).

Table 3

Measures to improve in-situ leaching of ores in blocks

Process	Essence of the process	Effect of implementation
1	2	3
Rock blasting and crushing	Advanced horizontal undercutting by blastholes (by a value of the thickness of a vertical layer)	Rationalization of compensation space formation, optimization of the ore grain size to be shrinked
	Blasting by layer with variable line of least resistance	
	Approximation of a layer shape to the vertical projection of the release shape	
Spraying with reagent solutions	Wells with casing and positioning of fine-grained layer in broken ore	Regular spraying by reagent solutions within the shrinked ore and in time
	Hydraulic rock fracturing	
Collection of solutions	Capturing solution leaks with electro-vacuum units	Optimization of reagent consumption
	Drainage by perforated pipes to a unit bottom	Minimizing environmental damage
	Creation of impervious screens made of polymeric materials	
Process intensification	Use of liquid explosives in blastholes for ore blasting	Displacement of leached ore pieces with destruction of colmataged zones
	Ore movement when breaking new layers on it	
	High-pressure compressed air pulse action	Increase in permeability through removing joint fillers and destruction of clay films Increasing the rate and completeness of metal recovery
	Ultrasound action during electromagnetic treatment of solutions with passing them through electric field	
	Action by pulsating electric current with low-frequency pulses	
Combining the extraction of different grade ores	Excavation of balance ores for conventional processing, shrinkage of a portion of balance and off-balance ores and leaching	Comprehensive improvement of deposit development performance

Table 4

Performance of metal recovery from solutions at different types of solution circulation

Component	N	Initial solution (wastewater)	Performance of metal recovery from solutions (brines)	
			with brine circulation through brine chambers	without circulation
			in dialysate	
Model options		1	2	3
Pb	1	2.2±0.3	0.1±0.02	0.08±0.02
Zn	2	40±1.2	0.4±0.05	0.3±0.03
Mg	3	70±1.9	10±2	8±1,1
Ca	4	200±6	30±1.2	40±1.7
Na	5	450±15	72±1.5	90±1.3
SO ₄	6	580±20	100±11	95±4
Cl	7	900±5	114±19	105±5

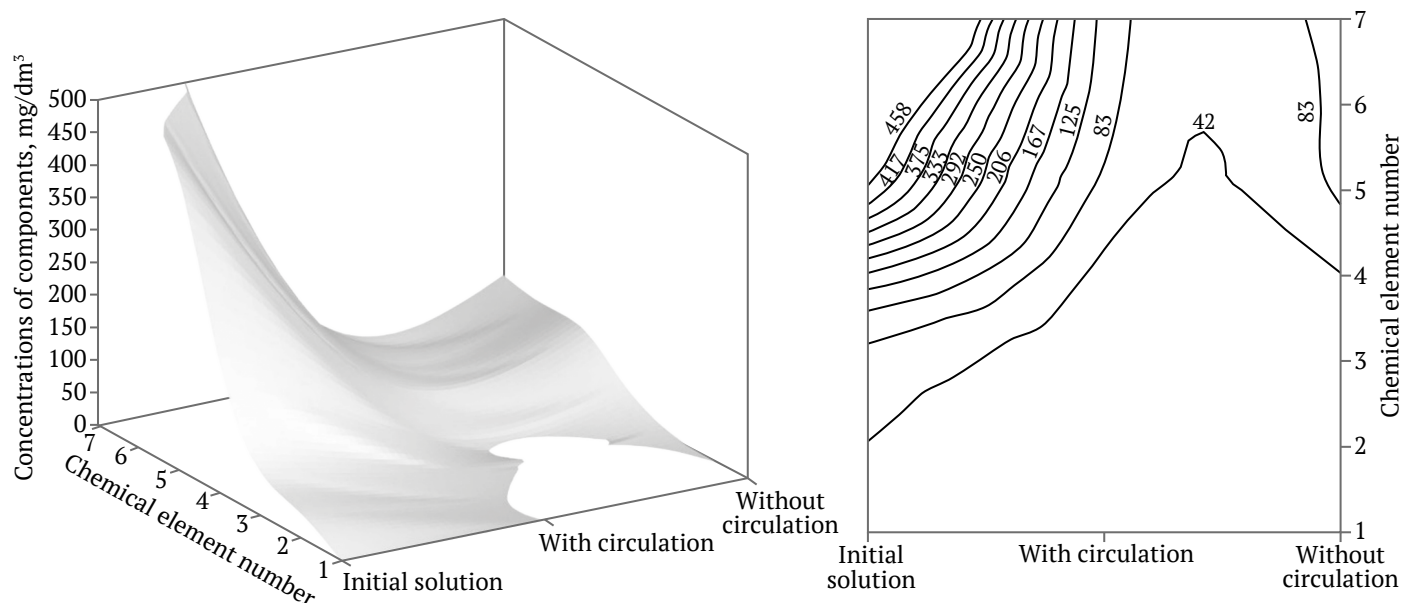


Fig. 1. Efficiency of chemical elements extraction at different parameters of electrochemical method

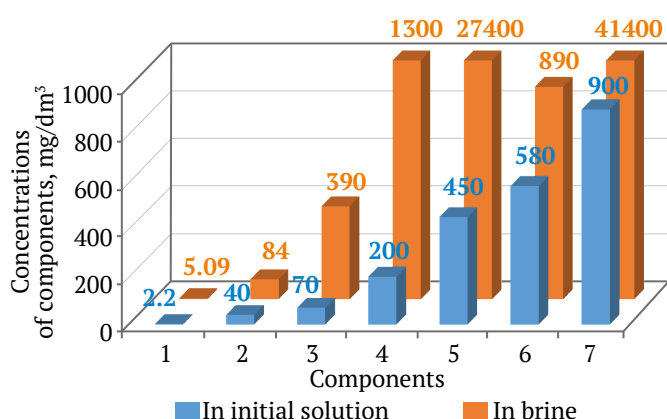


Fig. 2. Concentration of chemical elements in brines without circulation in comparison with initial solution

Metal recovery with preliminary mechanochemical activation of dry tailings

Since mechanoactivation is effectively used to convert tailings into a binding component of a back-fill material [42], it was decided to use the geomaterials activation effect to increase the yield of lead from tailings. Geomaterials were pre-milled in a laboratory ball mill, screened using a 4.0 mm mesh sieve and subjected to mechanoactivation (dry) in a DESI-11 disintegrator. The rotor speeds were 50 and 200 Hz. The testing program included the use of sulfuric acid and sodium chloride in different proportions. The acid concentration varied in the range including 20, 90 and 160 g/l, and that of sodium chloride, 2, 6, and 10 g/l. The preparation of the liquid fraction of the pulp implied preliminary preparation of chemical reagents (in separate flasks) in the proportions spe-

cified in the methodology of the test. All calculations were performed to obtain one liter of leaching solution with selected solid to liquid fraction ratio (S/L) values of 1/4.1, 1/7 and 1/10, respectively. After obtaining the activated solid fraction of the geomaterial, it was mixed with the liquid solution in a specified S/L fraction ratio to obtain a pulp. Agitation leaching was then carried out in laboratory columns.

Weight concentrations of leaching solution components in the final pulp, %, were determined by the following formula (using sulfuric acid as an example):

$$m_p(\text{H}_2\text{SO}_4) = \frac{m_L(\text{H}_2\text{SO}_4)}{M_p} \times 100, \quad (5)$$

where M_p is weight of pulp, consisting of the weight of solution (varying depending on the ratio of the concentrations of the reagents in 1 liter) and a constant weight of a subsample of solid dry waste, equal to 50 g; $m_L(\text{H}_2\text{SO}_4)$ is weight of sulfuric acid in the liquid fraction of the pulp at different concentrations of the acid and sodium chloride in it, g.

Lead concentration in the pulp was determined by standard method using atomic absorption spectrometer "KVANT-AFA" (KORTEK LLC). Q-Q plots (quantile-quantile plots – goodness-of-fit criterion of model construction) were plotted in Microsoft Excel 2010 software. The lead extraction performance at preliminary activation of the tailings and leaching time of 0.25 h (option I), as well as at preliminary activation of tailings by dry method in the disintegrator and leaching time of 1 h (option II) are presented in Table 5 and Fig. 3.

It follows from the analysis of Fig. 3, a, that the activation effect at $\nu = 50$ Hz and leaching duration of 0.25 h causes an increase in the beneficiation performance at H_2SO_4 (concentration) = 0.8–0.9% and NaCl = 11.5–14%. In addition, a pronounced second maximum is traced: Pb = 28% at $H_2SO_4 = 0.32$ –0.45% and NaCl = 5–7.6%. Increasing the leaching time from 0.25 to 1 h and ν to 200 Hz leads to an increase in the absolute values and the area of the second zone of lo-

cal maximum, which significantly changes the idea of the process (Fig. 3, b). At $H_2SO_4 = 0.9\%$, increasing the concentration of NaCl from 1 to 14% leads to a monotonic increase in lead yield from 4% to more than 40% (concentration of NaCl = 13.5%). The area of the local maximum is limited to the region from 0.5 to 0.7% of H_2SO_4 and from 7 to 14% of NaCl. The goodness-of-fit criterion for verifying the quality of the four three-dimensional Q–Q models is the graph shown in Fig. 4.

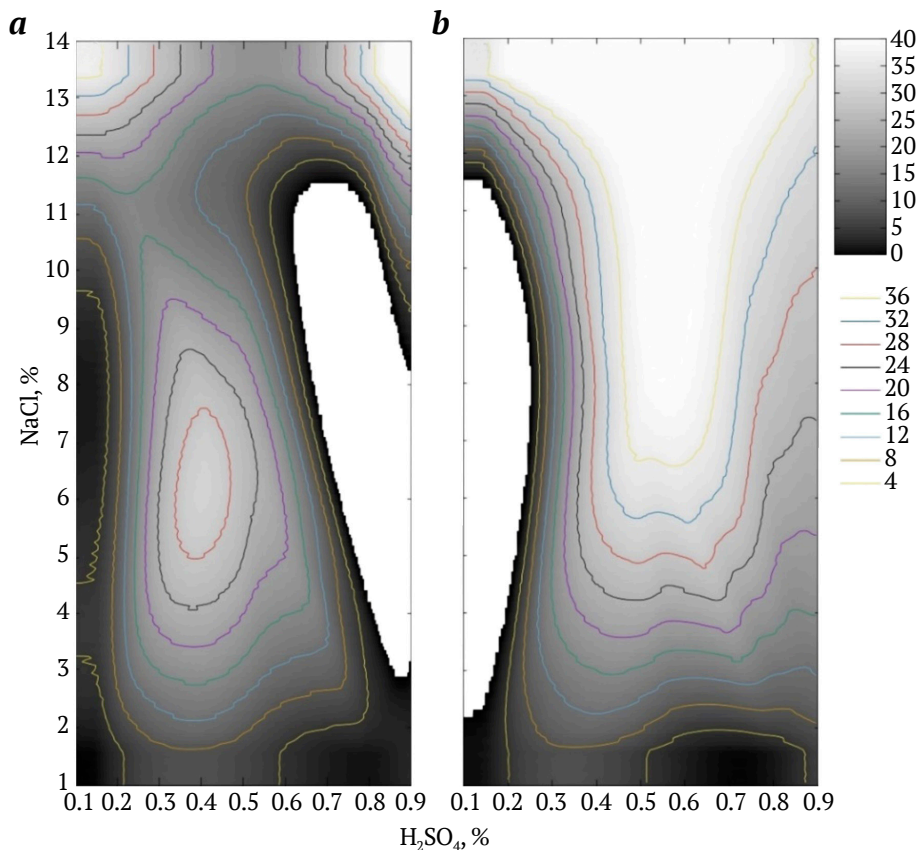


Fig. 3. Distribution of lead yield from Mizursky mill tailings:
a – leaching of Pb from pre-activated tailings $\nu = 50$ Hz, duration of 0.25 h (option II);
b – leaching of Pb from pre-activated tailings $\nu = 200$ Hz, duration of 1 h (option IV)

Table 5

Effect of pre-mechanoactivation of tailings by dry method

N of test	$m_p(H_2SO_4)$, weight concentration of sulfuric acid in pulp	$m_p(NaCl)$, weight concentration of sodium chloride in pulp	Test option	
	%	%	I	II
1	0.16	1.58	0.81	1.43
2	0.79	1.58	0.95	0.86
3	0.15	11.79	17.62	3.33
...
12	0.83	13.36	38.1	38.1
13	0.54	1.80	6.04	5.21
14	0.50	13.38	17.56	50.88

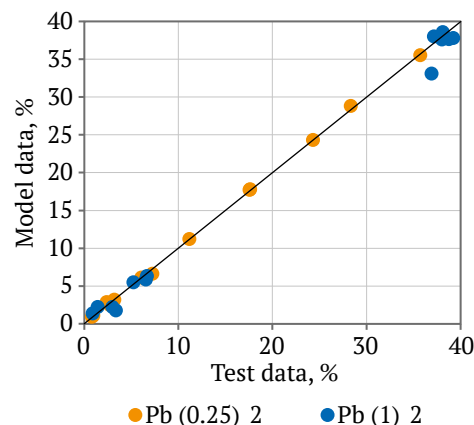


Fig. 4. Q–Q for the two model options



It follows from the analysis of the response surfaces that on the whole the obtained data are consistent with the results of studies [43, 44] on chalcopirite processing in a fine grinding mill, where the growth of H_2SO_4 concentration was higher by 30%. Leaching of Cu from ore with sulfuric acid [39] confirms the increase in epy process productivity with the increase of rotor speed in the disintegrator from 50 to 200 Hz. Studies [45, 46] also confirm the effectiveness of DESI-15 for mechano-activation of geomaterials.

Practical application

The practical significance of the obtained results lies in substantiating the feasibility of optimizing the flow sheet of electrochemical extraction of metals from wastewater on the basis of the obtained regularities of the use of brine circulation through brine chambers. In addition, the totality of the obtained results of using a disintegrator for re-extraction of lead from geomaterials will allow developing a methodology for calculating the parameters of mechanoactivation to increase the degree of metal recovery from the tailings of North Ossetia-Alania's (Zgidiskoe, Sadonskoe, Arkhonskoe deposits) polymetallic ores beneficiation.

Areas of further research

Further research should be focused on the specific changes in the parameters of existing geotechnologies not only in terms of greening of individual components or technological processes. In this regard, the most promising area for further research is to substantiate methods of using underground space for complete removal of wastes (wastewater and tailings) after their multistage treatment.

Conclusion

The main area of transformation of natural resources use paradigm should be the circulation management of mining and processing waste. The recession in mining production with decommissioning of existing rich ore and exploitable deposits can be mitigated with the development of in-situ leaching process with involving substandard reserves in exploitation. The proposed recommendations for improving in-situ leaching of ores in blocks make it possible to determine the optimal conditions for increasing the completeness of subsoil use and reducing environmental damage.

Environmental degradation caused by liquid wastes of in-situ leaching of ores can be minimized by technological means. The method of electrodialysis and activation in diaphragm electrolyzers is promising for treatment of mine wastewater. It was revealed that at metal extraction with solution circulation through brine chambers the concentrations of Na, Cl, SO_4 and Ca in dialysate was low, while without circulation through brine, they significantly exceeded MPCs (for Na, Cl, SO_4 and Ca). This proves the fundamental feasibility of controlling natural leaching processes by enhancing the oxidizing potential of natural solvents through the addition of industrial oxidizing agents.

Tailings storage facilities are man-made deposits within which natural leaching takes place. One of the key results of the study is the justification for expanding the scope of use of disintegrators in purposeful mechanical-chemical-activation action. Increasing the duration of agitation leaching (both with and without the use of mechanoactivation) leads to a uniform expansion of the local peaks of Pb yield from the pulp while the minimum NaCl concentration decreases from 11–12 to 7% at H_2SO_4 concentration of 0.6%.

References

1. Sinclair L., Thompson J. In situ leaching of copper: Challenges and future prospects. *Hydrometallurgy*. 2015;157:306–324. <https://doi.org/10.1016/j.hydromet.2015.08.022>
2. Liang W., Wang J., Leung C., Goh S., Sang S. Opportunities and challenges for gas coproduction from coal measure gas reservoirs with coal-shale-tight sandstone layers: A review. *Deep Underground Science and Engineering*. 2024. <https://doi.org/10.1002/dug2.12077>
3. Yanvarev G.S., Bobomurotov B.B. Volumetric digital model of deep horizons of the Main ore deposit of the Urupsky copper-crust deposit. *Geology and Geophysics of Russian South*. 2023;13(1):125–135. (In Russ.) <https://doi.org/10.46698/VNC.2023.90.90.009>
4. Kukartsev V., Kozlova A., Kuimova O., Nelyub V., Gantimurov A. Using digital twins to create an inventory management system. *E3S Web of Conferences*. 2023;431:05016. <https://doi.org/10.1051/e3sconf/202343105016>
5. Zakharov V.N., Kaplunov D.R., Klebanov D.A., Radchenko D.N. Methodical approaches to standardization of data acquisition, storage and analysis in management of geotechnical systems. *Gornyi Zhurnal*. 2022;(12):55–61. (In Russ.) <https://doi.org/10.17580/gzh.2022.12.10>
6. Reddivari B.R., Vadapalli S., Sanduru B., Buddi T., Vafaeva K.M., Joshi A. Fabrication and mechanical properties of hybrid fibre-reinforced polymer hybrid composite with graphene nanoplatelets and



- multiwalled carbon nanotubes. *Cogent Engineering*. 2024;11(1). <https://doi.org/10.1080/23311916.2024.2343586>
7. Ghorbani Y., Franzidis J.-P., Petersen J. Heap Leaching technology current state, innovations, and future directions: A review. *Mineral Processing and Extractive Metallurgy Review*. 2016;37(2):73–119. <https://doi.org/10.1080/08827508.2015.1115990>
 8. Panfilov I.A., Antamoshkin O.A., Fedorova N.V., Deryugin F.F., Byankin V.E. Prevention of air pollution during openpit mining of ore deposits. *Mining Informational and Analytical Bulletin*. 2023;(11–1):252–264. https://doi.org/10.25018/0236_1493_2023_111_0_252
 9. Chaikin L., Shoppert A., Valeev D., et al. Concentration of rare earth elements (Sc, Y, La, Ce, Nd, Sm) in bauxite residue (red mud) obtained by water and alkali leaching of bauxite sintering dust. *Minerals*. 2020;10(6):500. <https://doi.org/10.3390/min10060500>
 10. Evdokimov S.I., Makoeva A.K., Maksimov R.N., Dyatlova D.I. Development of a method and apparatus for measuring the forces in particle contacts under conditions of flotation of gold microdispersions. *Sustainable Development of Mountain Territories*. 2023;15(1):81–96. (In Russ.) <https://doi.org/10.21177/1998-4502-2023-15-1-81-96>
 11. Shoppert A., Loginova I., Valeev D. Kinetics study of al extraction from desilicated coal fly ash by NaOH at atmospheric pressure. *Materials*. 2021;14:7700. <https://doi.org/10.3390/ma14247700>
 12. Jiang H., Zhang H., Zhang X., Zhang J., Jiang Y. Experimental study on the influence of content and fineness of fly ash on the mechanical properties of grouting slurries. *Deep Underground Science and Engineering*. 2024. <https://doi.org/10.1002/dug2.12070>
 13. Rasskazova A.V., Sekisov A.G., Kirilchukirilchu M.S., Vasyanovvasyanov Y.A. Stage-activation leaching of ox-idized copper-gold ore: Theory and technology. *Eurasian Mining*. 2020;(1):52–55. <https://doi.org/10.17580/em.2020.01.10>
 14. Chen T., Lei C., Yan B., Xiao X. Metal recovery from the copper sulfide tailing with leaching and fractional precipitation technology. *Hydrometallurgy*. 2014;147–148:178–182. <https://doi.org/10.1016/j.hydromet.2014.05.018>
 15. Khayrutdinov M.M., Kongar-Syuryun Ch.B., Tyulyaeva Yu.S., Khayrutdinov A.M. Cementless backfill mixtures based on water-soluble manmade waste. *Bulletin of the Tomsk Polytechnic University. Geo Assets Engineering*. 2020;331(11):30–36. (In Russ.) <https://doi.org/10.18799/24131830/2020/11/2883>
 16. Vrancken C., Longhurst P.J., Wagland S.T. Critical review of real-time methods for solid waste characterisation: Informing material recovery and fuel production. *Waste Management*. 2017;61:40–57. <https://doi.org/10.1016/j.wasman.2017.01.019>
 17. Zhao H., Zhang Y., Zhang X., et al. The dissolution and passivation mechanism of chalcopyrite in bioleaching: An overview. *Minerals Engineering*. 2019;136:140–154. <https://doi.org/10.1016/j.mineng.2019.03.014>
 18. Podrezov D.R. Issues of improving control and increasing efficiency of production blocks at an ISL uranium mine. *Mining Science and Technology (Russia)*. 2020;5(2):131–153. (In Russ.) <https://doi.org/10.17073/2500-0632-2020-2-131-153>
 19. Garifulina I.Y., Abdulkhalimov A.H., Zaseev I.A., Maystrov Y.A. Prospects for development of sadon deposits by in-situ leaching. *Mining Science and Technology (Russia)*. 2020;5(4):358–366. (In Russ.) <https://doi.org/10.17073/2500-0632-2020-4-358-366>
 20. Dzhioeva A.K. Improvement of underground leaching technology while ensuring environmentally safe development of ore deposits. *Bezopasnost' Truda v Promyshlennosti*. 2022;(9):62–68. <https://doi.org/10.24000/0409-2961-2022-9-62-68>
 21. Feng X., Wang X. Characteristics of Electrical Resistance Alteration during in situ leaching of ion-adsorption-type rare earth ore. *Minerals*. 2024;14:92. <https://doi.org/10.3390/min14010092>
 22. Wu Zh., Liao H., Lu K. Mining consensus sequence in multi-criteria group decision making with incomparability of alternatives and conflicts of experts. *Information Sciences*. 2022;610:359–380. <https://doi.org/10.1016/j.ins.2022.07.058>
 23. Deveci M., Gokasar I., Brito-Parada P.R. A comprehensive model for socially responsible rehabilitation of mining sites using Q-rung orthopair fuzzy sets and combinative distance-based assessment. *Expert Systems with Applications*. 2022;200:117155. <https://doi.org/10.1016/j.eswa.2022.117155>
 24. McManus S., Rahman A., Coombes J., Horta A. Uncertainty assessment of spatial domain models in early stage mining projects – A review. *Ore Geology Reviews*. 2021;133:104098. <https://doi.org/10.1016/j.oregeorev.2021.104098>
 25. Abas Wisam Mahdi Abas, Arutyunyan R.V. Modeling of nonlinear dynamic and stationary systems based on Volterra integro–functional series and various classes of quadrature formulas. *Mathematical*



- Modeling and Computational Methods*. 2021;(2):68–85. (In Russ.) <https://doi.org/10.18698/2309-3684-2021-2-6885>
26. Yan J., Xu M. Energy and circular economy in sustainability transitions. *Resources, Conservation and Recycling*. 2021;169:105471. <https://doi.org/10.1016/j.resconrec.2021.105471>
 27. Shutaleva A. Ecological Culture and critical thinking: building of a sustainable future. *Sustainability*. 2023;15:13492. <https://doi.org/10.3390/su151813492>
 28. Ignatyeva M.N., Yurak V.V., Dushin A.V., Strovsky V.E. Technogenic mineral accumulations: problems of transition to circular economy. *Mining Science and Technology (Russia)*. 2021;6(2):73–89. <https://doi.org/10.17073/2500-0632-2021-2-73-89>
 29. Brigida V., Golik V.I., Voitovich E.V. et al. Technogenic reservoirs resources of mine methane when implementing the circular waste management concept. *Resources*. 2024;13(2):33. <https://doi.org/10.3390/resources13020033>
 30. Ma L., Ghorbani Y., Kongar-Syuryun C.B., Khayrutdinov M.M., Klyuev R.V., Petenko A. Dynamics of backfill compressive strength obtained from enrichment tails for the circular waste management. *Resources, Conservation and Recycling Advances*. 2024;23:200224. <https://doi.org/10.1016/j.rcadv.2024.200224>
 31. Klyuev R.V., Brigida V.S., Lobkov K.Y. et al. On the issue of monitoring crack formation in natural-technical systems during earth surface displacements. *Mining Informational and Analytical Bulletin*. 2023;(11–1):292–304. (In Russ.). https://doi.org/10.25018/0236_1493_2023_111_0_292
 32. Ayaz A., Ozyurt O., Al-Rahmi W.M., et al. Exploring gamification research trends using topic modeling. In: *IEEE Access*. 2023;11:119676–119692. <https://doi.org/10.1109/ACCESS.2023.3326444>
 33. Klyuev R., Tekiev M., Silaev V., et al. Sustainable operation analysis of the mining industry power supply system. In: *E3S Web of Conferences*. 2021;326:00016. <https://doi.org/10.1051/e3sconf/202132600016>
 34. Brigida V.S., Mishulina S.I., Stas G.V. Perspective directions of “ecologisation” of structural elements of a tourist product of Krasnodar region (case study of transportation component). *Sustainable Development of Mountain Territories*. 2020;12(1):24–25. (In Russ.) <https://doi.org/10.21177/1998-4502-2020-12-1-18-25>
 35. Pavlov M.V., Vafaeva K.M., Karpov D.F. et al. Impact of environmental factors on indoor air temperature in gas-fired radiant heated cultivated structures. In: *E3S Web of Conferences. International Conference on “Advanced Materials for Green Chemistry and Sustainable Environment” (AMGSE-2024)*. 2024;511:01036. <https://doi.org/10.1051/e3sconf/202451101036>
 36. Vafaeva K.M., Karpov D.F., Pavlov M.V. et al. Analyzing thermal images to evaluate thermal protection in residential structures: lessons from russian practices. In: *E3S Web of Conferences. International Conference on “Advanced Materials for Green Chemistry and Sustainable Environment” (AMGSE-2024)*. 2024;511:01037. <https://doi.org/10.1051/e3sconf/202451101037>
 37. Li G., Zhou Q., Zhu Z., et al. Selective leaching of nickel and cobalt from limonitic laterite using phosphoric acid: An alternative for value-added processing of laterite. *Journal of Cleaner Production*. 2018;189:620–626. <https://doi.org/10.1016/j.jclepro.2018.04.083>
 38. Kongar-Syuryun Ch.B., Kovalski E.R. Hardening backfill at potash mines: promising materials regulating stress-strain behavior of rock mass. *Geologiya i Geofizika Yuga Rossii*. 2023;13(4):177–187. <https://doi.org/10.46698/VNC.2023.34.99.014>
 39. Kondratyev Yu.I., Vyskrebenets A.S., Betrozov Z.C., Dzeranova K.B. Energy costs reduction on underground electrochemical metal leaching from ores. *Sustainable Development of Mountain Territories*. 2017;(4):419–426. (In Russ.) <https://doi.org/10.21177/1998-4502-2017-9-4-419-426>
 40. MacCarthy J., Nosrati A., Skinner W., Addai-Mensah J. Atmospheric acid leaching mechanisms and kinetics and rheological studies of a low grade saprolitic nickel laterite ore. *Hydrometallurgy*. 2016;160:26–37. <https://doi.org/10.1016/j.hydromet.2015.11.004>
 41. Lyashenko V.I., Khomenko O.E., Golik V.I. Friendly and Resource-Saving Methods of Underground Ore Mining in Disturbed Rock Masses. *Mining Science and Technology (Russia)*. 2020;5(2):104–118. <https://doi.org/10.17073/2500-0632-2020-2-104-118>
 42. Kovalski E., Kongar-Syuryun C., Petrov D. Challenges and prospects for several-stage stoping in potash minining. *Sustainable Development of Mountain Territories*. 2023;15(2):349–364. <https://doi.org/10.21177/1998-4502-2023-15-2-349-364>
 43. Palaniandy S. Impact of mechanochemical effect on chalcopryrite leaching. *International Journal of Mineral Processing*. 2015;136:56–65. <https://doi.org/10.1016/j.minpro.2014.10.005>
 44. Minagawa M., Hisatomi Sh., Kato T., et al. Enhancement of copper dissolution by mechanochemical activation of copper ores: Correlation between leaching experiments and DEM simulations. *Advanced Powder Technology*. 2018;29(3):471–478. <https://doi.org/10.1016/j.appt.2017.11.031>



45. Bumanisa G., Bajarea D. Compressive strength of cement mortar affected by sand micro filler obtained with collision milling in disintegrator. *Procedia Engineering*. 2017;172:149–156. <https://doi.org/10.1016/j.proeng.2017.02.037>
46. Basturkcü H., Achimovicova M., Kanuchova M., Acarkan N. Mechanochemical pre-treatment of lateritic nickel ore with sulfur followed by atmospheric leaching. *Hydrometallurgy*. 2018;181:43–52. <https://doi.org/10.1016/j.hydromet.2018.08.016>

Information about the authors

Vladimir I. Golik – Dr. Sci. (Eng.), Professor of Technique and Technology of Mining and Oil and Gas Production Department, Moscow Polytechnic University, Moscow, Russian Federation; Professor of Mining Department, North Caucasian Institute of Mining and Metallurgy (State Technological University), Vladikavkaz, Russian Federation; ORCID [0000-0002-1181-8452](https://orcid.org/0000-0002-1181-8452), Scopus ID [6602135324](https://scopus.id/6602135324); e-mail v.i.golik@mail.ru

Yuri I. Razorenov – Dr. Sci. (Eng.), Professor, Rector of Platov South-Russian State Polytechnic University NPI, Novocherkassk, Russian Federation; ORCID [0000-0001-8171-0749](https://orcid.org/0000-0001-8171-0749), Scopus ID [57194146509](https://scopus.id/57194146509); e-mail rektorat@npi-tu.ru

Niyaz G. Valiev – Dr. Sci. (Eng.), Professor, Head of the Department of Mining, Ural State Mining University, Ekaterinburg, Russian Federation; ORCID [0000-0002-5556-2217](https://orcid.org/0000-0002-5556-2217), Scopus ID [55749527900](https://scopus.id/55749527900); e-mail science@ursmu.ru

Oksana A. Gavrina – Cand. Sci. (Eng.), Senior Researcher of Mining Systems Control Laboratory, Research Institute of Comprehensive Exploitation of Mineral Resources of the Russian Academy of Sciences, Moscow, Russian Federation; ORCID [0000-0002-9712-9075](https://orcid.org/0000-0002-9712-9075), Scopus ID [57204639532](https://scopus.id/57204639532)

Received 24.11.2023

Revised 29.01.2024

Accepted 01.02.2024



SAFETY IN MINING AND PROCESSING INDUSTRY AND ENVIRONMENTAL PROTECTION

Research paper

<https://doi.org/10.17073/2500-0632-2024-04-259>

UDC 528.9

**Substantiation of environmental safety
in metro facility operations considering hydrogeological risks**

S. A. Zhukov

Mosinzhproekt JSC, Moscow, Russian Federation

fragrante@mail.ru**Abstract**

In today's world of rapid urbanization, environmental safety has become a key aspect of urban planning and management. The issue of environmental safety encompasses a wide range of concerns, from pollution reduction and biodiversity conservation to ensuring the sustainable use of natural resources. In this context, metro facilities, as an integral part of urban infrastructure, play a crucial role in providing mobility for urban populations, yet they also pose potential environmental challenges. The operation of metro facilities is associated with noise pollution, emissions of harmful substances due to the use of energy produced from fossil fuels, energy consumption, undesirable impacts on groundwater, and other negative environmental aspects. Equally important is the issue of waste disposal and the use of construction materials during the building and maintenance of metro systems. The aim of this study was to assess the environmental safety of metro facility operations. The consideration of this topic is particularly relevant in light of global efforts towards sustainable development and the need to ensure a high quality of life for urban populations. The assessment of environmental safety in metro operations is proposed to be conducted through a comprehensive approach, involving field studies and modelling the distribution patterns of defects in metro structures under the influence of hydrogeological risks. A systematic approach to evaluating environmental safety in metro operations, based on modelling the development of defects in tunnel structures under the influence of hydrogeological factors, will help organize existing information on potential accidents and develop monitoring methods and measures to minimize risks that compromise the environmental sustainability of underground transport infrastructure. The research results, which include the systematization of environmental safety criteria for metro operations and the analysis of tunnel structure defects caused by hydrogeological factors, provide the basis for further developing methods to ensure environmentally safe operation of urban transport tunnels.

Keywords

metro, environmental safety, sustainable development, urban transport system, environmental standards, innovative technologies, risks

For citation

Zhukov S. A. Substantiation of environmental safety in metro facility operations considering hydrogeological risks. *Mining Science and Technology (Russia)*. 2024;9(3):283–291. <https://doi.org/10.17073/2500-0632-2024-04-259>

**ТЕХНОЛОГИЧЕСКАЯ БЕЗОПАСНОСТЬ В МИНЕРАЛЬНО-СЫРЬЕВОМ КОМПЛЕКСЕ
И ОХРАНА ОКРУЖАЮЩЕЙ СРЕДЫ**

Научная статья

**Обоснование экологической безопасности при эксплуатации
объектов метрополитена с учетом гидрогеологического риска**

С. А. Жуков

АО «Мосинжпроект», г. Москва, Российская Федерация

fragrante@mail.ru**Аннотация**

В современном мире стремительной урбанизации экологическая безопасность становится ключевым аспектом городского планирования и управления. Проблематика экологической безопасности охватывает широкий спектр вопросов – от снижения уровня загрязнения и сохранения биоразнообразия до обеспечения устойчивого использования природных ресурсов. В этом контексте объекты метрополитена как неотъемлемая часть городской инфраструктуры играют важную роль в обеспечении мобильности городского населения, однако они также представляют собой потенциальный источник экологических проблем. Эксплуатация объектов метрополитена сопровождается шумовым загрязнением, эмиссией вредных веществ, так как системы метрополитена используют энергию, производимую из



ископаемых источников, энергопотреблением, нежелательным влиянием на подземные воды и другими негативными экологическими аспектами. Также не менее важным является вопрос утилизации отходов и строительных материалов, используемых при строительстве и ремонте метрополитенов. Целью данного исследования являлась оценка экологической безопасности при эксплуатации объектов метрополитена. Рассмотрение этой темы особенно актуально в свете глобального стремления к устойчивому развитию и необходимости обеспечения высокого качества жизни городского населения. Оценка экологической безопасности при эксплуатации объектов метрополитена предполагается осуществлять на основе комплексного подхода, подразумевающего проведение натурных исследований и моделирования характера распределения дефектов в конструкциях подземных сооружений метрополитена под воздействием гидрогеологических рисков. Системный подход к оценке экологической безопасности при эксплуатации объектов метрополитена, основанный на моделировании развития дефектов в конструкциях тоннелей под действием гидрогеологических факторов, позволит структурировать имеющуюся информацию по потенциальным авариям, выработать методы мониторинга и меры по минимизации рисков, ведущих к снижению экологической устойчивости подземных объектов транспортной структуры города. Полученные результаты исследований, включающие в себя систематизацию критериев экологической безопасности при эксплуатации метрополитена, анализ дефектов в конструкциях тоннелей под действием гидрогеологических факторов, являются основой для дальнейшей разработки методики обеспечения экологически безопасной эксплуатации городских транспортных тоннелей.

Ключевые слова

метрополитен, экологическая безопасность, устойчивое развитие, городская транспортная система, экологические стандарты, инновационные технологии, риски

Для цитирования

Zhukov S. A. Substantiation of environmental safety in metro facility operations considering hydrogeological risks. *Mining Science and Technology (Russia)*. 2024;9(3):283–291. <https://doi.org/10.17073/2500-0632-2024-04-259>

Introduction

To assess the environmental safety of metro systems, several key criteria must be considered to help ensure their sustainable operation.

Hydrogeological criterion. This includes determining the hydrostatic pressure of groundwater, its mineralization, and composition.

Pollutant emissions. This involves measuring levels of carbon dioxide emissions, nitrogen oxides, and other pollutants that may affect air quality in cities. Particular attention should be given to areas with high concentrations of people, such as metro stations and transfer hubs.

Noise pollution. Metro operations are often accompanied by high noise levels, which can negatively affect the health and quality of life of city residents. It is important to assess noise levels and take measures to reduce them.

Energy efficiency. Efficient energy use is a key factor in reducing the environmental impact of metro systems. This includes the use of energy-saving technologies and transitioning to renewable energy sources.

Waste management and material use. Proper waste management during the construction and operation of metro systems, as well as the selection of environmentally sustainable materials, are critical aspects.

Impact on ecosystems and biodiversity. It is necessary to consider the impact of metro systems on natural ecosystems, particularly during the construction of new metro lines and the development of infrastructure.

Applying these criteria requires a comprehensive approach that includes regular monitoring, the use of modern technologies, and innovative solutions. It is also essential to develop and implement regulatory frameworks that govern the environmental aspects of metro operations.

Environmental safety criteria should be regularly reviewed and updated in accordance with the latest scientific research and technological advancements. This will ensure adaptability and continuous improvement in response to changing conditions and potential emergencies.

Implementing these criteria will not only reduce the negative environmental impact of metro systems but also increase their efficiency and convenience for both staff and passengers, thus contributing to the sustainable development of urban transport systems.

Examples of best practices

Stockholm Metro, Sweden. One of the most environmentally friendly metro systems in the world. Thanks to the use of 100% renewable energy for metro trains, Stockholm has significantly reduced the carbon footprint of its transport system. Additionally, efficient ventilation and noise reduction systems have been implemented.

Singapore Metro. An example of a highly efficient and innovative transport system. The Singapore metro uses regenerative braking, which helps reduce overall energy consumption. Strict standards for noise and air pollution reduction are also applied.

London Underground, United Kingdom. A program has been introduced to reduce energy consumption and improve air quality. The London Underground is also actively working on improving its infrastructure to reduce noise and vibration levels.

Examples of problematic aspects

New York City Subway, USA. Despite its size and significance, it faces several environmental challenges, primarily related to outdated infrastructure and high noise levels. Projects for infrastructure modernization and energy efficiency improvement are in development and implementation stages.

Moscow Metro, Russia. Although steps have been taken in recent years to improve environmental safety, such as the introduction of energy-efficient lighting and improved ventilation, challenges remain related to the aging infrastructure and changing geological and hydrological conditions due to urban landscape transformations.

Materials and methods

One of the most hazardous environmental risks in underground metro facilities, which significantly reduces environmental safety, is hydrogeological risk. This refers to potential social and economic losses resulting from the development of adverse hydrogeological processes, which manifest as a reduction in the stability of metro tunnels and environmental safety within the “rock mass–underground structure–environment” system. Hydrogeological risks are evidenced by the formation of defects in the supporting structures of tunnels, such as leaks, water ingress, soil

washouts into underground facilities, water breakthroughs, and quicksand.

As an example, we can consider the assessment of environmental safety at an existing Moscow metro facility, based on data from engineering geological surveys conducted over different periods. Photographs of the Moscow metro tunnel are shown in Figs. 1–3.

During the in-situ inspection of the structures at the emergency section of the running tunnel of the Moscow Metro line, the following most characteristic defects and damages were identified:

- concrete spalling in wall blocks, including areas with exposed reinforcement;
- concrete spalling in roof slabs, including areas with exposed reinforcement;
- leaching observed on the wall blocks of the running tunnel;
- leaching observed on the roof slabs of the running tunnel;
- wet spots on the wall blocks of the running tunnel;
- disruption of joint sealing in wall blocks and roof slabs;
- active leakages;
- cracks in the roof slabs with an aperture width of up to 0.2 mm.

The classification of the identified defects is reflected in Table 1.

Results

The geological cross-sections of the examined section of the running tunnel, observed over different time periods, are shown in Figs. 4 and 5.



Fig. 1. Leaching and wet spots at the inter-ring and inter-block joints of the tubing lining, active leakage. Crack in the back of the tubing

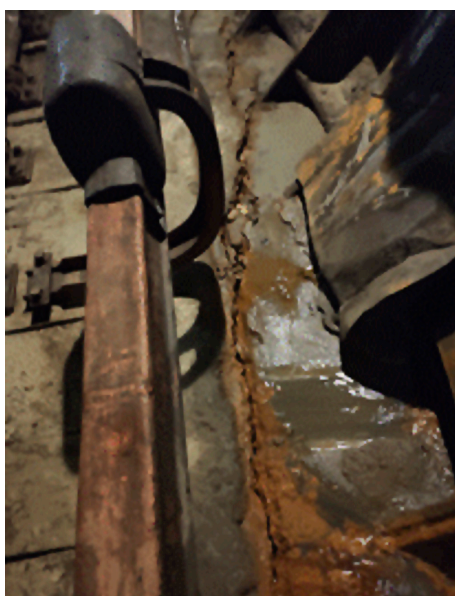


Fig. 2. Soil washout into the area of the contact rail



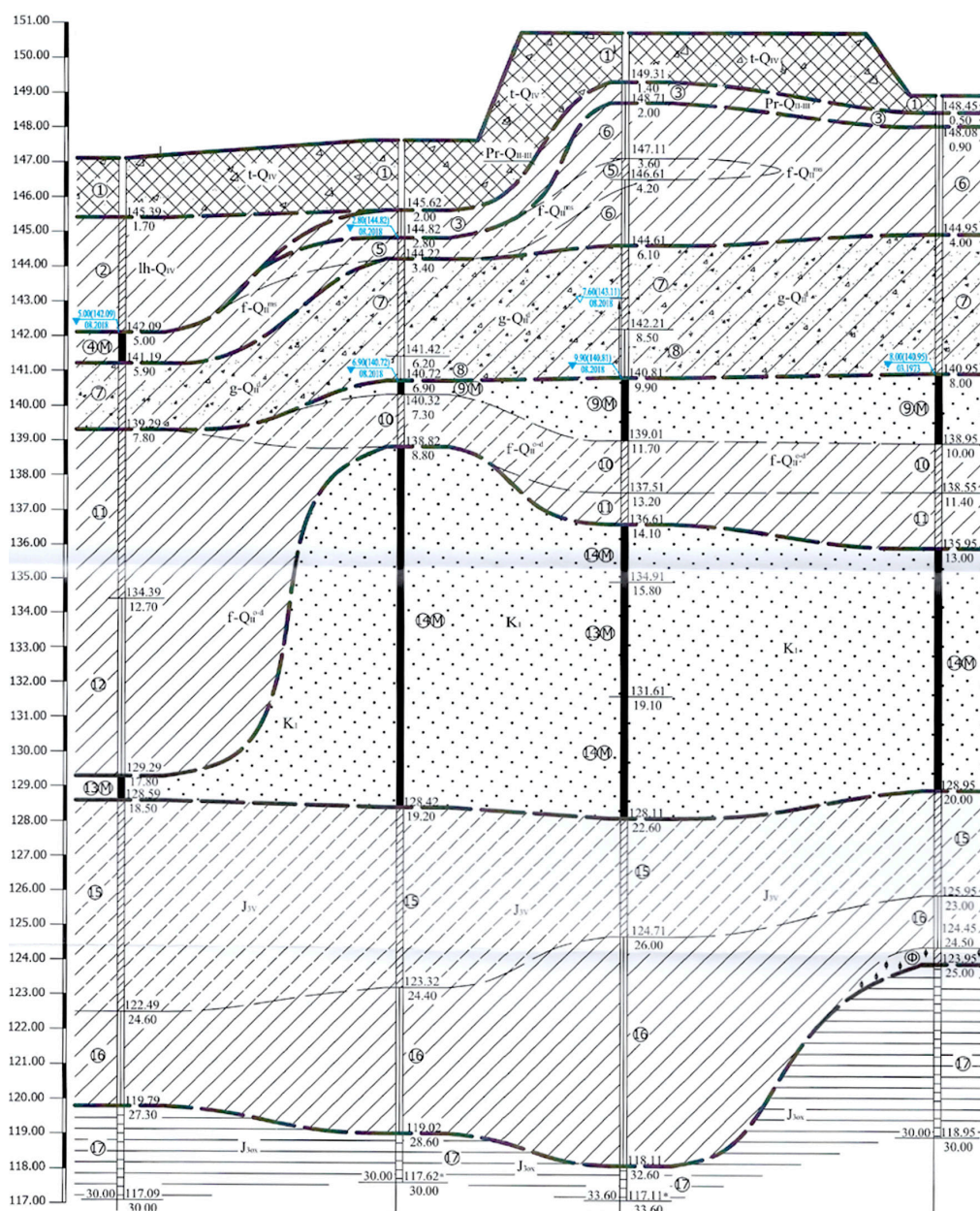
Fig. 3. Leaching and destruction of the concrete structure of the roof slab due to erosion of the waterproofing barrier



Table 1

Classification of defects (according to GOST R 57208–2016)

No	Type of defect	Possible causes	Potential consequences
1	Concrete spalling in wall blocks and roof slabs, including areas with exposed reinforcement	Mechanical impact	Reduction in load-bearing capacity proportional to the decrease in cross-sectional area
2	Leaching on wall blocks and roof slabs of the running tunnel. Wet spots on wall blocks. Dripping. Active leakages	Waterproofing failure	Concrete degradation, metal and reinforcement corrosion, reduction in operational performance
3	Steps at the joints of the roof slabs in the running tunnel up to 30 mm	Errors during manufacturing and installation	The degree of reduction in load-bearing capacity is determined by calculation
4	Cracks in roof slabs with an aperture width of up to 0.2 mm	Shrinkage due to the heat and moisture treatment of the concrete mix, properties of the cement, etc.	No effect on load-bearing capacity. May reduce durability
5	Disruption of joint sealing in wall blocks and roof slabs	Tunnel and metro operations (including vibrations from moving trains)	Increased water infiltration and reduced operational performance of the structure

Fig. 4. Geotechnical cross-section of the running tunnel section between stations at time period t_1

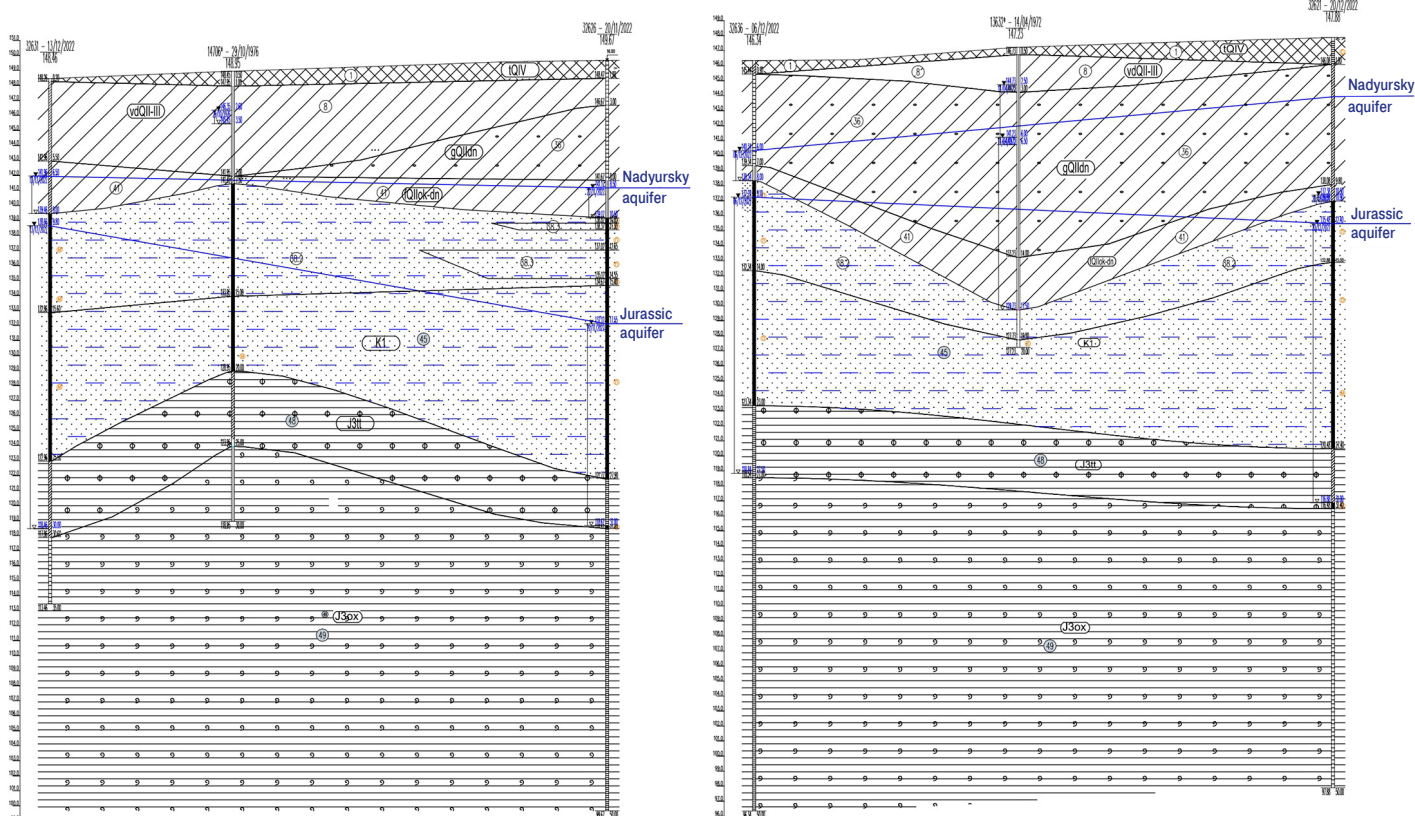


Fig. 5. Geotechnical cross-section of the running tunnel section between stations at time period t_2

From the presented cross-sections, it can be concluded that the level of the aquifer has changed over time, which significantly affected the physical and mechanical properties of the rock and the development of defects in the load-bearing structures of the tunnel, primarily influencing the geometry of the tunnel lining.

To determine the rate of decline and recovery of water inflow, calculations of the filtration properties of the aquifer near the running tunnel were conducted (Table 2).

Based on observations of the aquifer level near the running tunnel, changes in the hydrological regime were identified (Figs. 6 and 7). The presented graphs indicate that over an extended period, the aquifer level fluctuated within a range of 2 to 16 m.

As part of the inspection of the technical condition of problematic sections of running tunnels, in-situ measurements of the actual geometric dimensions of the tunnel structures were carried out. The measurements of the actual dimensions of the studied structures were conducted using a Leica DISTO D2 handheld laser distance meter. Measurement accuracy: ± 1.5 mm. Based on the measurement results, deviations of the actual geometric dimensions of the tunnel lining from the design values were

identified, with deviations exceeding 50 mm at the examined chain ages (Fig. 8). The area highlighted in Fig. 8, *a* represents an oversized section of the metro tunnel lining that could lead to the development of a potential emergency situation. The area highlighted in red in Fig. 8, *b* shows an oversized section of the metro tunnel lining before the process of reinforcing the base of the trough zone, which could also create a potential emergency risk. The blue-highlighted area shows the results of measurements taken after the reinforcement process, which reduced the deformation from 100 to 40 mm.

Table 2

Aquifer characteristics

Characteristics	Value
Type of aquifer	Confined
Aquifer thickness, H (m)	17.8
Well radius, m	0.063
Pumping duration, days	0.5
Discharge rate, m ³ /day	64.8
Static water level, m	7.2
Dynamic water level, m	23.45
Water level drawdown, m	16.25

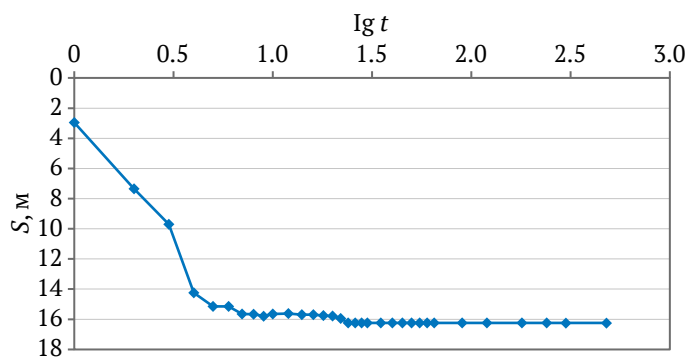


Fig. 6. Graph tracking the decline of the water level in the well

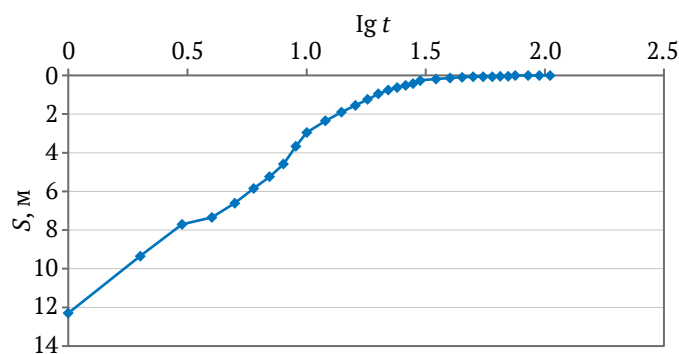
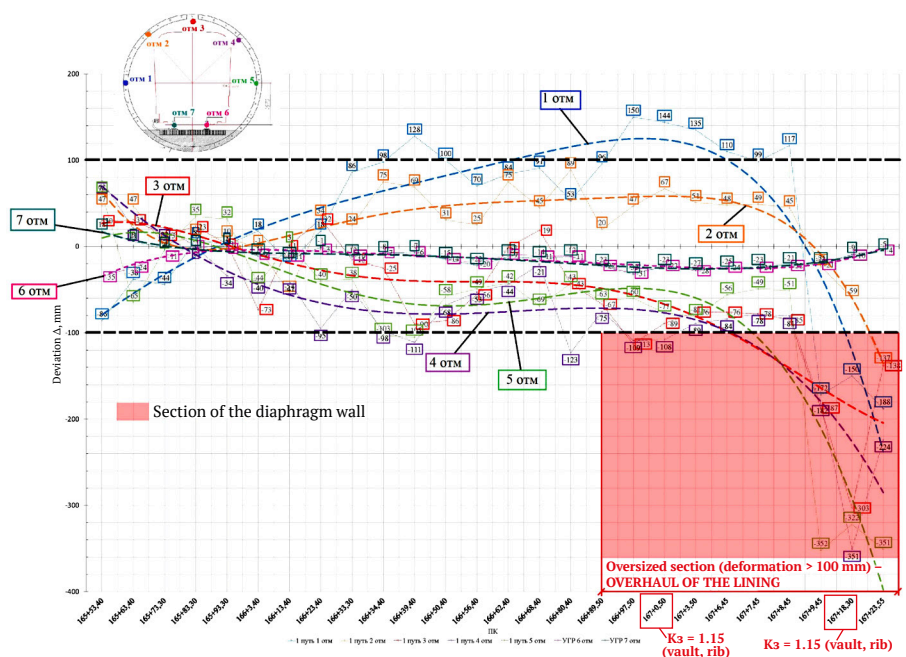
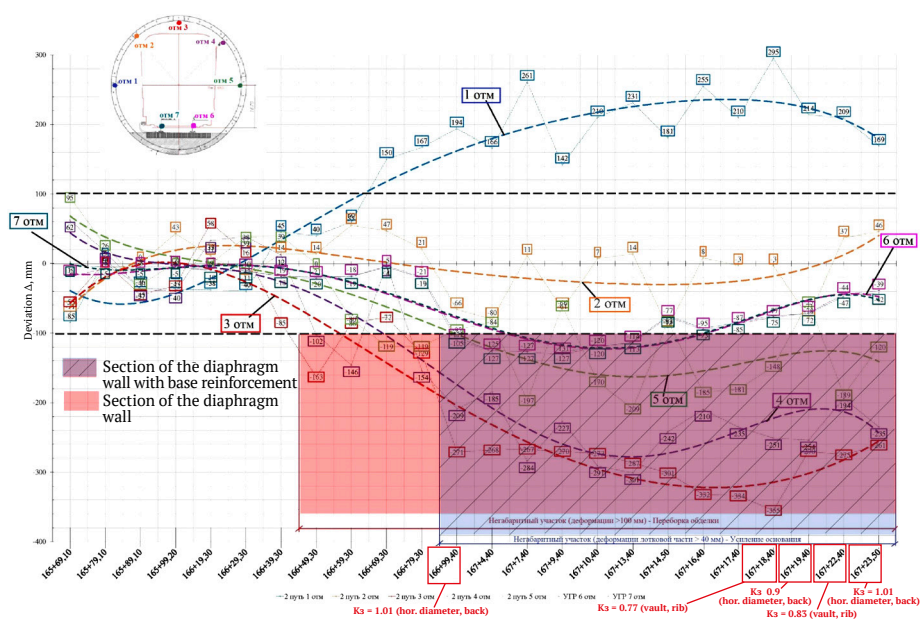


Fig. 7. Graph tracking the recovery of the water level in the well



a



b

Fig. 8. Deformation graph of the tunnel lining:
a – for the first track (left running tunnel); b – for the second track (right running tunnel)

From Fig. 8, it follows that deformation processes caused by increased groundwater inflow to the tunnel lining lead to cracking in the cast iron tubbing structure. This, in turn, contributes to the formation of leaks and soil washouts into the interior space of the tunnel, including onto the track sections.

Based on the results of the in-situ inspection, a defect map of the tunnel lining was created, with a fragment shown in Fig. 9.

Conclusions

The identified changes in the tunnel lining structure showed that 60% of the leaks are concentrated around the locations of construction joints. The tubbing itself also begins to filter water, exacerbating leaching processes, which leads to the appearance of

wet spots. Since the surrounding rock mass consists of weak, unstable soils, the washout of soil into the tunnel space could result in subsidence, which, in turn, would cause deformations and settlement of the ground surface. Consequently, there is a marked reduction in the environmental and geotechnical safety level of the metro running tunnel.

The obtained research results, including the analysis of defects in tunnel structures caused by hydrogeological factors, form the basis for further determination of acceptable risks and the development of methods for ensuring the environmentally safe operation of urban metro transport tunnels.

Future plans include the creation of a geomechanical impact model on metro structures. The modeling will allow for the evaluation of how geome-

Segmented rings of the tunnel lining

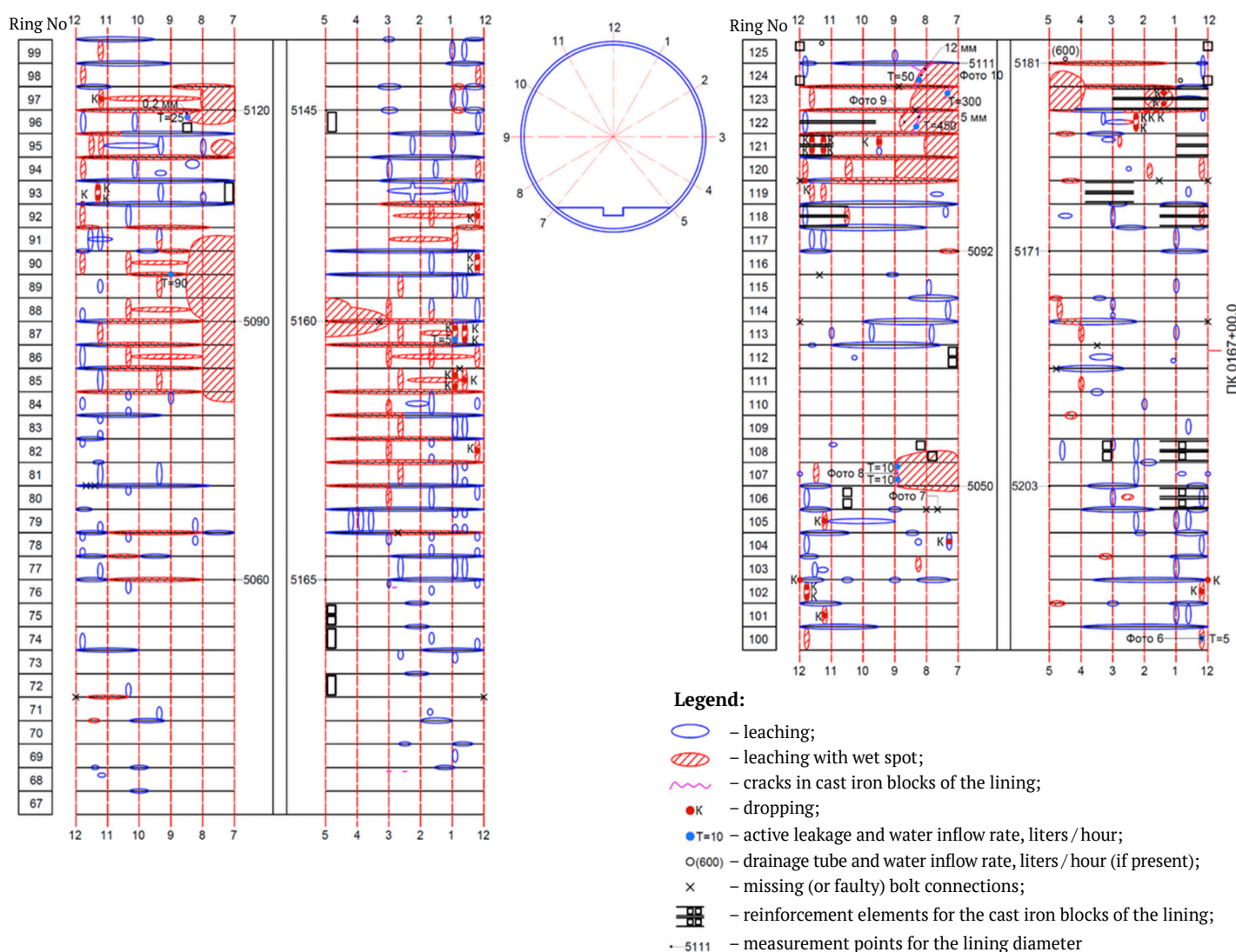


Fig. 9. Tunnel lining defect map, obtained from the in-situ inspection of operational facilities (PK167+00.0)



chanical phenomena such as karst processes, ground surface subsidence, soil heaving, and changes in the groundwater regime contribute to the stress-strain state of the prefabricated lining of metro running tunnels. The modeling is planned to be conducted

using a three-dimensional numerical method in the ANSYS Workbench software package. Comparing the results of the modeling with experimental data will allow for an assessment of the reliability of the proposed methodology.

References

1. Kulikova E. Yu., Balovtsev S. V., Skopintseva O. V. Complex estimation of geotechnical risks in mine and underground construction. *Sustainable Development of Mountain Territories*. 2023;15(1):7–16. (In Russ.) <https://doi.org/10.21177/1998-4502-2023-15-1-7-16>
2. Kulikova E. Yu. Safety and risk management in underground construction as a complex information process. *Mining Informational and Analytical Bulletin*. 2021;(2–1):134–143. (In Russ.) <https://doi.org/10.25018/0236-1493-2021-21-0-134-143>
3. He X. C., Xu Y. S., Shen S. L., Zhou A. N. Geological environment problems during metro shield tunnelling in Shenzhen, China. *Arabian Journal of Geosciences*. 2020;13(2):87. <https://doi.org/10.1007/s12517-020-5071-z>
4. Xu Y. S., Shen J. S., Zhou A. N., Arulrajah A. Geological and hydrogeological environment with geohazards during underground construction in Hangzhou: a review. *Arabian Journal of Geosciences*. 2018;11:544. <https://doi.org/10.1007/s12517-018-3894-7>
5. Lin X.-T., Chen R.-P., Wu H.-N., Cheng H.-Zh. Deformation behaviors of existing tunnels caused by shield tunneling undercrossing with oblique angle. *Tunnelling and Underground Space Technology*. 2019;89:78–90. <https://doi.org/10.1016/j.tust.2019.03.021>
6. Merisalu J., Sundell J., Rosén L. Probabilistic cost-benefit analysis for mitigating hydrogeological risks in underground construction. *Tunnelling and Underground Space Technology*. 2023;131(7):104815. <https://doi.org/10.1016/j.tust.2022.104815>
7. Konyukhov D. S. Criteria analysis of modern technologies of underground construction. *Geotekhnika*. 2021;(1):40–55. (In Russ.)
8. Konyukhov D. S. Analysis of mechanized tunneling parameters to determine the overcutting characteristics. *Mining Science and Technology (Russia)*. 2022;7(1):49–56. <https://doi.org/10.17073/2500-0632-2022-1-49-56>
9. Lebedev M. O. Choosing a calculation method for stress-strain of supports and lining of transport tunnels. In: *16th World Conference of the Associated Research Centers for the Urban Underground Space (ACUUS 2018)*. 5–7 November 2018, Hong Kong. Pp. 678–687.
10. Bourget A. P. F., Chiriotti E., Patrinieri E. Evolution of risk management during an underground project's life cycle. In: Peila D., Viggiani G., Celestino T. (Eds). *Tunnels and Underground Cities: Engineering and Innovation meet Archaeology, Architecture and Art*. London: CRC Press; 2019. Pp. 4375–4385. <https://doi.org/10.1201/9780429424441-463>
11. Mahdi S., Gastebled O., Ningre H., Senechal M. Grand Paris Express, Line 15 East – predictive damage analysis combining continuous settlement trough modeling, risk management, automated vulnerability checks and visualization in GIS. In: Peila D., Viggiani G., Celestino T. (Eds). *Tunnels and Underground Cities: Engineering and Innovation meet Archaeology, Architecture and Art*. London: CRC Press; 2019. Pp. 5855–5864. <https://doi.org/10.1201/9780429424441-619>
12. Hongjun W. Earth human settlement ecosystem and underground space research. *Procedia Engineering*. 2016;165:765–781. <https://doi.org/10.1016/j.proeng.2016.11.774>
13. Garber V. A. Abnormal situations at underground transport facilities. *Podzemnye Gorizonty*. 2018;(16):20–25. (In Russ.)
14. Kulikova E. Yu. Methodical principles for improving the ecological and technological reliability of urban underground structures. *Mining Informational and Analytical Bulletin*. 2020;(6–1):176–185. (In Russ.) <https://doi.org/10.25018/0236-1493-2020-61-0-176-185>
15. Kulikova E. Yu., Balovtsev S. V. Risk control system for the construction of urban underground structures. In: *IOP Conference Series: Materials Science and Engineering*. 2020;962(4):042020. <https://doi.org/10.1088/1757-899X/962/4/042020>
16. Kim D. Y., Farrokh E., Song M. K., Hyun K. S. Cutting tool wear evaluation for soft ground TBMs. In: *Proceeding of the World Tunnel Congress 2017. Surface challenges – Underground solutions*. 9–15th June 2017, Bergen, Norway. Bergen; 2017.



17. Potapova E.V. Typology of metro structures for the tasks of geotechnical risk classification. *Mining Science and Technology (Russia)*. 2021;6(1):52–60. (In Russ.) <https://doi.org/10.17073/2500-0632-2021-1-52-60>
18. Kuepferle J., Roettger A., Thesen W., Alber M. Wear prediction for soft-ground tunneling tools – a new approach regarding the dominant influencing factors in the tribological system of tunneling tools. In: *Proceeding of the World Tunnel Congress 2017. Surface challenges – Underground solutions*. 9–15th June 2017, Bergen, Norway. Bergen; 2017.

Information about the author

Sergey A. Zhukov – CEO, Mosinzhproekt JSC, Moscow, Russian federation; ORCID [0009-0007-6492-6696](https://orcid.org/0009-0007-6492-6696);
e-mail fragrante@mail.ru

Received 04.04.2024

Revised 26.05.2024

Accepted 05.06.2024




POWER ENGINEERING, AUTOMATION, AND ENERGY PERFORMANCE

Research paper

<https://doi.org/10.17073/2500-0632-2024-01-213>

UDC 622:62-83

**Stability of a controlled sucker-rod pump unit drive under operating conditions and during voltage dips in the electrical network**M. S. Ershov   , E. S. Efimov *Gubkin Russian State University of Oil and Gas (National Research University), Moscow, Russian Federation* msershov@yandex.ru**Abstract**

The use of a variable frequency drive (VFD) for sucker-rod pump units (SRPUs), widely employed in oil extraction, enhances the energy and technological efficiency of oil production and reduces equipment wear. However, its application is hindered by unstable operation under insufficient balancing of the SRPU and sensitivity to short-term voltage dips, which frequently occur in the extensive electrical networks of oil fields. Insufficient balancing of the SRPU leads to the occurrence of a period within the pumping cycle where the motor operates in generator mode, caused by the unevenness and reversal of the resistance torque of the working mechanism. The motor's transition to generator mode, as well as voltage dips in the power supply, causes the voltage in the DC link of the VFD to exceed the set limits, resulting in the drive being shut down. To investigate the processes during the operation of sucker-rod pump units and to test methods for mitigating the negative impact of generator mode and voltage dips in the power supply network on the VFD, a model of the "power grid – variable frequency SRPU drive" system with a load characteristic of this application was developed in Matlab Simulink. A series of experiments were conducted, and the results were analyzed. The suppression function of the generator mode was examined, and the feasibility of its application to real SRPUs was evaluated. The use of an uninterruptible power supply system based on battery energy storage to prevent operational interruptions during different levels of power supply voltage dips was analyzed. The resulting model can be used for general analysis of operability and stability, as well as for verifying the correct selection of key elements in the design of sucker-rod pump unit systems with variable frequency drives.

Keywords


sucker-rod pump unit, variable frequency drive, frequency converter, DC converter, battery storage, generator mode, voltage dip, computer modeling

For citation

Ershov M.S., Efimov E.S. Stability of a controlled sucker-rod pump unit drive under operating conditions and during voltage dips in the electrical network. *Mining Science and Technology (Russia)*. 2024;9(3):292–303. <https://doi.org/10.17073/2500-0632-2024-01-213>

ЭНЕРГЕТИКА, АВТОМАТИЗАЦИЯ И ЭНЕРГОЭФФЕКТИВНОСТЬ

Научная статья

Устойчивость регулируемого привода штанговой насосной установки в рабочих режимах и при провалах напряжения в сетиМ. С. Ершов   , Е. С. Ефимов *Российский государственный университет нефти и газа (НИУ) им. И.М. Губкина, г. Москва, Российская Федерация* msershov@yandex.ru**Аннотация**

Применение частотно-регулируемого привода штанговых насосных установок (ШНУ), широко используемых для добычи нефти, повышает энергетическую и технологическую эффективность добычи нефти, способствует снижению износа оборудования, но его применение сдерживается неустойчивой работой при недостаточной уравновешенности ШНУ и чувствительностью к кратковременным провалам напряжения, часто возникающим в протяженных электрических сетях нефтепромыслов. Недостаточная уравновешенность ШНУ приводит к появлению в цикле качания периода работы двигателя в генераторном режиме, обусловленном неравномерностью и изменением направления момента сопротивления рабочего механизма. Переход двигателя в генераторный режим так же, как и провалы питающего напряжения, приводит к выходу напряжения в звене постоянного тока преобразователя частоты за установленные пределы и к отключению преобразователя. Для исследования процессов при



работе штанговых насосных установок и проверки способов устранения негативного влияния на преобразователь частоты генераторного режима, а также провалов напряжения питающей электросети с целью повышения устойчивости системы в среде Matlab, Simulink создана модель «электрическая сеть – частотно-регулируемый привод ШНУ» с характерной для данного применения нагрузкой, проведен ряд опытов и выполнен анализ результатов. Рассмотрена программная функция подавления генераторного режима и дана оценка возможности ее применения для реальных установок. Проанализировано применение системы бесперебойного питания на основе аккумуляторных накопителей энергии для предотвращения прерывания работы при разных уровнях провалов питающего напряжения. Модель, полученная в результате работы, может быть применена для общего анализа работоспособности и устойчивости, а также проверки правильности подбора ключевых элементов проектируемых систем штанговых насосных установок с частотно-регулируемым приводом.

Ключевые слова

штанговая насосная установка, частотно-регулируемый привод, преобразователь частоты, преобразователь постоянного тока, аккумуляторная батарея, генераторный режим, провал напряжения, компьютерное моделирование

Для цитирования

Ershov M.S., Efimov E.S. Stability of a controlled sucker-rod pump unit drive under operating conditions and during voltage dips in the electrical network. *Mining Science and Technology (Russia)*. 2024;9(3):292–303. <https://doi.org/10.17073/2500-0632-2024-01-213>

Introduction

To enhance the technological and energy efficiency of sucker-rod pump units (SRPUs), widely used in oil extraction, they are equipped with a variable frequency drive (VFD). However, its application is constrained by instability during operation under conditions of insufficient balancing of pump jacks and frequent disturbances in the electrical networks of oil fields.

The practical application of VFDs in SRPUs has shown that the main causes of drive instability are short-term voltage dips in the electrical networks of oil fields and the presence of a generator mode period during the pumping cycle. This mode arises due to the uneven load caused by the inertia and vibration loads resulting from the movement of the rod string. A brief generator mode during pumping can occur even in well-balanced units with shallow pump depths and, consequently, low rod suspension force created by the weight of the fluid column when the difference between maximum and minimum loads per cycle is small. When transitioning to generator mode, the energy received from the motor through the inverter cannot be recovered into the grid via the uncontrolled rectifier of the frequency converter (FC). This leads to an increase in the DC link voltage, which subsequently results in the FC shutting down due to its built-in overvoltage protection [1].

To improve stability and prevent undesirable emergency shutdowns of the VFD in SRPUs during generator mode, several solutions can be employed: using a frequency converter with energy recovery capability, installing a braking resistor, or utilizing special software settings. Implementing a regenerative FC is associated with significant capital investment due to the use of an active rectifier. Installing a bra-

king resistor results in the unproductive consumption of recoverable energy, which is dissipated as heat. The software setting known as the anti-regeneration function (ARF) increases motor speed, which can lead to undesirable dynamic forces within the SRPU. Each method has its advantages and disadvantages, leading to ambiguity in solving the problem of the negative impact of generator mode on FC operation.

Another feature of VFDs is their increased sensitivity to power supply disruptions, particularly to voltage dips [2]. In the event of a significant voltage drop in the DC link, the FC will disconnect from the grid due to the activation of undervoltage protection, which is necessary to prevent a current surge when the capacitor charges after the voltage is restored [3]. Enhancing the reliability of SRPU operation during voltage dips can be achieved through the use of an uninterruptible power supply (UPS) system connected to the DC link.

In accordance with the identified problems and their potential solutions, modeling was conducted to examine methods for eliminating overvoltage in the DC link that occurs during the operation of VFDs in SRPUs, as well as the application of UPS systems to maintain operation during power supply voltage dips to determine the impact of these solutions on system stability.

Methods

To investigate methods for mitigating the impact of generator mode and voltage dips on the operation of the VFD, a simulation of the electrical complex of the sucker-rod pump unit was performed in Matlab Simulink (Sim Power Systems library). A model was developed, whose main components include: a section of the electrical network, a frequency converter,

a squirrel-cage induction motor, a four-bar linkage pump jack mechanism, a well, as well as a bidirectional DC converter (DC/DC converter) and a lead-acid battery (LAB).

The electrical system includes a power source with a short-circuit capacity of $S_{shc} = 100$ MVA; an overhead line (6 kV) 6 km in length, with an aluminum conductor cross-section of 16 mm²; a 6/0.4 kV transformer with a capacity of 40 kVA; a cable line from the transformer to the frequency converter, 20 m in length, with aluminum cores of 10 mm² cross-section; a frequency converter based on an uncontrolled rectifier and a three-phase inverter controlled by pulse-width modulation (PWM); and a squirrel-cage induction motor with two pole pairs, whose parameters include: nominal power $P_{nom} = 30$ kW; nominal speed $n_{nom} = 1485$ rpm; nominal efficiency $\eta = 0.91$; power factor $\cos \varphi = 0.86$; nominal current $I_{nom} = 60$ A; starting current ratio $i_s = 7.7$; starting torque ratio $m_s = 2.7$; maximum torque ratio $m_{max} = 3.2$ m; and moment of inertia $J = 0.1326$ kg·m². In this model, the VFD is controlled by a scalar control method with the motor speed being maintained at the setpoint.

The mathematical model of the squirrel-cage induction motor is represented by the system of equations (1), which is constructed for the rotor-aligned (dq -axes) two-phase orthogonal coordinate system. The mechanical part of the drive is represented by equation (2). The calculation of the equivalent circuit parameters used in the model is performed using the formulas presented in [4].

The sucker-rod pump unit was modeled for an axial-type pump jack, the kinematic diagram of which is shown in Fig. 1 [5, 6]. The following designations are used in Fig. 1: R – crank; P – connecting rod; C – rear arm of the balance beam; A – front arm of the balance beam. Additionally, auxiliary lengths and angles used in the modeling are presented.

$$\begin{aligned} U_{ds} &= R_s i_{ds} + \frac{d\psi_{ds}}{dt} - \omega \psi_{qs}; \\ U_{qs} &= R_s i_{qs} + \frac{d\psi_{qs}}{dt} - \omega \psi_{ds}; \\ U'_{dr} &= R'_r i'_{dr} + \frac{d\psi'_{dr}}{dt} - (\omega - \omega_r) \psi'_{qr}; \\ U'_{qr} &= R'_r i'_{qr} + \frac{d\psi'_{qr}}{dt} - (\omega - \omega_r) \psi'_{dr}; \\ T_e &= 1.5p(\psi_{ds} i_{qs} - \psi_{qs} i_{ds}); \\ J \frac{d\omega_m}{dt} &= T_{\gamma_2} - F\omega - T. \end{aligned} \quad (1)$$

$$(2)$$

The variables in equations (1) and (2) have the following designations: U_{ds}, i_{ds} – projections of stator

voltage and current on the d -axis; U_{qs}, i_{qs} – projections of stator voltage and current on the q -axis; U'_{dr}, i'_{dr} – projections of rotor voltage and current on the d -axis; U'_{qr}, i'_{qr} – projections of rotor voltage and current on the q -axis; ψ_{qs}, ψ_{qs} – projections of stator flux linkage on the d and q axes; ψ'_{dr}, ψ'_{qr} – projections of rotor flux linkage on the d and q axes; R_s, R'_r – active resistances of the stator and rotor windings; T_e, T_m – electromagnetic torque of the motor and the torque resistance of the mechanism referred to the motor shaft; ω, ω_m and ω_r – angular velocity of the coordinate system, mechanical angular velocity of the motor shaft, and electrical angular velocity of the motor rotor; J, F – moment of inertia and viscous friction coefficient of the rotor and load.

The operation of the sucker-rod pump unit (SRPU) is cyclical. An example of a dynamogram of normal operation is shown in Fig. 2, a , where the following periods are indicated [7]:

$A-B$ – The beginning of the upward movement of the rod string, during which the load (the weight of the fluid column) is transferred from the tubing to the rod string. The tubing shortens, and the rod string lengthens, while the pump valves are closed.

$B-C$ – The upward movement of the rod string continues after the load transfer process is completed. The intake valve opens, allowing fluid to enter the pump cylinder.

$C-D$ – The intake valve closes at the uppermost position of the rod string, marking the beginning of the downward movement of the rod string. The load is transferred from the rod string back to the tubing. The tubing lengthens, and the rod string shortens, with the pump valves closed.

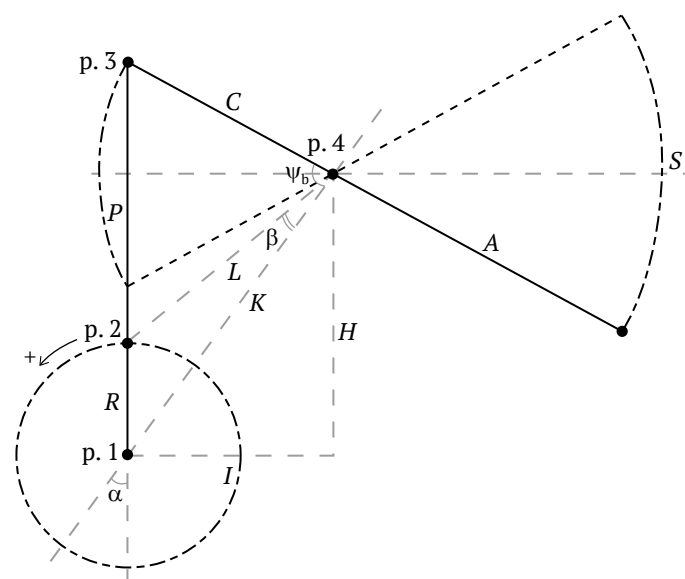


Fig. 1. Axial kinematic diagram of the pump jack

D–A – The downward movement of the rod string continues after the load transfer process is completed. The discharge valve opens. The cycle completes at the lowermost position.

Fig. 2, *b* presents a diagram showing the dependence of the pumping periods on the crankshaft angle, with the cycle divided into 4 quadrants. This representation is more convenient for adjusting the control settings of the unit.

As is well known, even the operation of a well-balanced pump jack can be accompanied by the motor transitioning into a brief generator mode during the first and third periods of the pumping cycle, as shown in Fig. 2. The duration of this mode may increase when the parameters of the SRPU change during operation due to equipment wear [1].

In the model of the sucker-rod pump unit, which includes the gearbox, the four-bar linkage pump jack mechanism, and the downhole section, the cyclic nature of the load, intake pressure, fluid density, dynamic fluid level in the well, the weight of the rod string in the fluid, the weight of the fluid column, the degree of balance of the pump jack, as well as the stroke loss of the rod suspension point, which is associated with elastic elongations during load transfer from the tubing string to the rod, are all considered [8, 9].

The equations and dependencies used in the mathematical model allow tracking the position, speed, and acceleration of the rod string suspension point based on the geometric dimensions of the pump jack mechanism. They also allow determining the coefficient for calculating the resistance torque on the crankshaft based on the load at the suspension point [10, 11].

Thus, the developed model allows evaluating the operating modes of the SRPU with different loads and degrees of pump jack balance, determining the energy consumed from the grid, and the energy dissipated on the braking resistor in the DC circuit of the VFD during the motor's generator mode, which occurs when the rod string moves downward under its own weight.

The model is supplemented with an uninterruptible power supply (UPS) system, and there are many implementation schemes. The simulation considers a system that consists of a *DC/DC* converter connected to the DC link of the SRPU's frequency converter. The *DC/DC* converter is similar to the inverter of the frequency converter, with the difference being in the control system and the law governing the control signals for the operation of the IGBT switches [12]. Inductors and battery packs (LABs) are connected to the output of the *DC/DC* converter, with the quantity and connection scheme depending on the duration of the backup. The control system must generate the gate drive signals for the power switches in such a way as to maintain the required voltage level in the DC link and regulate the charging and discharging current and voltages of the battery packs. It consists of an internal loop with current feedback from the *DC/DC* side of the battery pack and an external loop with feedback from the DC link voltage of the VFD during discharge and from the battery pack voltage during charging [13].

There are several types of battery models available: those based solely on experimental data, those relying on a mathematical description of chemical processes, and those utilizing electrical equivalent circuit models. For the simulation, the third type was employed, with a model available in the stan-

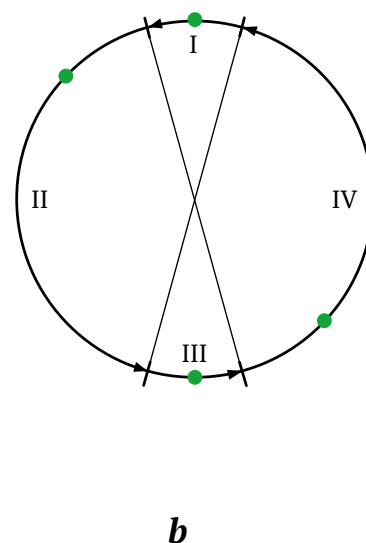
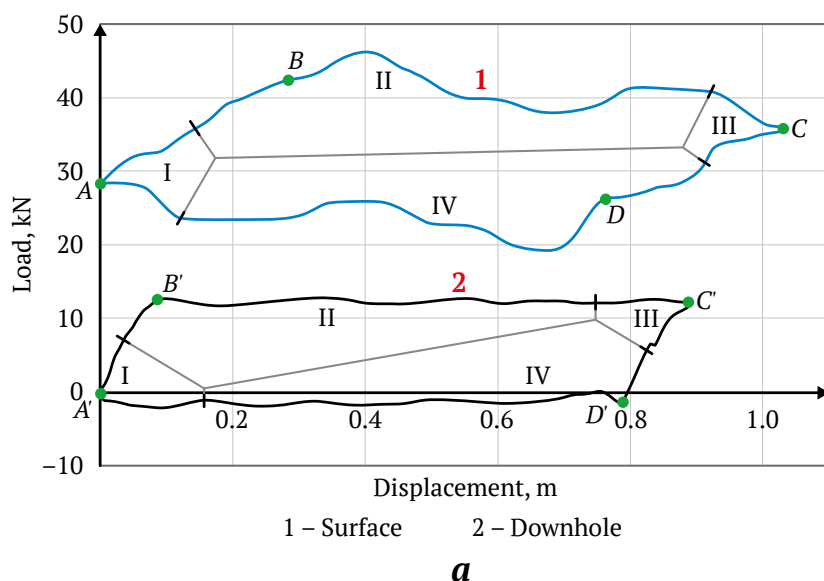


Fig. 2. Periods of the pumping cycle: *a* – on surface and downhole dynamograms; *b* – on the diagram of the polished rod position relative to the crankshaft angle

standard Simulink library. The parameters required for this model can be determined using technical specifications and discharge characteristics provided by the manufacturer [14]. However, the most precise calibration can be achieved by conducting real-world tests on the specific battery in question.

In the control system, the voltage range on the battery side is set between 310–435 V, and the voltage range on the DC link side of the VFD is set between 495–550 V. The maximum error for the LAB model in the standard Simulink library is 5% for a charge level range from 10% to 100%, with currents ranging from 0 to twice the battery capacity during charging, and from 0 to five times the battery capacity during discharging. The assumptions for the considered LAB model are as follows:

- the internal resistance does not change with current amplitude and remains constant throughout the charge and discharge cycles;
- discharge and charge characteristics are identical;
- the battery capacity does not change with current amplitude, and the Peukert effect [15] is absent;
- self-discharge of the LAB is not implemented in this model, but it can be realized by adding a large resistor in parallel with the battery terminals;
- the LAB does not have a memory effect.

The parameters for the LAB system of 32 units are selected to maintain operation for a 30 kW load

for 5 minutes, with each battery maintaining a voltage of 10.8 V. For this, it is required that during discharge at constant power, each LAB in the system must provide, W/battery:

$$P_{el} = \frac{P_{main}}{\eta_{DC/DC} \eta_{inv} \eta} = 1017.3. \quad (3)$$

Catalog data from various manufacturers indicate that for the case under consideration, a system of 32 LABs with a nominal capacity of 33 Ah each can sustain a discharge at constant power of 1020 W/battery. The parameters set in the model are similar to such a system of 32 LABs.

SRPU simulation results

The operation of the sucker-rod pump unit with a period of generator mode was simulated. Fig. 3 shows the graphs for a pump jack with a significant imbalance of approximately 50%, with the degree of imbalance determined using the current imbalance coefficient [16, 17]. Using the lower graph in Fig. 3, the beginning of the generator mode can be identified at 8.2 seconds when the load torque on the crankshaft becomes negative. On the upper graph, curve 1 represents the power dissipated on the braking resistor, and curve 2 represents the DC link voltage, which is limited to 757 V. When this value is reached, the braking resistor circuit is activated, and the excess energy is dissipated.

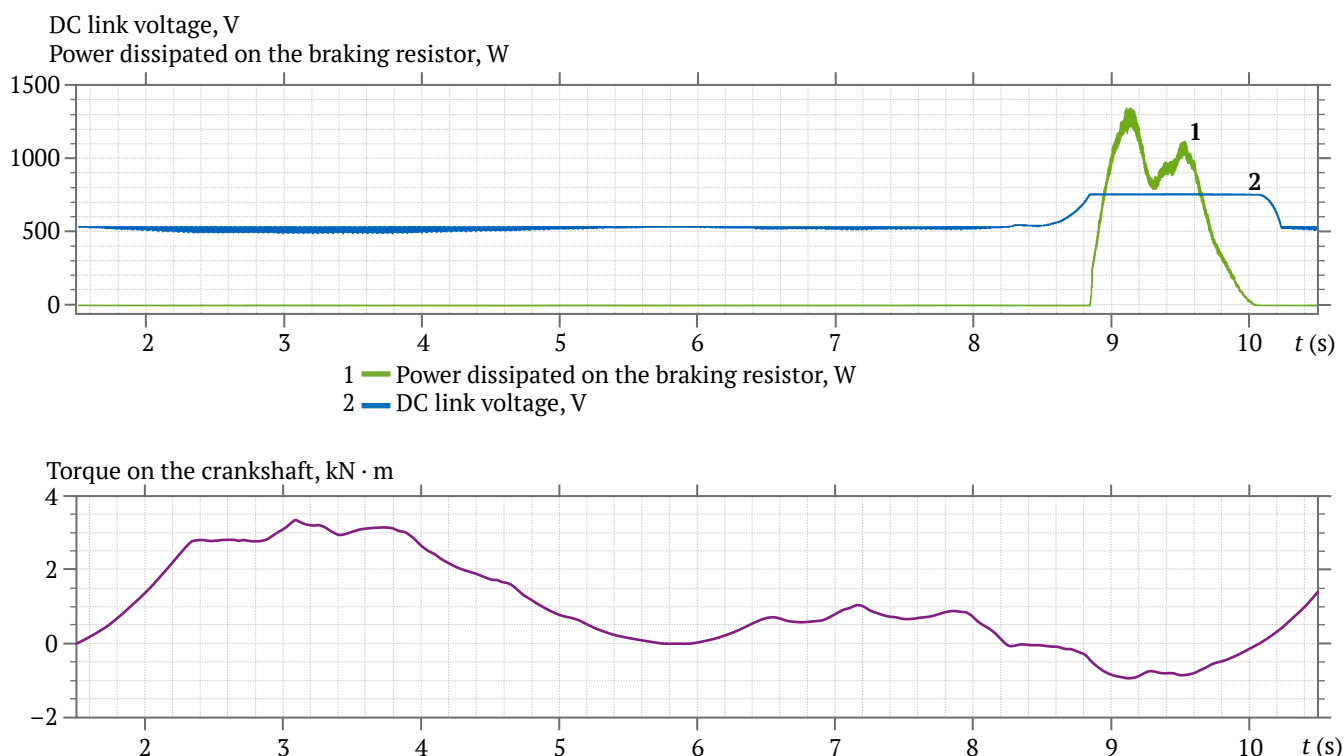


Fig. 3. DC link voltage and power dissipation curves on the braking resistor (upper graph), and the torque curve on the crankshaft considering the effect of counterweights (lower graph) at approximately 50% imbalance

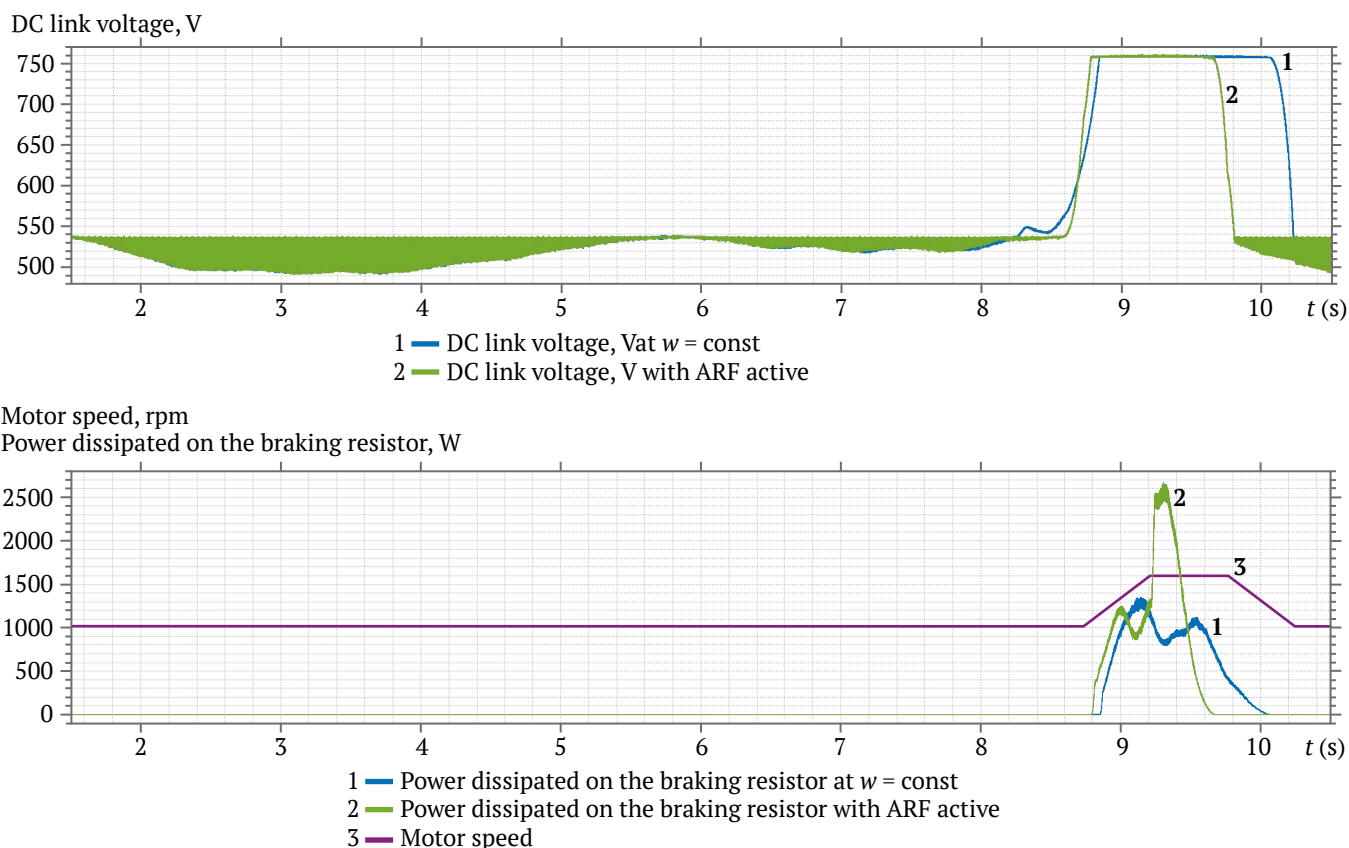


Fig. 4. DC link voltage curves (upper graph), speed and power dissipation curves on the braking resistor (lower graph) with ARF disabled and active, at approximately 50% imbalance

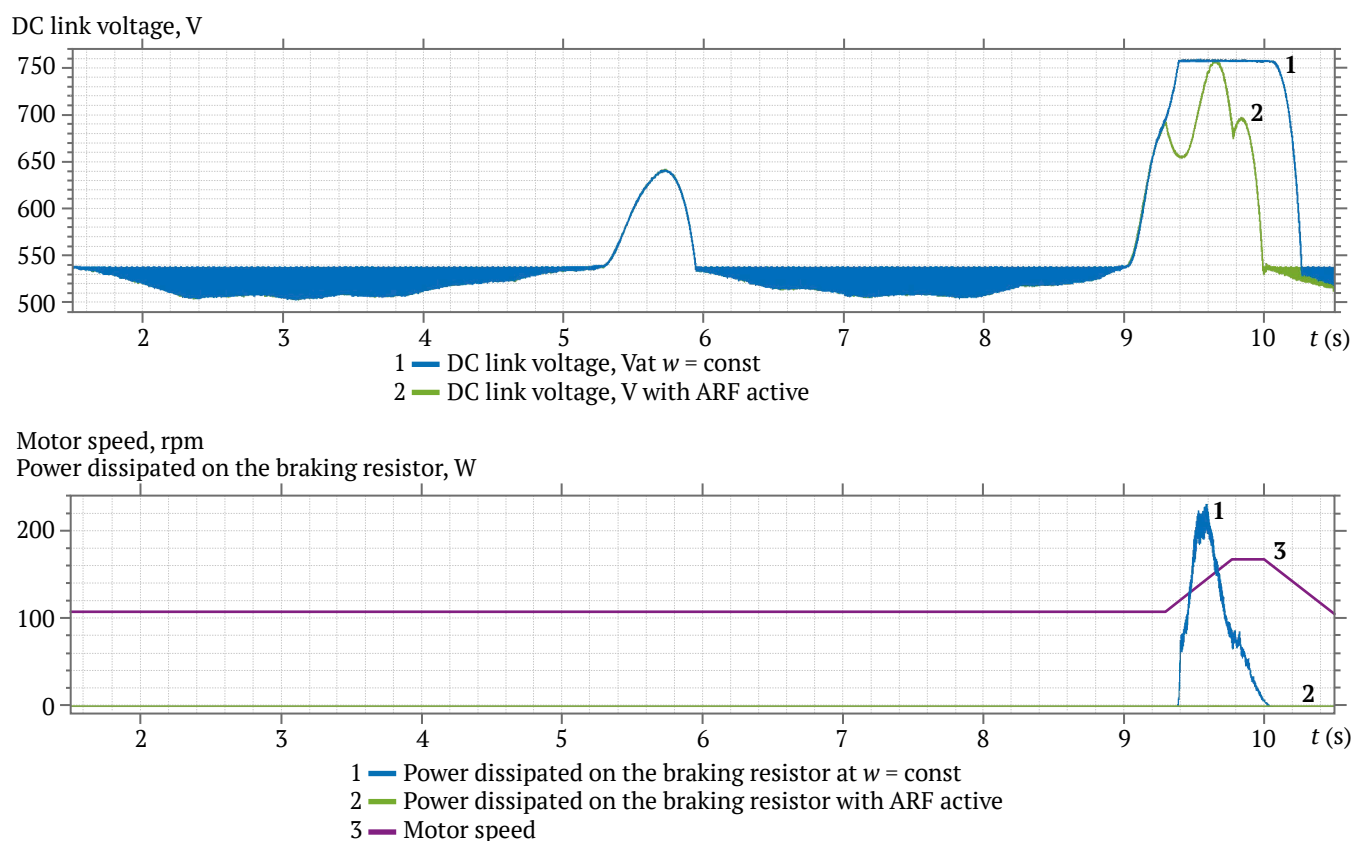


Fig. 5. DC link voltage curves (upper graph), speed and power dissipation curves on the braking resistor (lower graph) with ARF disabled and active, at approximately 5% imbalance

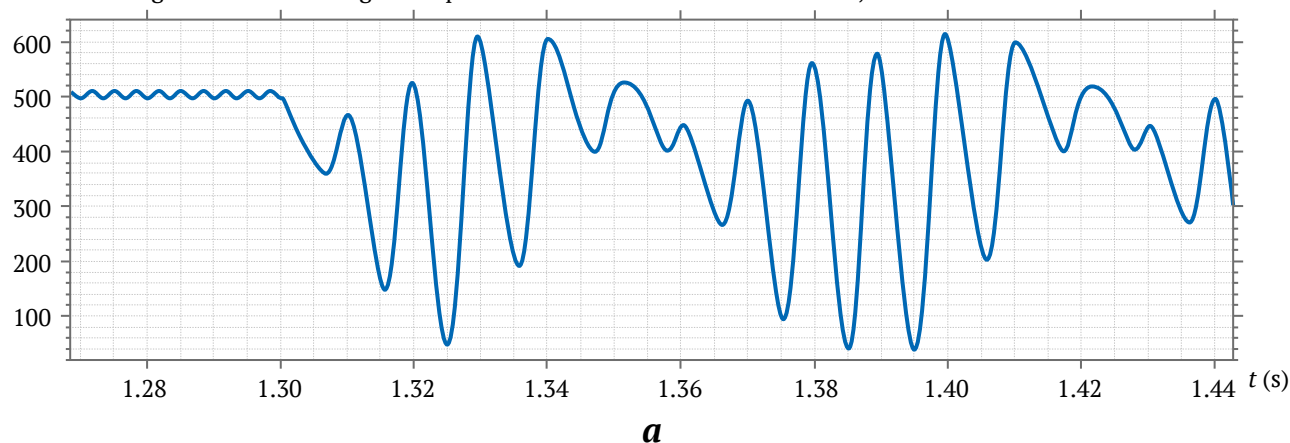
For different levels of imbalance, Figs. 4 and 5 show the DC link voltage curves on the upper graphs: curve 1 corresponds to constant speed (without ARF), and curve 2 corresponds to active ARF. To more clearly indicate the period of ARF activation, the speed graphs, labeled as curve 3, are shown in the lower part of these Figs. Additionally, curve 1 denotes the power dissipated on the braking resistor without ARF, and curve 2 denotes the power dissipated with active ARF.

Simulation results of voltage dips and the operation of the DC / DC converter

Disturbances in the electrical network are caused by short circuits, originating from nearby overhead transmission lines and from distant networks of 35 kV and above. The simulation of nearby short circuits was carried out at the node connected to the 6 kV overhead transmission line. It was found that during sin-

gle-phase short circuits in the 6 kV network, the drive operation can continue. However, three-phase and two-phase short circuits in the 6 kV network lead to shutdowns, with the SRPU's VFD losing power. In the case of a two-phase short circuit not being cleared, large voltage fluctuations occur in the DC link, as shown in Fig. 6, a, and large current fluctuations at the VFD input, as shown in Fig. 6, b, which are highly likely to cause equipment failure. It should be noted that when the 6/0.4 kV transformer windings are connected in a Δ/Y_0-11 configuration, the average voltage in the VFD's DC link is higher than when the transformer windings are connected in a Y/Y_0-12 configuration. In the event of a power supply not being disconnected during emergency conditions, individual drive protection should be activated. It is recommended to use both an automatic circuit breaker and a fast-acting fuse that match the drive's nominal parameters to ensure comprehensive protection.

DC link voltage of the VFD during a two-phase short circuit in the 6 kV network, V



Currents at the VFD input during a two-phase short circuit in the 6 kV network, A

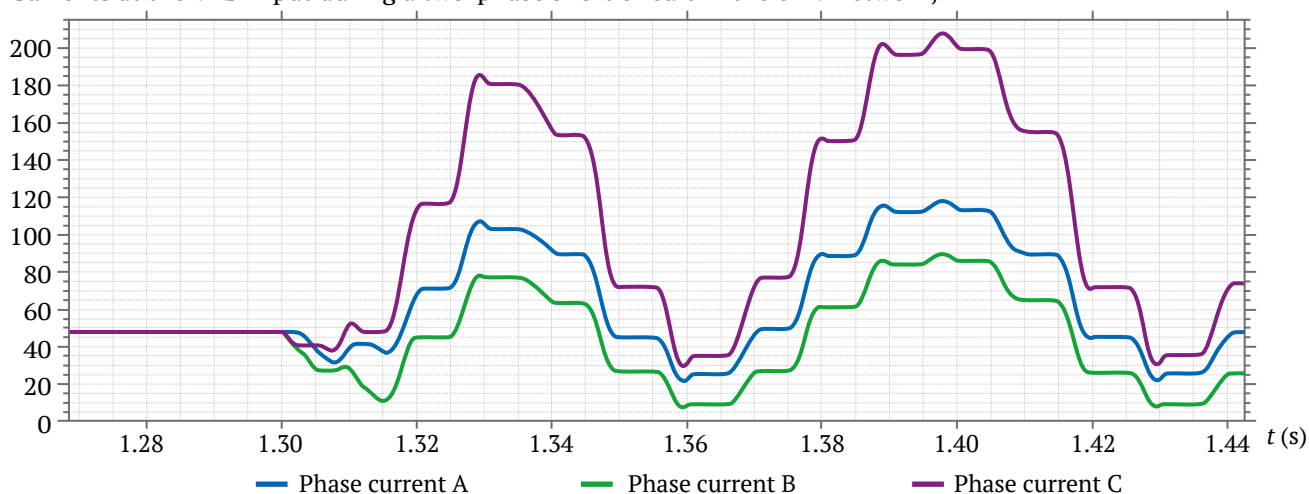


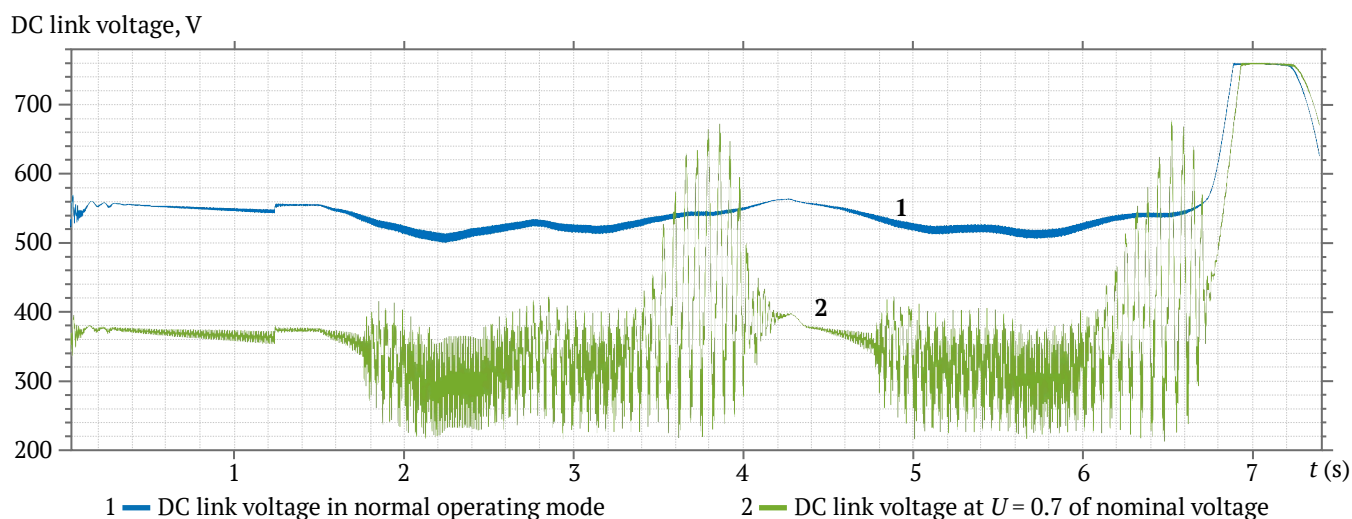
Рис. 6. Two-phase short circuit in the 6 kV power supply network:
a – DC link voltage of the VFD; b – input current of the VFD

Distant short circuits manifest in 6 kV load nodes and at the VFD inputs as voltage dips. To maintain the operation of the VFD with centrifugal working mechanisms, an effective means of improving stability is the “kinetic reserve” option [18], which essentially functions as the reverse of the anti-regeneration function mentioned earlier. The “kinetic reserve” option causes an accelerated reduction in motor speed by lowering the set frequency at the VFD output, with the excess motor energy being used to maintain the voltage in the DC link.

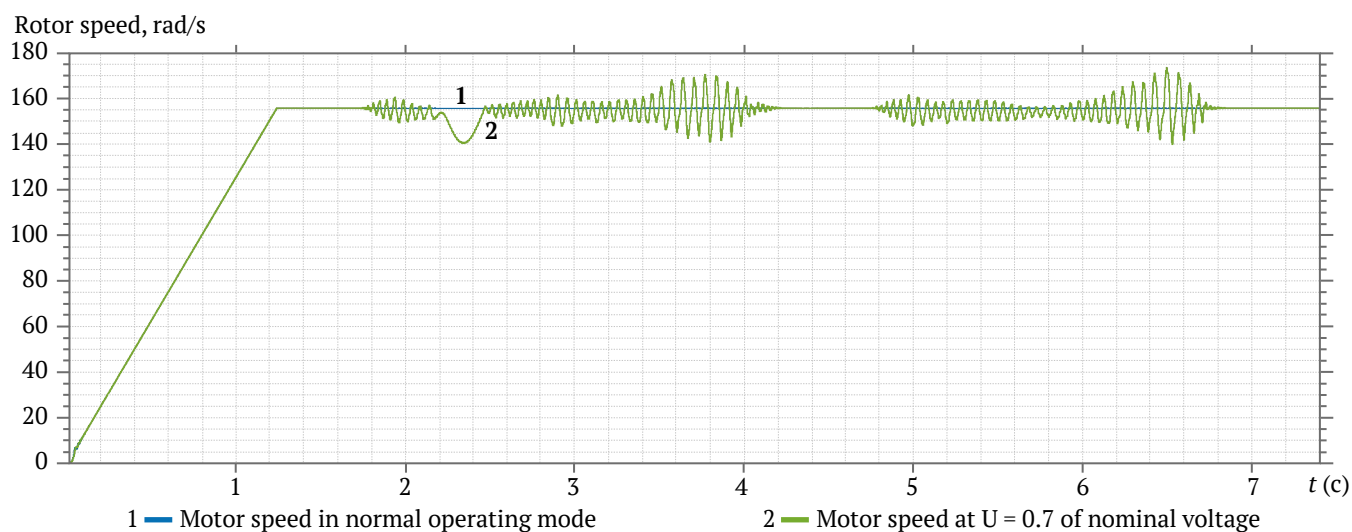
In the drive system of the SRPU, the use of the “kinetic reserve” option would be ineffective because the resistance torque of the mechanism does not depend proportionally on the square of the speed, as it does in centrifugal mechanisms, but follows a more complex law dependent on the position of the suspen-

sion point. The implementation of this option is only possible during a short period of the cycle. Therefore, the possibility of connecting a UPS system based on a DC/DC converter and LABs to the VFD’s DC link was investigated.

Typically, the VFD has built-in protection against voltage dips in the DC link – undervoltage protection (UVP), which is set by default within the range of 64–76% to 85–90% of the nominal voltage value [3]. The voltage level is determined by the permissible current value of the rectifier diodes during power restoration and the surge of the DC link capacitor charging current, which is mitigated by connecting the capacitor charging circuit. The voltage level is also related to the minimum allowable voltage necessary to maintain the normal operating mode of the of the sucker-rod pump unit.



a



b

Fig. 7. Mode characteristics: 1 – at nominal voltage and 2 – with a voltage reduction to 0.7 of the nominal value, the following curves are presented: a – DC link voltage; b – motor speed



The operation was simulated with a reduction in the DC link voltage to 0.7 of the nominal value. Fig. 7, *a* shows the voltages for two modes, and Fig. 7, *b* shows the corresponding motor speeds.

Fig. 8 shows the results of simulating a prolonged voltage dip in the DC ($U_{\text{пч}} = 0.7U_{\text{пчном}}$), link with the UPS connected to the DC link – curve number 2. The created model with the UPS is capable of maintaining the DC link voltage during voltage dips without causing negative oscillations in the motor shaft.

Fig. 9 presents the DC link voltage and the LAB voltage for the experiment, where the following voltage dip periods were used $U_{\text{пч}} = 0.3U_{\text{пчном}}$: 2–3 s; 4.1–5.1 s; 6.8–7.1 s.

Results and discussion

Based on the experiments conducted, it can be concluded that the anti-regeneration function (ARF) can completely eliminate the generator mode only when it is necessary to dissipate a small amount of

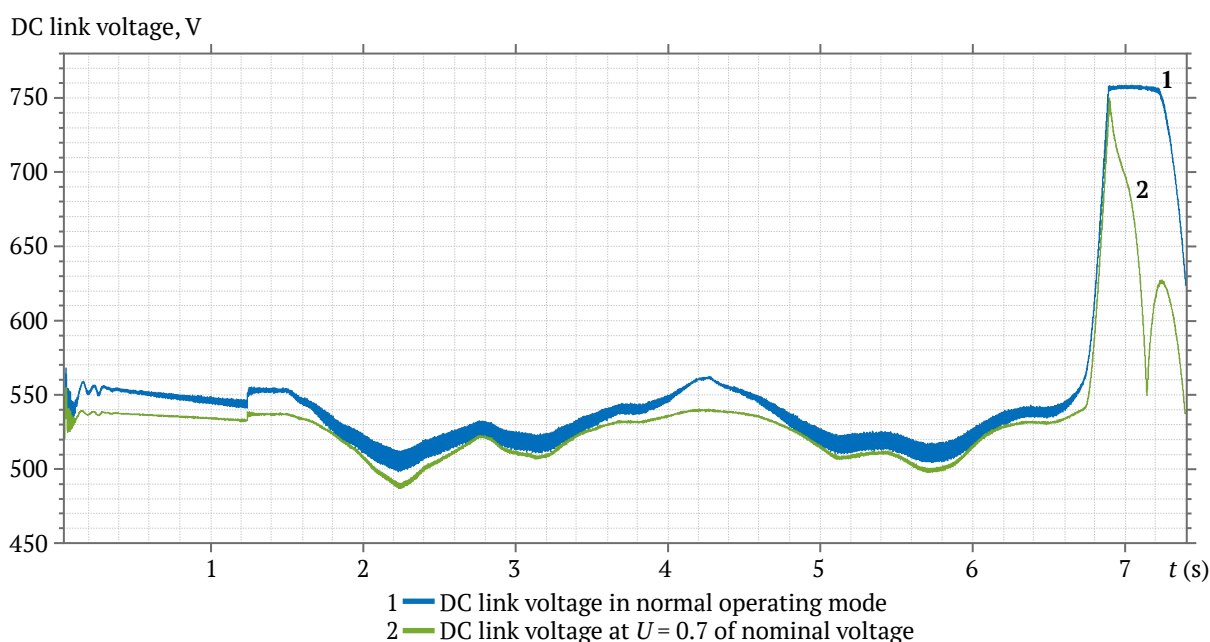


Fig. 8. DC link voltage in normal mode – curve 1, and in mode with a reduction of input voltage to 0.7 of the nominal value with the UPS connected – curve 2

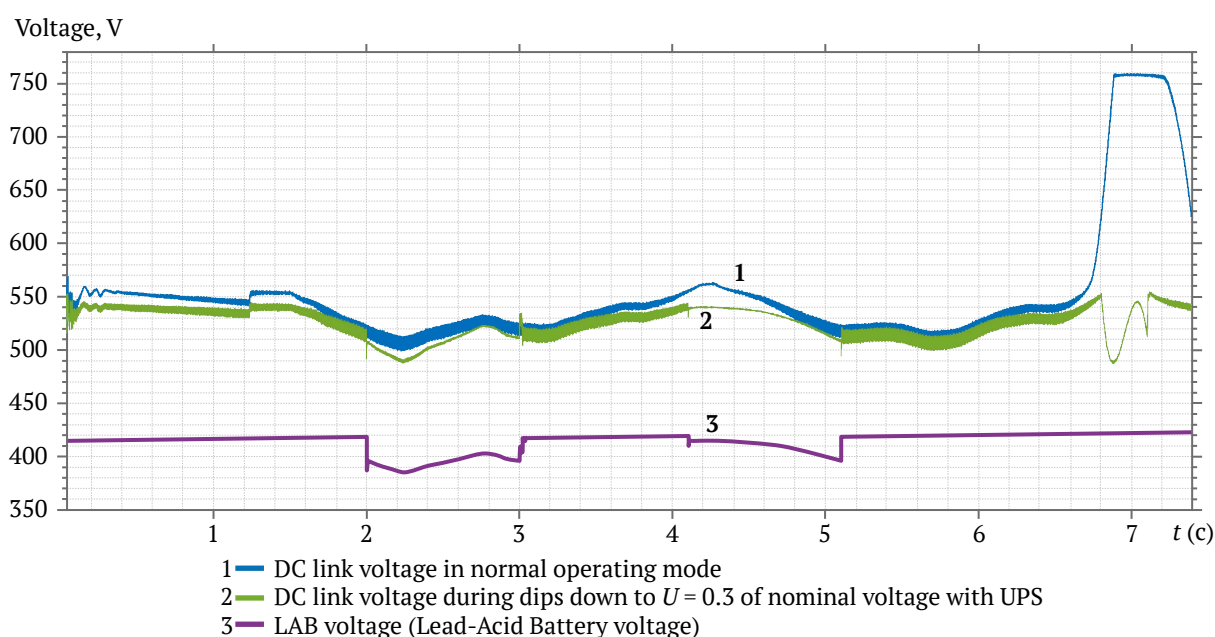


Fig. 9. DC link voltage and LAB voltage during short-term dips in input voltage in all three phases down to 0.3 of the nominal value with the UPS connected



power, as shown in Fig. 5. The acceleration settings when using the overvoltage suppression and speed and torque limiting functions must be configured with regard to the actual characteristics of the well and equipment, as in some cases, an increase in speed may lead to unacceptable mechanical stresses in SRPU parts. The ARF reduces the duration of the pumping cycle, which should be considered when planning the operation mode of the unit.

The electromagnetic torque exerts a braking effect on the rotor in generator mode, but with the ARF active, the electromagnetic torque remains rotational. When ARF is active, the electromagnetic torque and the resistance torque, which becomes negative during the downward movement of the rod string, increase the motor speed, and the deceleration of the rod string at the end of the downward stroke occurs more intensively and rapidly [1]. The simulation results confirm that the longer the generator mode lasts, the higher the instantaneous rotor speed must be. The lack of speed limitation with active ARF can lead to acceleration to a speed that exceeds the nominal by 50–70%, if this is permissible for the motor. Increased speed dynamics at the end of the fourth and the first period of the pumping cycle lead to additional inertial forces in the pump jack elements and dynamic impacts on the pump jack structure, which increases wear and leads to the failure of the unit. Thus, ARF without the additional use of braking resistors can be successfully applied if it does not lead to a critical increase in load; that is, for SRPUs with a short generator mode period, where significant speed increases are not required to eliminate it, or when the motor operates at a speed significantly lower than the nominal speed maintained by the VFD.

It should be noted that in the absence of the ability to transfer excess energy to the grid, it is recommended to use a braking resistor even with an active anti-regeneration function, if there is no complete confidence that the operating mode will not change over time and the generator mode period will not increase. It should also be considered that an overvoltage in the DC link can be caused not only by transitioning to generator mode, so it is recommended to take measures to reduce the likelihood of other causes, such as high output voltage, voltage spikes at the VFD output, incorrect grounding connection, motor malfunction, and others.

When the voltage decreases, torque oscillations increase, as shown in Fig. 7, b, where increased oscillations and the appearance of speed dips can be observed. The model under consideration did not use DC link undervoltage protection or VFD overload protec-

tion, which could be triggered under these conditions. Further voltage reduction leads to an even greater decrease in the stability of the unit and subsequent motor shutdown. Therefore, a UPS is recommended to maintain operation in the presence of significant voltage dips or short-term interruptions.

The UPS simulation results presented in Figs. 8 and 9 demonstrated its effectiveness during both prolonged voltage dips in the power supply network and short-term dips. The obtained results are close to ideal, and measurements taken on a real object or physical modeling of the UPS with such a load will allow adjustments to be made to this model if necessary.

It should be noted that the considered lead-acid batteries (LABs) have several limitations and requirements related to depth of discharge, voltage, and charge current at different battery charge levels, parameters for operation in buffer mode, temperature range, and the need for temperature compensation of the charging voltage. These requirements are specified in the LAB manual and should be considered by the charge and discharge management system – the DC/DC converter control system – to ensure the maximum possible service life. An alternative option is supercapacitors, which generally have a longer service life, can operate in a wider temperature range, and have fewer restrictions on permissible voltage, current, and charge levels. Detailed specifications are usually provided in the datasheets and catalogs for the respective equipment.

Future research directions may involve improving the accuracy of this model and examining the possibility of using a dynamic voltage distortion compensator (DVD compensator) with the SRPU VFD to compensate for voltage deviations and dips.

Conclusion

A model was developed to analyze the stability of the variable frequency drive (VFD) of a sucker-rod pump unit (SRPU), which takes into account the cyclical and uneven nature of the load, the balance of the pump jack, processes associated with the occurrence of generator mode, and the impact of voltage dips in the network. The method of eliminating overvoltage in the DC link by using the overvoltage suppression function was examined. It was determined that this function has several limitations, primarily related to the duration of the generator mode (degree of imbalance) and the period of its occurrence in the pumping cycle. With significant imbalance, the ARF will be less effective, and the use of a braking resistor will be required. If the generator mode occurs at the end of the upward or downward movement of the rod string, the



increase in rotational speed will lead to undesirable mechanical forces, additional wear, or even equipment failure.

Another task of the study was to simulate voltage dips in the power supply network and examine their impact on the stability of SRPU operation. With minor voltage dips, the VFD is able to remain operational, and in some VFD models, special control algorithms are applied to maintain operational stability. It is known that with more significant voltage dips, the undervoltage protection (UVP) will activate. One way

to maintain operation even during a short-term loss of voltage is through the use of an uninterruptible power supply (UPS). The operation of such a system was examined during the simulation, the results of which demonstrated the effectiveness of this method in improving operational stability. The model developed in this study can be used to perform a general assessment of the operability of a similar designed system and to verify the correct selection of the DC link capacitor and inductors at the input of the DC/DC converter.

References

1. Yarish R.F., Garifullina A.R., Garifullin R.I., Yakunin A.N. Investigation of operating modes of frequency-regulated electric drive of pumpjack. *Power Engineering: Research, Equipment, Technology*. 2018;20(11–12):56–64. (In Russ.) <https://doi.org/10.30724/1998-9903-2018-20-11-12-56-64>
2. Egorov A.V., Ershov M.S. Experimental study of the stability of asynchronous variable-speed drives (VSD) during short-term voltage failures. *Industrial Power Engineering*. 2018;(4):9–12. (In Russ.)
3. Xu Y., Lu W., Wang K. et al. Sensitivity of low-voltage variable-frequency devices to voltage sags. *IEEE Access*. 2019;7:2068–2079. <https://doi.org/10.1109/ACCESS.2018.2885402>
4. Pantel O.V. Method of calculating the parameters of an asynchronous motor to model its operating modes in the Matlab / Simulink environment. *Academy*. 2015;2(2):7–11. (In Russ.)
5. Haisen Z., Yilong W., Yang Z. et al. Practical model for energy consumption analysis of beam pumping motor systems and its energy saving applications. In: *2017 IEEE Industry Applications Society Annual Meeting*. 1–5 October 2017, Cincinnati, OH, USA. Pp. 1–9. <http://dx.doi.org/10.1109/IAS.2017.8101721>
6. Zheng B., Gao X., Li X. Fault detection for sucker rod pump based on motor power. *Control Engineering Practice*. 2019;86:37–47. <https://doi.org/10.1016/j.conengprac.2019.02.001>
7. Fakher S., Khlaifat A., Hossain M.E., Nameer H. A comprehensive review of sucker rod pumps' components, diagnostics, mathematical models, and common failures and mitigations. *Journal of Petroleum Exploration and Production Technology*. 2021;11:3815–3839. <https://doi.org/10.1007/s13202-021-01270-7>
8. Ershov M.S., Efimov E.S. Modeling of the energy efficiency of an electric drive for a rod pumping unit. In: Martynov V.G. (ed.) *Gubkin University in Addressing Issues of the Russian Oil and Gas Industry: VI Regional Scientific and Technical Conference dedicated to the 100th Anniversary of M.M. Ivanov*. September 19–21, 2022, Moscow. Abstracts of Reports, Moscow: Gubkin Russian State University of Oil and Gas (NRU); 2022. Pp. 766–767. (In Russ.)
9. Langbauer C., Langbauer T., Fruhwirth R., Mastobaev B. Sucker rod pump frequency-elastic drive mode development – from the numerical model to the field test. *Liquid and Gaseous Energy Resources*. 2021;1(1):64–85. <https://doi.org/10.21595/lger.2021.22074>
10. Urazakov K.R., Molchanova V.A., Tugunov P.M. Method for calculating dynamic loads and energy consumption of a sucker rod installation with an automatic balancing system. *Journal of Mining Institute*. 2020;246:640–649. (In Russ.) <https://doi.org/10.31897/PMI.2020.6.6>
11. Solodkiy E.M., Kazantsev V.P., Dadenkov D.A. Improving the energy efficiency of the sucker-rod pump via its optimal counterbalancing. *International Russian Automation Conference (RusAutoCon)*. 8–14 September 2019, Sochi, Russia. Pp. 1–5. <https://doi.org/10.1109/RUSAUTOCON.2019.8867737>
12. Higure H., Hoshi N., Haruna J. Inductor current control of three-phase interleaved DC-DC converter using single DC-link current sensor. In: *2012 IEEE International Conference on Power Electronics, Drives and Energy Systems (PEDES)*. 16–19 December 2012, Bengaluru, India. Pp. 1–5. <https://doi.org/10.1109/PEDES.2012.6484495>
13. Nandankar P., Rothe J.P. Design and implementation of efficient three-phase interleaved DC-DC converter. In: *2016 International Conference on Electrical, Electronics, and Optimization Techniques (ICEEOT)*. 3–5 March 2016, Chennai, India. Pp. 1632–1637. <https://doi.org/10.1109/ICEEOT.2016.7754962>
14. Tremblay O., Dessaint L.-A. Experimental validation of a battery dynamic model. *World Electric Vehicle Journal*. 2009;3(2):289–298. <https://doi.org/10.3390/wevj3020289>
15. Cugnet M., Dubarry M., Liaw B.Y. Peukert's law of a lead-acid battery simulated by a mathematical model. *ECS Transactions*. 2010;25(35):223–233. <https://doi.org/10.1149/1.3414021>



16. Zyuzev A.M., Bubnov M.V. Diagnostics of the balance of the rod deep-well pumping unit by wattmetrogram. *Bulletin of the Tomsk Polytechnic University. Geo Assets Engineering*. 2019;330(4):178–187. (In Russ.) <https://doi.org/10.18799/24131830/2019/4/226>
17. Galeev A.S., Nurgaliev R.Z., Bikbulatova G.I., Sabanov S.L., Boltneva Yu.A. Criterion of equilibrium of the slow-speed drive of the downhole rod pumping unit to improve the reliability of the gearbox. *Petroleum Engineering*. 2019;17(6):96–101. (In Russ.) <https://doi.org/10.17122/ngdelo-2019-6-96-101>
18. Belousenko I.V., Ershov M.S., Chernov M.Yu. Improving the stability of electrical systems in continuous oil and gas production complexes. *Industrial Power Engineering*. 2019;(2):8–15. (In Russ.)

Information about the authors

Mikhail S. Ershov – Dr. Sci. (Eng.), Professor, Department of Theoretical Electrical Engineering and Electrification of Oil and Gas Industry, I.M. Gubkin Russian State University of Oil and Gas (National Research University), Moscow, Russian Federation; ORCID [0000-0002-7772-0095](https://orcid.org/0000-0002-7772-0095), Scopus ID [56261333000](https://scopus.org/56261333000); e-mail msershov@yandex.ru

Evgeniy S. Efimov – PhD-Student, Department of Theoretical Electrical Engineering and Electrification of Oil and Gas Industry, I.M. Gubkin Russian State University of Oil and Gas (National Research University), Moscow, Russian Federation; ORCID [0009-0007-9189-8029](https://orcid.org/0009-0007-9189-8029); e-mail efimov.evgeniy@yandex.ru

Received 30.01.2024

Revised 14.03.2024

Accepted 22.05.2024